STUDIES OF INTERPARTICULATE ADHESION AND COHESION IN DRY POWDER INHALATION SYSTEMS

Amanda Sue Clarke, BPharm (Hons), MRPharmS.

A thesis submitted in partial fulfilment of the requirements of the degree of Doctor of Philosophy

Department of Pharmacy, De Montfort University, Leicester
in collaboration with
Fisons Pharmaceuticals, Loughborough.

This thesis is dedicated to my parents

Studies of Interparticulate Adhesion and Cohesion in Dry Powder Inhalation Systems

Clarke A. S. PhD thesis, January 1997.
Department of Pharmacy, De Montfort University, The Gateway, Leicester, LE1 9BH, UK.

Abstract

Natural barriers prevent the inhalation and pulmonary penetration of particles larger than about 10 μm diameter. Therefore, in order to deliver powdered particles of drug directly to the lung the particle size must be less than 10 μm. A particle diameter between 2 μm-5 μm is considered optimum for pulmonary delivery. Particles in this size range are inherently cohesive. This cohesive nature presents a problem for uniformed dosing due to the associated poor flow properties. Binary mixes of larger, pharmacologically inert particles with small particles of drug are often formulated to improve the flow characteristics. The aim of this work was to investigate the particle-particle interactions which occur in such binary mixes, and evaluate their effect upon pulmonary drug delivery.

A comprehensive study was made into the roles of adhesion and cohesion within binary powder blends. The relationship between blend structure and pulmonary delivery was evaluated. Development of methodologies with the aim to quantify the interactive forces were reported.

Materials were characterised using a variety of techniques. Particles of α-lactose monohydrate were mixed with the drug species nedocromil sodium, sodium cromoglycate or reporterol to prepare binary interactive mixes. Evaluation of the structure of the mixes identified complex interactive units as well as non-adhered drug aggregates. The formation of the non-adhering drug aggregates occurred regardless of the area of lactose surface available for adhesive interactions.

Deposition of drug at the target site was evaluated *in vitro* using a multi-stage liquid impinger. Examination of the blend structure before and after inspiration of a dose, and evaluation of multi-stage liquid impinger data indicates that the majority of inspirable particles originate from the surface held drug aggregates.

In order to investigate the apparent competition between adhesive and cohesive interactions novel methodologies were developed. A centrifuge technique and a cone penetration technique were developed in order to quantify the magnitude of the adhesive and cohesive forces respectively.

Preparation of mixes which encouraged a random mix had a similar structure to the interactive mixes. Specific areas of the lactose surface appear to be preferential for adhesive interactions. Surface-held drug clusters are present in binary powder mixes, regardless of the method of preparation and drug load.

This work has shown that adhesive interactions are responsible for maintaining the integrity of the interactive units, whereas the deposition of drug at the target site is cohesion dependent.

"It is the product of knowledge to speak, but the privilege of wisdom to listen."

Anon.

Presentations

A part of the work described in this thesis has been presented in the following:

1. A. Clarke; A. H. de Boer, P. Wright, D. Y. T. Wong, M. Aulton.
Composition of binary interactive powder mixtures before and after *in vitro* inhalation testing.

Presented at the 9th Annual Meeting of the American Association of Pharmaceutical Scientists, San Diego, U.S.A.
November 1994.

2. Mike Aulton, Amanda Clarke.
Powder technology and powder characterisation in dry powder inhalation systems.

Presented at European Continuing Education College Course.
Pharmaceutical aerosols and dry powder inhalation systems, London, U.K.
September 1996.

Acknowledgements

The author wishes to thank:

Prof. M. E. Aulton for his supervision for the duration of the project;

Prof. C. LERK of Rijksuniversiteit Groningen, Netherlands, for his participation in the ERASMUS program;

Dr. Ing. A. H. deBOER, D. GJALTEMA and P. HAGEDOORN for making the stay in the Netherlands so productive and enjoyable;

all TECHNICAL STAFF of De Montfort University, Leicester, in particular Mr. R. WEBSTER for his technical expertise and assistance;

FISONS PHARMACEUTICALS for financial support;

Dr. P. WRIGHT and Dr. D.Y.T. WONG for their supervision;

all FAMILY and FRIENDS for all their various forms of encouragement.

CHAPTER FOUR: DETERMINATION OF THE PERFORMANCE OF BINARY POWDER MIXES AS INHALATION DOSAGE FORMS

Chapter One

Introduction

1.1 Introduction

Asthma is a major cause of ill health in populations with a westernised culture. It has been estimated that the prevalence of asthma sufficiently severe to require regular medical supervision in England is from 4 % to 6 % in children and about 4 % in adults [1].

The diagnosis of asthma is best confirmed by evidence of variable or reversible airflow obstruction accompanying the symptoms of wheeze, cough, chest tightness and dyspnoea. These symptoms may be exacerbated by exposure to allergens such as house dust mites, animal dusts, pollen, fungal spores, passive smoking or other air pollution: More general factors such as exposure to cold air or stress may also trigger attacks. This hyper-reaction to non-specific stimuli causes bronchoconstriction.

Asthma was the term used by Hippocrates in reference to the symptom of panting. It has been defined as "a clinical syndrome characterised by widespread airways obstruction, which is reversible either spontaneously or with treatment" [2]. Asthma is diagnosed by evidence of this reversible airflow obstruction which accompanies the symptoms of wheeze, cough, chest tightness and dyspnoea.

The function of the airway is to allow air to come into close contact with blood in order that gaseous exchange can take place. The consistently branching structure of the airways can be described as a pulmonary tree. The trachea of the airways which bifurcates to form main bronchi, is analogous to the tree trunk. These airways divide to

form smaller bronchi that lead to individual lung lobes: three lobes on the right side and two on the left side. Within each lobe the bronchi undergo further bifurcation to form new generations of smaller calibre airways, the bronchioles. This process continues through the terminal bronchioles, the respiratory bronchioles, alveolar ducts, and terminates with the alveolar sacs.

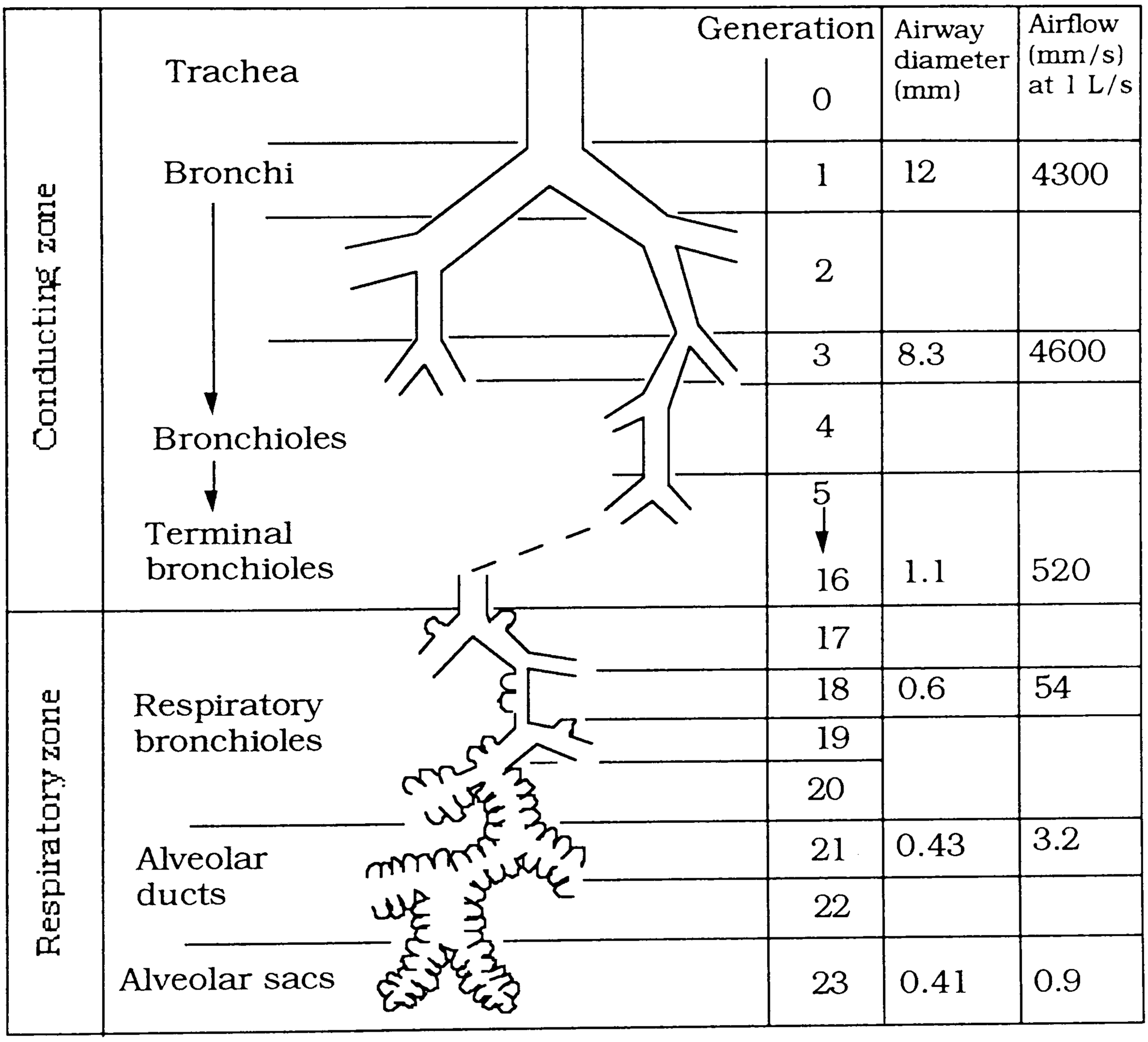

Generation	Airway diameter (mm)	Airflow (mm/s) at 1 L/s
0		
1	12	4300
2		
3	8.3	4600
4		
5		
↓		
16	1.1	520
17		
18	0.6	54
19		
20		
21	0.43	3.2
22		
23	0.41	0.9

Figure 1.1 Lung structure

The airways which do not participate in gaseous exchange, from the trachea to the terminal bronchioles, are categorised as the conducting zone. The respiratory zone comprises of respiratory bronchioles,

alveolar ducts and alveolar sacs, which do participate in gaseous exchange.

This structure forms an organ with a capacity of about 3000 mL after quiet, normal expiration, and 3400 mL upon normal inspiration. The total surface area at the level of the human alveolus is in the order of $140 m^2$. There is a change in the total cross sectional area of the conducting airways, from 2.5 to 180 cm^2. This allows the rapid bulk flow of inspired air down to the terminal bronchiole. In contrast to this, within the respiratory zone the cross-sectional area increases, from 180 to 10 000 cm^2. This results in a significant decrease in the velocity of airflow to such an extent that the flow velocity fails to exceed that of diffusing oxygen molecules. Of the 400 mL of air inspired by contraction of the inspiratory muscles the first 250 mL reaches the alveoli, the last 150 mL remains in the conducting airways when inspiration ceases and is exhaled as unchanged room air. The histology of each region of the pulmonary tree has a distinct effect on the functional aspects of the airway under physiological and pathophysiological conditions.

Smooth muscle is separated from the epithelium by the lamina propria, a region of connective tissue containing nerves and blood vessels. The trachea is supported by incomplete cartilage rings. The smooth muscle supports the open ends of these rings, and therefore constitutes only a small proportion of this component of the airway. Further down the pulmonary tree, through the bronchi and bronchioles, the contribution of the smooth muscle to the airway wall increases to a point of completely encircling the airway.

The epithelium is a continuous sheet of cells lining the luminal surface of the airways. It comprises a variety of cell types. Throughout the conducting airways the luminal surface is lined with ciliated cells. Co-ordinated beating of these cilia propels a blanket of mucus towards the upper airway and pharynx where it is either swallowed or ejected. This mucus, secreted by goblet cells and mucus glands, fulfils three functions: (i) it protects the epithelia from becoming dehydrated; (ii) the water in the mucus is involved in saturation of the inhaled air; (iii) and it is involved in the protection of the airway from xenoparticles. This mucociliary escalator, the movement of the mucus up the pulmonary tree, is the method of clearing non-dissolving particles from the lung.

Mast cells are distributed widely throughout the human respiratory tract. They are found in large numbers in the walls of the alveoli and airways. An appreciable number are found intercalcated between the epithelial cells and adjacent to the surface of the lumen.

β-adrenergic receptors are also widely distributed in human airway and alveoli. The greatest density is seen on airway epithelium and alveolar walls, with a less dense distribution over airway and vascular smooth muscle. The receptors on airway and vascular smooth muscle, and on airway epithelium appear to be entirely β_2-receptors whilst β_1-receptors account for 30 % of the β-receptors on the alveolar walls.

The functional abnormalities characteristic of the airways of asthmatic patients include hyper-responsiveness to non-specific stimuli, reversible airflow limitation, and excess mucus production.

The hyper-responsiveness of the airways results in a narrowing of the airways by stimuli which does not cause a change in normal airways. It is unlikely that the responsiveness is related to an inherent abnormality of bronchial smooth muscle, which has normal reactivity *in vitro*. Damage to the epithelia increases responsiveness, which has led to the suggestion that a loss of putative epithelial-derived relaxation factor may be responsible.

Airway narrowing results from the combined effects of mucosal inflammation and oedema, excessive intraluminal secretions and smooth muscle contraction. These effects are thought to be the consequence of an exaggerated inflammatory process.

The distribution of the mast cells throughout the airways results in these cells coming into immediate contact with an inhaled antigen. Degranulation of the mast cell results in the release of mediators. Some of these mediators cause rapid bronchoconstriction which characterises the acute phase of an asthma attack. Other mediators stimulate mucus production and recruit other inflammatory cells which are responsible for the delayed response. This late asthmatic response is complex and incompletely understood. It involves release of mediators from eosinophils which can produce epithelial damage, contribute to bronchoconstriction, increased vascular permeability, mucus secretion and further chemotaxis.

Relief of the symptoms of asthma can be achieved by the administration of β_2-adrenoceptor agonists, mast cell stabilising drugs, and corticosteroids. Agonists of β_2-adrenoceptors are potent smooth

muscle relaxants which attenuate the bronchospasm induced by released mediators. They provide symptomatic relief where bronchoconstriction is the predominant cause of reduced airway calibre. Stabilisation of the mast cell membrane inhibits mediator release and prevents the ensuing inflammatory process. These type of drugs have no bronchodilator activity. Corticosteroids influence several immune system functions and thereby interfere with the inflammatory processes at several loci. Their main effect is to block late-onset asthmatic responses, and may prevent or reverse airway hypersensitivity. They may also modify β-adrenoreceptor populations and exert a permissive effect on β-adrenoreceptor function.

Local drug delivery to the airways for the treatment of the symptoms of asthma has clear advantages over the oral or intravenous route. A faster onset of action and longer bronchodilation caused by β_2-adrenoceptor agonists occurs when comparing the effect of pulmonary delivery to that caused by similar intravenous, or much larger oral doses [3]. The low drug doses needed for the local route, due to the precise delivery of the drug at the site of action, leads to very little systemic absorption. This reduces the side effects associated with these drugs which occurs when they are distributed systemically. These include tremor and tachycardia associated with β_2-adrenoceptor agonists and adrenal suppression associated with corticosteroids. It also offers a route for drug species which are active at sites in the airways but poorly adsorbed from the gastrointestinal tract, or readily eliminated, such as sodium cromoglycate.

In order to exert its pharmacological effect the drug must penetrate the pulmonary tree to the respiratory zone (Figure 1.1). The nature of the condition which causes high airflow resistance, and limitations of the inhalation device can result in as little as 10 % of the dose reaching the correct site within the lungs [4].

Delivery of drugs to active sites within the airways requires penetration of the drug into the pulmonary tree, overcoming the natural barriers to particles, to reach the distal regions of the lungs. In order to exert a pharmacological effect an inhaled drug particle must negotiate a route through the complex structure of the respiratory tract and impinge onto the lung surface in the alveolar region. Deposition of particles from the inhaled airstream onto the luminal mucus occurs by three principal phenomena: impaction, sedimentation and diffusion [5]. The mechanism of deposition is determined by the particle diameter.

Deposition by impaction occurs when a particle has an inertia which makes it unable to change direction with the air flow. This occurs in the upper airways where the airstream changes direction entering the throat, and the upper airway bifurcations. This method removes particles with a diameter greater than 5 μm from the inspired air. Impaction deposition is enhanced when the air velocity is high, the airways are partially obstructed and by turbulent airflow in the trachea and major bronchi.

Sedimentation describes the process of particles settling under the influence of gravity. Deposition by sedimentation is most likely to occur when the airflow is not turbulent and the air velocity is low.

For very small particles, under 5 μm, removal from the airstream occurs by Brownian motion. Random bombardment of the particles by gas molecules causes collision with the airway walls.

Interception is a less important mechanism. Deposition by interception occurs when the diameter of a particle approaches the diameter of the airway. Particles large enough to deposit by interception in the lower airways often have sufficient mass to cause deposition by impaction or sedimentation in the upper airways. The role of interception, however, increases as a particle shape deviates from spherical [6].

The effect of the particle size on the location of its deposition can be described by Figure 1.2 [7].

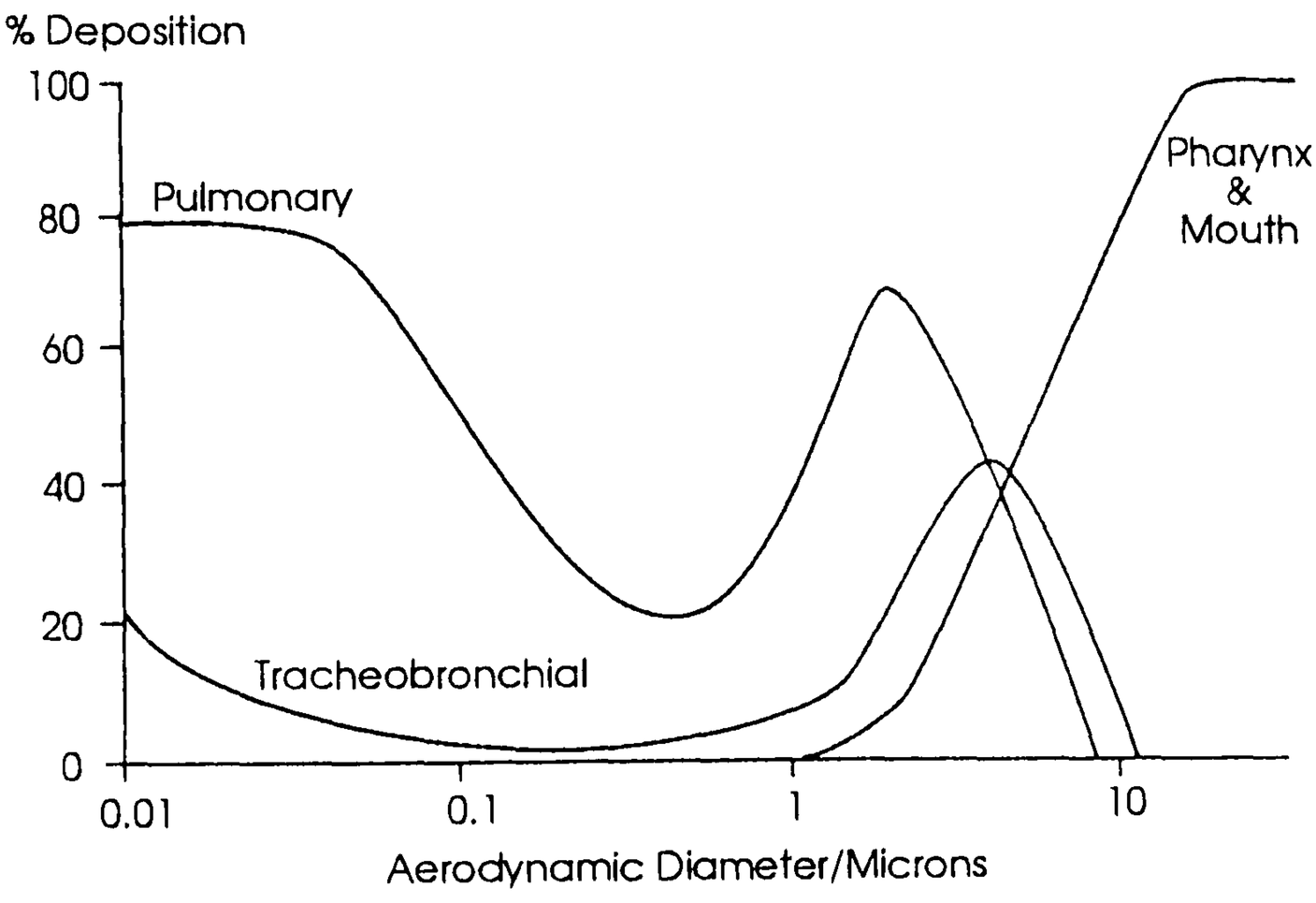

Figure 1.2 Effect of particle size on deposition of a monodisperse aerosol (redrawn from [7])

According to this model therefore, for maximum deposition in the respiratory zone particle size must be restricted between 2 μm and

5 μm. Particles larger than this are removed in the upper airways. Particles smaller than this may not be removed from the airstream and therefore will be exhaled with the expired air.

Such a small size of drug which will penetrate into the pulmonary tree can be presented from a nebuliser, a pressurised aerosol or a dry powder inhaler.

Pressurised aerosols deliver a fine spray of either drug solution or suspension. Most metered dose pressurised inhalers rely on the patient to release a dose from the aerosol in co-ordination with inspiration. This co-ordination is essential for optimum administration of the dose, but difficult to perform correctly. Recent studies have shown that at least 50 % of adults have difficulty using conventional MDIs efficiently [8, 9]. Breath-actuated pressurised aerosols [10] and spacer devices have been developed in order to overcome this problem.

Chlorofluorocarbon propellants are used extensively in the formulation of MDIs as a dispersion medium for the drug, and more importantly, as the driving force for aerosolisation. With the implication that CFC compounds were partially responsible for the depletion of the ozone layer [11] global production and use has declined. The Montreal Protocol on Substances That Deplete The Ozone Layer (1994) has reduced the use of CFCs in all of the signatory countries in all but essential uses. Although medicinal purposes are recognised as essential use alternative propellant systems are being developed [12] as are inhalation systems which do not require propellants.

Nebulisers produce clouds of liquid droplets in a gas. These droplets are solutions of the drug in aqueous solvents. To produce the cloud, a jet of compressed air is passed over the solution. This involves cumbersome equipment which is expensive and noisy. Treatment requires the patient to be stationary and takes at least five minutes per dose. The dosing technique using a nebuliser involves normal breathing through a mouthpiece or a facemask. It can therefore be used for all ages and severities of the condition, and does not rely on co-ordination to inhale and deliver a dose.

Dry powder inhalers are breath-actuated, propellant-free devices. The delivery of drug from the dose to the lungs is dependent upon the act of inspiration from the patient. It is influenced by the severity of the disease, the age of the patient, the dry powder formulation and the inhaler device.

The pressure drop at the mouthpiece, created by the act of inspiration, causes the flow of air through the device. Turbulent airflow within the device is responsible for dispersing the powder mix from a static bed to a powder cloud. Turbulent airflow within the device inherently increases the resistance to airflow through the device. For any dry powder device the magnitude of this resistance is influenced by the tortousity of the airflow path and the minimum orifice diameter. The relationship between the airflow, resistance and pressure drop is shown in equation 1.1 [13].

$$\sqrt{\Delta P_d} = R_d \times Q \qquad \text{(equation 1.1)}$$

where ΔP_d = pressure drop
R_d = specific resistance
Q = volumetric flow rate

The resistance to airflow is dependent upon the design of the device, and is therefore device specific. The specific resistance (gradient of $\sqrt{\Delta P}$ vs. Q) of several dry powder inhalers has been evaluated [13]. The results of which are shown in Table 1.1.

Device	**Resistance** ($cmH_2O^{1/2}/(L/min)$)
Rotahaler	0.040
Spinhaler	0.051
ISF inhaler	0.055
Diskhaler	0.067
Turbuhaler	0.100
Inhalator	0.180

Table 1.1 Specific resistance of six types of dry powder inhalers

The flow rate attained by a patient depends upon the air flow resistance of the device and the effort expended by the patient. The amount of work required by the patient to create the airflow is known as the inspiratory effort. This is directly proportional to the pressure drop [14]. Experimentally is has been shown that the energy input that can be achieved varies considerably between patients [15].

In vitro determination has evaluated that for a specific dry powder inhaler, increasing the flow rate (equivalent to increasing the pressure drop or the inspiratory effort) increases the percentage of the dose which would reach the respiratory zone of the lungs [16].

The results from *in vitro* and *in vivo* deposition testing indicate only a small percentage of the dose from dry powder inhalers reaches the respiratory zone of the lungs. *In vivo* results have shown that the fraction of a dose from a dry powder inhaler found in the lung is in the range of 6.2 % to 16.4 % [17].

The dose of drug from a dry powder inhaler is presented either as drug aggregates or a binary powder mix. Currently [18], Spinhaler™ and Turbohaler™ present doses as drug only formulations. The Rotahaler™, Inhalator Ingelheim™, Cyclohaler™ and Diskhaler™ all present doses as a binary powder mix, usually with α-lactose monohydrate crystals. As discussed previously the energy to create the turbulent airflow is provided by the patient. It is this airflow which causes dissociation of the particles in the dose, and creates a powder cloud containing single drug particles. This dissociation takes place in the inhaler device.

The small fraction of the dose which is delivered to the respiratory zone indicates that the whole dose of active drug does not exist in the powder cloud as single particle entities.

1.2 Scope of thesis

Numerous investigations have been carried out into the effect of the testing conditions upon the performance of dry powder inhalers, both *in vivo* and *in vitro*. These include altering the environmental conditions [19, 20], varying flow rates [19, 21, 22], investigating the effect of the inhaler design [17] and altering the formulation of the dry powder dose [23]. Fundamental research, however, into the behaviour

of drug particles within the dose and the resultant dispersion characteristics are not so prevalent. The aim of this thesis was to investigate particle-particle interactions which take place within binary powder mixes which are used for inhalation therapy, and relate these to the delivery characteristics of the dose.

Within a powder mix for inhalation therapy cohesive interactions occur between like particles (drug-drug), whilst adhesive interactions occur between dissimilar particles (drug-carrier). These interactions are responsible for the structure of the powder mix. In order to deliver drug particles into the pulmonary system during the delivery of the dose, the structure of the mix must disintegrate to produce isolated, airborne particles of drug.

This investigation examined the degree of adhesive and cohesive interactions within powder mixes. The structure of the mix was related to the delivery characteristics, using *in vitro* inhalation test apparatus. Methodologies were developed with the aim of determining the magnitude of these inter-particle interactions. Such an understanding of the relationship between the interactions within the powder blend and the drug delivery from the blend would allow manipulation of the dose to achieve a more efficacious drug delivery system.

Chapter Two

Materials characterisation

2.1 Aim

The aim of this chapter was to characterise the materials used throughout this work. This was done using a variety of analytical technologies in order to establish physical properties which may relate to the behaviour of the powders under investigation.

2.2 Materials

2.2.1 Nedocromil sodium

Nedocromil sodium powder was used throughout this work. Five batches of the drug were characterised in order to establish any interbatch physical variation.

Nedocromil sodium is a pharmacologically active drug used in inhalation therapy. It is a non-steroid agent which has anti-inflammatory properties when administered topically to the lung. *In vivo*, *ex vivo* and *in vitro* studies have shown that nedocromil sodium has beneficial effects on cellular, humoral and neuronal mechanisms thought to be involved in the inflammation of bronchial asthma [24].

Nedocromil sodium is a yellow crystalline odourless powder which can exist as a number of hydrates. The trihydrate form is thermodynamically stable in ambient atmospheres, between 6.4 % and 79.5 % relative humidity at 22 °C [25]. The nedocromil sodium molecule has the chemical structure shown below. It has an anhydrous molecular weight of 415.3 Da.

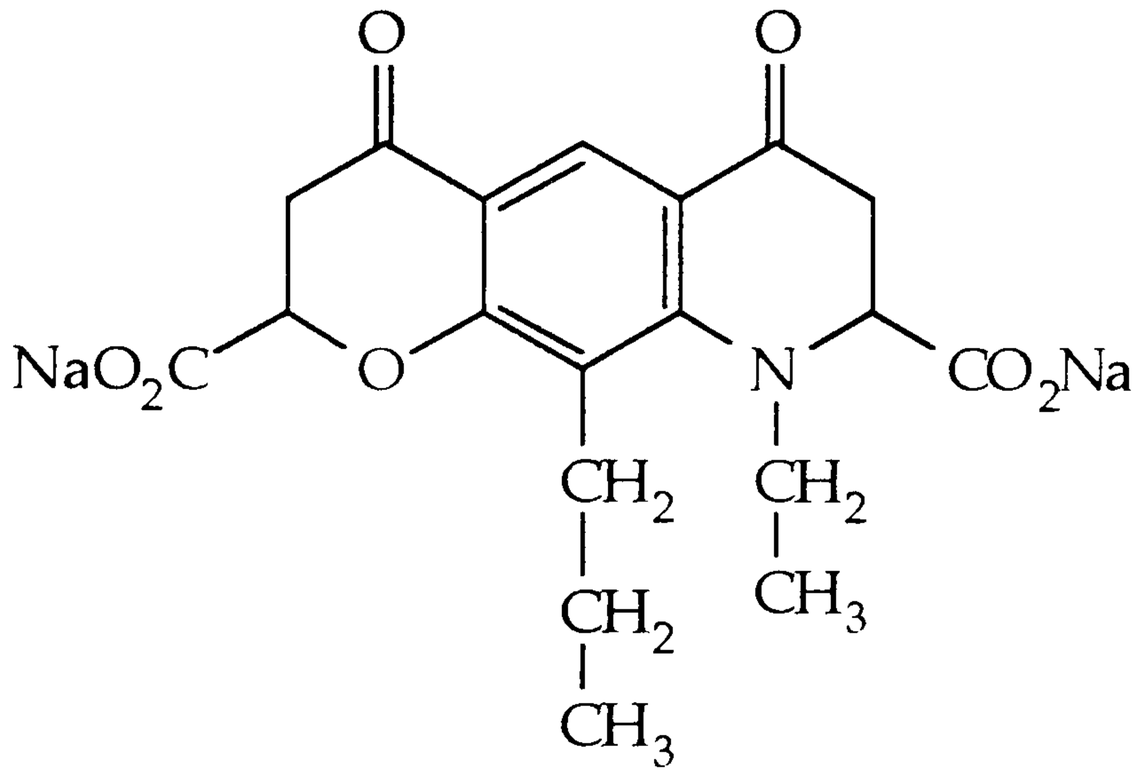

Figure 2.2.1 Chemical structure of nedocromil sodium

The following batches of nedocromil sodium were used in this work:

Batch number	Preparation	Supplier
Z403V	Apex Milled	Fisons, Holmes Chapel.
ZBB9A	Apex Milled	Fisons, Holmes Chapel.
3B1	Apex Milled	Fisons, Holmes Chapel.
4B1	Apex Milled	Fisons, Holmes Chapel.
5B1	Apex Milled	Fisons, Holmes Chapel.
2001B1	Apex Milled	Fisons, Holmes Chapel.
2002B1	Apex Milled	Fisons, Holmes Chapel.

Table 2.2.1 Nedocromil sodium batch information

2.2.2 Sodium cromoglycate

Sodium cromoglycate powder was used in the investigation of binary powder mixes and their performance in the multi-stage liquid impinger.

Sodium cromoglycate is a pharmacologically active drug which is used in inhalation therapy. Its action inhibits the release from sensitised mast cells of mediators of the allergic reaction. In the lungs this inhibition of mediator release prevents both the immediate and the late asthmatic response to immunological stimuli. Sodium cromoglycate also prevents the bronchoconstriction caused by exercise, cold air and chemical irritants [24].

Sodium cromoglycate is a white crystalline odourless powder. It is soluble in water up to approximately 5 %w/v. The sodium cromoglycate molecule has the chemical structure shown below. It has an anhydrous molecular weight of 512.3 Da.

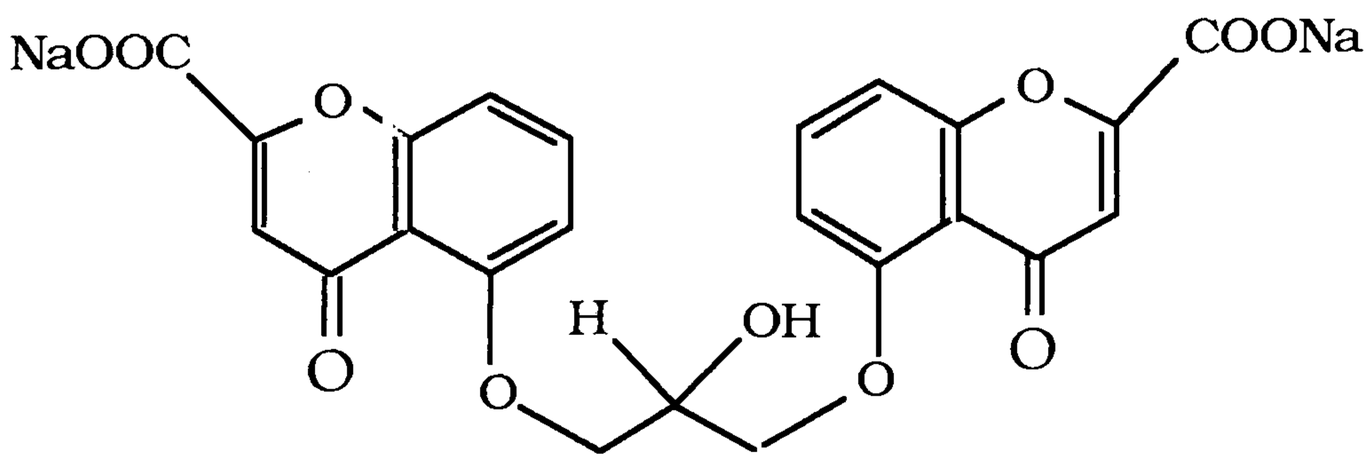

Figure 2.2.2 Chemical structure of sodium cromoglycate

The following batch of sodium cromoglycate was used in this work:

Batch Number	Preparation	Supplier
XC13 CIA M150	Apex Milled	Fisons, Holmes Chapel.

Table 2.2.2 Sodium cromoglycate batch information

2.2.3 Lactose

Samples of lactose were used throughout this work. Lactose is a white crystalline odourless powder and is pharmacologically inert [26]. Lactose can exist in several different crystal forms, depending upon the method of its preparation. The crystal form used for this work was α-lactose monohydrate. The chemical structure for the molecule is shown below. It has an anhydrous molecular weight of 342.3 Da.

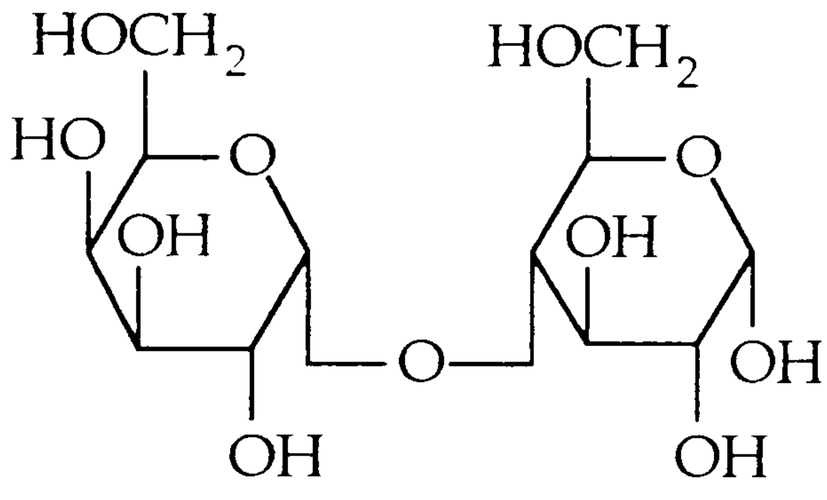

Figure 2.2.3 chemical structure of α-lactose monohydrate

The following batches of α-lactose monohydrate were used in this work:

Batch Number	Grade	Supplier
022303	150 Mesh Mean diameter 50 μm 100%< 315 μm.	DMV
3217C	325 Mesh Mean diameter 50 μm 100%< 100 μm.	Fisons, Loughborough.

Table 2.2.3 Lactose batch information

2.2.4 Reproterol

Reproterol powder was used in the investigation of binary powder mixes and their performance in the multi-stage liquid impinger. Reproterol is a pharmacologically active drug used in inhalation therapy. The following batch of reproterol was used for this work.

Batch Number	Preparation	Supplier
092125	Apex milled	Asta Medica AG

Table 2.2.4 Reproterol batch information

2.2.5 Budesonide

A sample of budesonide powder was used in the particle sizing analysis as a contrast to samples prepared by milling techniques. Budesonide is a pharmacologically active drug which is used in inhalation therapy. The following batch of budesonide was used for this work.

Batch Number	Preparation	Supplier
3189/M1M101	Spray dried	Astra, Sweden.

Table 2.2.5 Budesonide batch information

2.2.6 Starch 1500

A sample of Starch 1500 (pregelatinised maize starch) was used in the investigation of particle cohesion. The batch used for this work was:

Batch Number	Supplier
1500 DM 486	Thornton & Ross

Table 2.2.6 Starch 1500 batch information

2.2.7 Kaolin

A sample of Light Kaolin B.P was used in the investigation of particle cohesion. The batch used for this work was

Batch Number	Supplier
18CL	Thornton & Ross

Table 2.2.7 Light Kaolin batch information

2.3 Scanning electron microscopy

Scanning electron microscopy is a visual technique which, following production of a photomicrograph, can be used to observe particle shape, surface characteristics and to quantify particle size. A fine beam of electrons of medium energy scan across a gold coated sample in a series of parallel tracks. The electrons interact with the gold coat producing secondary electron emission, back scattered electrons, light or cathodoluminescence and X-rays [27]. Each of these signals can be detected and displayed on a cathode ray tube. These images are captured on a photomicrograph.

2.3.1 Materials

Scanning electron microscopy was carried out on the following samples:

Sample	Batch Number	Figure number
nedocromil sodium	3B1	2.3.1
nedocromil sodium	4B1	2.3.2
nedocromil sodium	5B1	2.3.3
nedocromil sodium	2001B1	2.3.4
nedocromil sodium	2002B1	2.3.5
nedocromil sodium	5B1	2.3.6
sodium cromoglycate	XC13CIAM150	2.3.7
reproterol	092125	2.3.8
lactose	022303	2.3.9
starch 1500	1500DM 486	2.3.10
light kaolin	18CL	2.3.11

Table 2.3.1 Scanning electron micrograph summary

2.3.2 Apparatus

Photomicrographs of the samples were produced using a Jeol JSM35 scanning electron microscope and an International Scientific Instruments DS130 scanning electron microscope. Gold coating of the samples was carried out using Blazer apparatus and Polaron co-stage sputter coater apparatus respectively.

2.3.3 Method

Samples were taken from stock bottles and dropped from a spatula onto a prepared adhesive disc. The disc was gently tapped to remove any particles not held by the adhesive. Sample preparation involved coating the particles with a thin layer of gold, under vacuum conditions. A total time of 5 minutes sputtering was sufficient to coat the particles with a layer of approximately 30 nm depth.

2.3.4 Results

2.3.4 a Nedocromil sodium

Examples of the scanning electron micrographs taken of the samples of nedocromil sodium are reproduced in Figures 2.3.1 to 2.3.5. The crystal habit of the powder particles from all five samples is columnar. Each photomicrograph shows examples of particles in the size range between 0.5 μm to 3 μm. The surface of the larger particles exhibit deep pores and cracks. It is possible that these surface

irregularities are an artefact of the sample preparation procedure, or caused by the incident beam of electrons. There is some suggestion from the photomicrographs that particles much larger than 3 μm are present in the bulk powders. These can been seen in Figures 2.3.2 and 2.3.5. The sample of batch 5B1 taken for scanning electron microscopy, Figure 2.3.3, contains a higher proportion of particles towards the smaller end of the size range.

Figure 2.3.1 Scanning electron micrograph of nedocromil sodium particles batch 3B1. Picture no. 0664.

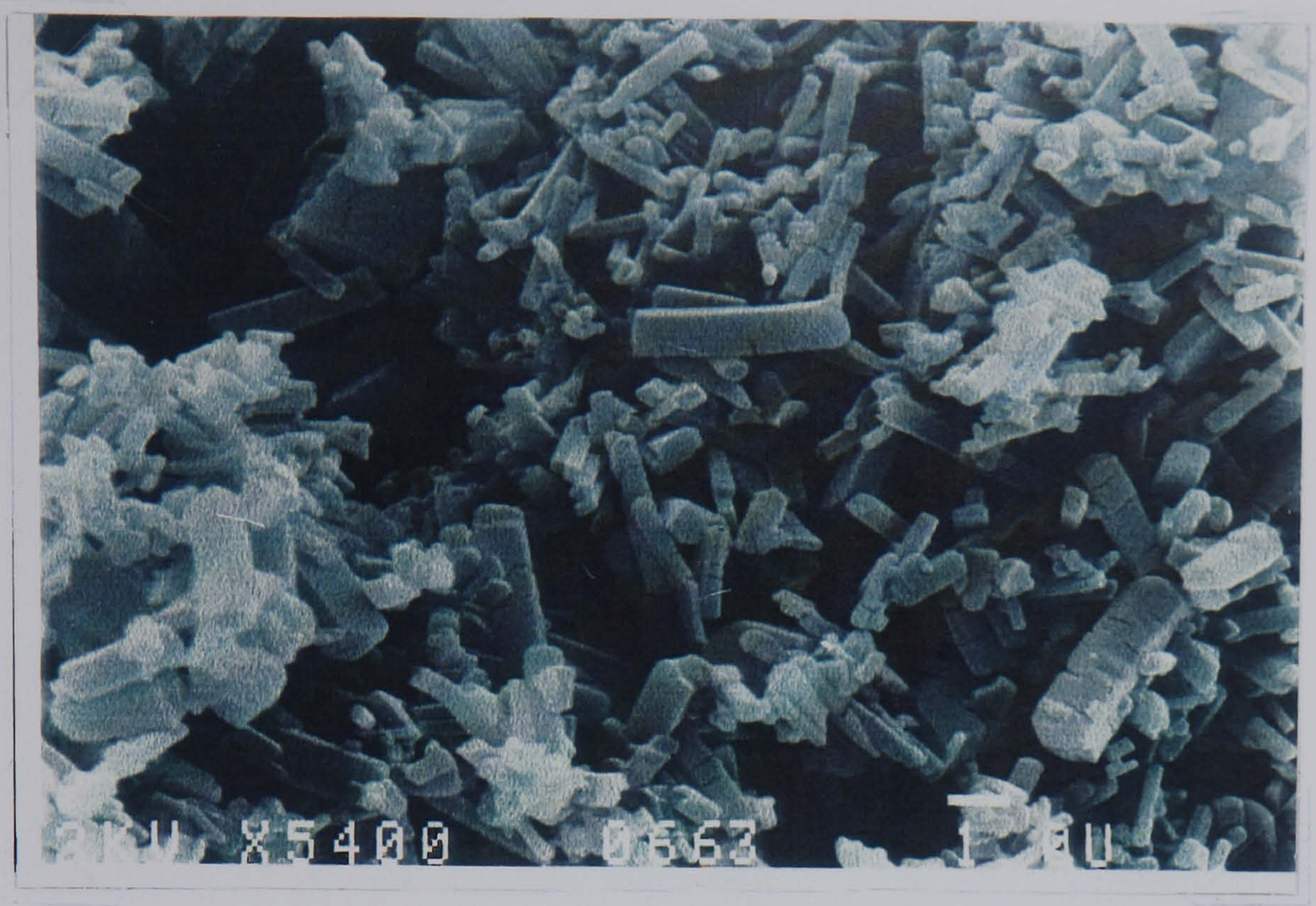

Figure 2.3.2 Scanning electron micrograph of nedocromil sodium particles batch 4B1. Picture number 0663.

Figure 2.3.3 Scanning electron micrograph of nedocromil sodium particles batch 5B1. Picture number 0665.

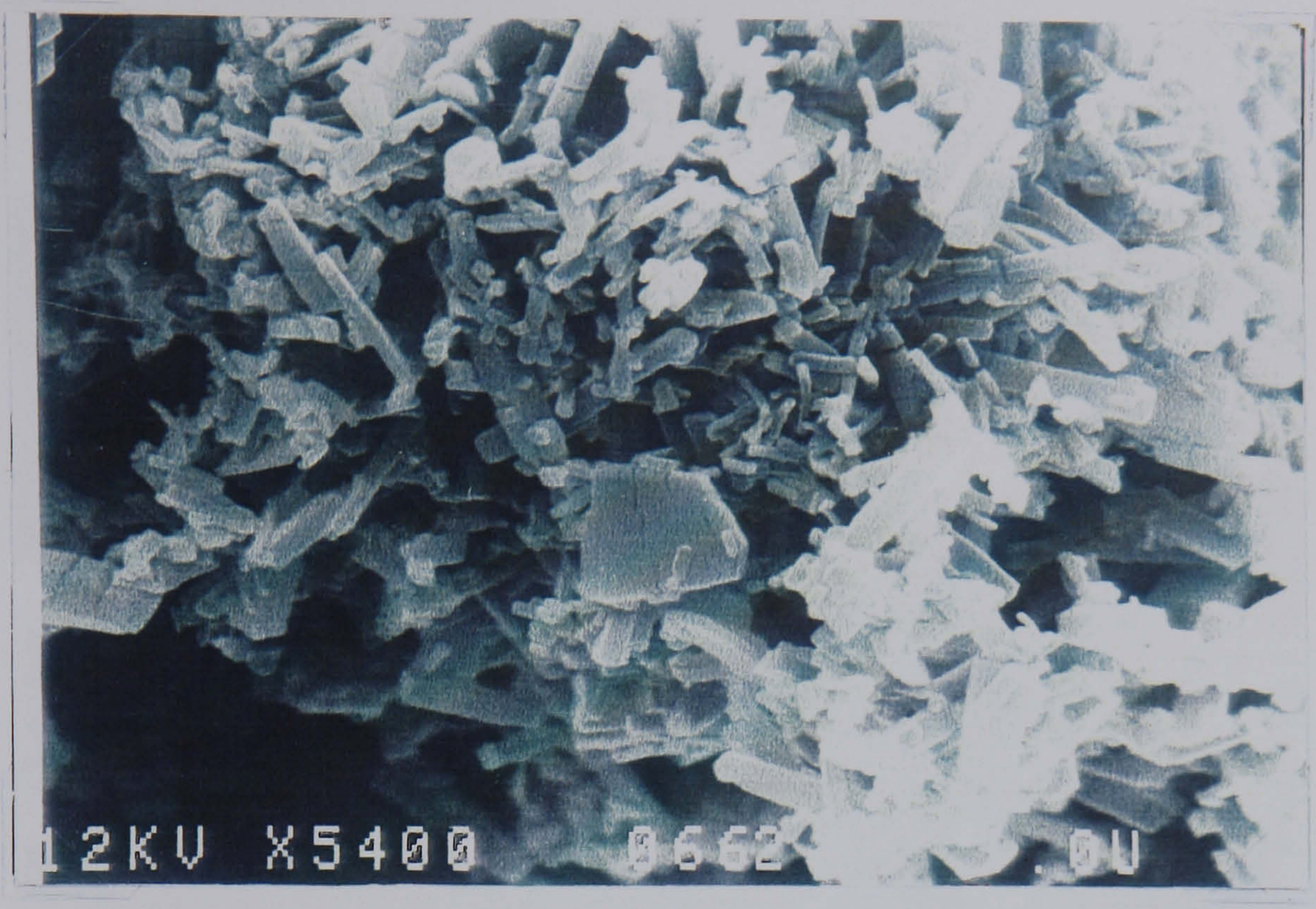

Figure 2.3.4 Scanning electron micrograph of nedocromil sodium particles batch 2001B1. Picture number 0662.

Figure 2.3.5 Scanning electron micrograph of nedocromil sodium particles batch 2002B1. Picture number 0661.

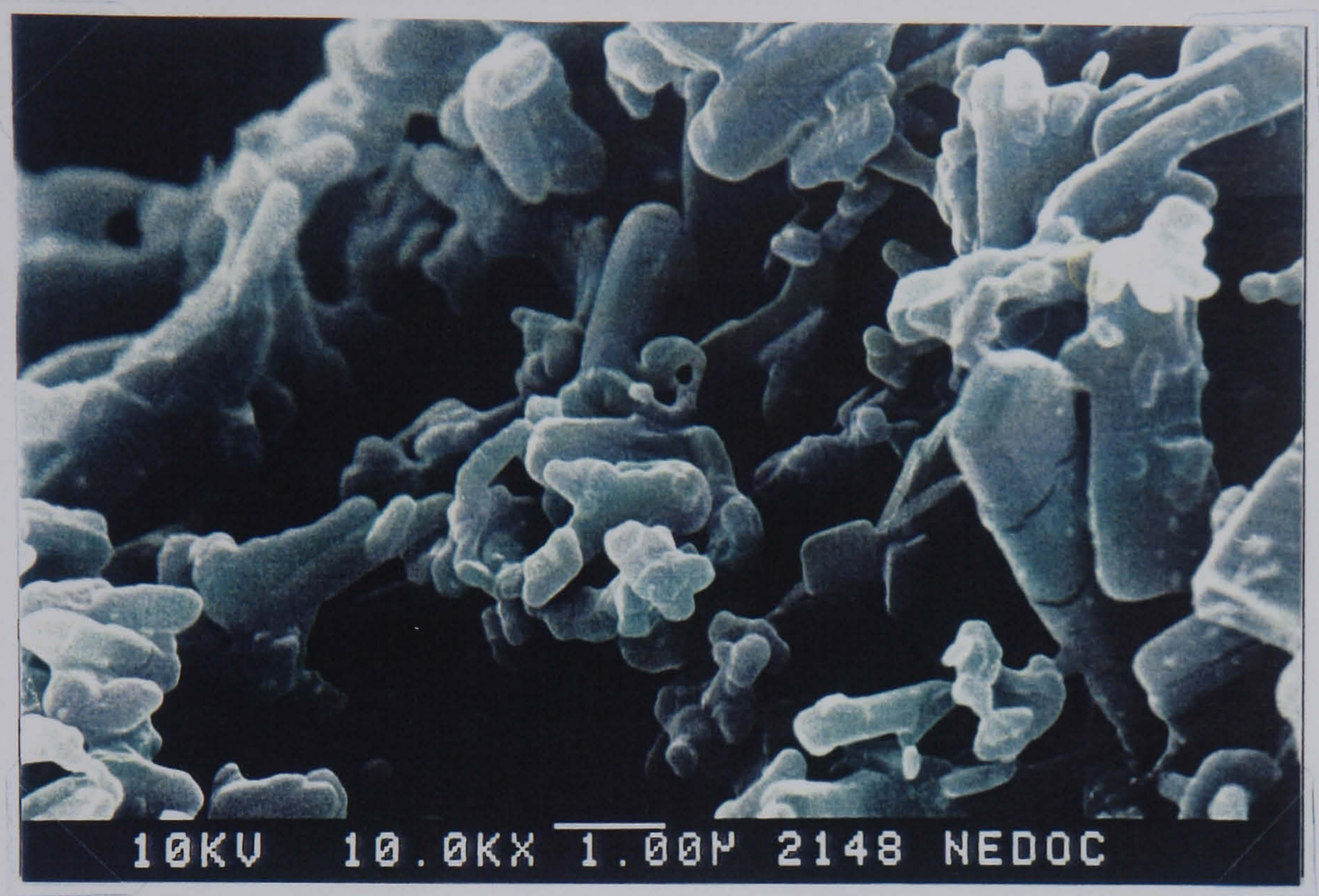

Figure 2.3.6 Scanning electron micrograph of nedocromil sodium particles batch 5B1. Picture number 2148.

2.3.4.b Sodium cromoglycate

The sample of sodium cromoglycate investigated using scanning electron microscopy shows the particles have a columnar structure. The size distribution of these particles appears similar to that of nedocromil sodium when comparing Figures 2.3.6. and 2.3.7.

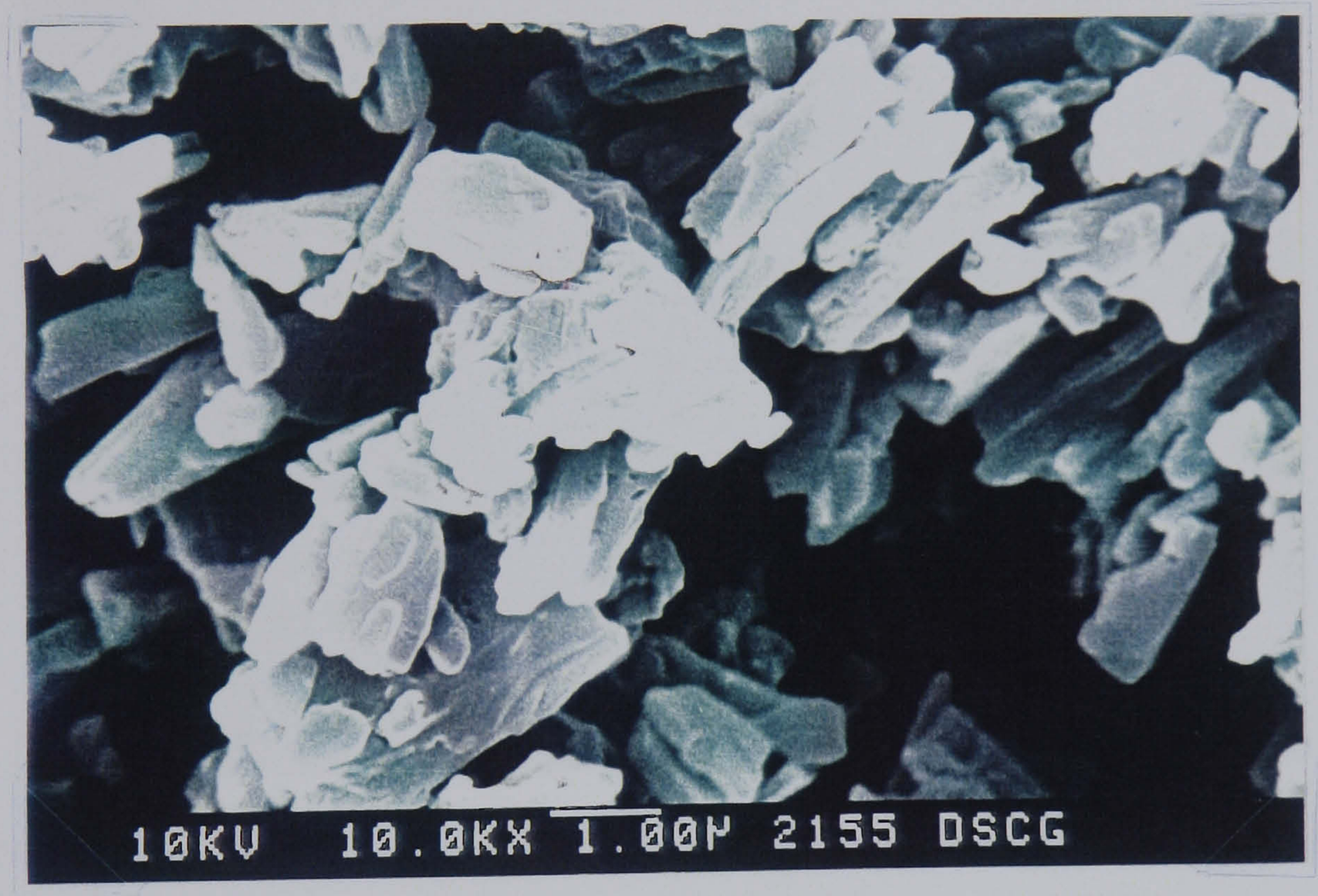

Figure 2.3.7 Scanning electron micrograph of sodium cromoglycate particles batch. Picture number 2155.

2.3.4.c Reproterol

A photomicrograph of a sample of reproterol is reproduced in Figure 2.3.8. The sample contains particles up to 3 μm in length. The smaller particles appear isodiametric with a diameter of about 0.25 μm.

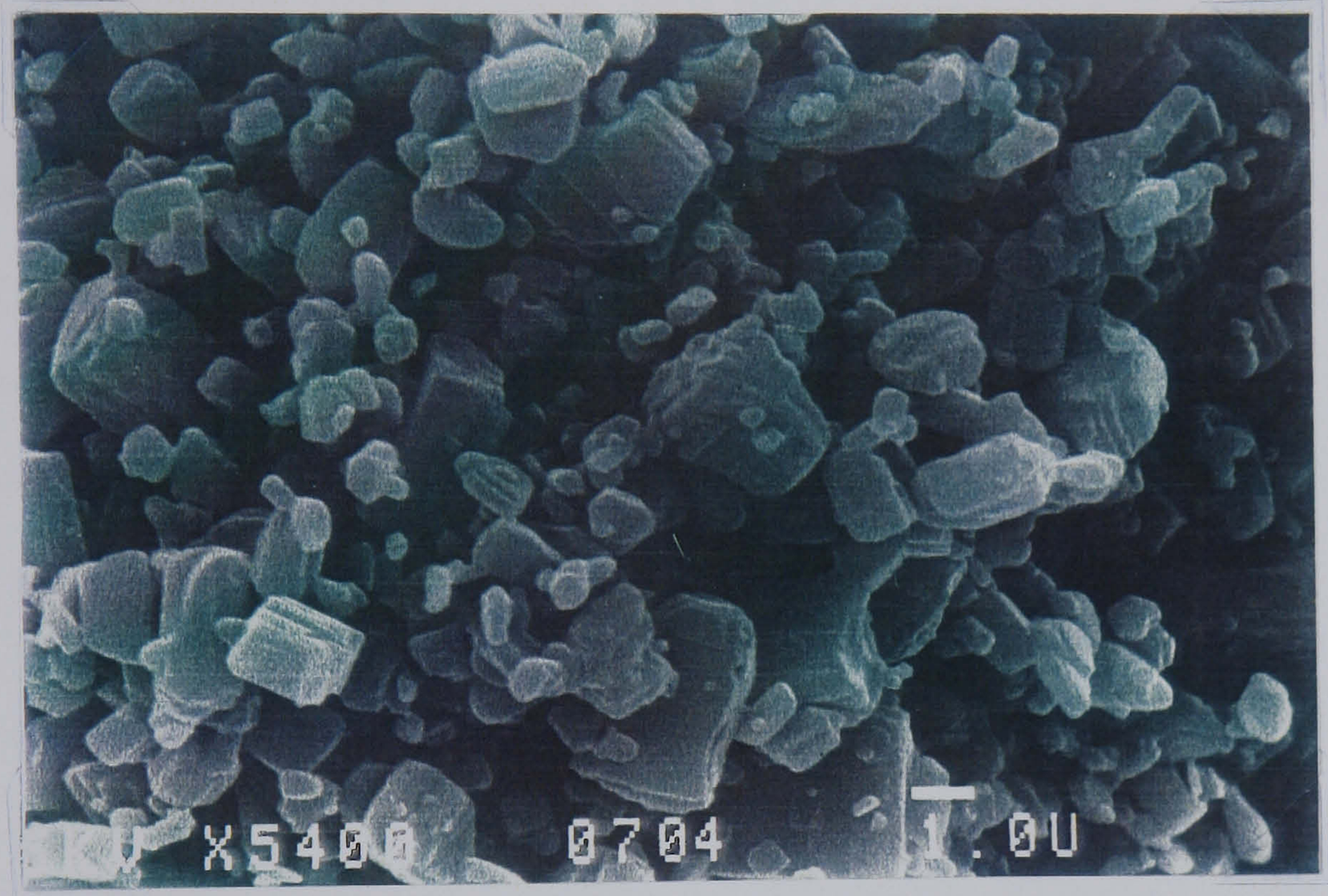

Figure 2.32.8 Scanning electron micrograph of reproterol particles. Picture number 0704.

2.3.4.d α-Lactose monohydrate

A photomicrograph of a sample of lactose is reproduced in Figure 2.3.9. The sample of lactose taken for scanning electron microscopy analysis shows the typical 'tomahawk'-shaped particles. These are in the size range 63 μm to 90 μm. Sieving was used to size classify the particles, indicating that at least two dimensions of the particles are below 90 μm. Some particles present in the sample show a third dimension greater than 90 μm. Very fine lactose particles can be seen adhering to the surface of larger particles. These surface-cohered fines are created during the screening procedure which is performed during the preparation of this grade of lactose.

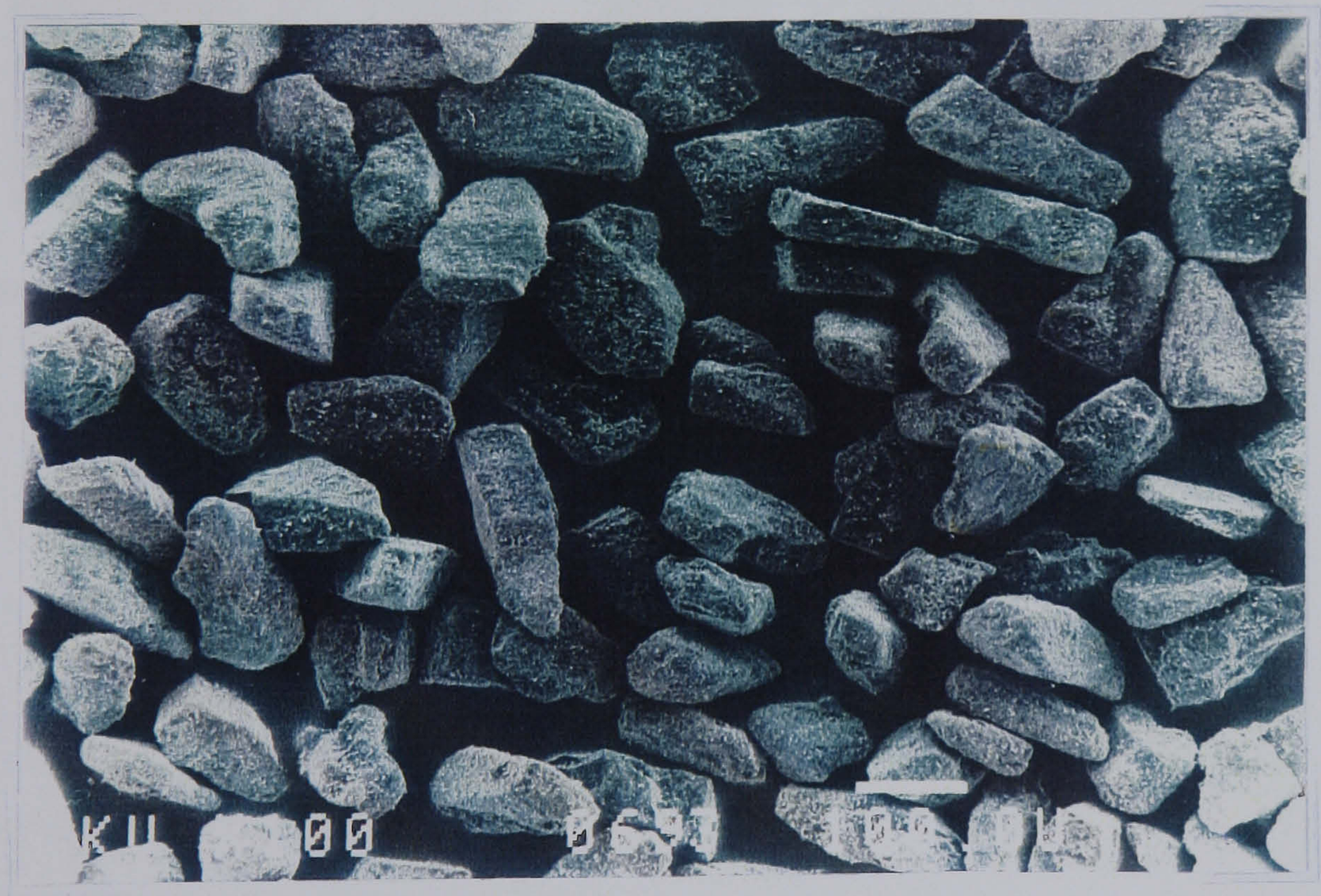

Figure 2.3.9 Scanning electron micrograph of lactose particles. Picture number 0693.

2.3.4.e Kaolin

A photomicrograph of a sample of kaolin is reproduced in Figure 2.3.10. The sample of kaolin shows flaky particles. These range in size from approximately 0.5 μm to 1 μm diameter.

Figure 2.3.10 Scanning electron micrograph of kaolin particles.
Picture number 2144

2.3.4.f Starch 1500

A photomicrograph of a sample of the modified starch is reproduced in Figure 2.3.11. These irregularly shaped particles range from approximately 6.5 μm to 53 μm diameter.

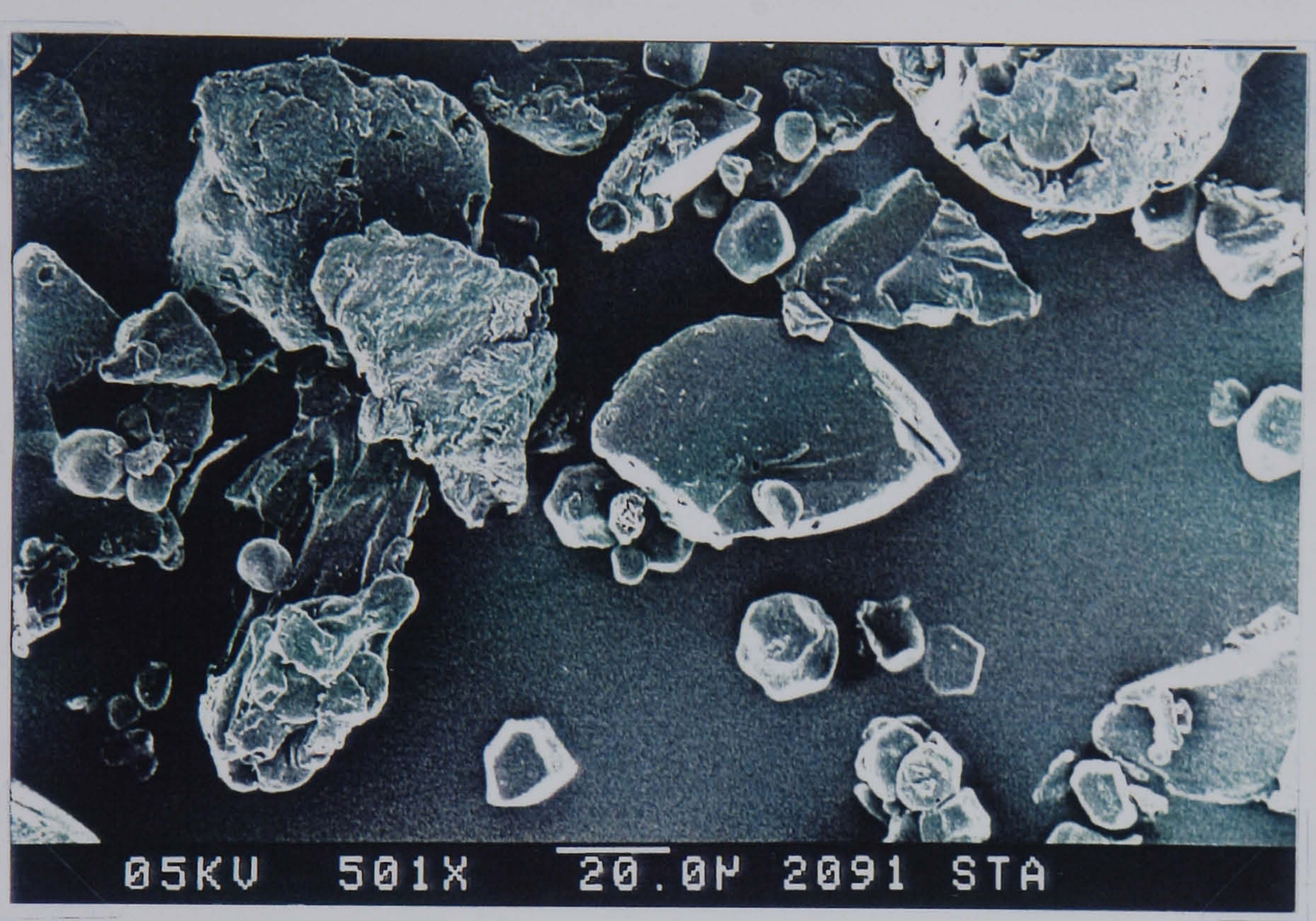

Figure 2.3.11 Scanning electron micrograph of starch particles.
Picture number 2091

2.3.5 Concluding comments

All of the nedocromil sodium batches exhibit particles of a very similar size and shape. Therefore differences in behaviour ~~is~~ are not due to differences in these parameters.

The size and morphology of particles of sodium cromoglycate are very similar to the particles of nedocromil sodium. Both drug samples were prepared by recrystallisation followed by milling.

2.4 Laser diffraction

The laser diffraction size analysis technique is based on the calculation of particle size by analysis of diffraction patterns formed by low angle laser light scattering. A sample cell containing powder dispersed in a liquid in which it is not soluble, is held in the path of a laser beam. A diffraction pattern is formed when a powder particle is illuminated by the parallel beam of monochromatic coherent light. Size analysis can be carried out as the angle of diffraction is dependent upon the particle size. Small particles diffract the beam through greater angles than large particles. The detector of the diffracted light is split into a series of concentric rings, each one corresponding to the diffraction angles for a range of particle sizes. The intensity of light reaching each detector is proportional to the number of particles in a particular size range.

2.4.1 Materials

Laser diffraction size analysis was carried out on the following samples.

Sample	Batch Number
Nedocromil sodium	5B1
Sodium cromoglycate	XC13CIAM150
Reproterol	092125
Budesonide	3189/M1 M101

Table 2.4.1 Laser diffraction sample summary

2.4.2 Apparatus

A coulter LS 130 apparatus was used for the determination of the particle size distribution of the samples. This apparatus is capable of calculating size distributions within the range 0.1 μm to 800 μm by measuring the diffraction angle and then applying Fraunhofer theory.

2.4.3 Method

A filtered saturated solution of each drug in analytical grade butanone containing 4.0 %w/v magnesium perchlorate was prepared as the suspending medium for nedocromil sodium, sodium cromoglycate and reproterol. Budesonide was suspended in a filtered saturated solution of the drug in HPLC grade water. This suspending medium was filtered through Whatman glass microfibre filters, type GF/B, pore size 1 μm.

A small amount of the powder sample was added to about 20 mL of the suspending solution and subjected to sonication in an ultrasonic bath for 3 minutes. A few drops of this suspension were then added to the micro-volume diffraction cell which contained filtered suspending solution. Freshly filtered suspending solution was used as the blank. The procedure was carried out a total of three times for each drug type.

2.4.4 Results

The frequency and cumulative size distributions of the samples are reproduced in Figures 2.4.1 to 2.4.4.

COULTER^R LS Particle Size Analysis 1.51.19 11:39 24 Mar 1993

nedoc.$01

File name:	NEDOC.$01	Group ID:	nedoc
Sample ID:	nedocromil	Run number:	2
Operator:			
Comments:			
Start time:	11:32 24 Mar 1993	Run length:	30 Seconds
Obscuration:	19%		
Optical model:	Fraunhofer		
Fluid:	2-Butanone		
LS 130	Micro-volume module		
Software:	1.51.19	Firmware:	1.3 1.8

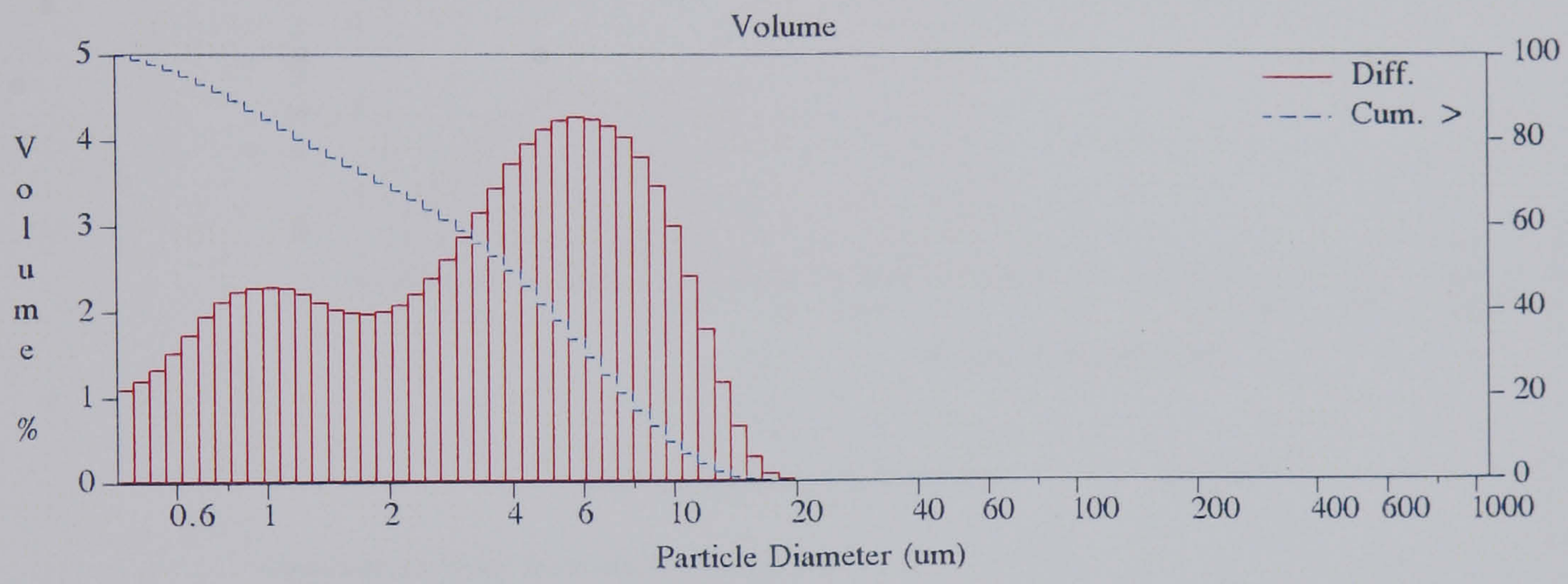

Volume Statistics (Arithmetic) nedoc.$01

Calculations from 0.43 um to 900.00 um

Volume	100.0%		
Mean:	4.434 um	95% Conf. Limits:	3.776-5.092 um
Median:	3.749 um	Std. Dev.:	3.357 um
D(3,2):	2.017 um	Variance:	11.27 um^2
Mean/Median Ratio:	1.183	Coef. Var.:	75.72%
Mode:	5.750 um	Skewness:	0.869 Right skewed
Specific Surf. Area	29745 cm^2/ml	Kurtosis:	0.150 Leptokurtic

% >	10	25	50	75	90
Size um	9.332	6.564	3.749	1.461	0.784

Figure 2.4.1 Particle size distribution for nedocromil sodium batch 5B1 using laser diffraction analysis

COULTER^R LS Particle Size Analysis 1.51.19 12:52 24 Mar 1993

dscg.$01

File name:	dscg.$01	Group ID:	dscg
Sample ID:		Run number:	7
Operator:			
Comments:			
Start time:	12:26 24 Mar 1993	Run length:	30 Seconds
Obscuration:	14%		
Optical model:	Fraunhofer		
Fluid:	2-Butanone		
LS 130	Micro-volume module		
Software:	1.51.19	Firmware:	1.3 1.8

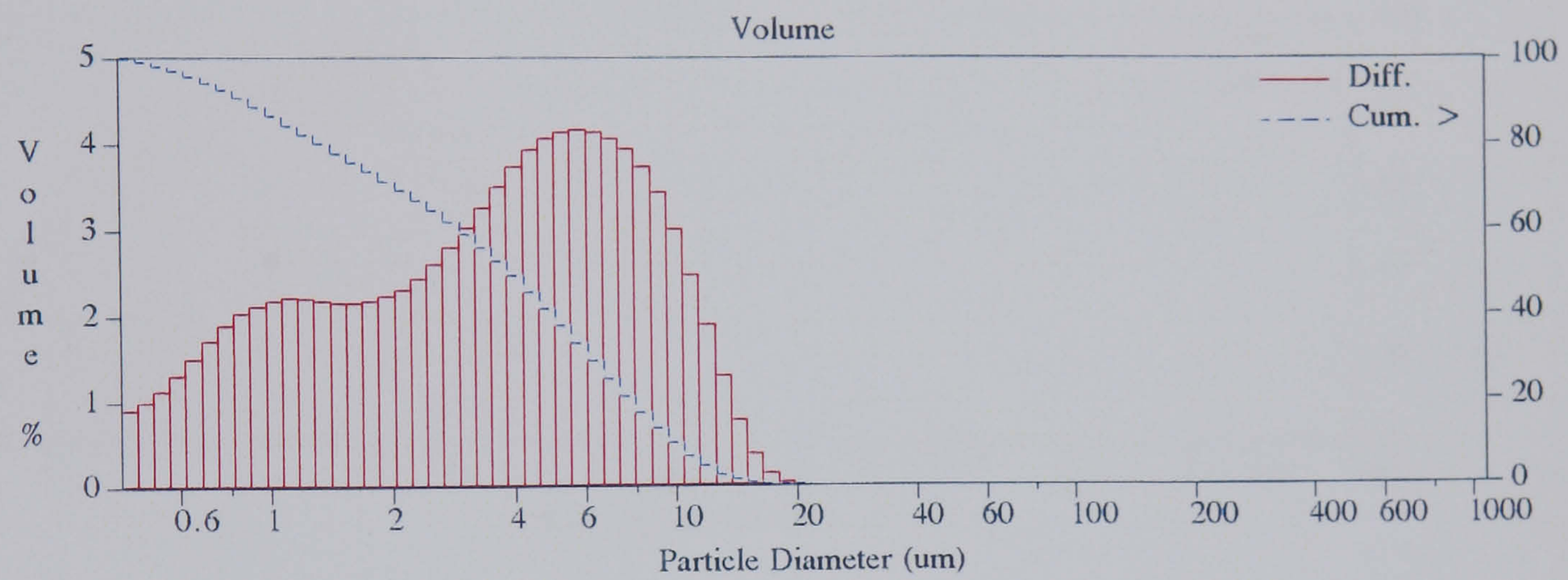

Volume Statistics (Arithmetic) dscg.$01

Calculations from 0.43 um to 900.00 um

Volume	100.0%		
Mean:	4.506 um	95% Conf. Limits:	3.838-5.174 um
Median:	3.745 um	Std. Dev.:	3.406 um
D(3,2):	2.108 um	Variance:	11.60 um^2
Mean/Median Ratio:	1.203	Coef. Var.:	75.59%
Mode:	5.750 um	Skewness:	0.927 Right skewed
Specific Surf. Area	28470 cm^2/ml	Kurtosis:	0.306 Leptokurtic

% >	10	25	50	75	90
Size um	9.477	6.610	3.745	1.580	0.837

Figure 2.4.2 Particle size distribution for sodium cromoglycate using laser diffraction analysis

COULTER^R LS Particle Size Analysis 1.51.19 13:05 24 Mar 1993

repro.$01

File name:	REPRO.$01	Group ID:	repro
Sample ID:		Run number:	10
Operator:			
Comments:			
Start time:	13:03 24 Mar 1993	Run length:	30 Seconds
Obscuration:	11%		
Optical model:	Fraunhofer		
Fluid:	2-Butanone		
LS 130	Micro-volume module		
Software:	1.51.19	Firmware:	1.3 1.8

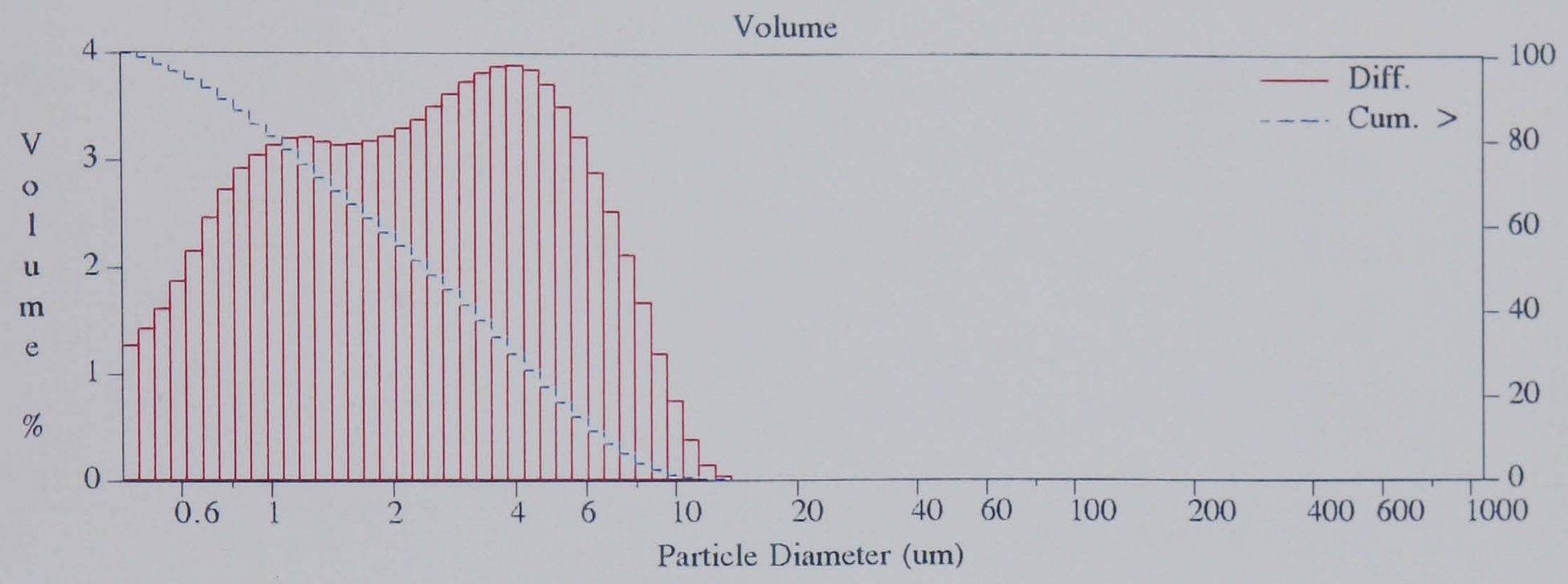

Volume Statistics (Arithmetic) repro.$01

Calculations from 0.43 um to 900.00 um

Volume	100.0%		
Mean:	2.991 um	95% Conf. Limits:	2.545-3.437 um
Median:	2.323 um	Std. Dev.:	2.275 um
D(3,2):	1.613 um	Variance:	5.173 um^2
Mean/Median Ratio:	1.288	Coef. Var.:	76.05%
Mode:	3.995 um	Skewness:	1.136 Right skewed
Specific Surf. Area	37195 cm^2/ml	Kurtosis:	0.829 Leptokurtic

% >	10	25	50	75	90
Size um	6.353	4.282	2.323	1.142	0.721

Figure 2.4.3 Particle size distribution for reproterol using laser diffraction analysis

COULTER^R LS Particle Size Analysis 1.51.19 14:02 24 Mar 1993

budes.$01

File name:	budes.$01	Group ID:	budes
Sample ID:	budesonide	Run number:	15
Operator:			
Comments:			
Start time:	13:56 24 Mar 1993	Run length:	30 Seconds
Obscuration:	13%		
Optical model:	Fraunhofer		
Fluid:	Water		
LS 130	Micro-volume module		
Software:	1.51.19	Firmware:	1.3 1.8

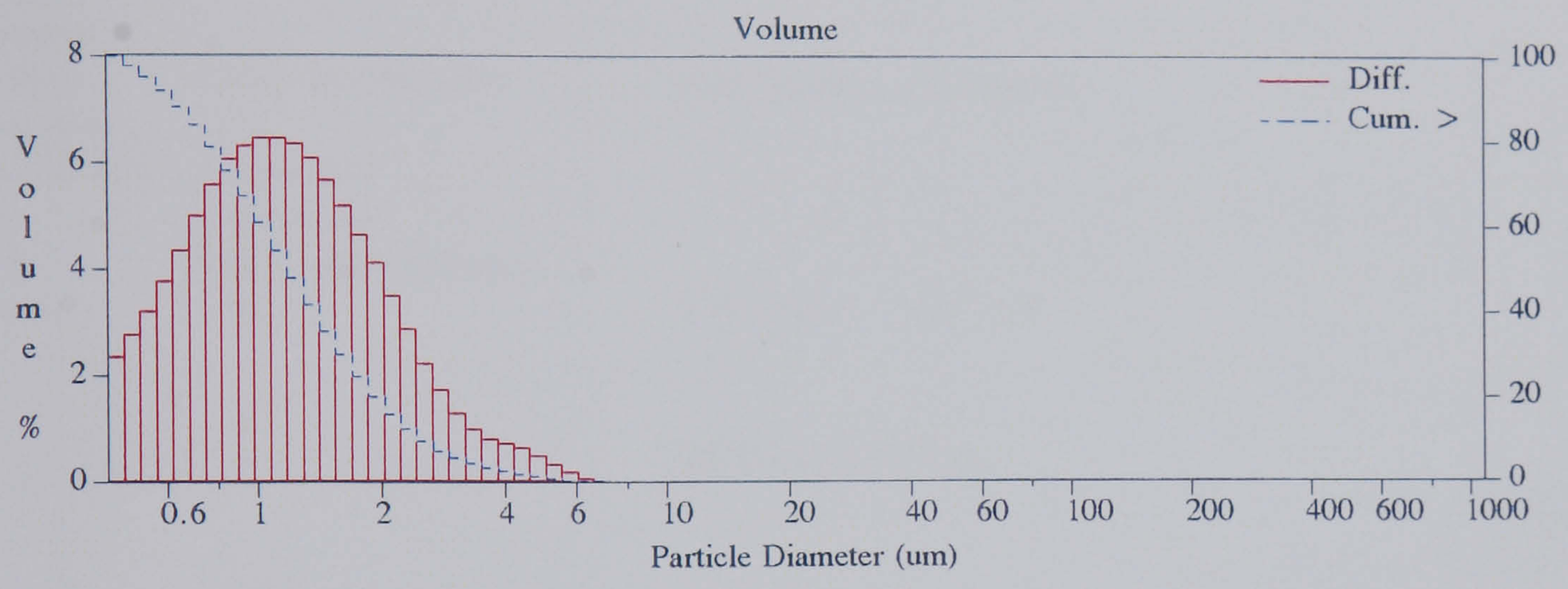

Volume Statistics (Arithmetic) budes.$01

Calculations from 0.43 um to 900.00 um

Volume	100.0%		
Mean:	1.361 um	95% Conf. Limits:	1.197-1.526 um
Median:	1.134 um	Std. Dev.:	0.841 um
D(3,2):	1.026 um	Variance:	0.706 um^2
Mean/Median Ratio:	1.201	Coef. Var.:	61.74%
Mode:	1.116 um	Skewness:	1.987 Right skewed
Specific Surf. Area	58488 cm^2/ml	Kurtosis:	5.322 Leptokurtic

% >	10	25	50	75	90
Size um	2.380	1.669	1.134	0.787	0.588

Figure 2.4.4 Particle size distribution for budesonide using laser diffraction analysis

COULTER^{R} LS Particle Size Analysis 1.51.19 14:10 24 Mar 1993

budes.$01, dscg.$01, nedoc.$01, repro.$01

File name:	repro.$01	Group ID:	repro
Sample ID:		Run number:	10
Operator:			
Comments:			
Start time:	13:03 24 Mar 1993	Run length:	30 Seconds
Obscuration:	11%		
Optical model:	Fraunhofer		
Fluid:	2-Butanone		
LS 130	Micro-volume module		
Software:	1.51.19	Firmware:	1.3 1.8

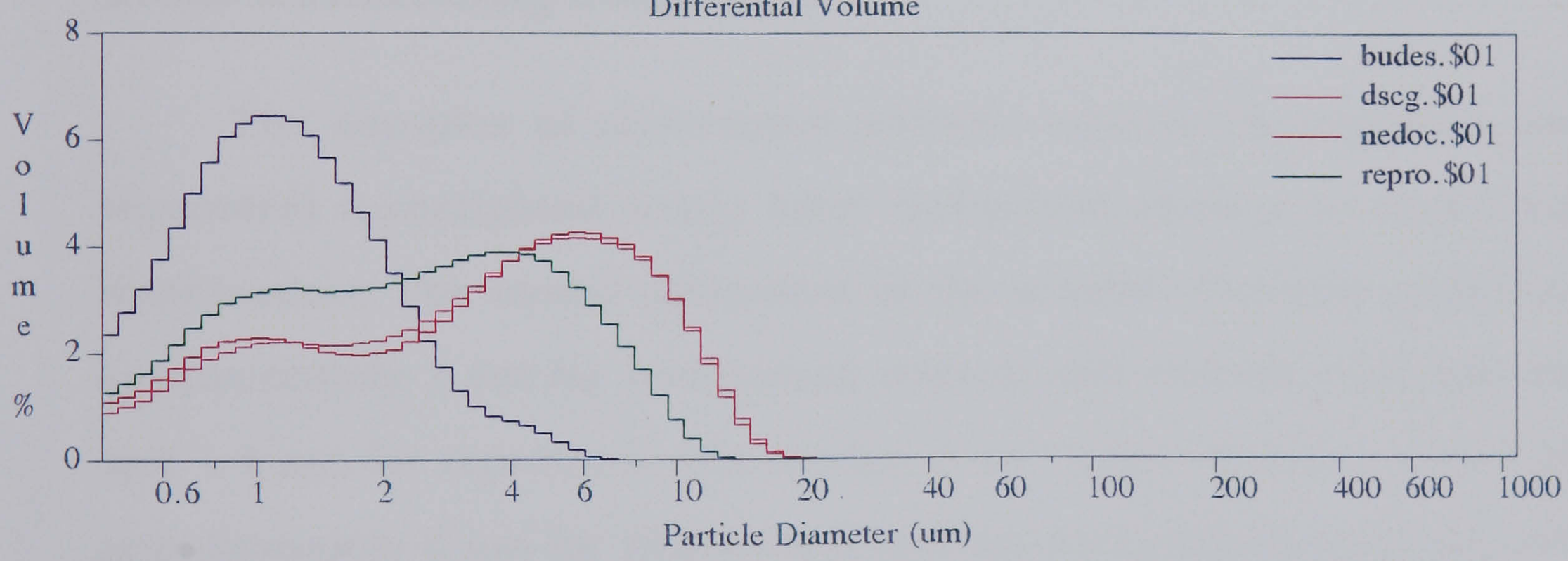

Figure 2.4.5 Summary of particle size distributions for nedocromil sodium, sodium cromoglycate, reproterol and budesonide

A summary of the derived equivalent particle sizes are shown in Table 2.4.2.

Sample	Median volume diameter (μm)	Arithmetic mean volume diameter (μm)	Standard deviation (μm)
Nedocromil sodium	3.75	4.43	3.36
Sodium cromoglycate	3.75	4.51	3.41
Reproterol	2.32	2.99	2.28
Budesonide	1.13	1.36	0.84

Table 2.4.2 Derived mean particle sizes using laser diffraction particle size analysis

2.4.5 Concluding comments

The samples of nedocromil sodium, sodium cromoglycate and reproterol investigated using laser diffraction show a bi-modal size distribution. The modal diameters of the smaller diameter peaks are approximately 1 μm for nedocromil sodium and sodium cromoglycate, and 1.4 μm for reproterol. The modes of the larger diameter peaks are approximately 6 μm for nedocromil sodium and sodium cromoglycate, and 4.5 μm for reproterol. The sample of budesonide exhibits a single peak at approximately 1.2 μm.

The reasons for this type of distribution are discussed in section 2.6.

2.5 Electrical stream sensing zone method

The electrical stream sensing zone (ESZ or Coulter counter) technique is a method which determines the number and size of particles suspended in an electrolyte. The particles pass through a small orifice, on either side of which is immersed an electrode. The flow of electrical current between the electrodes submerged in the solution is measured by the electrical resistance across the aperture. When a particle passes through the orifice an amount of solution equal to the particle volume is displaced. This results in a change of electrical impedance, the amplitude of which is proportional to the volume of particles, and the number of which is equal to the number of particles. The parameter calculated is the diameter of a sphere causing an equivalent change in electrical resistance.

2.5.1 Materials

ESZ analysis was carried out using the following samples.

Sample	Batch Number
Nedocromil sodium	5B1
Sodium cromoglycate	XC13CIAM150
Reproterol	092125
Budesonide	3189/M1 M101

Table 2.5.1 ESZ analysis sample summary

2.5.2 Apparatus

A Coulter Counter Multisizer was used for the determination of the particle size of the samples. A 30 μm orifice tube was used which enabled accurate particle size determinations between 0.6 μm and 18 μm diameter.

2.5.3 Method

A filtered saturated solution of each drug in analytical grade butanone containing 4.0 % magnesium perchlorate was prepared as the suspending medium for nedocromil sodium, sodium cromoglycate and reproterol. The magnesium perchlorate is the electrolyte which conducts electricity in the solution. Budesonide was suspended in a filtered saturated solution of the drug in a sodium chloride solution. The suspending medium was filtered using a 0.05 μm pore size filter. This solution was also used to prime the Coulter Counter. A small amount (approximately 1 mg) of the powder sample was added to about 20 mL of this solution and subjected to sonication for 3 minutes. A few drops of the resulting suspension were added to a beaker containing 100 mL of the electrolyte solution into which the orifice tube and electrodes were submerged.

2.5.4 Results

The frequency and cumulative size distributions of the samples are reproduced in Figures 2.5.1 to 2.5.4.

TEXT BOUND INTO

THE SPINE

quired at: 17:00 Wed Mar 24 1993

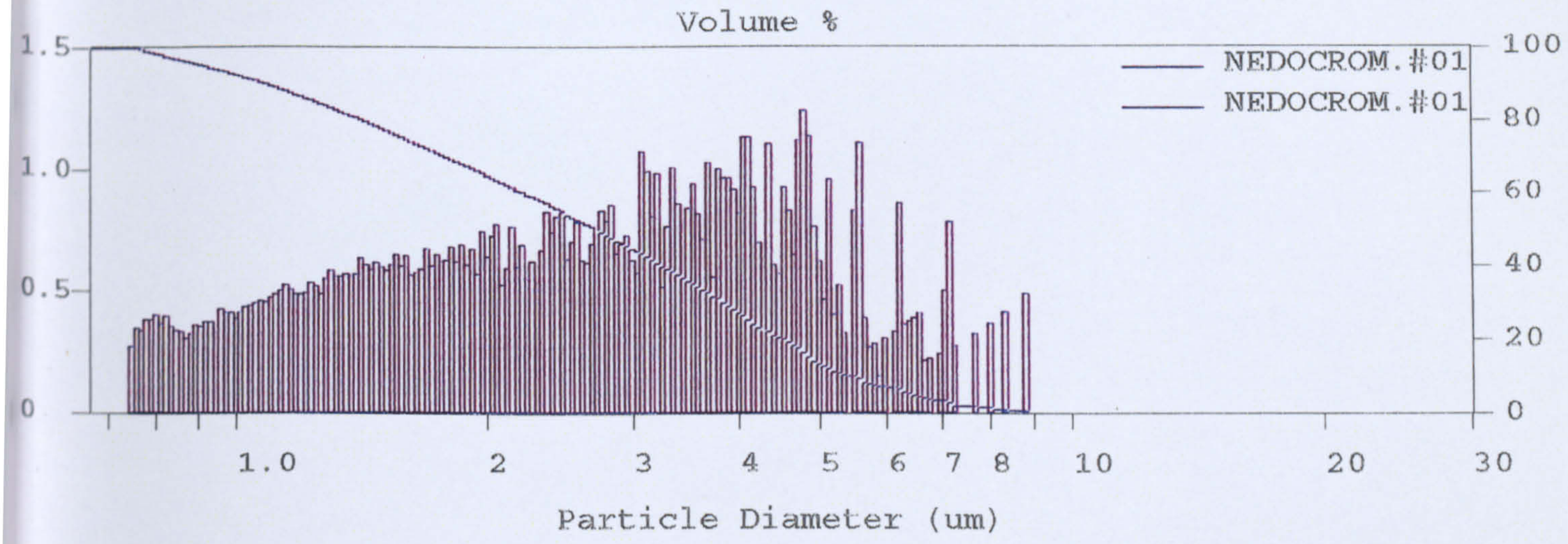

Figure 2.5.1 Particle size distribution for nedocromil sodium using ESZ analysis

cquired at: 16:35 Wed Mar 24 1993

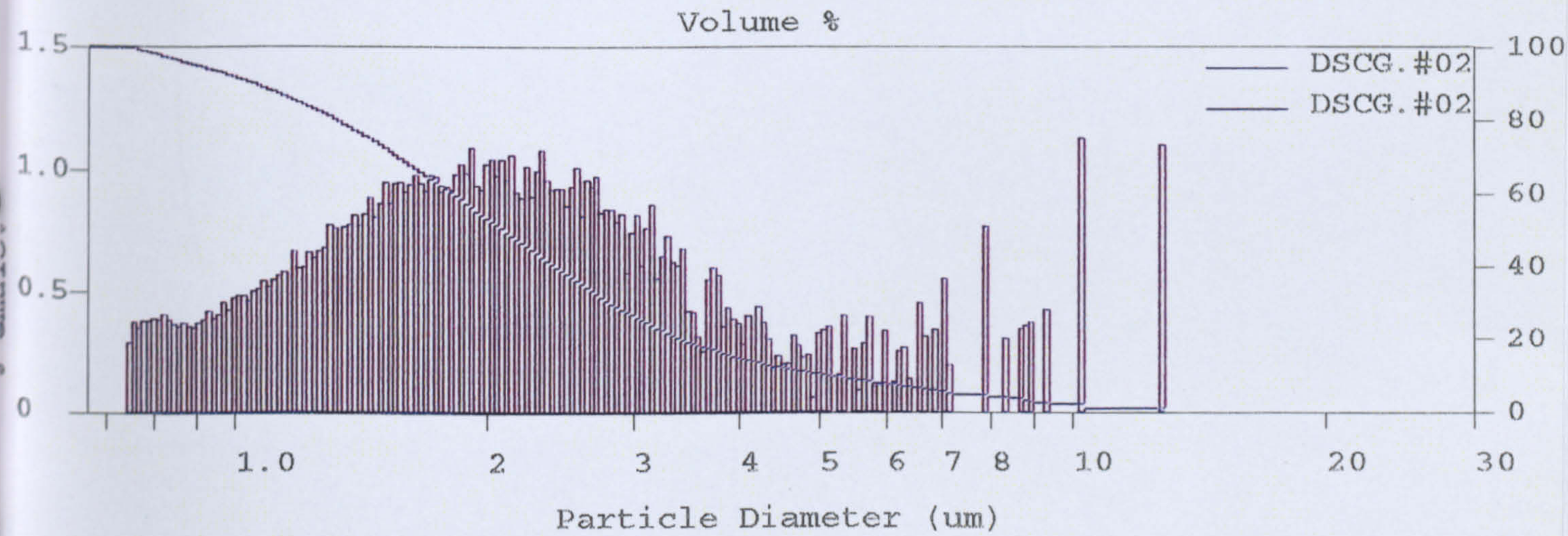

Figure 2.5.2 Particle size distribution for sodium cromoglycate using ESZ analysis

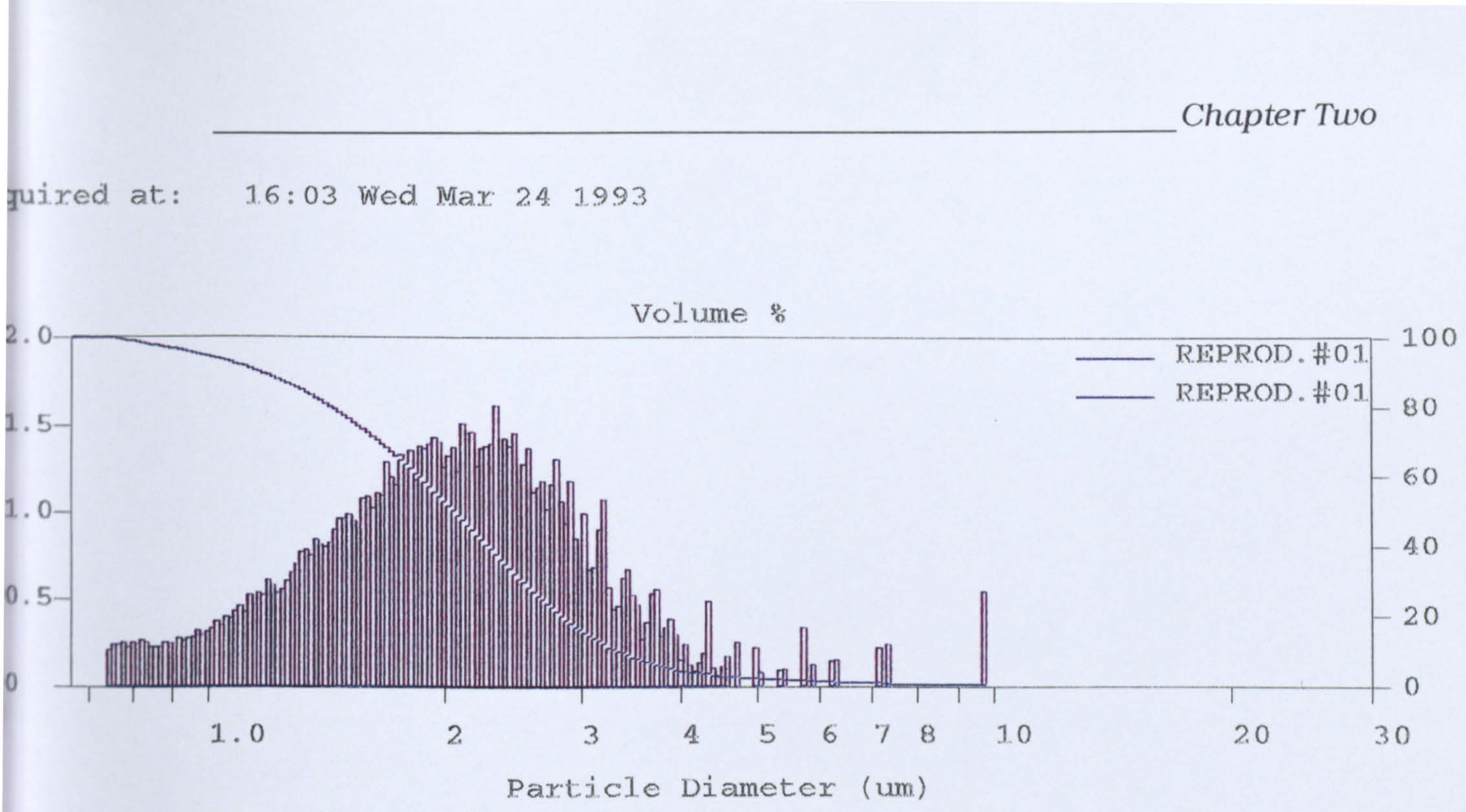

Figure 2.5.3 Particle size distribution for reproterol using ESZ analysis

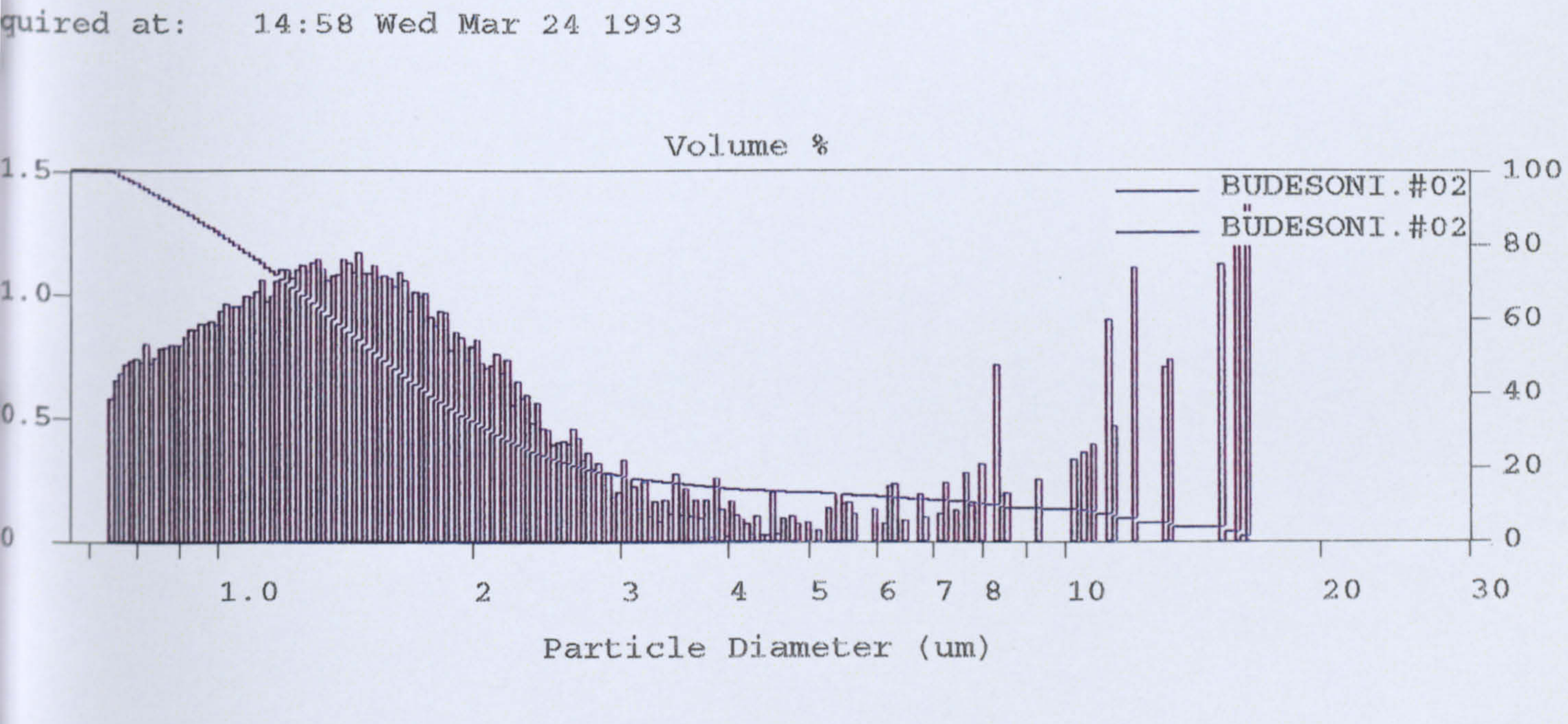

Figure 2.5.4 Particle size distribution for budesonide using ESZ analysis

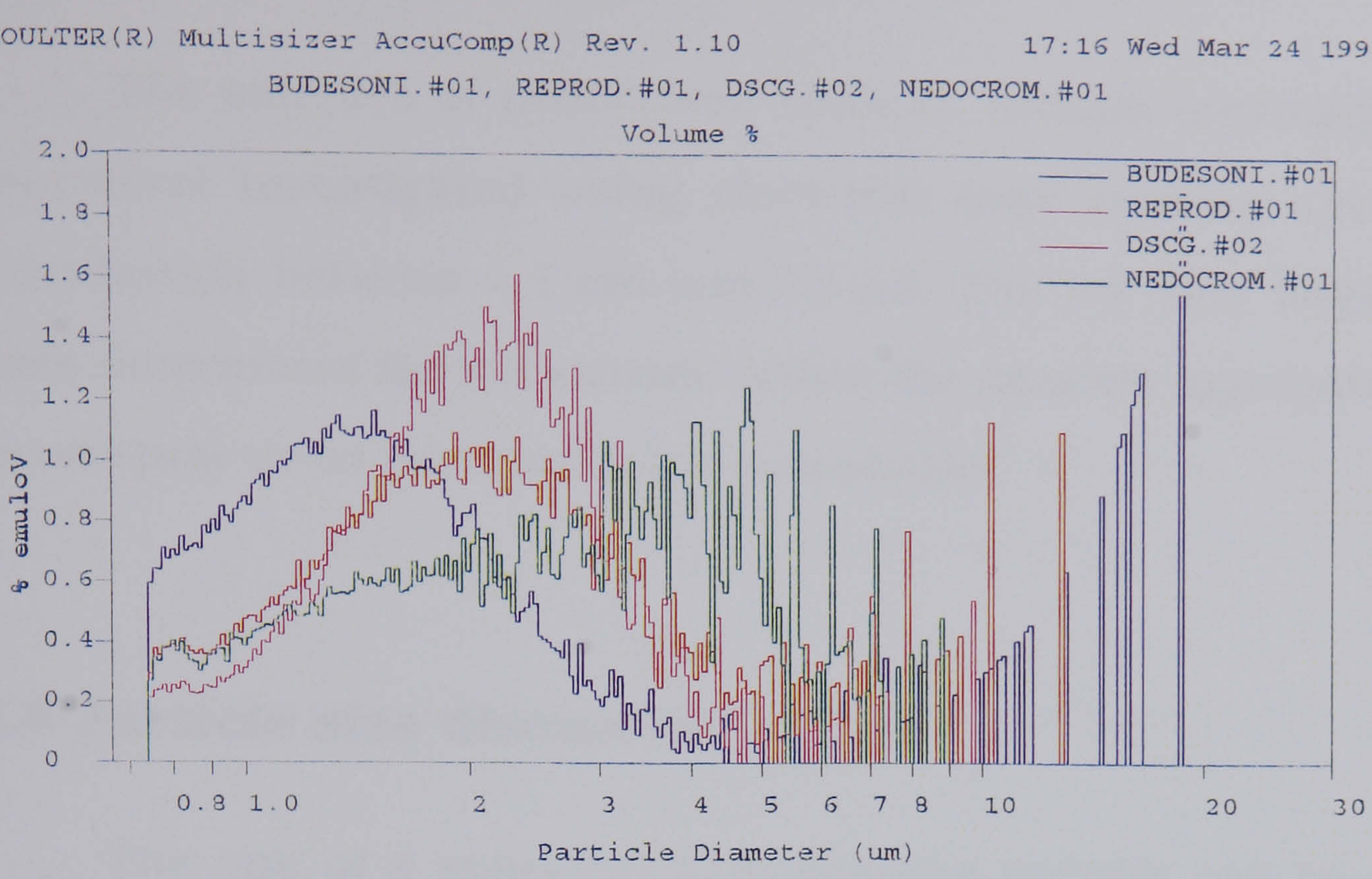

Figure 2.5.5 Summary of particle size distributions for nedocromil sodium, sodium cromoglycate, reproterol and budesonide

A summary of the derived equivalent particle sizes are shown in Table 2.5.2.

Sample	**Median volume diameter (μm)**	**Geometric mean volume diameter (μm)**	**Standard deviation (μm)**
Nedocromil sodium	2.68	2.53	0.60
Sodium cromoglycate	2.08	2.20	0.60
Reproterol	2.04	2.02	0.42
Budesonide	1.54	1.91	0.78

Table 2.5.2 Derived mean particle sizes using ESZ particle size analysis

2.5.5 Concluding comments

The samples of nedocromil sodium, sodium cromoglycate and reproterol investigated using electrical zone sensing show a size distribution between < 1 μm and 10 μm. The few very large particle sizes determined for budesonide reflect the possible aggregation of the small spray dried particles in the suspension.

2.6 Particle size discussion

The size of a spherical homogeneous particle can be uniquely defined by its diameter. Derived equivalent diameters are determined by relating a size dependent property of a particle to a linear dimension. The equivalent spherical diameter is the most widely determined diameter.

Laser diffraction sizing determines the diameter of a sphere which causes the equivalent scattering of light through a defined angle as the sample particle. Electrical zone sensing analysis determines the diameter of a sphere which causes an equivalent change in electrical resistance as the sample particle.

For irregular shaped particles the size determination method is often dependent upon the method of measurement. The evaluation of particle shape, carried out by scanning electron microscopy (Section 2.3) showed that the samples of nedocromil sodium, sodium cromoglycate, reproterol and budesonide are non-spherical. This is reflected in the variation of particle size determination between the

laser diffraction and electrical zone sensing methods. However, the particle size distributions of the samples relative to each other remain constant, regardless of the analytical method.

Bi-modal size distributions are observed for the samples of nedocromil sodium, sodium cromoglycate and reproterol. This type of size distribution is typical of powder samples which have undergone a process of particle size reduction. Differences in the fracture behaviour of coarse and fine particles leads to a size reduced bi-modal population of particles from an approximately normal initial size distribution. This can be described by Figure 2.6.1. All of the three samples which showed this bi-modal distribution had undergone particle size reduction in an Apex Mill.

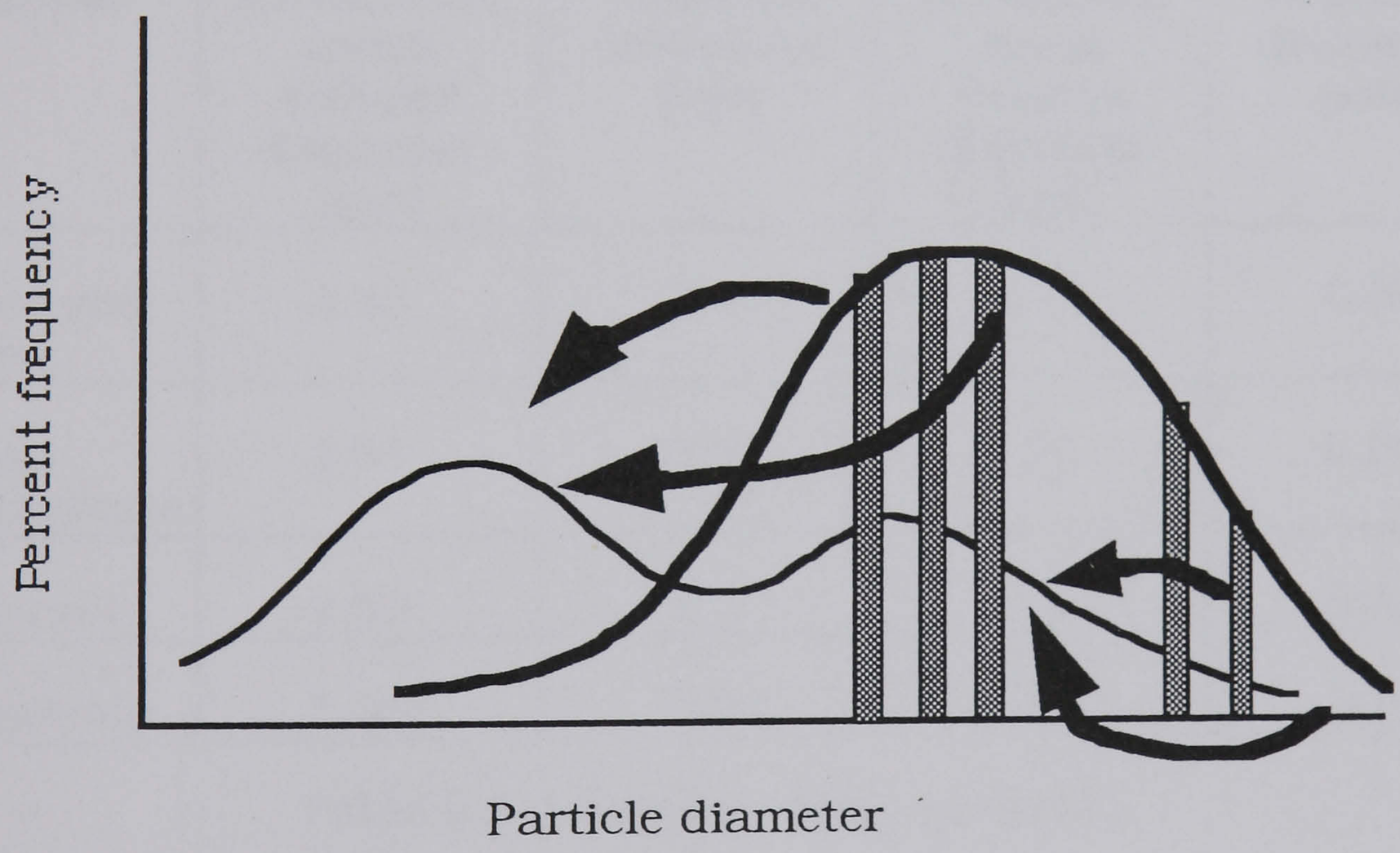

Figure 2.6.1 Transformation of approximate normal particle size distribution into finer bi-modal distribution following particle size reduction [28]

The particle size distribution of budesonide was also determined. This was carried out in order to verify that the distribution of size

exhibited by nedocromil sodium, sodium cromoglycate and reproterol was not an artefact of the analysis techniques. Budesonide particles had been prepared by spray drying. No particle size reduction of the spray dried product had been performed. This produced the log-normal distribution as expected, confirming that the previous distributions were not influenced by the sizing procedure.

The summary of the particle size distributions evaluated using laser diffraction and electrical zone sensing are reproduced in Table 2.6.1.

	Laser diffraction		**Electrical zone sensing**	
Sample	**Arithmetic mean volume diameter (μm)**	**Standard deviation (μm)**	**Geometric mean volume diameter (μm)**	**Standard deviation (μm)**
Nedocromil sodium	4.43	3.36	2.53	0.60
Sodium cromoglycate	4.51	3.41	2.20	0.60
Reproterol	2.99	2.28	2.02	0.42
Budesonide	1.36	0.84	1.91	0.78

Table 2.6.1 Particle sizing summary

2.7 Mass loss on drying

In order to quantify the mass of water released by nedocromil sodium (batches 3B1, 4B1, 5B1, 2001B1, 2002B1) and sodium cromoglycate (batch XC13 CIA M150) during dehydration the following procedure was carried out.

2.7.1 Method

About 1 g of drug sample was weighed accurately and placed into a glass heating vessel with the lid positioned to allow air circulation. The vessel was then placed into the oven alongside a blank containing no sample. The samples were heated to 200° C. The samples were held at this temperature for two hours. The vessels were then transferred to a desiccator through which nitrogen was flowing. After an hour in these conditions the lids were replaced securely and the samples weighed again.

2.7.2 Results

The results from the experimental provides the mass lost per gram of hydrated sample. The percentage initial moisture content (M.C.) can be calculated using the formula

$$\frac{(\text{mass of hydrated sample}) - (\text{mass of anhydrous sample})}{\text{mass of anhydrous sample}} \times 100 = \text{M.C.}$$

(equation 2.7.1)

The corresponding number of moles of water associated with each mole of anhydrous nedocromil sodium can then be calculated using the formula

$$\frac{M.C. \times MW_{\text{nedocromil sodium anhydrous}}}{100} \times \frac{1}{MW_{H_2O}} = \text{No. of moles of } H_2O$$

(equation 2.7.2)

where

$MW_{\text{nedocromil sodium anhydrous}} = 415$ Da

$MW_{H_2O} = 18$ Da

Table 2.7.1 shows the calculated values for the five nedocromil sodium batches.

Batch number	**Mass (g) lost per gram of hydrated sample**	**Moisture content (%)**	**No. of moles of water per mole of drug sample**
3B1	0.043	4.49	1.0
4B1	0.045	4.71	1.1
5B1	0.088	9.65	2.2
2001B1	0.080	8.70	2.0
2002B1	0.052	5.49	1.3

Table 2.7.1 Summary of the water content of five nedocromil sodium batches

Using the same method, the moisture content results for the sample of sodium cromoglycate was found to be 5.71 % [29] which corresponds to 1.6 moles of water per mole of anhydrous sodium cromoglycate.

Reproterol and budesonide exhibited negligible weight loss [29] indicating that the crystals were not hydrated.

2.7.3 Discussion

At ambient temperature and relative humidity nedocromil sodium exists as a trihydrate, as described in Figure 2.7.1. The mass lost from the nedocromil sodium samples during the drying experiment does not correspond to the loss expected from a trihydrate form of the crystal. Two types of bound water are held in the nedocromil molecular crystal and when heated, leave it in different ways. The trihydrate form is converted to a monohydrate at temperatures ≥70° C. This corresponds to the "loosely bound" water which is hydrogen bonded [30]. This water is lost anisotropically along the crystal axis. During the second dehydration event "tightly bound" water molecules, which are bonded to the carboxylic acid groups [30], are lost. This results in fragmentation of the crystal structure [25]. Visual observation of the samples after they had been heated for the predetermined time revealed yellow crystals similar to those observed before heating, rather than darker brown crystals. This indicates that after heating in the oven and cooling under nitrogen, the nedocromil sodium crystals were not fully dehydrated. Therefore the corresponding three moles of water were not lost. It is suggested that batches 5B1 and 2001B1 more readily lose the "loosely bound" water compared with the remaining three batches. Alternatively batches 5B1 and 2001B1 may have more adsorbed water due to a possible difference in the surface behaviour of the particles.

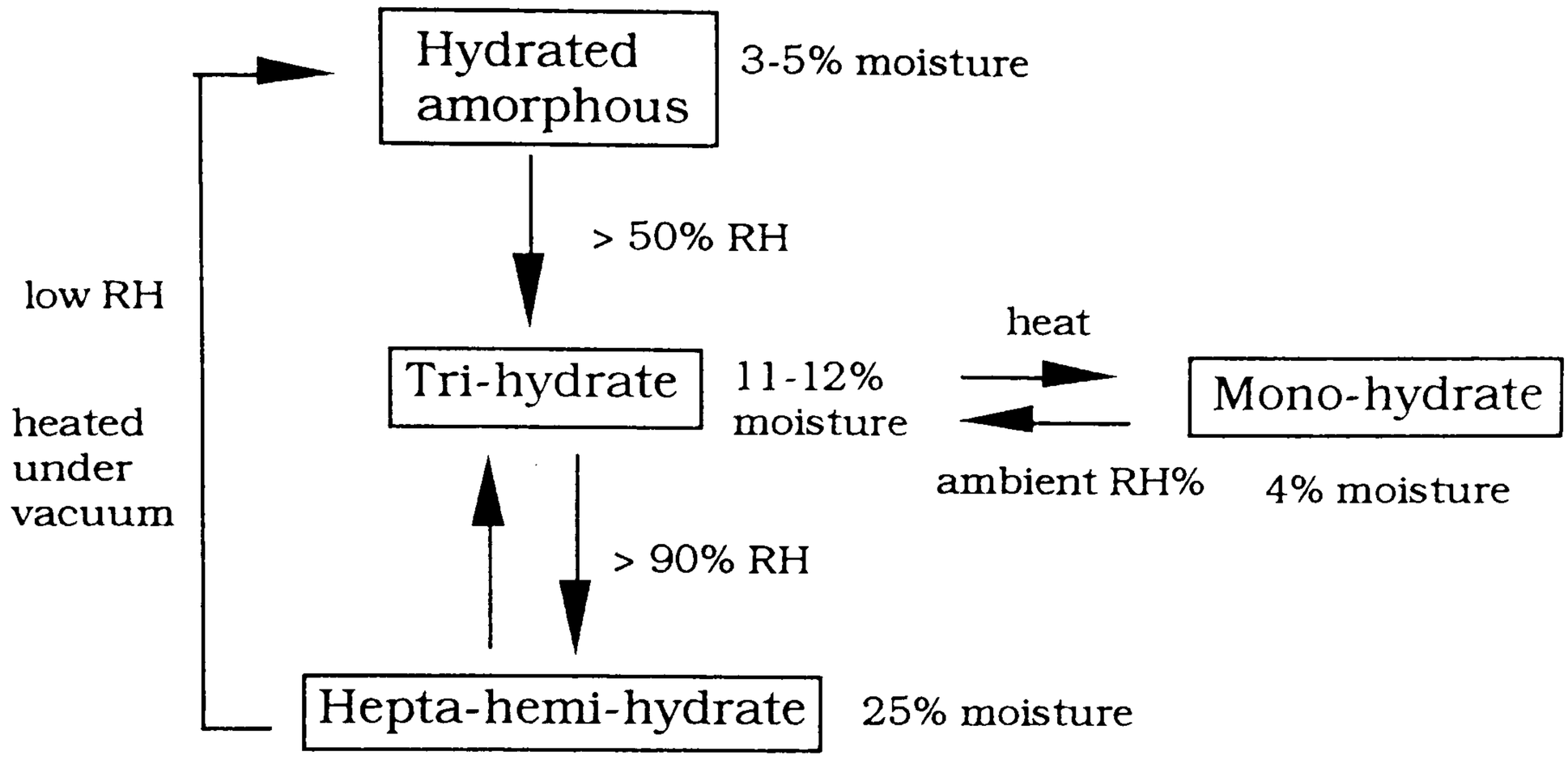

Figure 2.7.1 Hydrated states of nedocromil sodium [30]

Sodium cromoglycate does not exist as a fixed hydrate. The crystals can absorb or lose water as a continuous series of interstitial solid solutions, with water as the interstitial component. The amount of water absorbed, or lost, is proportional to the relative humidity environment of the crystals. Between 30-70 % relative humidity at ambient atmosphere the interstitial water approaches five to six molecules per molecule of sodium cromoglycate [31]. This corresponds to the moisture content determined for sodium cromoglycate.

2.8 Differential Scanning Calorimetry

Differential scanning calorimetry (DSC) is a method of thermal analysis. It can be used to identify dehydration events which occur in a solid samples as its temperature is increased.

Dehydration is an energy requiring (endothermic) transition. This can be detected and quantified by the DSC apparatus. A sample is loaded into a small aluminium pan. An empty pan is used as a reference. A constantan disc transfers heat to the reference sample and the sample for analysis, which are positioned within the oven chamber of the apparatus. The sample is heated at a constant rate by heat transfer from the constantan disc, through the sample pan to the sample. A thermocouple detects any differential heat flow at the sample and reference positions. The power associated with an endothermic transition is recorded as a peak on a plot of ΔH against temperature for the system.

2.8.1 Materials

Differential scanning calorimetry was used to identify dehydration events in the following samples.

Sample	Batch Number
nedocromil sodium	3B1
nedocromil sodium	4B1
nedocromil sodium	5B1
nedocromil sodium	2001B1
nedocromil sodium	2002B1
sodium cromoglycate	XC13ClAM150
lactose	022303

Table 2.8.1 Differential scanning calorimetry sample summary

Nedocromil sodium samples were prepared for analysis as shown in Table 2.8.2

Sample preparation	**Batch Number**
From ambient conditions	3B1, 4B1, 5B1, 2001B1, 2002B1
Stored at 60 % relative humidity for 14 days	4B1, 2002B1
Heated to 240 °C, allowed to cool to ambient temperature in a nitrogen environment	4B1
Heated to 240 °C, allowed to cool to ambient temperature in the laboratory environment	4B1

Table 2.8.2 Preparation of nedocromil sodium samples tested using differential scanning calorimetry

Interactive binary mixes of nedocromil sodium with α-lactose monohydrate, and sodium cromoglycate with α-lactose monohydrate (as prepared in Chapter Three) were also investigated using differential

scanning calorimetry. The mixes investigated are presented in Table 2.8.3.

Mix	Drug concentration in mix
Nedocromil sodium (5B1) with α-lactose monohydrate	2 % w/w
Sodium cromoglycate with α-lactose monohydrate	2 % w/w

Table 2.8.3 Powder blends analysed using differential scanning calorimetry

2.8.2 Apparatus

A DuPont series 99 thermal analyser and 910 differential scanning calorimeter was used to determine the DSC profiles of the samples.

2.8.3 Method

A precisely known mass, about 4 mg, of sample was weighed into the aluminium sample cap. This was placed in the oven chamber of the apparatus alongside the reference cap. A gentle stream of helium flowed through the oven chamber in order to create an inert atmosphere. The oven was then warmed at a constant rate between two predetermined temperatures.

2.8.4 Results

2.8.4.a Nedocromil sodium

The DSC plots are reproduced in Figures 2.8.1 to 2.8.5.

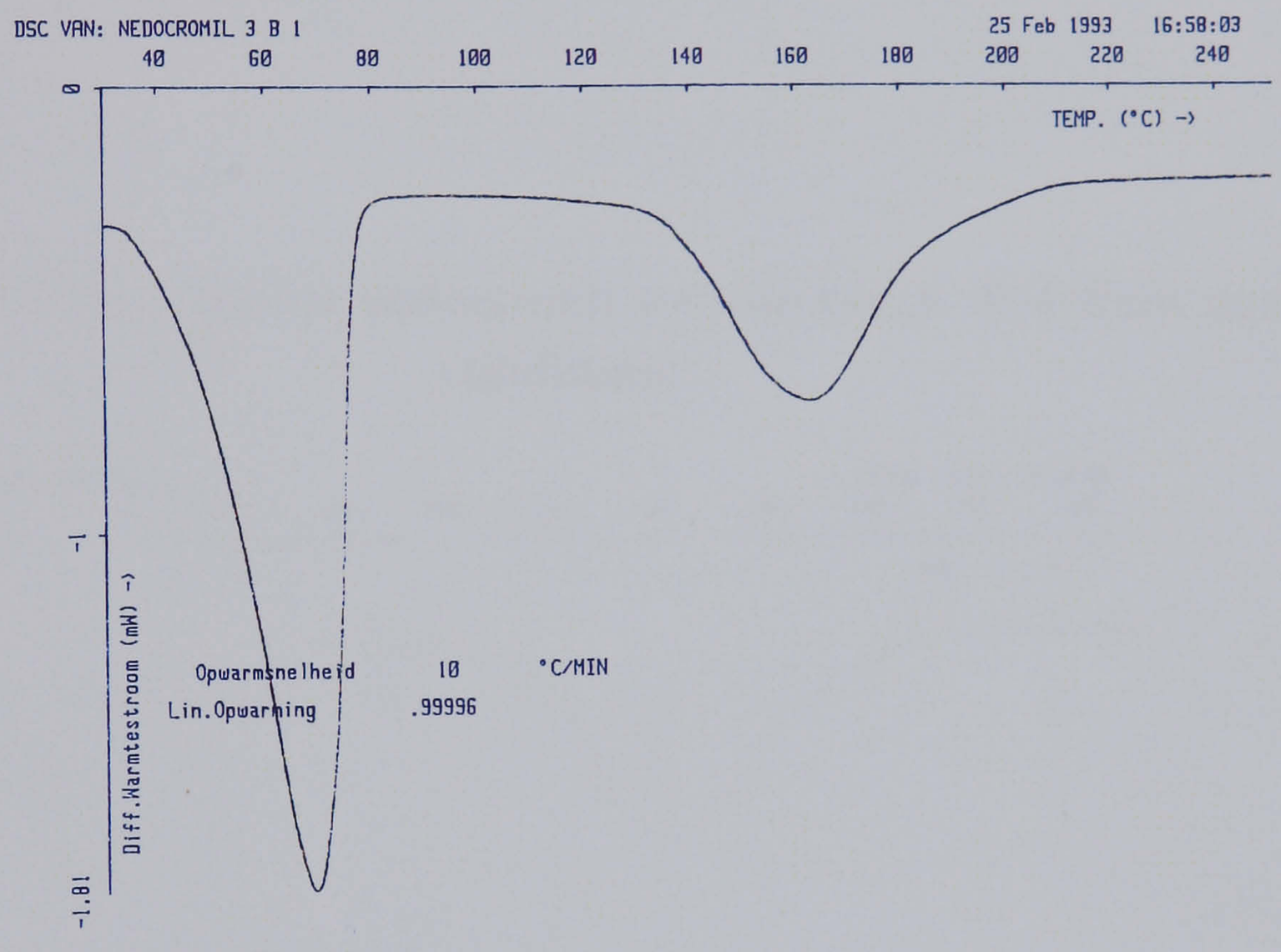

Figure 2.8.1 DSC scan for nedocromil sodium batch 3B1 from ambient conditions

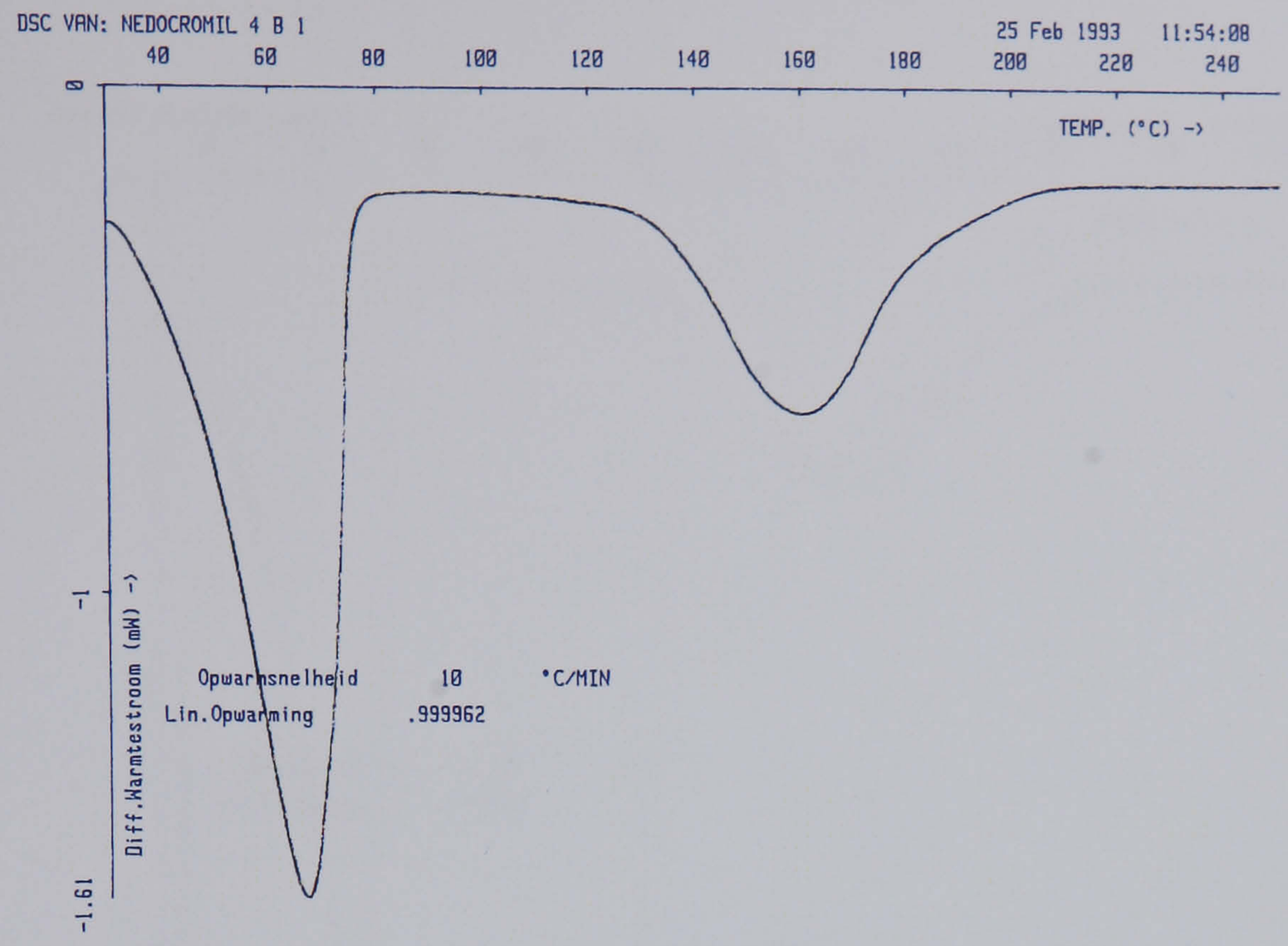

Figure 2.8.2 DSC scan for nedocromil sodium batch 4B1 from ambient conditions

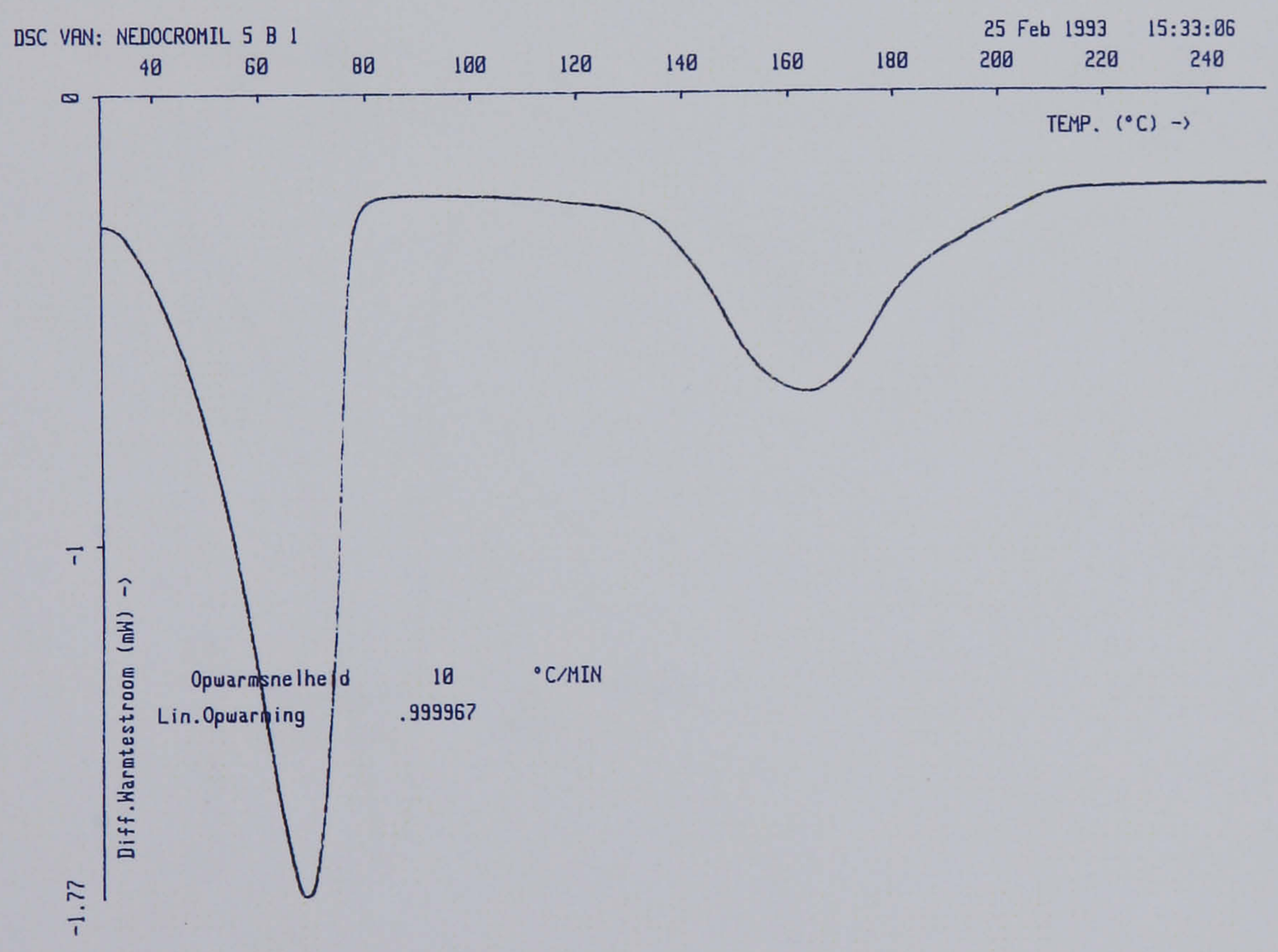

Figure 2.8.3 DSC scan for nedocromil sodium batch 5B1 from ambient conditions

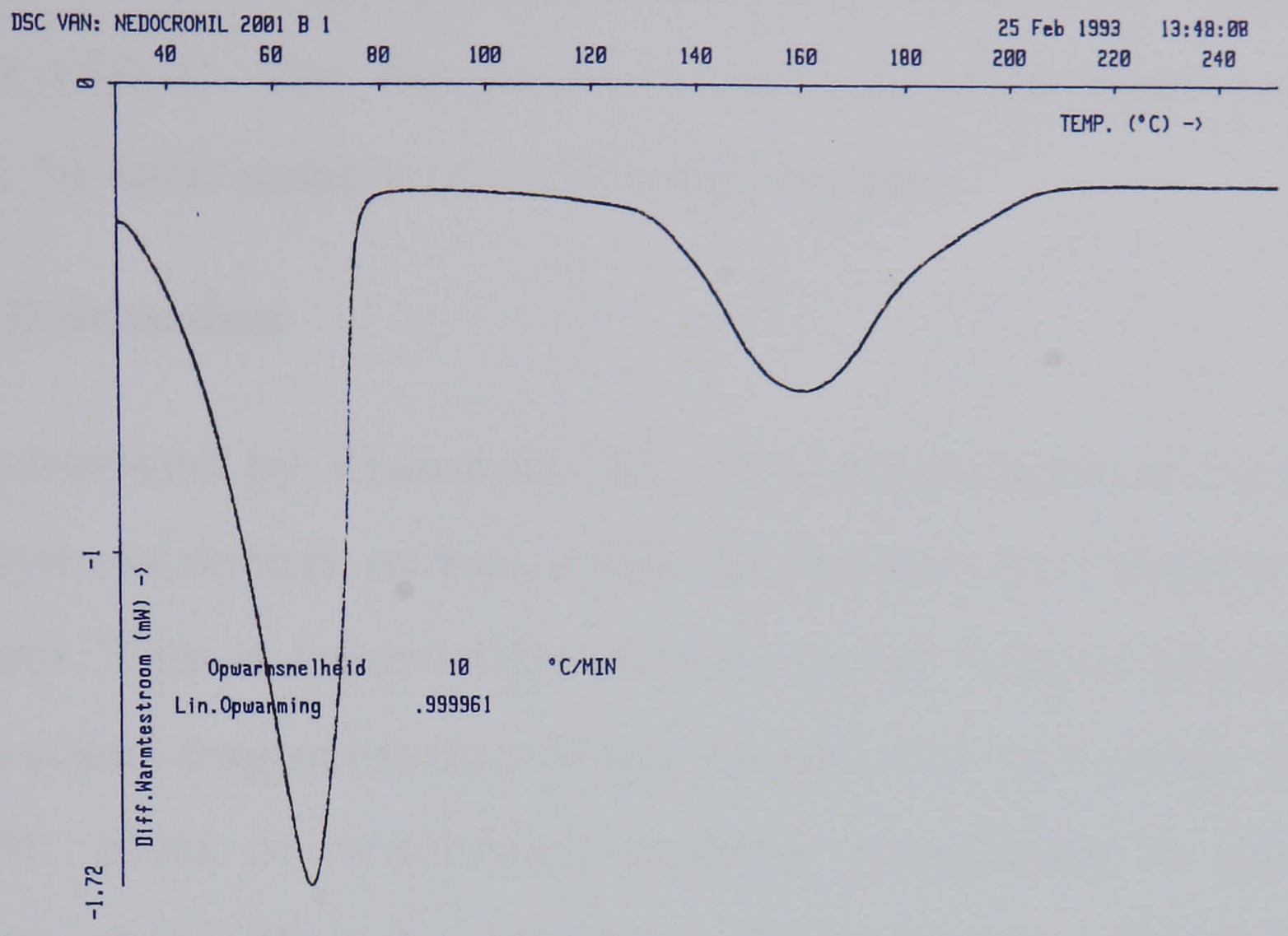

Figure 2.8.4 DSC scan for nedocromil sodium batch 2001B1 from ambient conditions

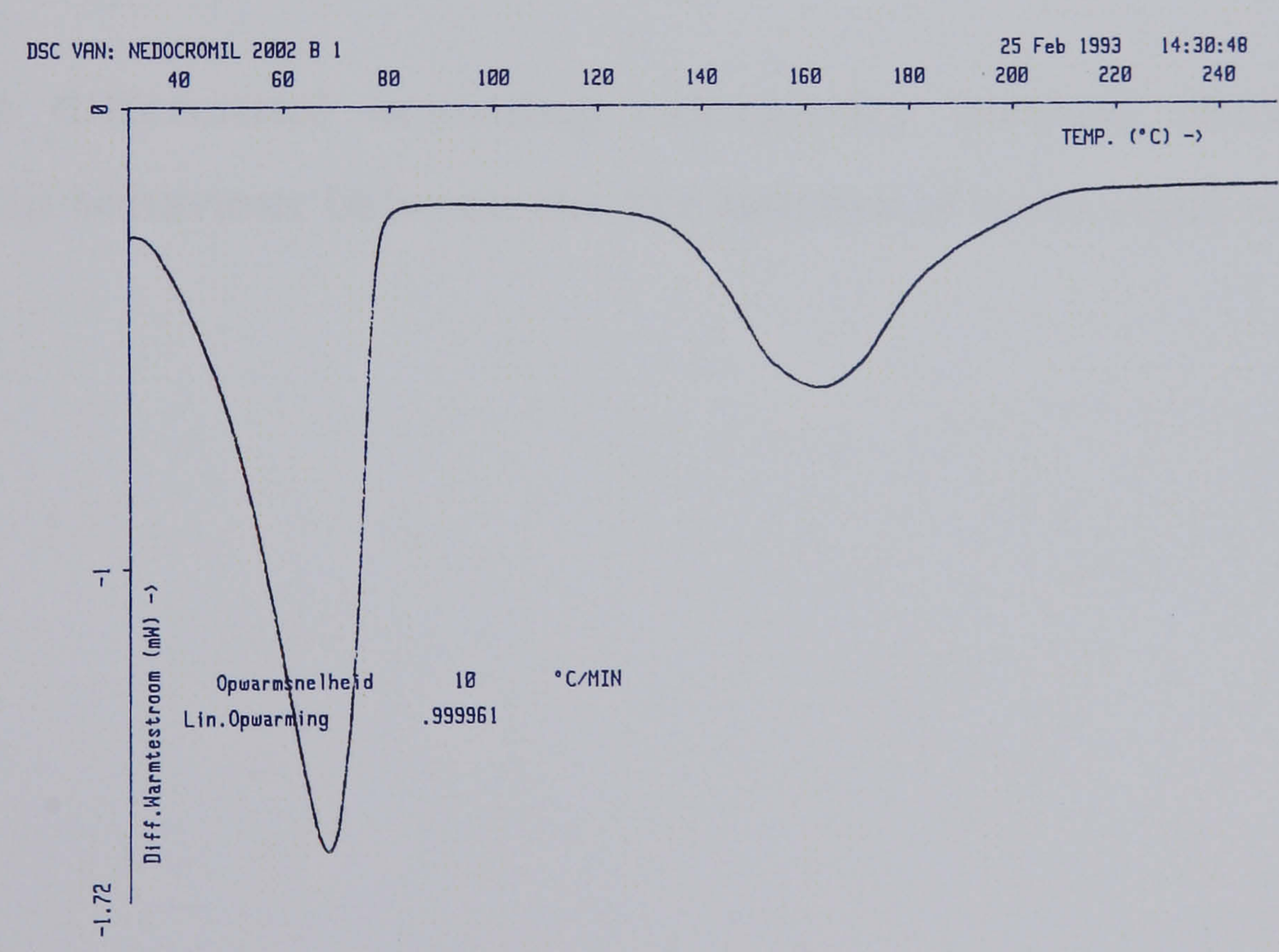

Figure 2.8.5 DSC scan for nedocromil sodium batch 2002B1 from ambient conditions

2.8.4.a.i Results

The DSC plot identifies two endothermic events. These lie at 65 °C and 160 °C. The temperature and extent of these peaks are consistent for each sample of nedocromil sodium.

2.8.4.a.ii Discussion

As observed by Khankari [25], the dehydration of nedocromil sodium crystals occurs in two steps. In the first the "loosely bound" water is lost. This is followed by the loss of the "tightly bound" water and subsequent fragmentation of the crystal. The two peaks observed in the DSC plots of nedocromil sodium correspond to these two dehydration steps. Visual inspection of the sample after heating to 250 °C revealed the sample had changed in appearance from yellow to dark brown.

This differential scanning calorimetry method showed no difference in behaviour between the five batches of nedocromil sodium.

2.8.4.a.iii Elevated humidity

The plots obtained from the samples of nedocromil sodium stored at 60 % relative humidity for 14 days are reproduced in Figures 2.8.6 and 2.8.7.

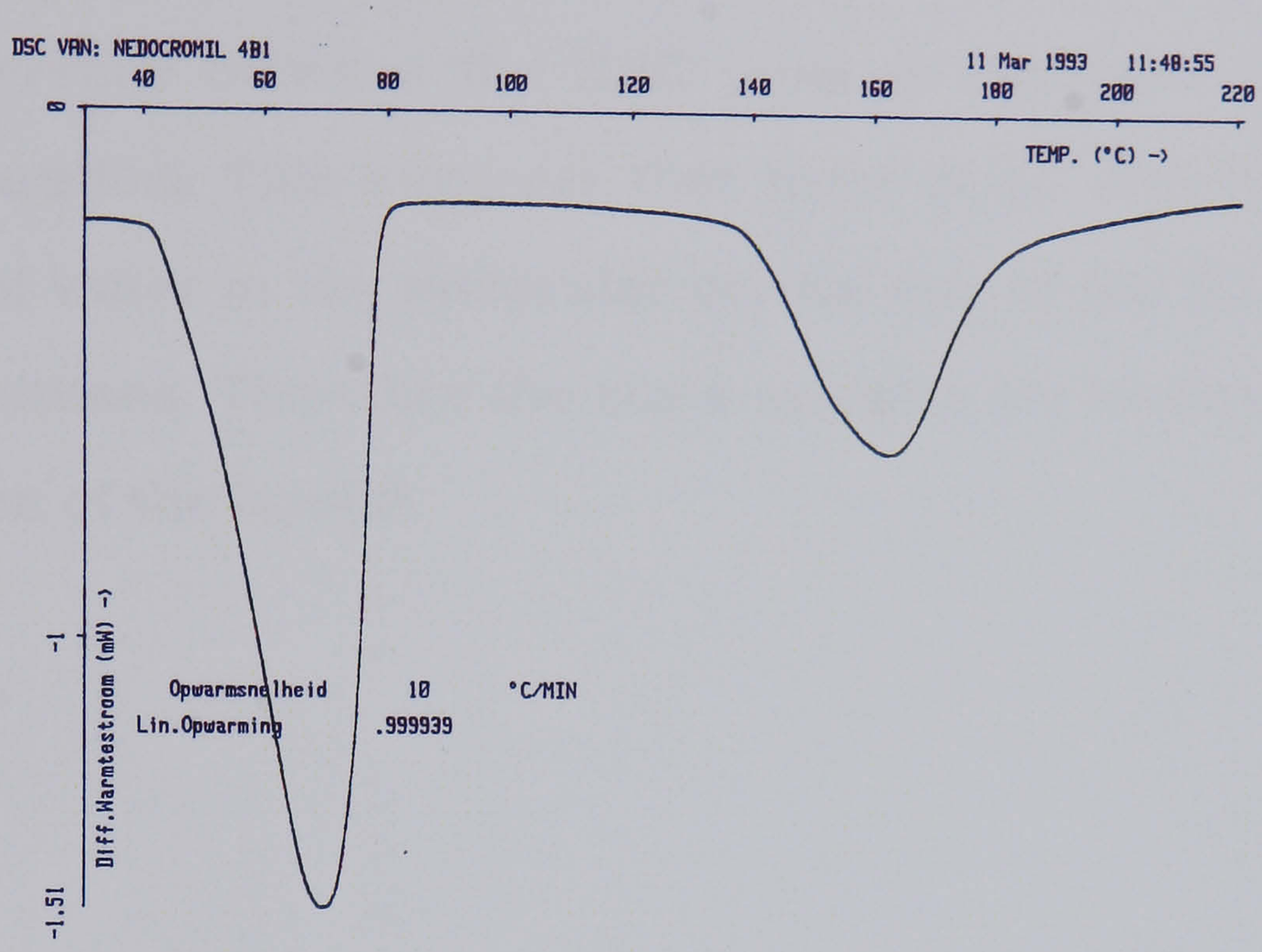

Figure 2.8.6 DSC scan for nedocromil sodium batch 4B1 stored at 60 % relative humidity

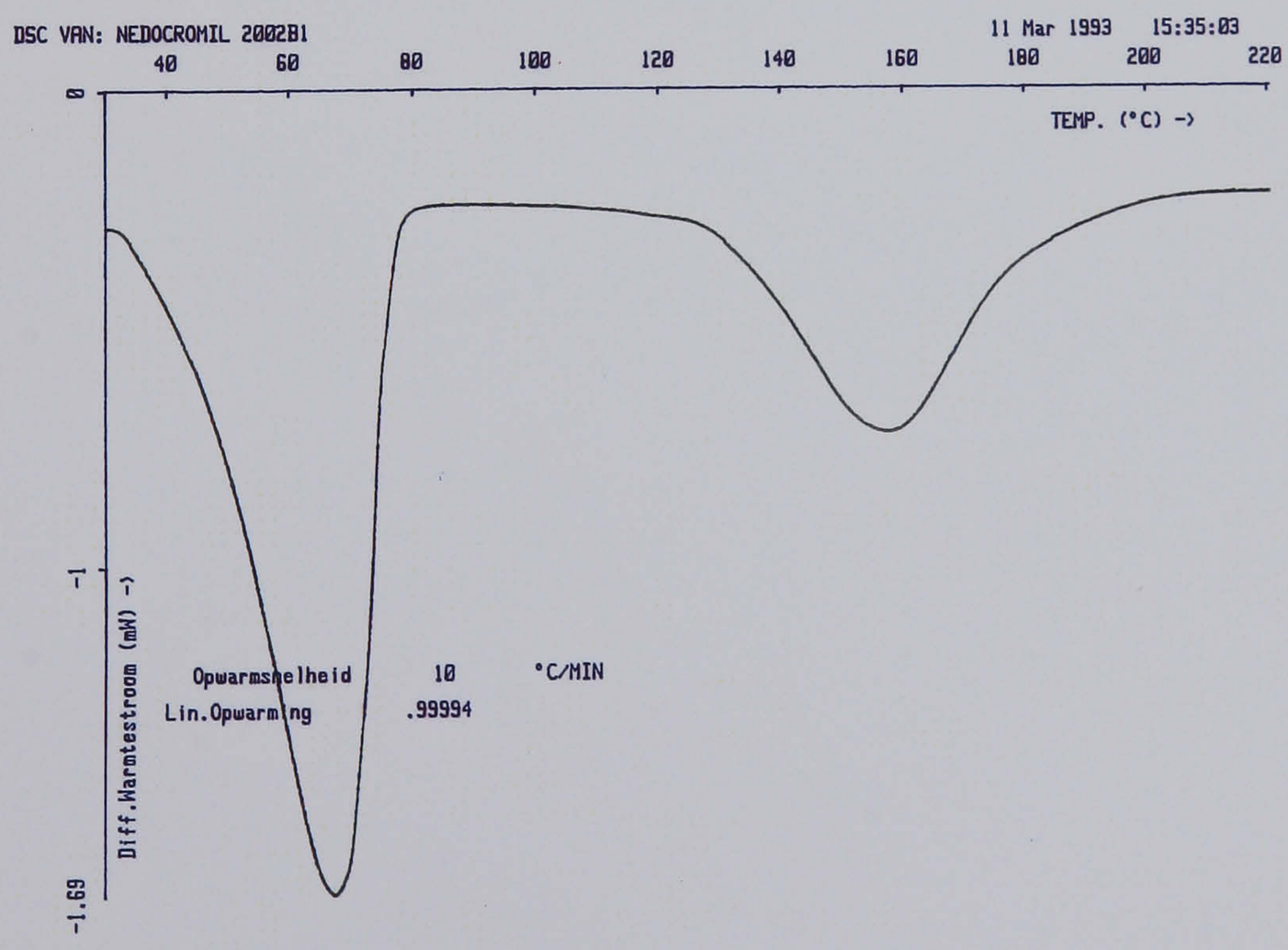

Figure 2.8.7 DSC scan for nedocromil sodium batch 2002B1 stored at 60 % relative humidity

The DSC plot identifies two endothermic reactions. These lie at 65 °C and 160 °C. These peaks are consistent for both samples of nedocromil sodium which had been stored at an elevated humidity.

2.8.4.a.iv Concluding comment

No difference between the DSC plots is observed due to this sample preparation. This suggests that there is no alteration in the distribution of water in the molecular crystal due to the 60 % relative humidity conditions. Therefore the stock samples are confirmed as the trihydrate form of the crystal.

2.8.4.a.v. Moisture re-uptake

The efficiency of moisture re-uptake by nedocromil sodium crystals was studied by heating the samples to 240 °C in a gentle stream of helium. The samples were then allowed to cool either in a steady flow of nitrogen, or in the laboratory environment (22 °C, 67 % R.H). The resultant DSC traces are reproduced in Figures 2.8.8 and 2.8.9.

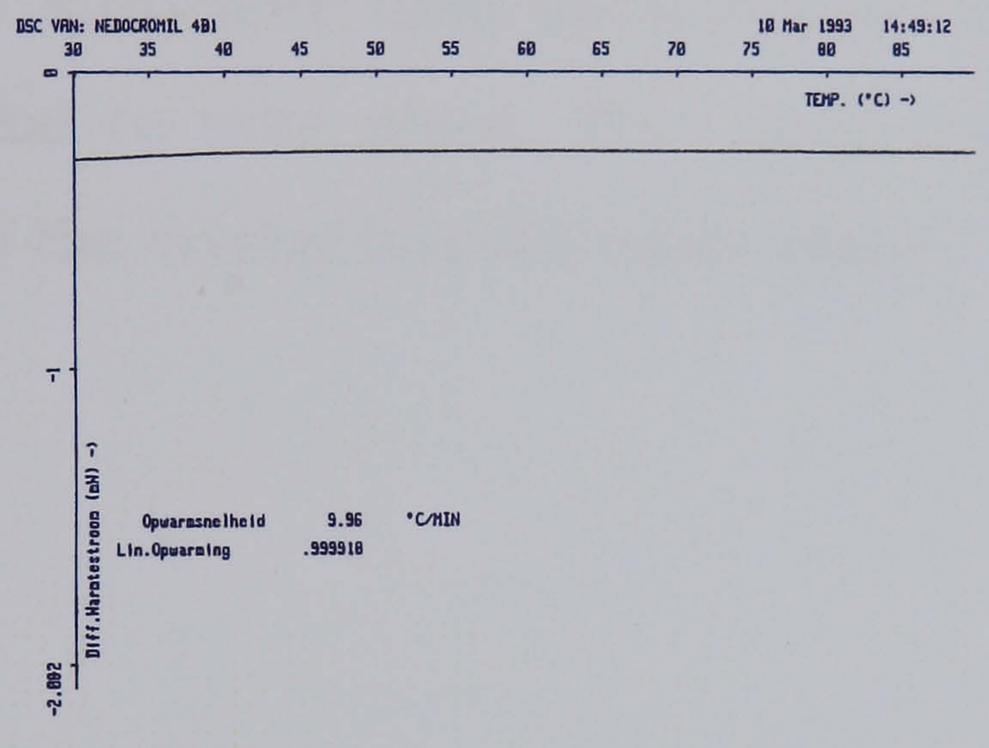

Figure 2.8.8 DSC scan for nedocromil sodium batch 4B1 heated to 240 °C, cooled in nitrogen

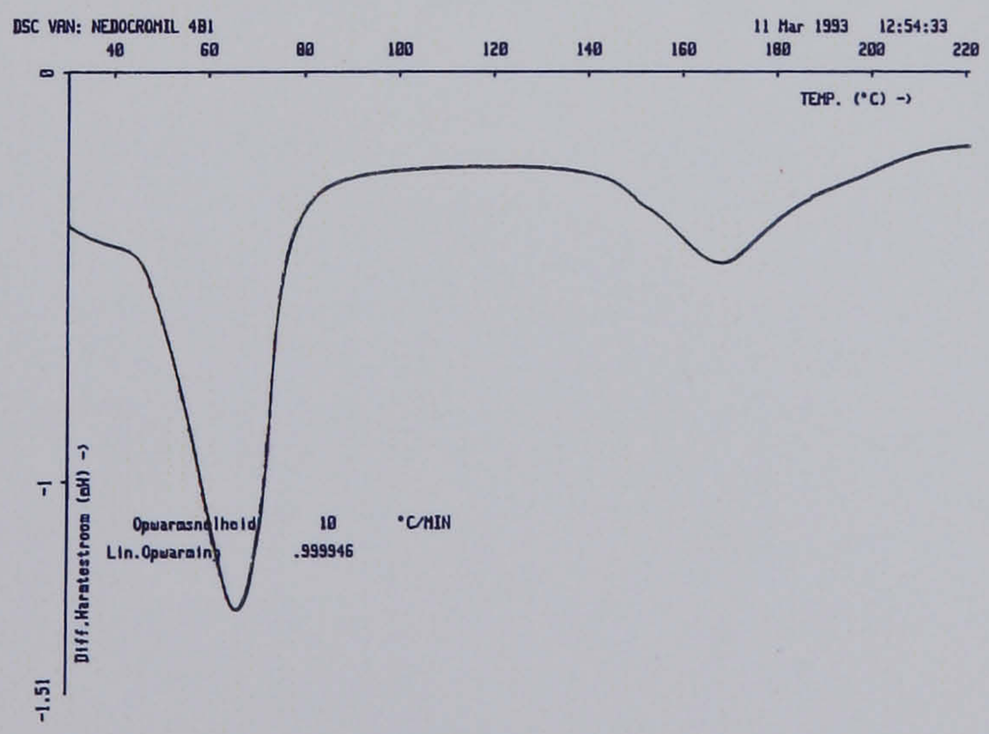

Figure 2.8.9 DSC scan for nedocromil sodium batch 4B1 heated to 240 °C, cooled in laboratory conditions

2.8.4.a.vi. Results

The sample cooled in the absence of moisture (Figure 2.8.8) reveals no endothermic transitions, as expected. When cooled in ambient conditions the DSC trace shows the typical two dehydration peaks.

2.8.4.a.vii Concluding comment

These results indicate that 30 minutes in an ambient environment is sufficient time for a degree of rehydration of the molecular crystal to take place. This suggests that non-reversible fragmentation of the crystal has not taken place.

2.8.4.b Sodium cromoglycate

The DSC plot identifies a single endothermic event. This corresponds to dehydration of the removal of adsorbed water associated with the crystal.

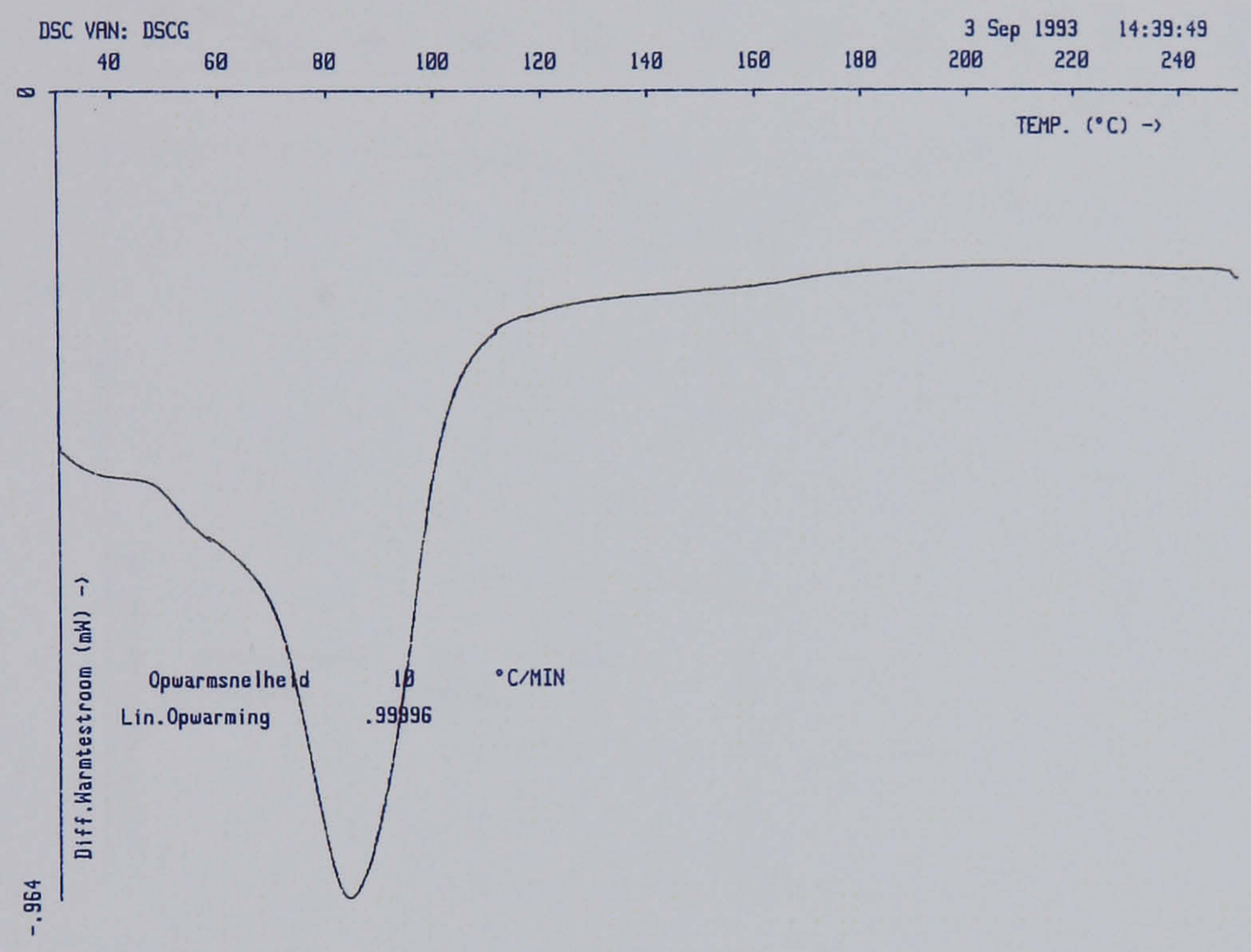

Figure 2.8.10 DSC scan for sodium cromoglycate from ambient conditions

2.8.4.c α-lactose monohydrate

The DSC plot obtained for lactose was typical of those exhibited by the α-lactose monohydrate form of the crystal [32]. The endothermic transition at 140 °C corresponds to dehydration of the product. A melting endotherm is present at 210 °C.

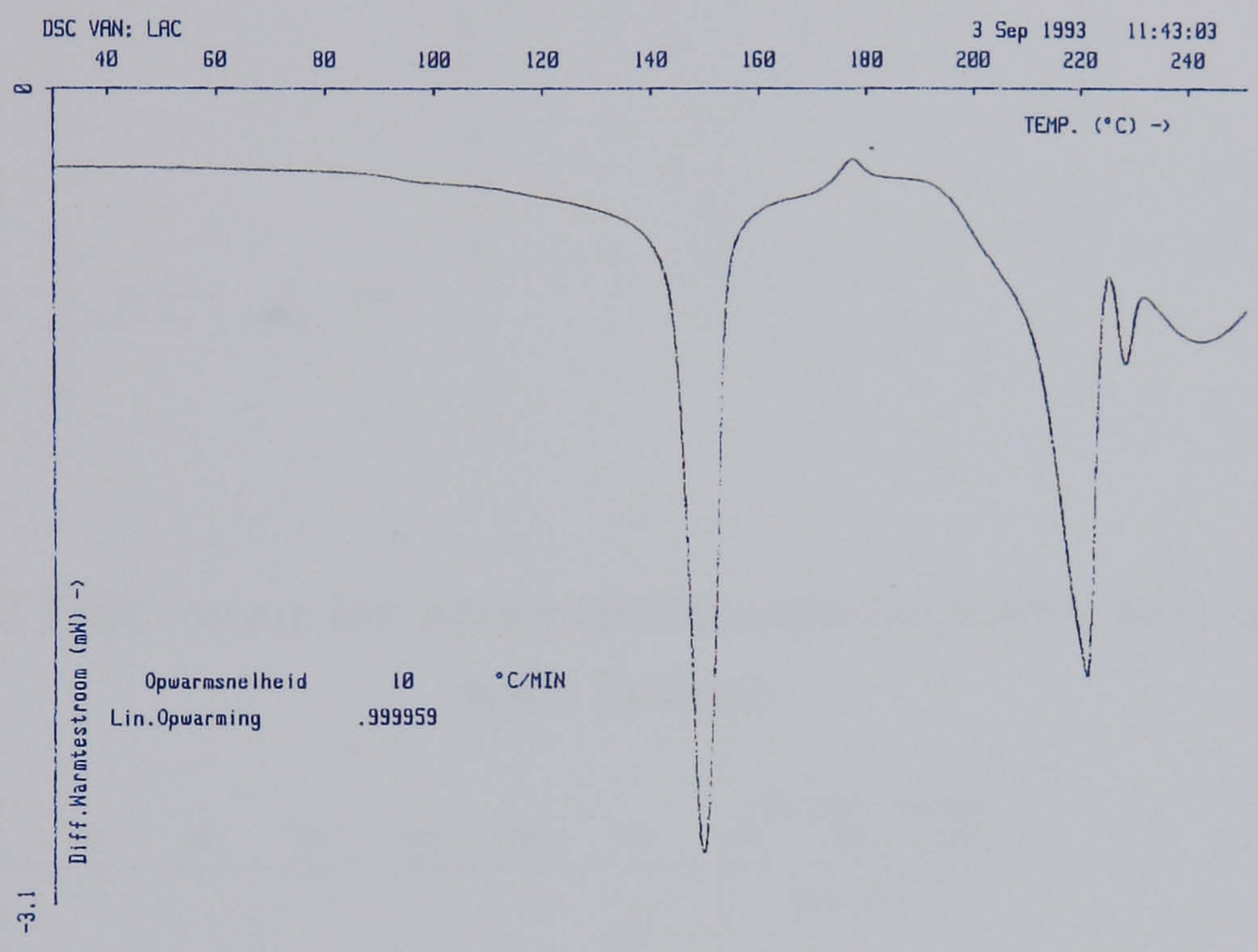

Figure 2.8.11 DSC scan for lactose from ambient conditions

2.8.4.d Drug-lactose mixes

The DSC plots recorded for these samples are reproduced in figures 2.8.12 and 2.8.13. These show a combination of the traces from the components in the powder mix. There appears to be no interactions affecting the transition stages from either component, in either mix.

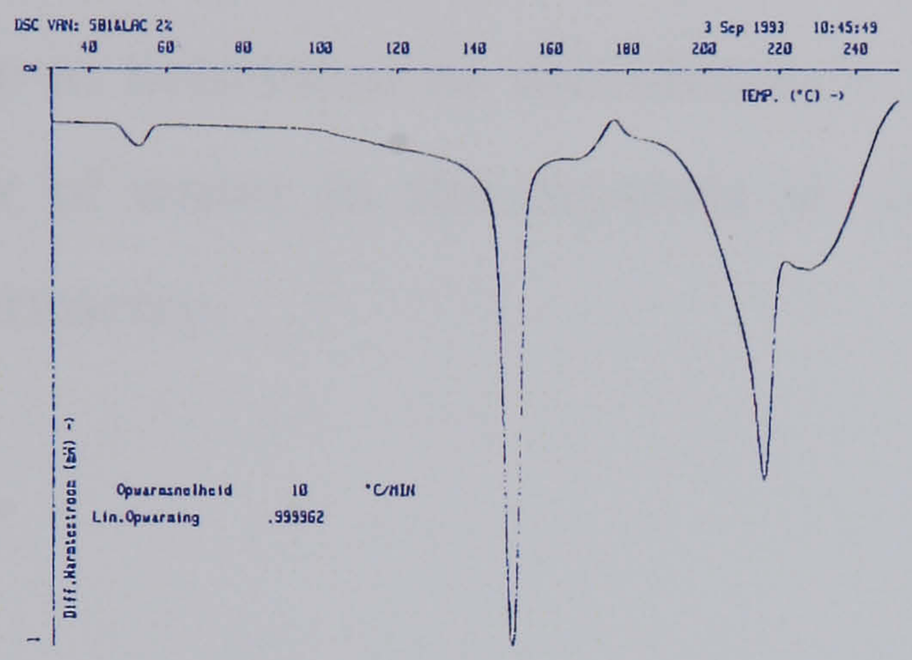

Figure 2.8.12 DSC scan for nedocromil sodium batch 5B1 2 %w/w mix with lactose

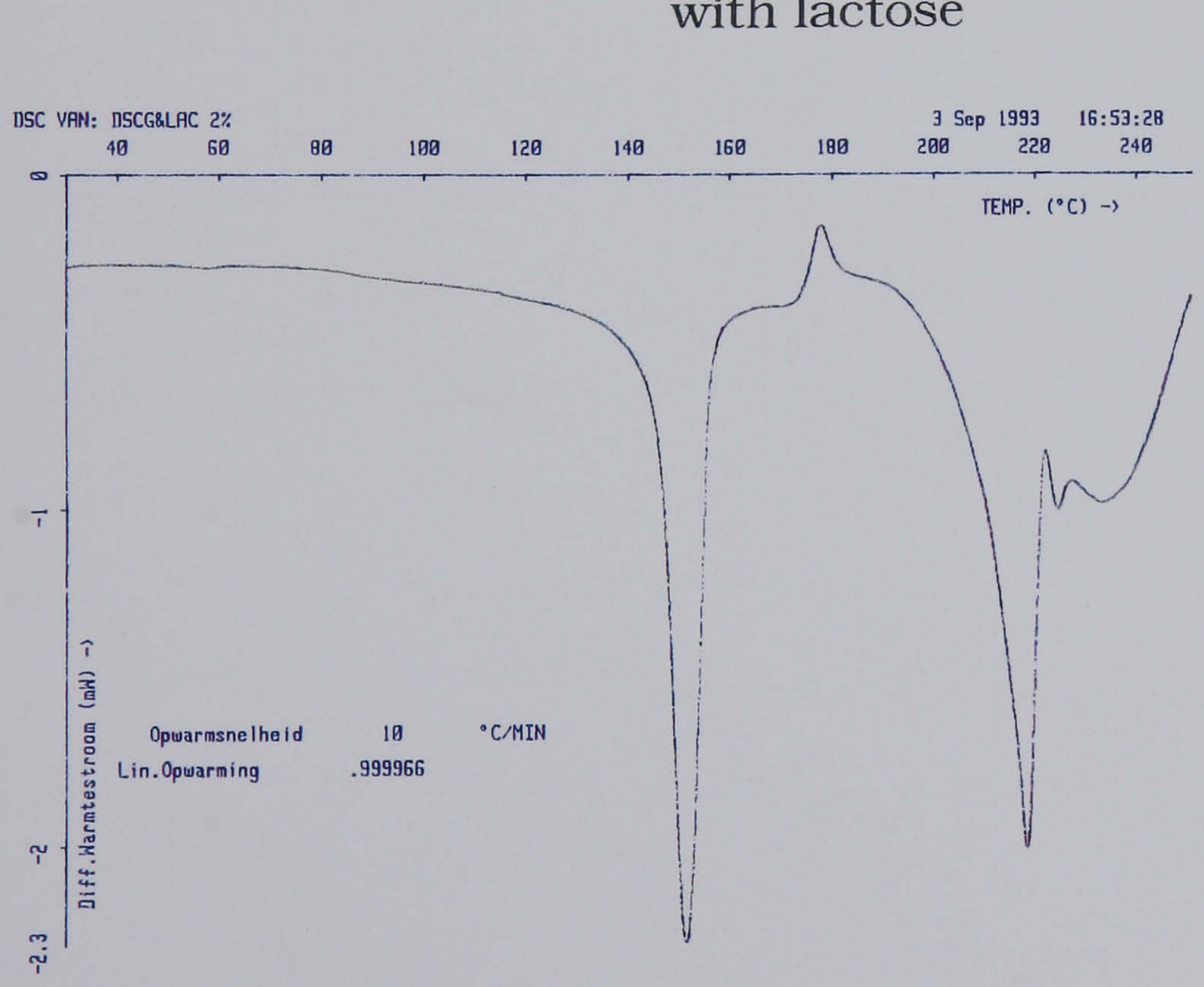

Figure 2.8.13 DSC scan for sodium cromoglycate 2 %w/w mix with lactose

2.8.5 Concluding comments

Dehydration events, identified by differential scanning calorimetry confirm the materials used for this work behave in the manner expected for nedocromil sodium trihydrate, sodium cromoglycate and α-lactose monohydrate.

All batches of nedocromil behaved in an identical way, suggesting that difference in behaviour as an inhalation dosage form is not due to the behaviour of water in the crystals as detected using differential scanning calorimetry.

2.9 Pycnometry

The technique of pycnometry determines the volume of irregularly shaped particles, the results of which are used to calculate true density. The sample volume is determined by displacement of gas from a sample chamber of accurately known dimensions, due to the sample. The pycnometer apparatus consists of two gas chambers: a sample chamber and an expansion chamber. The powder sample is placed into the sample chamber and sealed into the apparatus. Helium gas is used to charge this chamber, the small molecules of gas are able to penetrate pores and surface irregularities of the sample. The chamber is raised to an elevated pressure. The volume occupied by the gas is then increased by a precisely known expansion volume by opening a valve connecting the sample chamber to the expansion chamber. The new lower pressure associated with this increase in volume is inversely proportional to the volume of gas in the sample chamber under pressure. Powder samples which displace a large volume of helium from the sample chamber, therefore, are associated with a large pressure difference upon expansion of the gas.

2.9.1 Materials

Sample	Batch Number
nedocromil sodium	3B1
nedocromil sodium	4B1
nedocromil sodium	5B1
nedocromil sodium	2001B1
nedocromil sodium	2002B1
sodium cromoglycate	XC13CIAM150
reproterol	092125
budesonide	3189/M1 M101
lactose	022303

Table 2.9.1 True particle density determination sample summary

2.9.2 Apparatus

A Quantachrome Multivolume Helium Pycnometer, using a large volume sample cell was used to determine the volume of the samples. Helium was used as the purge gas.

2.9.3 Method

Prior to use the instrument was calibrated by determining the volume of a precision ball bearing, which by design occupied the maximum possible volume of the sample cup. Thorough cleaning of the

apparatus ensured that the sample chamber and sample cup were free from particulate contamination.

The sample cup was loaded to two thirds of its capacity with the sample and placed in the sample chamber. The sample chamber was purged with Helium gas three times prior to taking readings. This was to ensure that any residual air or moisture which may have been present on the sample was displaced.

The sample chamber was then raised to a Helium gas pressure of approximately 19.5 ± 0.2 psi (equivalent to approximately 134 kPa). allowed to equilibrate and the pressure recorded (P_1). The valve connecting the sample and expansion chambers was opened. The Helium gas then expanded into the expansion chamber, was allowed to equilibrate, and the expansion pressure (P_2) recorded. The mass of the sample and empty sample cup were recorded at the end of testing. This ensured that the mass recorded was a reflection of the true mass of the sample, free of air and moisture vapour.

2.9.4 Results

The sample volume was calculated using the following equation

$$V_{samp} = V_{cell} - \frac{V_{exp}}{(P_1/P_2 - 1)} \qquad \text{(equation 2.9.1)}$$

where V_{samp} = sample volume

V_{cell} = empty volume of the sample cell with the empty sample cup in place

V_{exp} = expansion volume

P_1 = charge pressure (psi)

P_2 = expansion pressure (psi)

Calculation of sample density follows the evaluation of the sample volume. The density of a material is, by definition, the mass per unit volume of that sample. This may be expressed as:

$$\rho_{samp} = \frac{M_{samp}}{V_{samp}} = \frac{\text{gross mass} - \text{cup mass}}{V_{samp}} \qquad \text{(equation. 2.9.2)}$$

where ρ_{samp} = sample density

M_{samp} = sample mass

V_{samp} = sample volume

The following densities for the powder samples were determined:

Sample	Hydrated density (g/cm^3)	Sample	Hydrated density (g/cm^3)
Nedocromil sodium batch number:		Sodium cromoglycate	1.590
3B1	1.571		
4B1	1.580		
5B1	1.583	Reproterol	1.445
2001B1	1.558	Budesonide	1.264
2002B1	1.572	Lactose	1.533

Table 2.9.2 Sample densities evaluated using helium pycnometry

2.9.4 Concluding comments

Statistical analysis using one-way analysis of variance ($P<0.05$) shows no significant difference between the evaluated density values for nedocromil sodium samples.

The density values derived for the samples of nedocromil sodium and sodium cromoglycate are significantly different ($P<0.05$).

2.10 BET Analysis

BET analysis is a gas adsorption technique which can be used to quantify particle surface area. In this context, adsorption is the phenomenon which occurs when gas molecules impinge upon a solid and reside on the surface for a finite time. The amount of gas adsorbed depends upon the nature of the gas (adsorbate) and the solid (adsorbent), and the pressure at which adsorption takes place.

The derivation of surface area from gas adsorption data assumes that the total amount of gas adsorbed will form a complete monolayer coverage of the powder particles. However, as the solid surface becomes progressively coated, the probability increases that a gas molecule will strike and be adsorbed onto a previously bound molecule. The Brunauer, Emmett and Teller (BET) theory [33] enables an experimental determination of the number of gas molecules required to form a monolayer, despite the fact that exactly one monomolecular layer is never actually formed.

The BET equation is expressed below:

$$\frac{1}{V\left(P_0/P-1\right)} = \frac{1}{V_m c} + \frac{c-1}{V_m c}\left(\frac{P}{P_0}\right) \qquad \text{(equation. 2.10.1)}$$

where P = partial pressure of the adsorbate

P_0 = saturated vapour pressure of the adsorbate

V = volume of adsorbed gas

V_m = volume of adsorbed gas in a completed monolayer

c = constant = $e^{(\Theta_1-\Theta_L)/RT}$ where Θ_1 = heat of adsorption of the first layer

Θ_L = heat of liquefaction of the bulk liquid

The determination of surface area from the BET theory follows the construction of a plot of $1/V\left(P_0/P-1\right)$ against P/P_0. This yields a straight line with a gradient $(c-1)/V_m c$ and intercept $1/V_m c$. A value for V_m can then be determined, by solving equation 2.10.2

$$V_m = 1/(\text{gradient} + \text{intercept}). \qquad \text{(equation. 2.10.2)}$$

Single point BET analysis can be used as an alternative to construction of the above plot. As the name suggests a single point of data is evaluated rather than a complete isotherm. The errors introduced by this method are very small [33]. This method is possible using the following approximation of the BET equation.

For high values of c the intercept is small compared to the gradient, which can be considered negligible. The BET equation therefore simplifies to:

$$V_m = V(1 - P/P_0) \qquad \text{(equation. 2.10.3)}$$

The evaluation of V_m, the volume of adsorbed gas required to form a monolayer, leads to the determination of particle surface area using a working formula such as equation 2.10.4 (see section 2.10.4).

2.10.1 Materials

Sample	Batch Number
Nedocromil sodium	5B1
Nedocromil sodium	2001B1
Lactose	022303

Table 2.10.1 Surface area determination sample summary

Samples of nedocromil sodium for which the extreme values of density were derived were analysed using gas adsorption. The samples were prepared for analysis as shown in Table 2.10.2.

Sample preparation	Batch Number
Ambient conditions	5B1, 2001B1
60 % relative humidity	5B1, 2001B1
Heated to 80 °C under helium for 12 hours	5B1, 2001B1

Table 2.10.2 Sample preparation prior to BET analysis

2.10.2 Apparatus

A Quantachrome BET apparatus was used to determine the surface area of the samples. Nitrogen gas was used as the adsorbate with helium as the carrier.

2.10.3 Method

The single point BET method used determined the amount of gas adsorbed by the sample volumetrically. In this method the sample is situated in a steadily flowing stream of a mixture of two gasses. One is the adsorbate and the other the 'carrier' gas. An environment is created in which the adsorbate is removed from the gas mix and retained on the sample surface. This is followed by a change in conditions such that the adsorbate is no longer associated with the sample. The desorption of the adsorbate causes an increase in pressure of the gas mix flowing from the sample. The magnitude of the pressure increase is translated to a deflection from normal on a chart recorder. Prior to use the recorder was calibrated by injecting a precise volume of adsorbate to the stream of gas flowing from the sample. The deflection caused by the pressure increase due to the calibration volume was recorded. A calibration injection producing a similar deflection as that caused by release of adsorbate was also carried out after every adsorbate determination.

A known mass of sample was measured into the sample tube of the apparatus. The mix of the nitrogen and helium gasses was set so

that 15 % of the total pressure of the gas mix was due to nitrogen. At a given pressure the quantity of physically adsorbed gas increases with a decreasing temperature. The adsorption measurements were therefore carried out at the temperature of liquid nitrogen. A vessel containing liquid nitrogen was positioned such that the tube containing the sample was submerged fully. This was held in position until nitrogen adsorption was completed and the total gas pressure returned to the normal. The vessel containing liquid nitrogen was then replaced by a beaker containing water at ambient temperature. The pressure increase of the gas mix was recorded on the chart recorder. A calibration volume was the injected and the resultant pressure increase recorded.

2.10.4 Results

Single point BET analyses can be carried out to determine the surface area of the powder sample. The use of nitrogen as the adsorbate at liquid nitrogen temperatures results in a high value for c, the constant in the BET equation [34]. Therefore equation 2.10.3 can be applied.

The sample surface area was evaluated using the following working formula.

$$S_t = \left(\frac{A}{A_c}\right) V_c \left(1 - \frac{P}{P_0}\right) \overline{N} A_{cs} \frac{P_a}{RT} \qquad \text{(equation. 2.10.4)}$$

where S_t = sample surface area (m^2)

A = signal height

A_c = calibration height

V_c = calibration volume (m^2)

P = partial pressure of adsorbate (Pa)

P_0 = saturated pressure of adsorbate (Pa)

$\overline{N}$ = Avogadro's number (mol^{-1})

A_{cs} = adsorbate molecule cross-sectional area (m^2)

P_a = ambient pressure (Pa)

R = molar gas constant ($J\ mol^{-1}K^{-1}$)

T = ambient temperature (K)

Samples of nedocromil sodium were used from ambient conditions, from conditioning at 60 % relative humidity, and from conditioning overnight in a stream of helium being heated to 80 °C.

The single point BET analysis derived the following values for the surface area of the samples.

Drug sample and storage conditions	**Specific surface area** (m^2g^{-1})
Nedocromil sodium, ambient conditions batch 5B1	8.46 (SD±0.13)
Nedocromil sodium, 60 % relative humidity batch 5B1	4.65 (SD±0.09)
Nedocromil sodium, heated to 80 °C under helium for 12 hours batch 5B1	8.88 (SD±0.20)
Nedocromil sodium, ambient conditions batch 2001B1	8.52 (SD±0.06)
Nedocromil sodium, 60 % relative humidity batch 2001B1	4.88 (SD±0.19)
Nedocromil sodium, heated to 80 °C under helium for 12 hours batch 2001B1	9.05 (SD±0.11)
Lactose, ambient conditions	0.16 (SD±0.004)

Table 2.10.3 Surface area values

2.10.5 Concluding comments

Statistical analysis shows no significant difference in specific surface area between the two drug batches when stored in laboratory conditions, and when heated under helium ($P<0.05$). The values derived for the surface area of samples stored at 60 % relative humidity show a significant difference.

2.11 Drug assay

Ultraviolet spectroscopy was used as the assay method for the aqueous solutions of nedocromil sodium, sodium cromoglycate and reproterol. It was necessary to determine the compliance of these drug solutions with the Beer-Lambert equation.

The ultraviolet and visible spectra of organic compounds are associated with transitions between electronic energy levels. Excitation of electrons above 200 nm from p- and d- orbitals, and π-orbitals and π-conjugated systems, give rise to spectra which is easily measured.

The energy of electronic excitation is related to wavelength by the following:

$$E(\text{kJ/mol}) = {1.19 \times 10^5}/{\lambda(\text{nm})} \qquad \text{(equation 2.11.1)}$$

The energy of electronic excitation for each drug compound can be calculated after determination of the λ_{max} wavelength for each solution. This was done by performing a scan over the wavelength range 300-220 nm. The energy of excitation for nedocromil sodium, sodium cromoglycate and reproterol was found to be 469 kJ, 365 kJ and 433 kJ, respectively.

Two empirical rules have been formulated to describe adsorption intensity. Lambert's Law states that the fraction of incident light absorbed is independent of the intensity of the source. Beer's Law states that the absorption is proportional to the number of absorbing

molecules. The combined Beer-Lambert equation is shown in equation (2.9.2). i.e. Beer-Lambert Law.

$$\log_{10}(I_0/I) = \in cl = A \qquad \text{(equation 2.11.2)}$$

where I_0 = intensity of incident light

I = intensity of transmitted light

$\in$ = molar extinction coefficient ($dm^3 mol^{-1} cm^{-1}$)

c = solution concentration ($mol\ dm^{-3}$)

l = path length (cm)

A = absorbance

The factor $\log_{10}(I_0/I)$ is therefore proportional to the amount of absorbing material present in the sample. The absorbance, also known as optical density, is related to the transmittance (T) as shown in equation 2.11.3

$$A = 1/T = \in cl \qquad \text{(equation 2.11.3)}$$

Since $\in$ and l are constant, a linear relationship between absorbance and concentration of drug indicates compliance of the compound with the Beer-Lambert Law.

2.11.1 Method

Solutions were prepared of the sample drug in deionised water. U.V spectroscopy was carried out using a Philips PU 8729 UV/Vis Scanning spectrophotometer with a 1 cm path length.

2.11.2 Results

Figures 2.11.1, 2.11.2, and 2.11.3 show the Beer-Lambert plots for nedocromil sodium, sodium cromoglycate and reproterol respectively.

In order to ascertain the effect of the presence of lactose on the absorption spectra, solutions of lactose were assayed at the λ_{max} values for each compound. No interference was observed due to the presence of lactose in any of the solution.

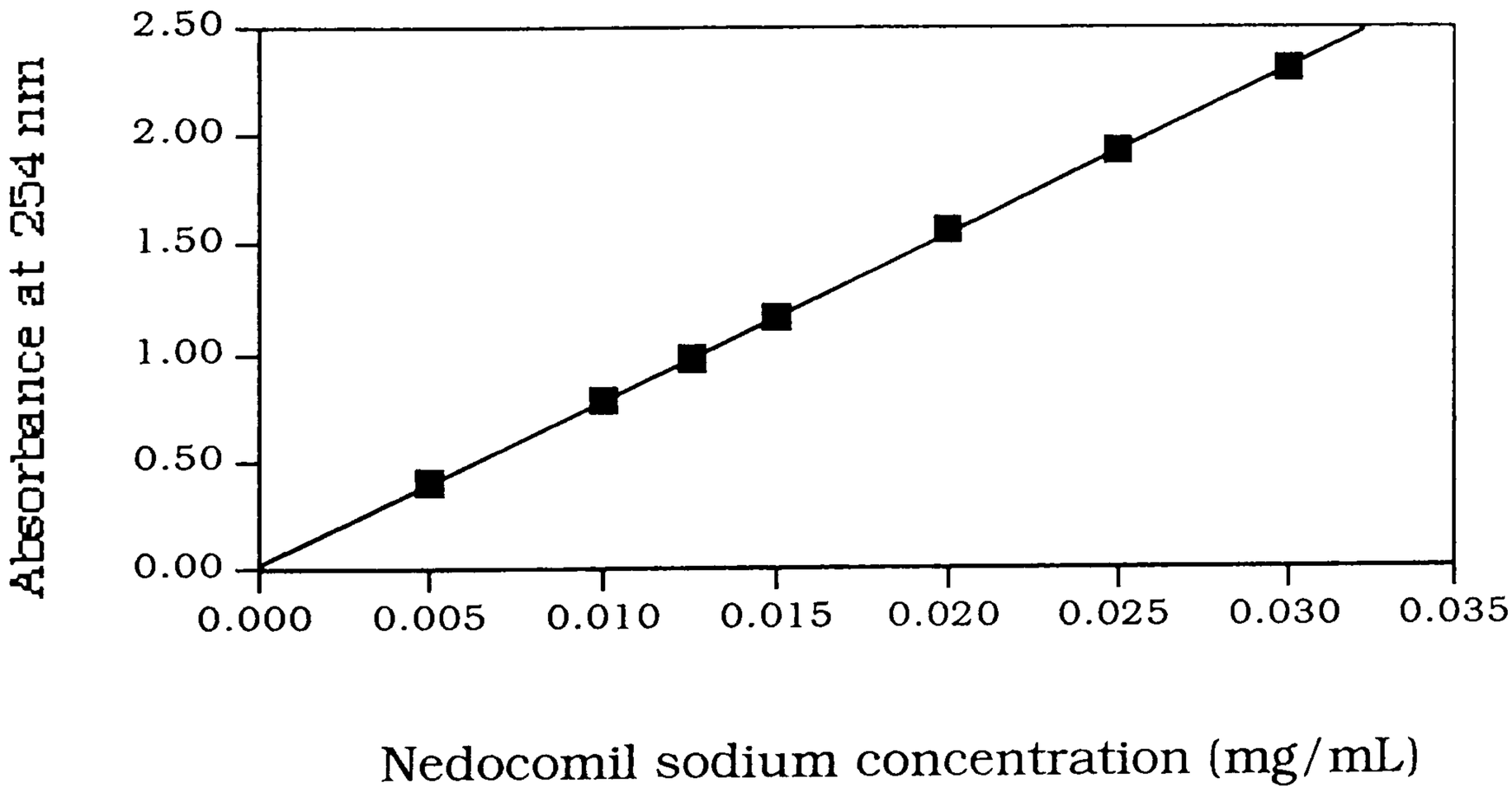

Figure 2.11.1 Beer-Lambert plot for nedocromil sodium in deionised water at 254 nm

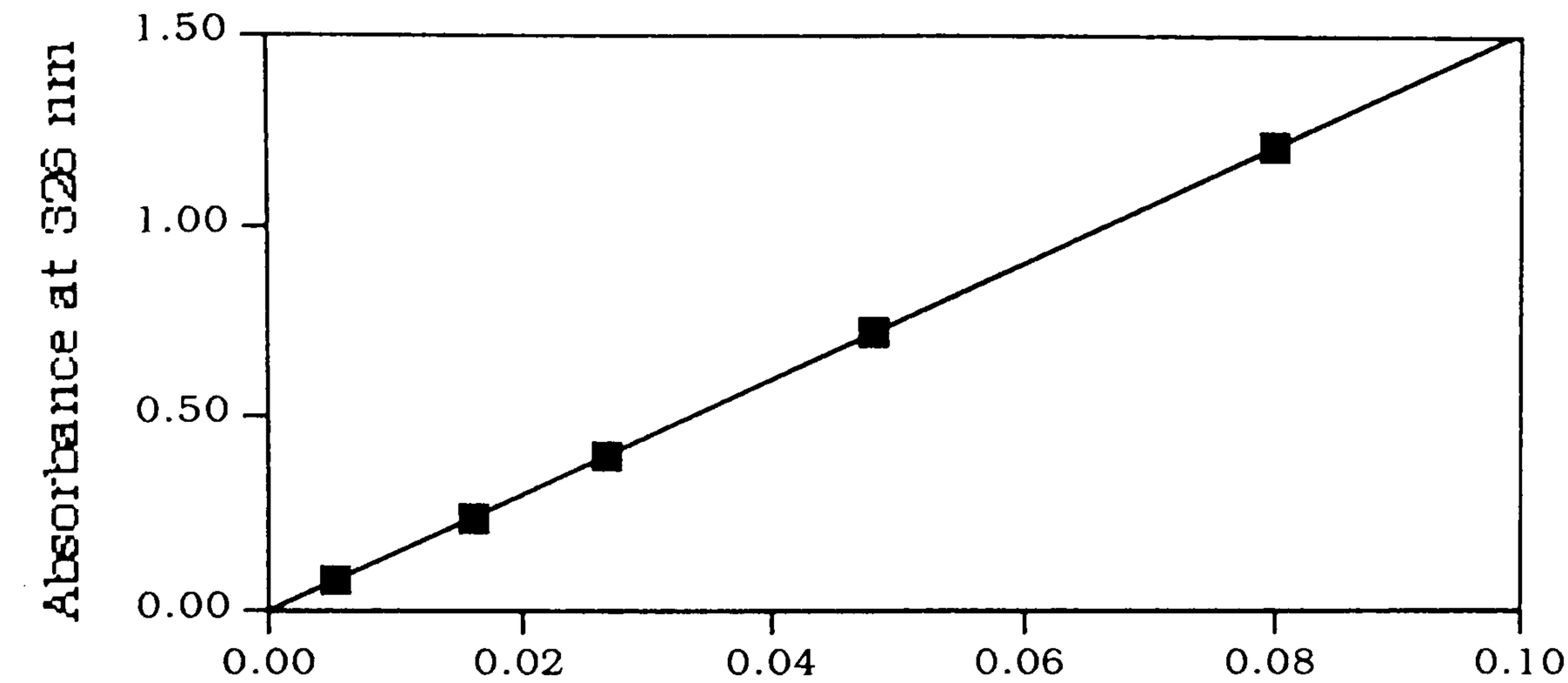

Figure 2.11.2 Beer-Lambert plot for sodium cromoglycate in deionised water at 326 nm

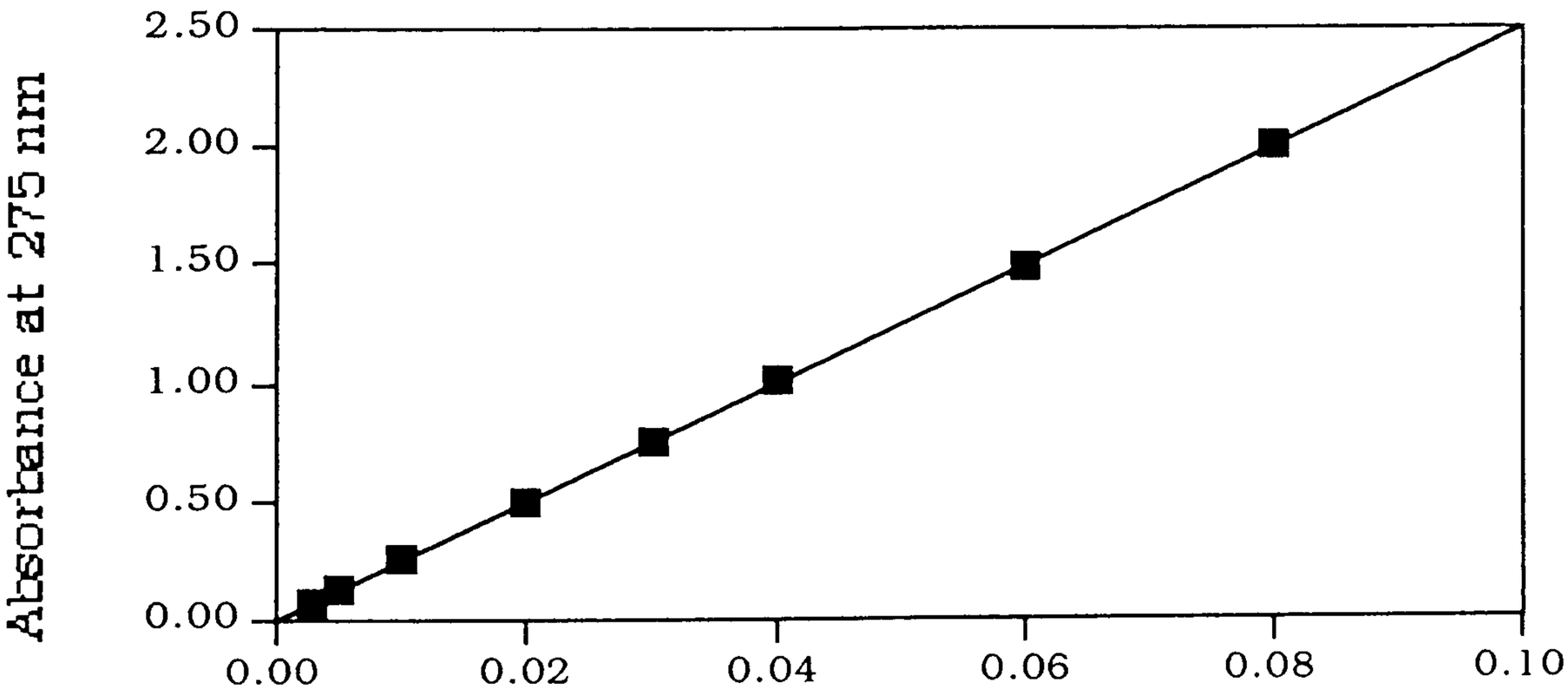

Figure 2.11.3 Beer-Lambert plot for reproterol in deionised water at 275 nm

2.11.3 Summary of standard curve equations

Drug species	Wavelength of maximum U.V absorbance	Standard curve equation
Nedocromil sodium	254 nm	$\text{Conc}_{(\text{mg/mL})} = \frac{\text{Abs} - 0.012}{77.009}$
Sodium cromoglycate	326 nm	$\text{Conc}_{(\text{mg/mL})} = \frac{\text{Abs} - 0.001}{15.103}$
Reproterol	275 nm	$\text{Conc}_{(\text{mg/mL})} = \frac{\text{Abs} - 0.004}{24.937}$

Table 2.11.1 Standard curve equations

2.12 Discussion

Particle characterisation was carried out for the five batches of the drug nedocromil sodium. No significant physical differences were detected between the batches using these testing procedures. However, interbatch variation has been observed with respect to the performance of the drug with respect to blending with lactose and drug release evaluated using a multi-stage liquid impinger. This variation may be due to the possible introduction of crystalline disorder onto particle surfaces due to the size reduction process.

The particles of nedocromil sodium have been subjected to Apex milling in order to achieve the small size fraction required for pulmonary delivery. Gross changes in the physical states of raw materials have been observed due to particle size reduction [35-38]. The energy input during communition can impart amorphous character to once highly crystalline particles. Often these amorphous regions constitute only a small percent of the total mass. Because these regions are very small they are beyond the limits of detection by traditional analytical methodologies [39]. However, these small areas of amorphous material can have profound physical effects [40]. Aggregation of small particles in suspension as a response to the processing techniques used to prepare micronised material had been observed [39]. This change affects the surface energy of the particles and consequently their interfacial interactions may be responsible for the batch variation behaviour of nedocromil sodium.

These subtle changes of the surface of the particle have been detected by the recently developed techniques of microcalorimetry [41, 42] and water sorption [43]. Unfortunately these techniques were not available to me at the time of doing this study.

12.13 Conclusion

A series of characterisation techniques have not unveiled a detectable difference in the behaviour of five batches of nedocromil sodium. More sensitive techniques may have to be employed in order to ascertain the reasons that cause variable batch behaviour when the drug is presented as an inhalation dosage form.

The characterisation confirms the batches of materials as nedocromil sodium trihydrate, sodium cromoglycate with a typical content of associated water, anhydrous reproterol and budesonide and α-lactose monohydrate.

Chapter Three

Preparation and structure determination of binary powder mixes used for inhalation therapy

3.1 Aim

The aim of this chapter was to prepare binary interactive powder mixes and evaluate their structure. The materials characterised in Chapter Two were used to prepare the powder blends. The structure of the blends was investigated using scanning electron microscopy.

3.2 Introduction

Mixing may be defined as a process where two or more components are treated so as to lie as nearly as possible in contact with a particle of each of the other components [44]. Two distinct structures of powder mixes have been classified. These are non-interactive mixes, in which the constituent particles are independent of each other, and interactive mixes in which a degree of association takes place between the constituents.

Non-interactive mixing

Analysis of a non-interacting powder system provides the contrast for the interactive type powder mixes. Two species of equally sized and weighted non-interacting particles combine to form a mix of this type. The distribution of the particles prior to mixing can be represented diagrammatically by Figure 3.2.1. The solid and open circles represent the two powder species. Before the mixing process is started the two groups are totally unmixed, or perfectly segregated.

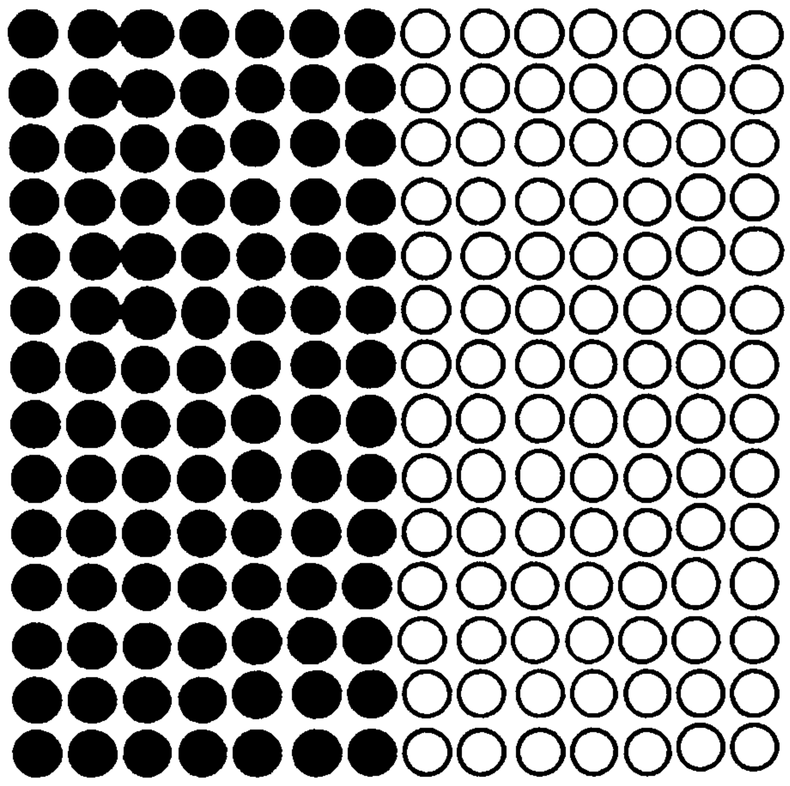

Figure 3.2.1

If a perfect mix were formed, both species of powder would have the same distribution throughout the mix, each particle being adjacent to a particle of the different species for a 50:50 mix of each component. This can be represented diagrammatically by Figure 3.2.2.

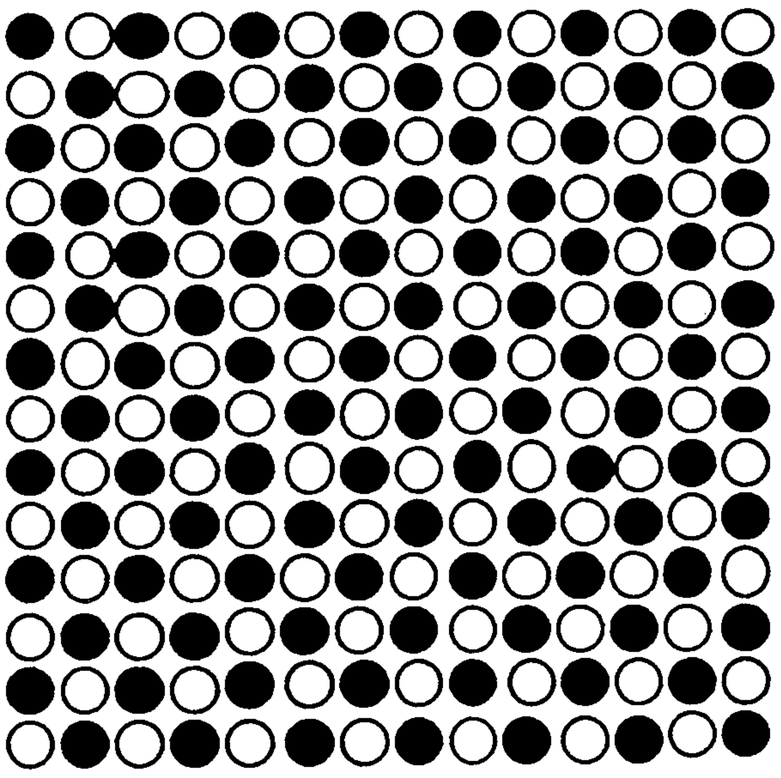

Figure 3.2.2

Mixing is a disorder-creating process and is very unlikely to produce the regularity seen in the system of a perfect mix. The best attainable mix is the result of a mixing mechanism in which there is equal chance of any individual particle being at any given point at any one time. The diagrammatic representation of this random mix is shown in Figure 3.2.3.

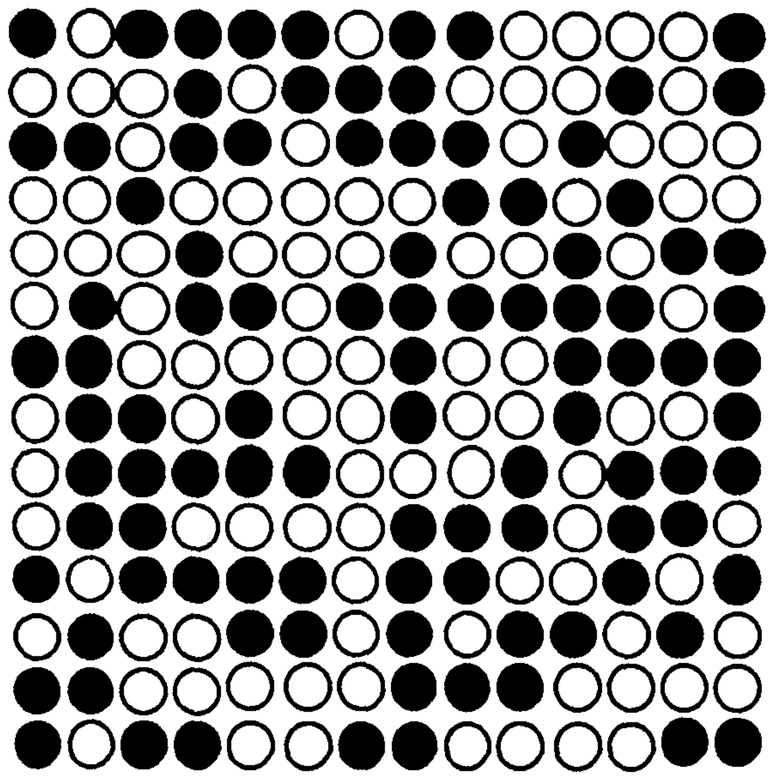

Figure 3.2.3

Homogeneity

The probability of locating a given particle at a given point in a non-interactive powder mix containing similar quantities of each species can be described by a binomial distribution. From this the quality of the random mix can be determined by calculating the variance or standard deviation of the drug content of samples taken from the mix. Theoretical variances relating to totally unmixed (Figure 3.1, equation 3.1) and the random type of mix (Figure 3.3, equation 3.2) were developed by Lacey [45].

$$\sigma_0^2 = x.y \qquad \text{(equation 3.2.1)}$$

$$\sigma_R^2 = {}^{x.y}/_{n} \qquad \text{(equation 3.2.2)}$$

where x and y are the proportions of the two component powders, n is the number of particles and σ_o and σ_R are the theoretical variances for the unmixed and random systems respectively.

From this basic principle many formulae have been derived to describe real situations where components differ in physical

characteristics, and sampling is carried out by different means [46, 47]. These theoretical calculations aim to define the lowest value for the standard deviation of samples taken from the mix when the best attainable mix has been formed.

Segregation

The process of mixing is in dynamic equilibrium with the demixing process, segregation [48]. Segregation describes the preference of particles, possessing a similar property, for being at some part of the system [49]. Segregation of a powder is caused by differences in the physical and mechanical properties of the constituent particles. The properties of powders which are known to cause segregation include relative density, shape or roughness, resilience and relative size of the particles [46]. Of all the causes of segregation, particle size is considered to be the most important [50].

Mechanisms of segregation can be considered according to the forces acting on the particles. Trajectory segregation occurs when particles of different mass are set in motion. Larger particles with larger kinetic energies tend to have increased stopping distances. Therefore similar particles, having similar stopping distances tend to travel to the same areas in the powder bed. Percolation segregation describes the mechanism of particles travelling through the voids in the powder bed. This can occur either when the powder bed is at rest, or when slip planes are formed. Densification segregation occurs when powders of a dissimilar size are vibrated. The smaller particles tend to fall through

the interstices between the large particles and travel to the bottom of the powder bed.

According to the mechanisms above, mixing a micronised powder with larger solid particles would create a mix in which segregation would dominate due to the size differences of the powder components. A very poor homogeneity would be expected from such a mix. However it was first observed by Travers and White [51] that these type of mixes exhibited a resistance to segregation.

Interactive mixes

According to Jones and Pilpel [52] particles below 50 μm in diameter tend to be adsorbed onto the surfaces of coarser particles in a powder mix to form a coating which may or may not be continuous. The prevention of segregation by the adsorption of fine particles onto larger crystals was identified by Travers and White [51]. Hersey [53] introduced the term of 'ordered mixing' implying the presence of adhesion due to particulate interactions. Unfortunately the term ordered mixing was used subsequently in the literature with different meanings, leading to misunderstanding and ambiguity.

The term 'order' was originally proposed to distinguish the type of mixture and describe its structure [54]. Mixes of interactive powders in which adhesion takes place between constituents, and mixes of free flowing constituents were named 'ordered mixes' and 'random mixes' respectively.

The term 'ordered mix' has been misinterpreted, and has been used to describe the degree of homogeneity within the powder blend. An incomplete mix, where the standard deviation of drug content in the samples is greater than the theoretical best attainable mix according to random theory, has been contrasted with an 'ordered mix' in which the standard deviation is smaller than expected.

This confusing terminology was addressed with the suggestion to use two terms, one to define the type of mix, and a second to describe the level of homogeneity [54, 55]. The terms interactive and non-interactive have now become more acceptable to describe the types of mix in which the constituents are cohesive or free flowing respectively [56, 57]. Description of the degree of mixing relates the real mix to the best attainable mix according to random theory. The terminology incomplete, random and ordered has been suggested to differentiate between mixes in which the level of homogeneity corresponds to worse than, equal to, and better than that of the theoretical best attainable mix [55]. However, as much confusion has surrounded the term 'ordered', it has been suggested that it is preferential to describe the level of homogeneity by use of a measure such as standard deviation, or simply by a descriptive phrase [54].

Adhesion mechanisms

The mechanisms which cause adhesion between solid particles are listed below:

A) Van der Waals' forces

B) Electrostatic forces

C) Forces due to liquid bridges

D) Mechanical forces, resulting from interlocking of irregularly shaped particles

E) Solid bridging forces, present when individual particles have been joined at points of contact by sintering or precipitated impurities.

F) Magnetic forces, associated with materials having an appreciable magnetic moment [58].

Applied to the situation of dry, solid particles, it is the van der Waals' forces which play the most important part in the adhesion mechanism [59].

Van der Waals' forces are short range intermolecular forces, which are noticeable only when particles come sufficiently close together, that is, separation distances of the order 0.2 nm to 1 nm. All intermolecular forces are essentially electrostatic in origin. The three types of force which contribute to the total van der Waals' force are orientation (Keesom forces), induction (Debye forces) and dispersion (London forces) [60].

Orientation forces are due to atoms or molecules with permanent dipoles. A permanent dipole moment can also polarise a non-polar medium, the resultant force being the induction force. Whilst the time average variation of charge is zero, the charges and dipoles generated by the movement of the charges is subject to statistical variation, the same as any other physical variable. These interacting dipoles cause a steady, fluctuating electromagnetic field, which results in the omnipresent dispersion forces [61].

The magnitude of van der Waals' forces is proportional to the particle diameter. The gravitational force is proportional to the cube of the diameter. Therefore, when the particle diameter exceeds a few microns, the magnitude of the van der Waals' force becomes negligible when compared with that of the gravitational force.

The electrostatic attraction between particles can occur to a greater extent if the powders are subjected to triboelectrification. The relative difference in energy levels of the Fermi electrons can allow excipient and drug particles to have different surface charge signs which causes interparticulate attraction. The electrostatic charge is lost through earth leakage relatively quickly. However, improved van der Waals' bonding can take place due to the close surface contacts facilitated by the triboelectrification [62].

Mechanical interlocking creates multiple interparticle contacts which increases the magnitude of the van der Waals' forces experienced by the particle. It also prevents removal of the adhered particle due to abrasion, as the adhered particle experiences a degree of protection. This can be seen in Figure 3.2.4.

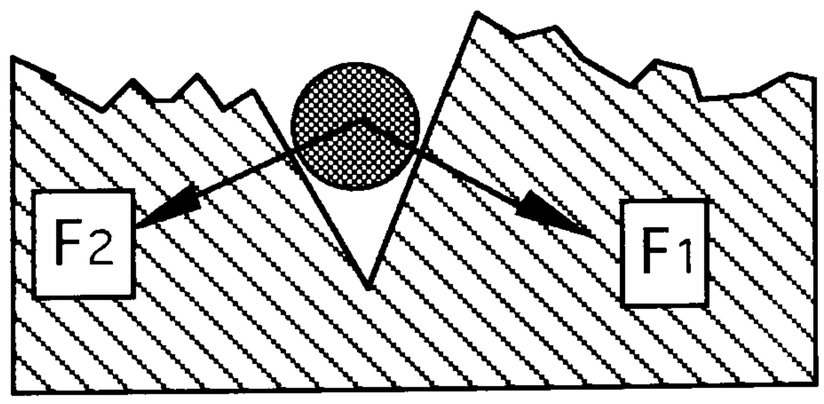

Figure 3.2.4 Mechanical interlocking of a small adhered particle [62] .F_1 F_2 represent the adhesion forces.

Structure of interactive mixes

It has been stated that ideally the weight of particles of drug bound to the carrier particle is in direct proportion to the surface area of the carrier particle [63], implying that the carrier particles are covered with a monolayer of fine particles [64]. The number of fine particles which can be accommodated on the surface of each carrier particle, assuming a hexagonal close packed arrangement of the fine particles, can be calculated from equation 3.3 [52].

$$n = \frac{4\pi(R + r)^2 \phi}{2r^2\sqrt{3}} \qquad \text{(equation 3.2.3)}$$

where n = number of fine particles
R,r = large particle and small particle radius
ϕ = fraction of the maximum number of small particles associated with the carrier particle

If ϕ is taken as unity, then the calculation relates to a saturated monolayer of fine particles covering the surface of the carrier particle.

Only one piece of published experimental work has found good agreement between the theoretical number of fines associated with each carrier particle and the number determined experimentally [65].

According to Hersey [53], using a lower concentration of fine particles than the saturation value would lead to the total number of sites for adhesion not being filled. Conversely, more fine particles than the saturation number would lead to the excess fines not adhering and behaving as non-interacting particles dispersed in the mix in a random

manner. Experimental evaluation has led to the determination of non-adhered fine particles in the powder mix [66].

When the concentration of fine particles surpasses the number required to form a monolayer, carrier particles have been observed to become spherical or elliptical in shape. It has been suggested that this formation of a multi-layer coverage follows a monolayer coverage. As the concentration of fines in the mix increases, the multilayer, initially filling the void space or surface indentations continues to produce a smooth particle [64], as described in Figure 3.2.5.

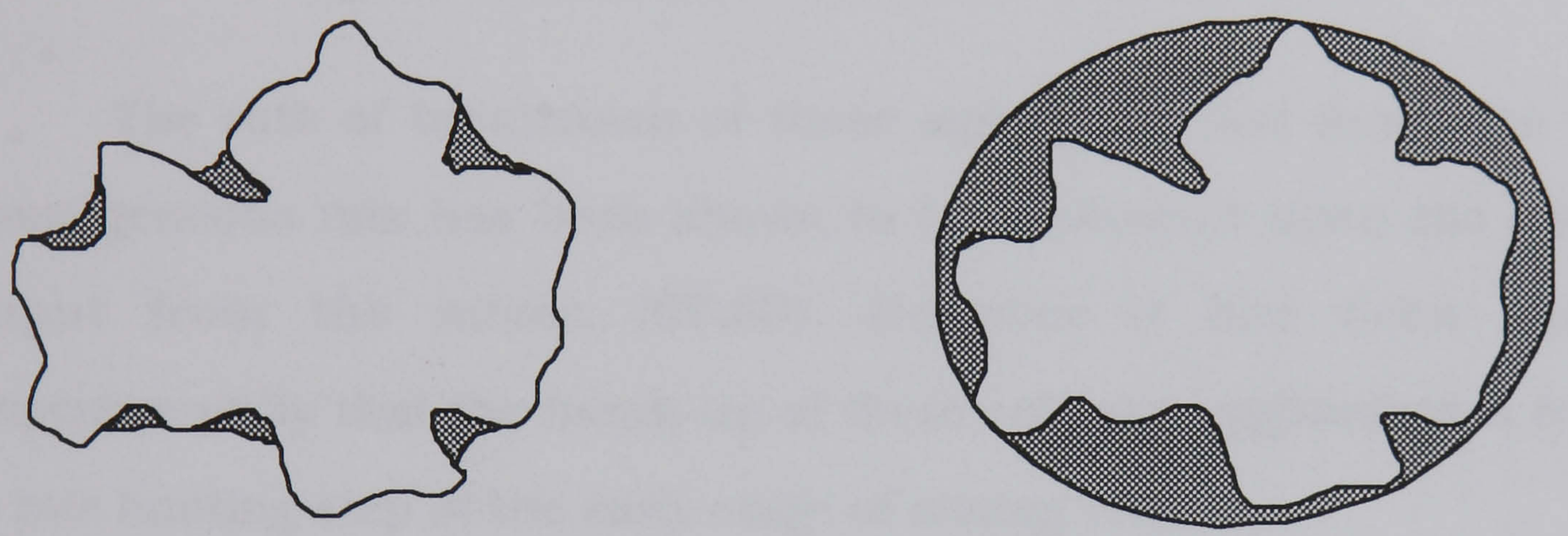

Figure 3.2.5 Schematic representation of multi-layer formation [64]

In order to adhere single cohesive particles the mixing process must first break down aggregates of the fine powder. This two step mechanism for the production of an interactive mix has been suggested by Stephenson and Thiel [67] and can be represented diagrammatically as shown in Figure 3.2.6.

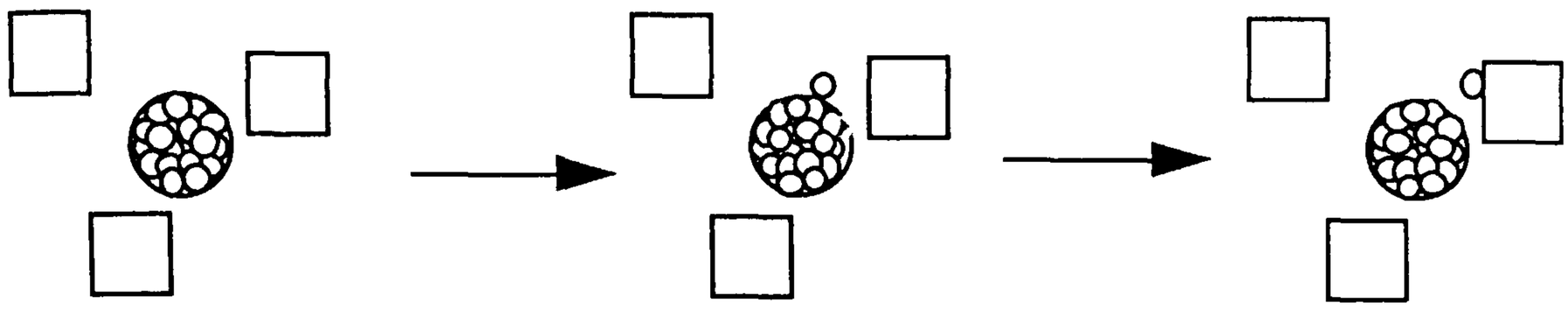

○ Adherent particle

Agglomerate of adherent particles

Carrier particle

Figure 3.2.6 Formation of an interactive unit

The rate of breakdown of these aggregates and formation of a homogeneous mix has been shown to be dependent upon the energy input from the mixer. [67-69]. However it has been shown experimentally that the break-up of these cohesive agglomerates is not a rate limiting step at the early stage of mixing [70].

It has been suggested that the agglomerates formed due to the cohesive nature of the fine particles could randomly mix with the coarse particles, in a non-interactive manner [71]. A combination of interactive and non-interactive behaviour has also been suggested, whereby a uniformed weight fraction leaves the agglomerates and adheres uniformly to the carrier particles [72]. Each adhesive interaction which has been considered involves a single fine particle adhering to a carrier particle as part of the process to form a monolayer coverage of the carrier.

Homogeneity

As with non-interactive powder mixes, the degree of mixing can be expressed by the comparison of the sample standard deviation of drug content of the withdrawn samples and the sample deviation for a random mixture, σ_R, of the same system.

With the introduction of the concept of fine particle adhesion in interactive mixes came the suggestion that the homogeneity of such powder mixes would be of a higher degree than that observed in the best attainable non-interacting random mix [53]. This has been supported by experimental findings [67, 68, 73].

Increased homogeneity in interactive mixes has since been established as an ideal situation, and is unlikely to occur in real powder mixes [54]. Statistical and experimental analysis have shown that the best degree of homogeneity seen in interactive mixes corresponds to that of a fully randomised system [65, 74, 75]. This is due to non-uniform distribution of fine particles on the carrier, a range of carrier and fine particle sizes, and unsatisfactory calculation of the sample variance of a random mix for the same system.

In order for homogeneity to increase, complete adhesion of an identical number of equally sized fine particles to each coarse, monosized carrier particle must take place [75].

Microscopic examination of interactive mixes has shown that the drug particles have a tendency to adhere to surface irregularities of the carrier particle [76]. This verifies the suggestion that indentations of

the carrier's surface are initially the sites of adherence for the fine particles [51, 66, 77]. This has led to the implication that the physical properties of the carrier particle surfaces are more important than pure stereometry [76].

Sites for adhesion due to surface indentations trapping particles, electrostatic forces [62], van der Waals' forces [64] and moisture bonding [78] have been suggested.

Individual carrier particles are not equivalent with respect to their relevant surface properties, and therefore to their binding capacity [75]. This erratic distribution of fine particles on the surface of the carrier has been observed experimentally [79, 80].

Therefore, because no mechanism exists to control the distribution of the adhering small particles, the state of **random adhesion** has been suggested [75]. This implies a random distribution of fine particles on the carrier surface. If the adherence occurs in a random fashion, then the quality of a fully randomised system can be achieved at best.

The Stange-Poole equation [81], a derivation from Lacey's binomial approach, was used to calculate the sample variance for the random mixture when a greater degree of homogeneity for the interactive mixes was claimed [67, 68, 73]. Theoretically, the variance of a random mix for a system containing a minor drug component, as is often the case in pharmaceutical powders, should be derived from the Poisson distribution [82]. Achieving a lower sample variation experimentally than that estimated for a random mix cannot,

therefore, imply a greater degree of homogeneity as the equation used to estimate the random quality did not apply to the system examined [83].

For pharmaceutical preparations, it is not the absolute standard deviation but the coefficient of variation which is of interest. This follows from the tolerance limits for the drug content variation of dose units being stated as a percentage of the mean drug content. The percentage coefficient of variation is the standard deviation (σ) expressed as a percentage of the arithmetic mean (μ):

$$C.V = (\sigma/\mu) \times 100 \qquad \text{(equation 3.2.4)}$$

Since σ and μ are both expressed in the same units as the variate, C.V. is independent of the units of measurement [84].

As stated earlier, the theoretical best possible mix of interactive constituents is one in which the fine particles are adhered in a random manner. The homogeneity of such a mix can be estimated from the Poisson distribution. Equation 3.2.5 derived by Johnson [85] and modified by Ergermann [86] describes this homogeneity

$$C_R = 100\sqrt{\frac{\overline{m}}{G}} \qquad \text{(equation 3.2.5)}$$

where C_R is the coefficient of variation of drug content as a percentage of the mean content G of the adherent ingredient per sample, and $\overline{m}$ is the volume-weighted mean particle mass of the ingredient. This assumes a mono-disperse diluent.

Identification of an interactive mix

It has been suggested in the literature that the creation of an interactive powder mix could be identified by the relationship between the sample variance and the sample size. When dealing with non-interacting powder mixes the relationship between the sample size and the sample deviation is such that the variance of the sample decays inversely with the sample size [45, 87]. Formation of an interactive powder mix has been suggested to lead to a constant standard deviation (σ) of the samples which is independent of the sample size [68]. This relates to the ideal interactive mix where complete adhesion of an identical number of equally sized fine particles to each coarse, monosized carrier particle takes place, and $\sigma = 0$ is purely theoretical [54]. The experimental data to support this suggestion [67, 68, 73] has been questioned by Orr [88], who suggested the real relationship between sample variance and size was being masked by large standard errors due to sampling and analytical procedures. A computer simulation of ordered mixes [89] showed that there was an inverse relationship between the sample standard deviation and the square root of the sample size for both interacting mixes and non-interacting random mixes.

Segregation

The interest in interactive mixes developed from the phenomena that this type of mix showed a unexpected resistance to segregation [51]. However this does not imply that segregation does not take place. Drug-lean and drug-rich areas have been determined in interactive

mixes [50]. These can be explained with the concepts of 'constituent' and 'ordered unit' segregation [90].

Constituent segregation results from the disassociation of the adhered fine particle and the larger carrier particle. This occurs if the force applied to the mixture is sufficient to break the adhering bond between the particles [90]. After the breakdown of the interactive units the two ingredients have to separate and travel to distinct parts of the powder bed [50]. The mechanism for this is identical to percolation segregation as observed in non-interacting mixes [91].

The term 'ordered unit' has been used to describe a single carrier particle with its associated small particles adhered to the surface. The segregation of these ordered units can occur due to differences in carrier particle size and/or density. Assuming an ideal interactive mix, where a complete monolayer of fine particles covers the surface of the larger particle, segregation of particle size of the vehicle will lead to rich and poor fractions of the drug. Fractions containing large particles of vehicle will have a low surface area and hence be poor in drug content. The converse will also be true [90].

The stability of interactive mixes has been studied experimentally [50, 76, 90, 92, 93]. Although the ideal interactive mix is not achieved when mixing real powders examples of both 'constituent' and 'ordered unit' segregation were observed.

The structure of an interactive powder mix, therefore is a reflection of any adhesive and cohesive interactions which are taking place. These interactions, whilst improving flow characteristics of

powder doses, and providing a means of delivering very small doses of potent actives, may influence the delivery of drug from the powder blend. Therefore, the determination of the structure of binary powder blends used for inhalation therapy will elucidate the extent of adhesive and cohesive interactions. The investigation of the effect of drug concentration and drug type may lead to different drug release characteristics, and will be reflected in the structure of the mix.

3.3 Experimental

Two component, drug and carrier, powder mixes were prepared. The drug species investigated were nedocromil sodium, sodium cromoglycate and reproterol. The carrier species was α-lactose monohydrate. The mixes were assessed for their homogeneity. Image analysis and scanning electron microscopy were carried out in order to observe the structure of the mixes.

3.4 Materials

The following drug and lactose samples were used to prepare the binary mixes.

Sample	Batch
Nedocromil sodium	5B1
Sodium cromoglycate	XC13 CIA M150
Reproterol	092125 M153
α lactose monohydrate	022303 and 022301

Table 3.4.1 Powder samples

3.5 Methods

3.5.1 Mixing

3.5.1.a Theory

The maximum number of fine particles which can be accommodated by the surface of a carrier particle can be derived using equation 3.2.3 [52], as discussed earlier in section 3.2.

$$n = \frac{4\pi(R + r)^2 \phi}{2r^2\sqrt{3}} \qquad \text{(equation 3.2.3)}$$

Taking ϕ to be unity assumes a saturated monolayer. The drug concentrations which correspond to a monolayer coverage of every carrier particle in the mix, calculated using equation 3.5.1 are shown in Table 3.5.1.

Drug	Number of drug particles per carrier particle	Maximum drug concentration (%w/w) for monolayer formation
Nedocromil sodium	384	7.15
Sodium cromoglycate	373	7.32
Reproterol	816	4.40

Table 3.5.1 Drug concentrations for binary interactive mixes

The coefficient of variation for the mixes of nedocromil sodium, sodium cromoglycate and reproterol calculated using equation 3.2.3 are shown below.

Nedocromil sodium

Mean volume diameter (Coulter Counter Analysis) = 2.677 μm

True particle density = 1.583 g/cm^3

Mean particle mass of drug particles = 1.583×10^{-11} g

% w/w drug content in mix	Mean content of drug per 25 mg sample (g) ('G' eqn 3.2.5)	Calculated coefficient of variation (%)
0.4	1.0×10^{-4}	4.0×10^{-2}
1.0	2.5×10^{-4}	2.5×10^{-2}
2.0	5.0×10^{-4}	2.0×10^{-2}
4.0	1.0×10^{-3}	1.3×10^{-2}
40.0	1.0×10^{-2}	4.0×10^{-3}

Table 3.5.2 Calculated values for nedocromil sodium powder mixes

Sodium cromoglycate

Mean volume diameter (Coulter Counter Analysis) = 2.078 μm

True particle density = 1.590 g/cm^3

Mean particle mass of drug particles = 7.470×10^{-12} g

% w/w drug content in mix	Mean content of drug per 25 mg sample (g) ('G' eqn 3.2.5)	Calculated coefficient of variation (%)
0.4	1.0×10^{-4}	2.7×10^{-2}
1.0	2.5×10^{-4}	1.7×10^{-2}
2.0	5.0×10^{-4}	1.2×10^{-2}
4.0	1.0×10^{-3}	8.6×10^{-3}
40.0	1.0×10^{-2}	2.7×10^{-3}

Table 3.5.3 Calculated values for sodium cromoglycate powder mixes

Reproterol

Mean volume diameter (Coulter Counter Analysis) = 2.041 μm

True particle density = 1.445 g/cm^3

Mean particle mass of drug particles = 6.432×10^{-12} g

% w/w drug content in mix	Mean content of drug per 25 mg sample (g) ('G' eqn 3.2.5)	Calculated coefficient of variation (%)
0.15	3.8×10^{-5}	4.1×10^{-2}
1.5	3.8×10^{-4}	1.3×10^{-2}
4.0	1.0×10^{-3}	8.0×10^{-3}

Table 3.5.4 Calculated values for reproterol powder mixes

These values represent the theoretical best attainable mix for the systems in question and therefore the smallest possible values for the coefficient of variation.

A poor quality mix will be reflected by a large value for the coefficient of variation. Experimental determination has led to an acceptable coefficient of variation of less than 2.5 %. Values greater than this suggest binary mixes which are not composed of interactive units [94].

3.5.1.b Method

Drug and lactose samples were weighed using a Mettler AT261 balance. The quantity of each powder mix allowed a 50 % void space within the mixing container.

A specially constructed stainless steel mixing cylinder was used to prepare the mixes. Curved internal joints replacing the 90° angles reduced the dead space in the vessel. The capacity of the vessel was 160 cm^3.

The weighed samples were transferred to the mixing vessel and were mixed for 5 minutes using a Turbula mixer (T2C, W. A. Bachofen, Switzerland) set at 90 revolutions per minute (corresponding to 1.5 Hz). The vessel was then removed from the mixer and gently tapped in order to dislodge any mix which had become adhered to the vertices of the vessel. This was followed by another 5 minute mixing time at the same settings.

Mixes were initially produced with no preparation of the sample. Subsequent mixes used drug powder which had been screened through a 63 μm sieve.

3.5.2 Homogeneity testing

The quality of the mixes was assessed by evaluating the homogeneity. Samples of the dose size, 25 mg, were taken from the mix. The samples were dissolved in deionised water and immediately assayed for drug content by U.V spectroscopy. The percentage

coefficient of variation for the ten samples was acceptable at a value below 2.5%.

3.5.3 Image analysis and scanning electron microscopy

Image analysis and scanning electron microscopy were employed in order to identify the structure of the interactive mixes. Image analysis was carried out using a Zeiss Axioskop microscope, images being produced using a Mitsubishi colour video copy processor (CP 100B). International Scientific Instruments DS130 and a Jeol JSM35 scanning electron microscopes were both used to produce photomicrographs of the powder mixes. Particles were sputtered with gold to a depth of 30 μm prior to analysis by scanning electron microscopy.

3.6 Results

3.6.1 Homogeneity testing

3.6.1a Nedocromil sodium

Binary mixes of nedocromil sodium with lactose at a concentration of 0.4% w/w hydrated drug were prepared from drug samples which had been previously either unscreened or screened through a 63 μm sieve. The assay results of the samples taken from the mixes are shown in Figure 3.6.1.

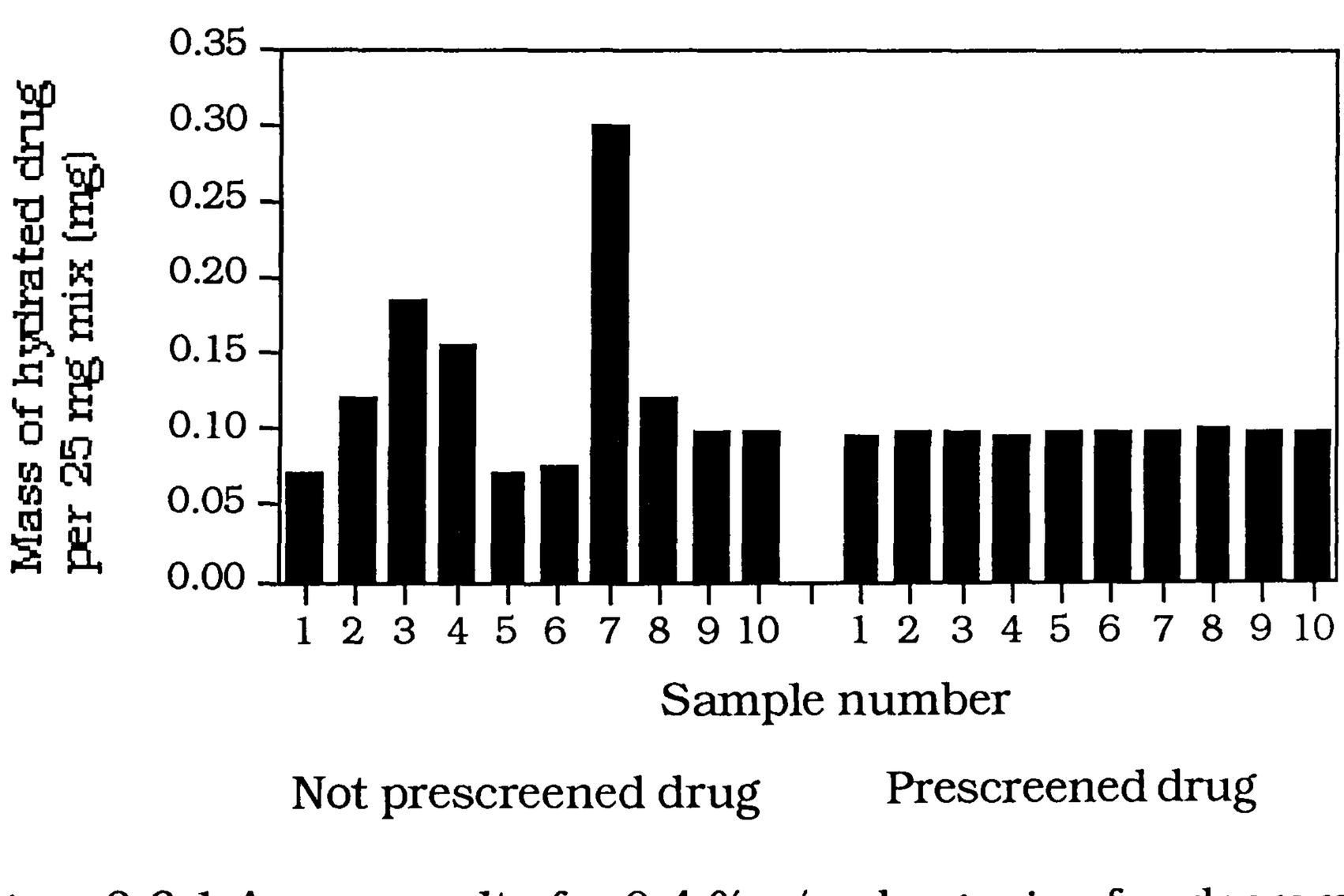

Figure 3.6.1 Assay results for 0.4 %w/w drug mix of nedocromil sodium with lactose

The mean and coefficient of variation for both mixes are shown in Table 3.6.1.

Sample preparation	Mean drug content per sample (mg)	Drug content coefficient of variation (%)
Not pre-screened	0.129	54.399
Pre-screened	0.098	0.985

Table 3.6.1 Comparison of the effect of nedocromil sodium sample preparation upon the powder mix homogeneity

All of the binary mixes subsequently prepared used nedocromil sodium which had been screened through a 63 μm sieve.

The following powder blends were prepared. The corresponding percentage coefficient of variation for ten dose weight samples taken from each batch is shown in Table 3.6.2.

% w/w hydrated drug content	Drug content coefficient of variation (%)	% w/w drug content by assay
0.4	0.985	0.392
1.0	0.854	0.985
2.0	0.450	1.956
4.0	0.750	3.908
40.0	7.371	37.629

Table 3.6.2 Nedocromil sodium powder mix homogeneity data

3.6.1b Sodium cromoglycate

Binary mixes of sodium cromoglycate with lactose at a concentration of 0.4% w/w hydrated drug were prepared from drug samples which had been previously either unscreened or screened through a 63 μm sieve. The assay results of the samples taken from the mixes are shown in Figure 3.6.2.

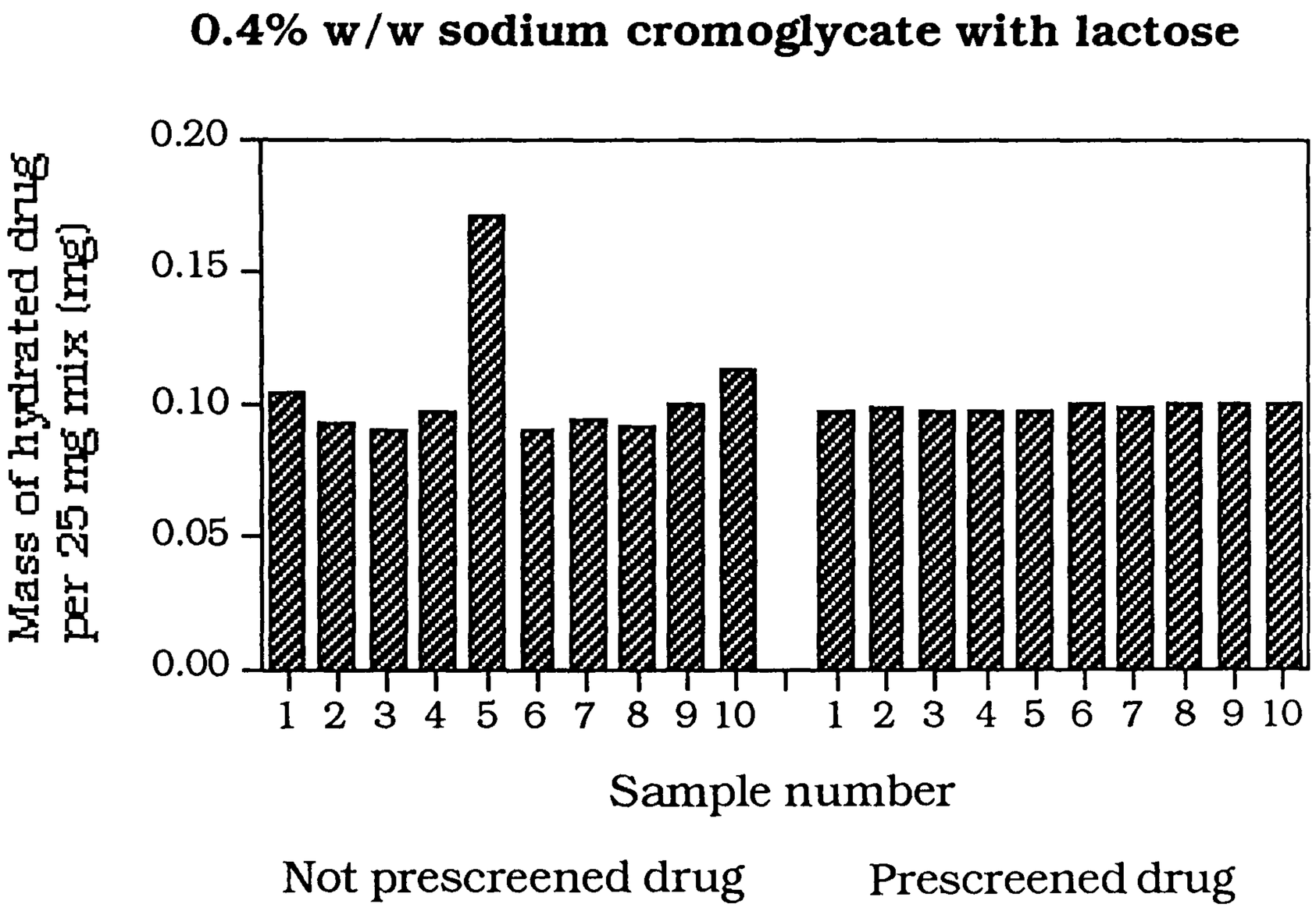

Figure 3.6.2 Assay results for 0.4 %w/w drug mix of sodium cromoglycate with lactose

The mean and coefficient of variation for both mixes are shown in Table 3.6.3.

Sample preparation	Mean drug content per sample (mg)	Drug content coefficient of variation (%)
Not pre-screened	0.104	23.591
Pre-screened	0.099	1.444

Table 3.6.3 Comparison of the effect of sodium cromoglycate sample preparation upon the powder mix homogeneity

All of the binary mixes subsequently prepared used sodium cromoglycate which had been screened through a 63 μm sieve.

The following powder blends were prepared. The corresponding percentage coefficient of variation for ten dose weight samples taken from each batch is shown in Table 3.6.4.

% w/w hydrated drug content	Drug content coefficient of variation (%)	% w/w drug content by assay
0.4	1.444	0.394
1.0	0.937	0.960
2.0	2.318	1.905
4.0	1.684	3.704
40.0	2.130	39.156

Table 3.6.4 Sodium cromoglycate powder mix homogeneity data

3.6.1c Reproterol

Binary mixes of reproterol with lactose at a concentration of 0.15% w/w drug were prepared using drug samples from drug samples which had been previously either unscreened or screened through a 63 μm sieve. The assay results of the samples taken from the mixes are shown in Figure 3.6.3.

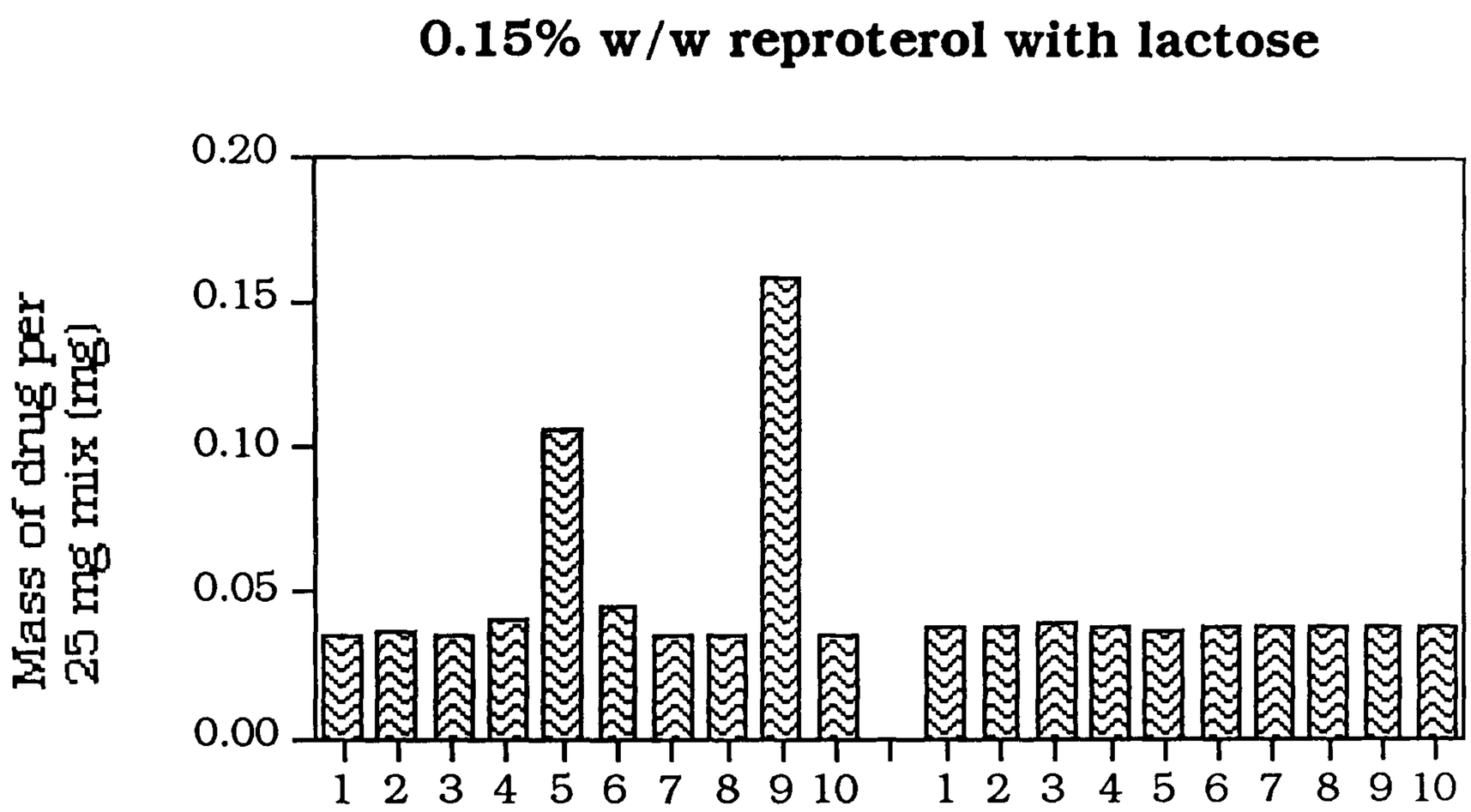

Figure 3.6.3 Assay results for 0.15 %w/w mix of reproterol with lactose

The mean and coefficient of variation for both mixes are shown in Table 3.6.5.

Sample preparation	Mean drug content per sample (mg)	Drug content coefficient of variation (%)
Not pre-screened	0.056	75.297
Pre-screened	0.038	1.454

Table 3.6.5 Comparison of the effect of reproterol sample preparation upon the powder mix homogeneity

All of the binary mixes subsequently prepared used reproterol which had been screened through a 63 μm sieve.

The following powder blends were prepared. The corresponding percentage coefficient of variation for ten dose weight samples taken from each batch is shown in Table 3.6.6.

% w/w hydrated drug content	Drug content coefficient of variation (%)	% w/w drug content by assay
0.15	1.454	0.150
1.50	1.179	1.475
4.0	9.062	4.034

Table 3.6.6 Reproterol mix homogeneity data

3.6.2 Discussion

All of the powder mixes exhibit a very poor homogeneity when the drug sample was not sieved prior to mixing. This is due to incomplete deaggregation of drug clusters which form in the bulk powder upon storage. The samples taken for homogeneity analysis which are very rich in drug content suggests that drug aggregates are present. These are in contrast with the very drug lean samples which suggest that very little drug has become adhered onto the carrier particles. Therefore interactive units have not been formed,

Preparing the drug by sieving immediately before mixing breaks down the clusters of drug which form during storage. The short range

van der Waalss bonds are disrupted and the structure of the aggregate breaks down. The very small sample coefficient of variation suggests that the process of pre-sieving encourages the formation of interactive units. Had interactive units not been created the expected constituent segregation would lead to a very poor homogeneity reflected by a high sample standard deviation and corresponding coefficient of variation.

The percentage coefficient of variation achieved for the mixes containing 40 % w/w nedocromil sodium and 4 % w/w reproterol lie outside the acceptable limit for interactive mix formation.

3.6.3 Visual analysis of the powder blends

Microscopic image analysis and scanning electron microscopy and were used to produce visual images of the powder mixes.

Photomicrographs produced from image analysis of the series of powder mixes increasing in drug concentration show the progressive change in structure of the mix with an increasing drug load.

Figure number	Drug species	Drug concentration
3.6.4	nedocromil sodium	0.4 % w/w
3.6.5	nedocromil sodium	1.0 % w/w
3.6.6	nedocromil sodium	2.0 % w/w
3.6.7	nedocromil sodium	4.0 % w/w
3.6.8	nedocromil sodium	40 % w/w
3.6.9	sodium cromoglycate	0.4 % w/w
3.6.10	sodium cromoglycate	1.0 % w/w
3.6.11	sodium cromoglycate	2.0 % w/w
3.6.12	sodium cromoglycate	4.0 % w/w
3.6.13	sodium cromoglycate	40 % w/w
3.6.14	reproterol	0.15 % w/w
3.6.15	reproterol	1.5% w/w
3.6.16	reproterol	4.0 % w/w

Table 3.6.7 Scanning electron micrograph summary

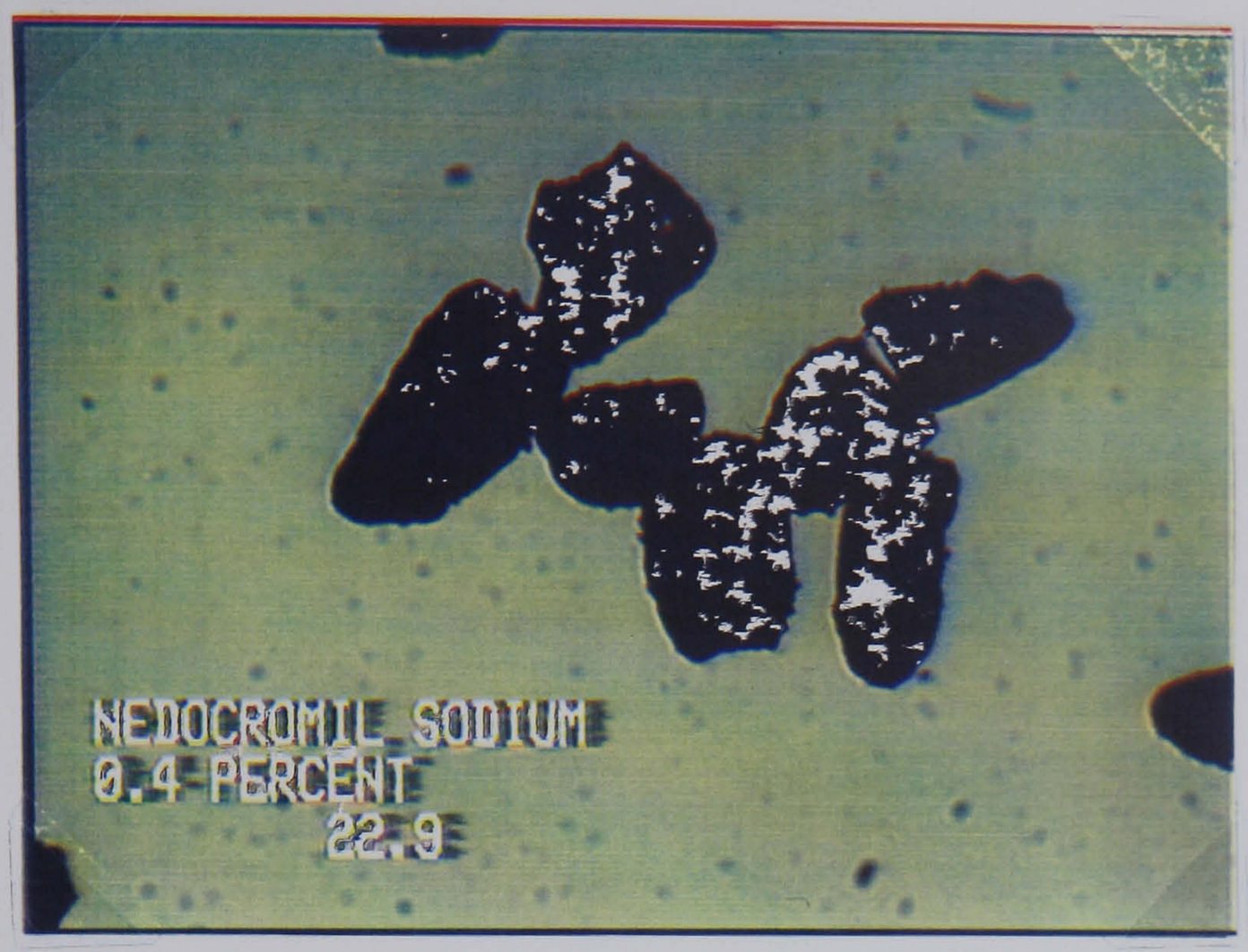

Figure 3.6.4. Nedocromil sodium/lactose powder mix 0.4 % w/w drug concentration. Magnification ×160 .

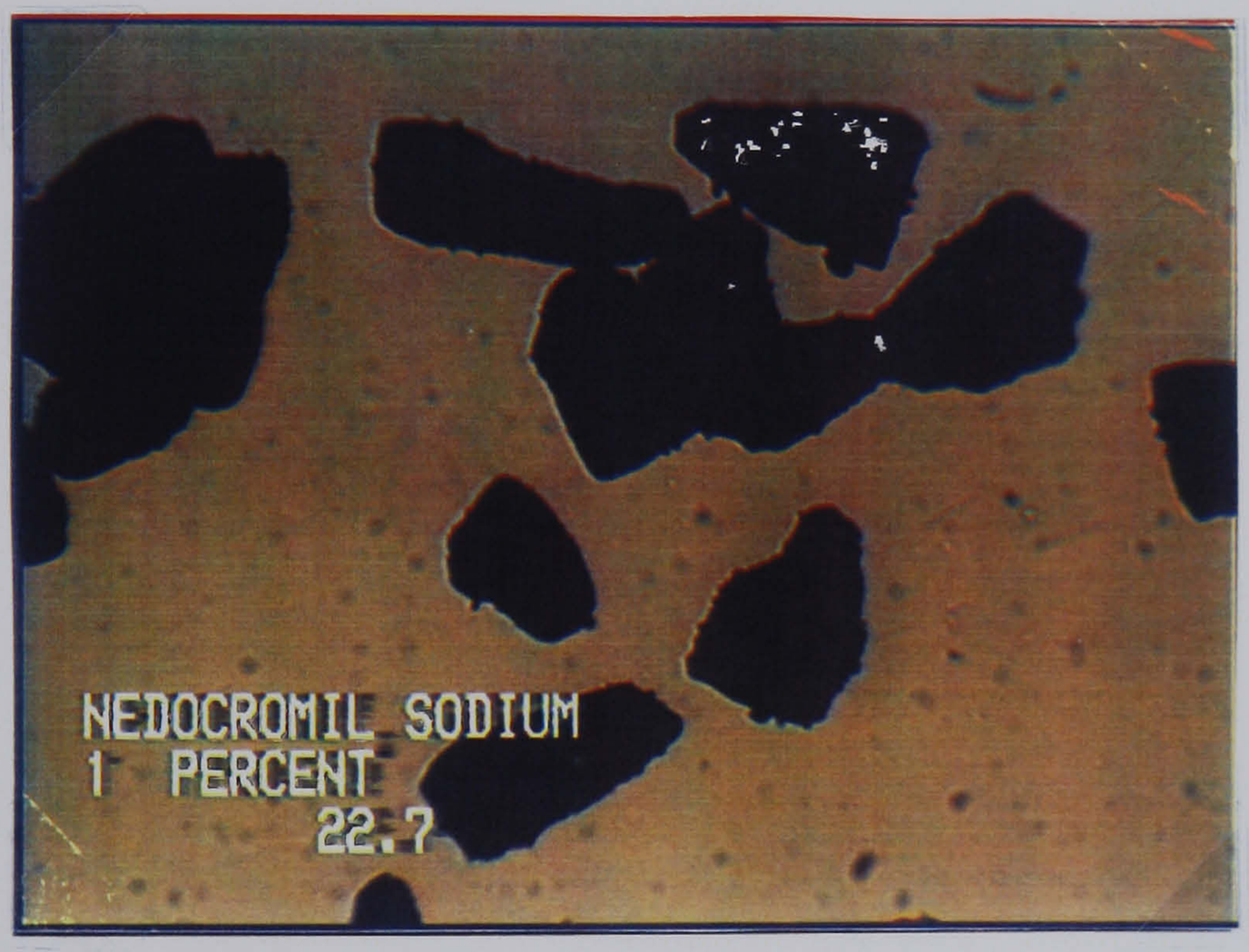

Figure 3.6.5. Nedocromil sodium/lactose powder mix 1.0 % w/w drug concentration. Magnification ×160 .

Figure 3.6.6. Nedocromil sodium/lactose powder mix 2.0 % w/w drug concentration. Magnification ×160 .

Figure 3.6.7. Nedocromil sodium/lactose powder mix 4.0 % w/w drug concentration. Magnification ×160 .

Figure 3.6.8. Nedocromil sodium/lactose powder mix 40 % w/w drug concentration. Magnification ×160 .

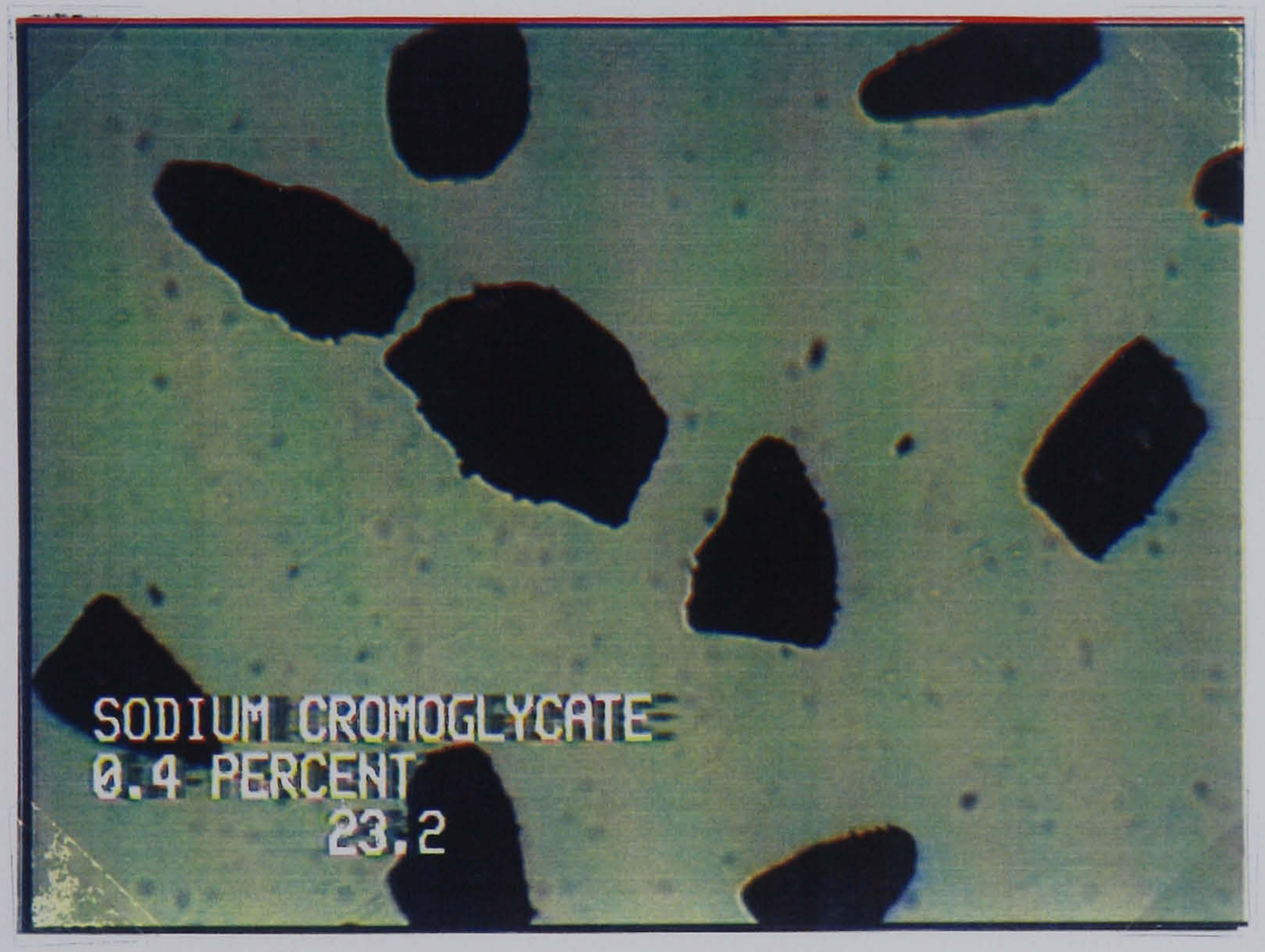

Figure 3.6.9. Sodium cromoglycate/lactose powder mix 0.4 % w/w drug concentration. Magnification ×160 .

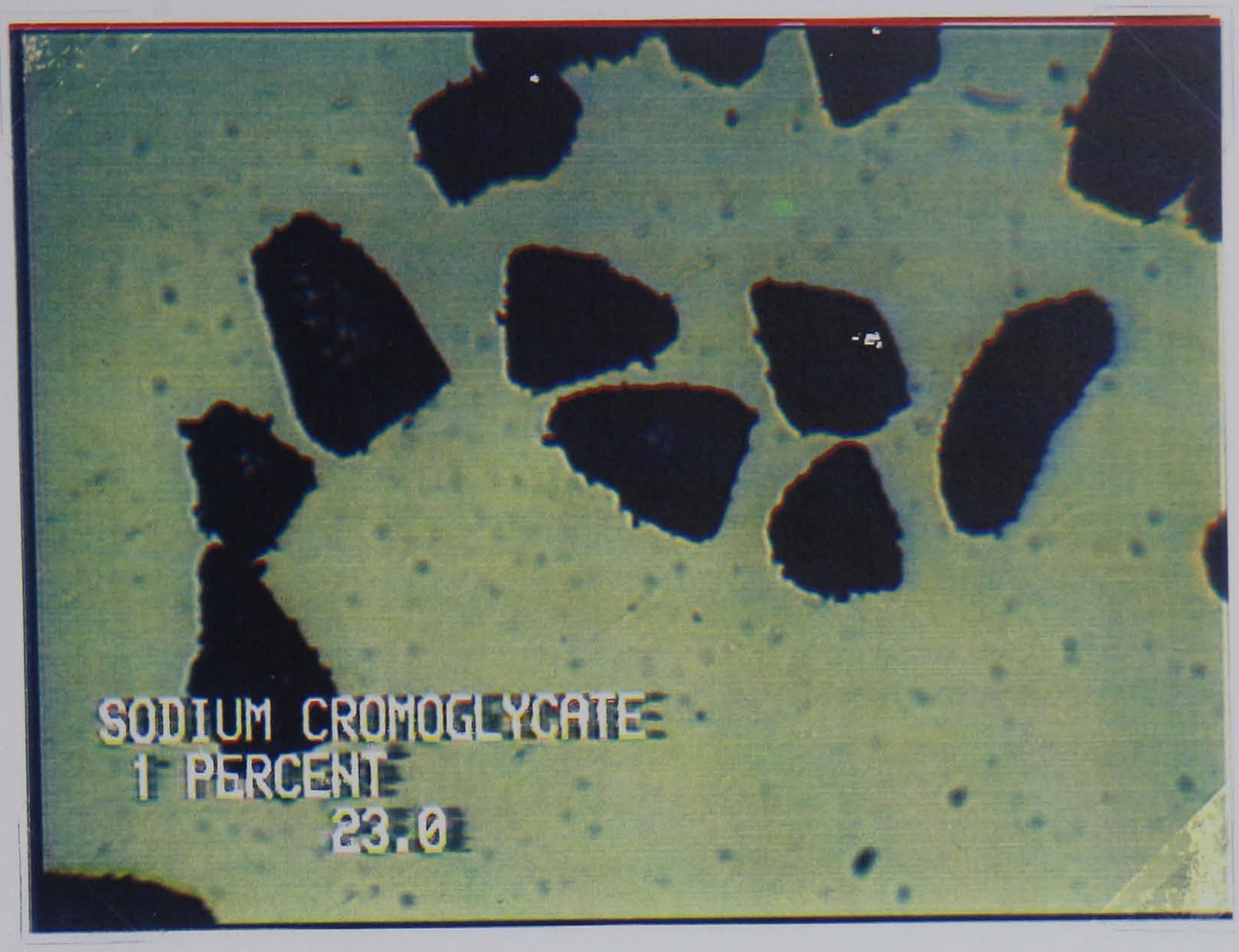

Figure 3.6.10. Sodium cromoglycate/lactose powder mix 1.0 % w/w drug concentration. Magnification ×160 .

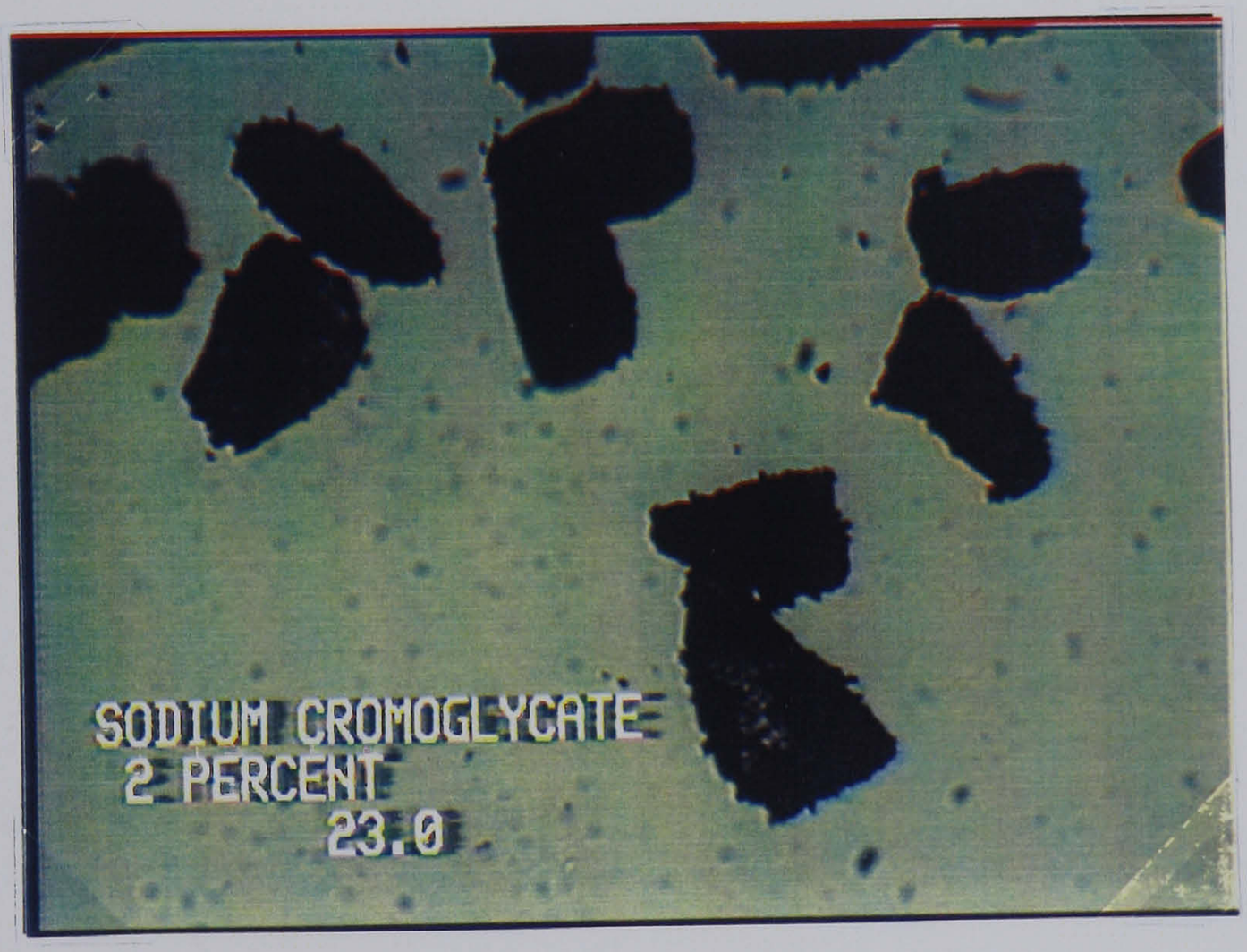

Figure 3.6.11. Sodium cromoglycate/lactose powder mix 2.0 % w/w drug concentration. Magnification ×160 .

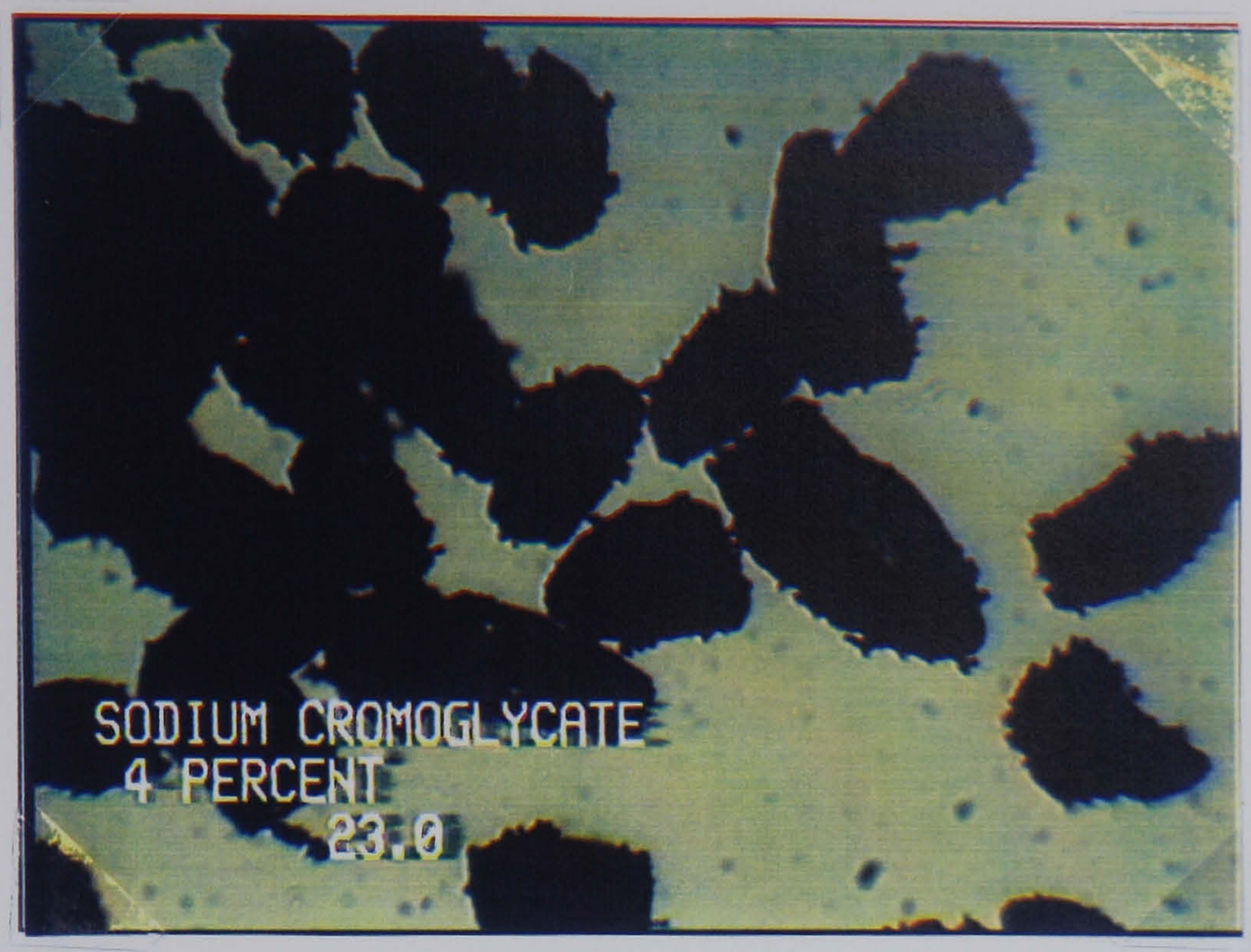

Figure 3.6.12. Sodium cromoglycate/lactose powder mix 4.0 % w/w drug concentration. Magnification ×160 .

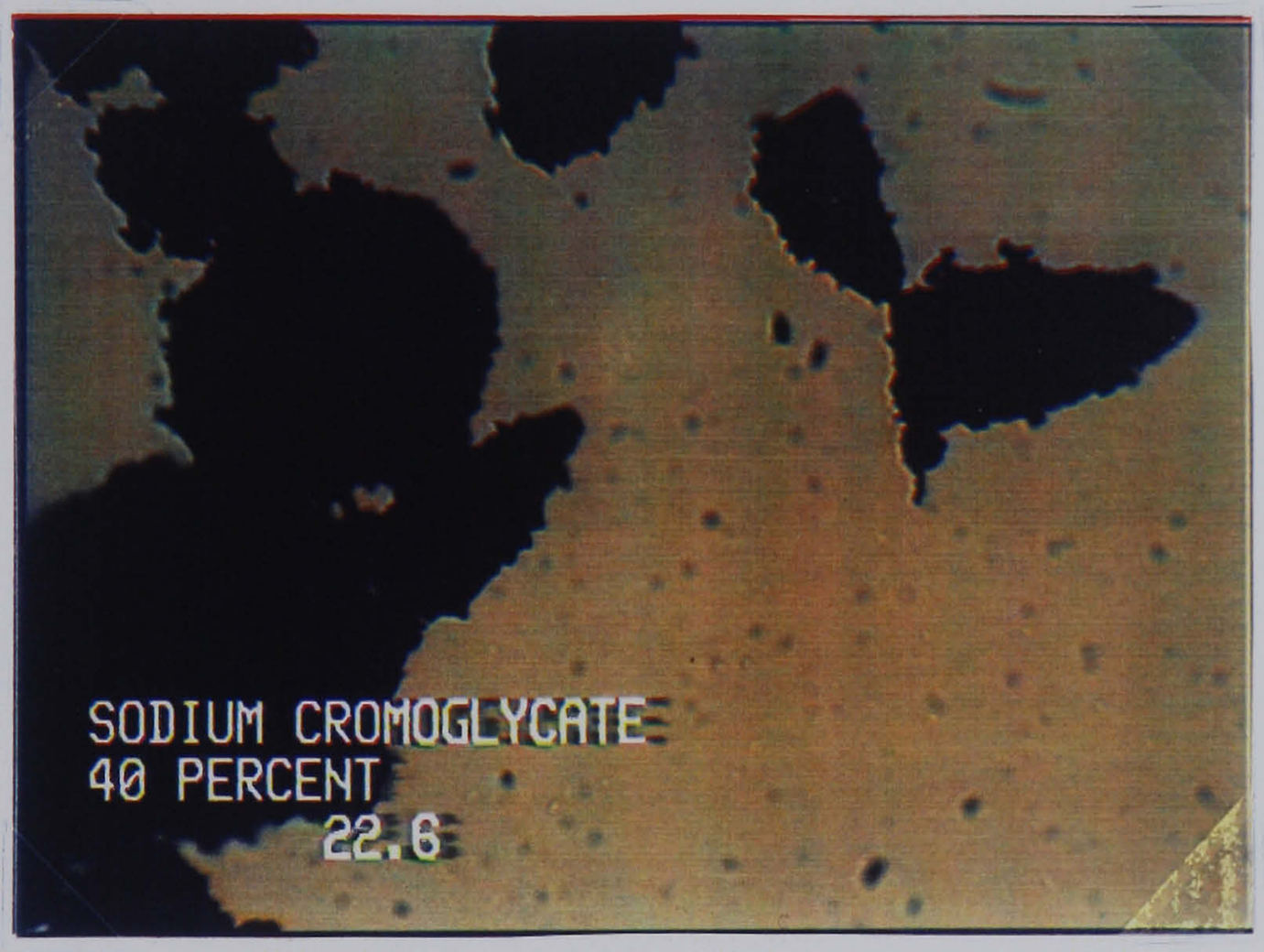

Figure 3.6.13. Sodium cromoglycate/lactose powder mix 40 % w/w drug concentration. Magnification ×160 .

Figure 3.6.14. Reproterol/lactose powder mix 0.15 % w/w drug concentration. Magnification ×160 .

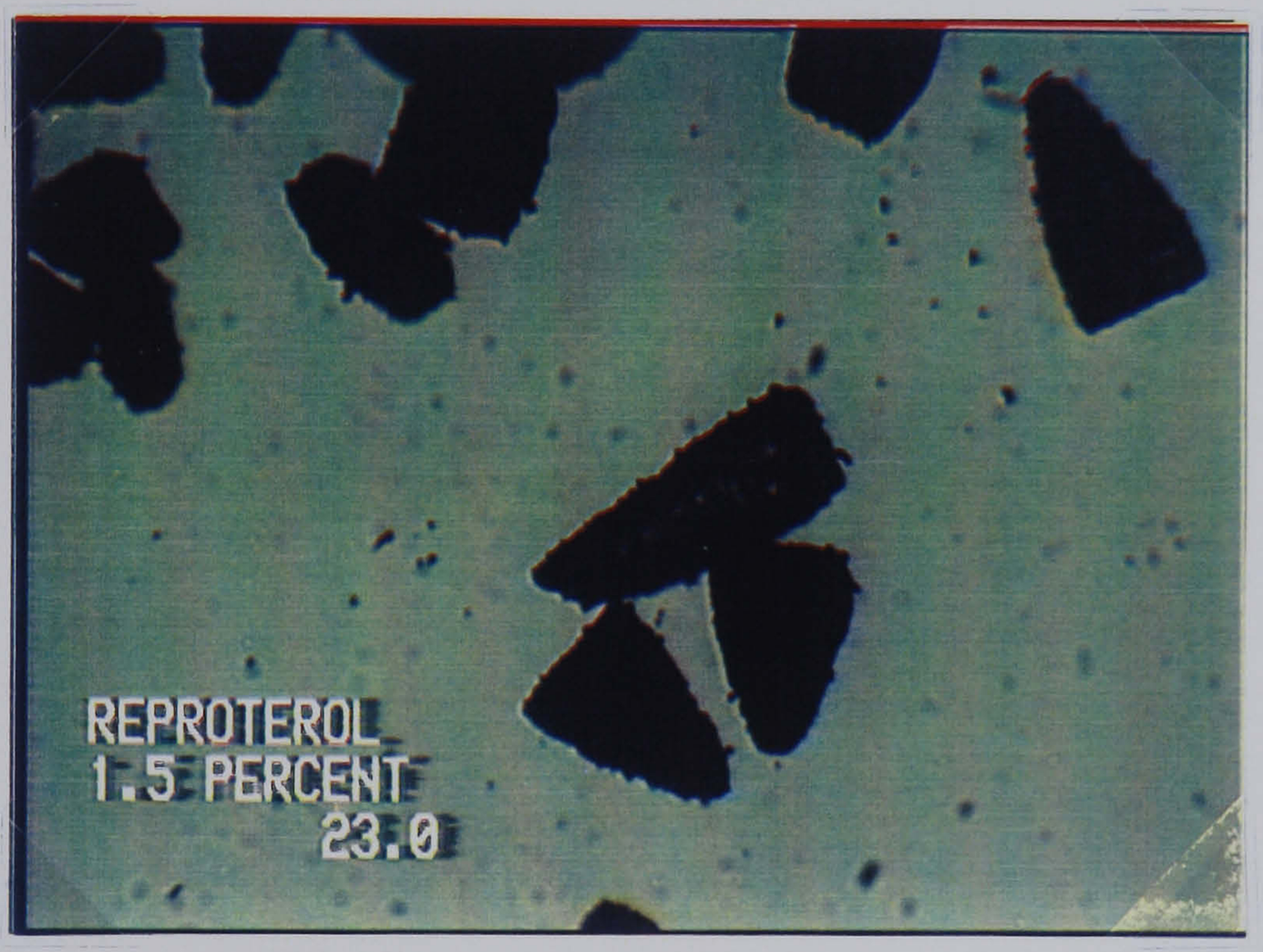

Figure 3.6.15. Reproterol/lactose powder mix 1.5 % w/w drug concentration. Magnification ×160 .

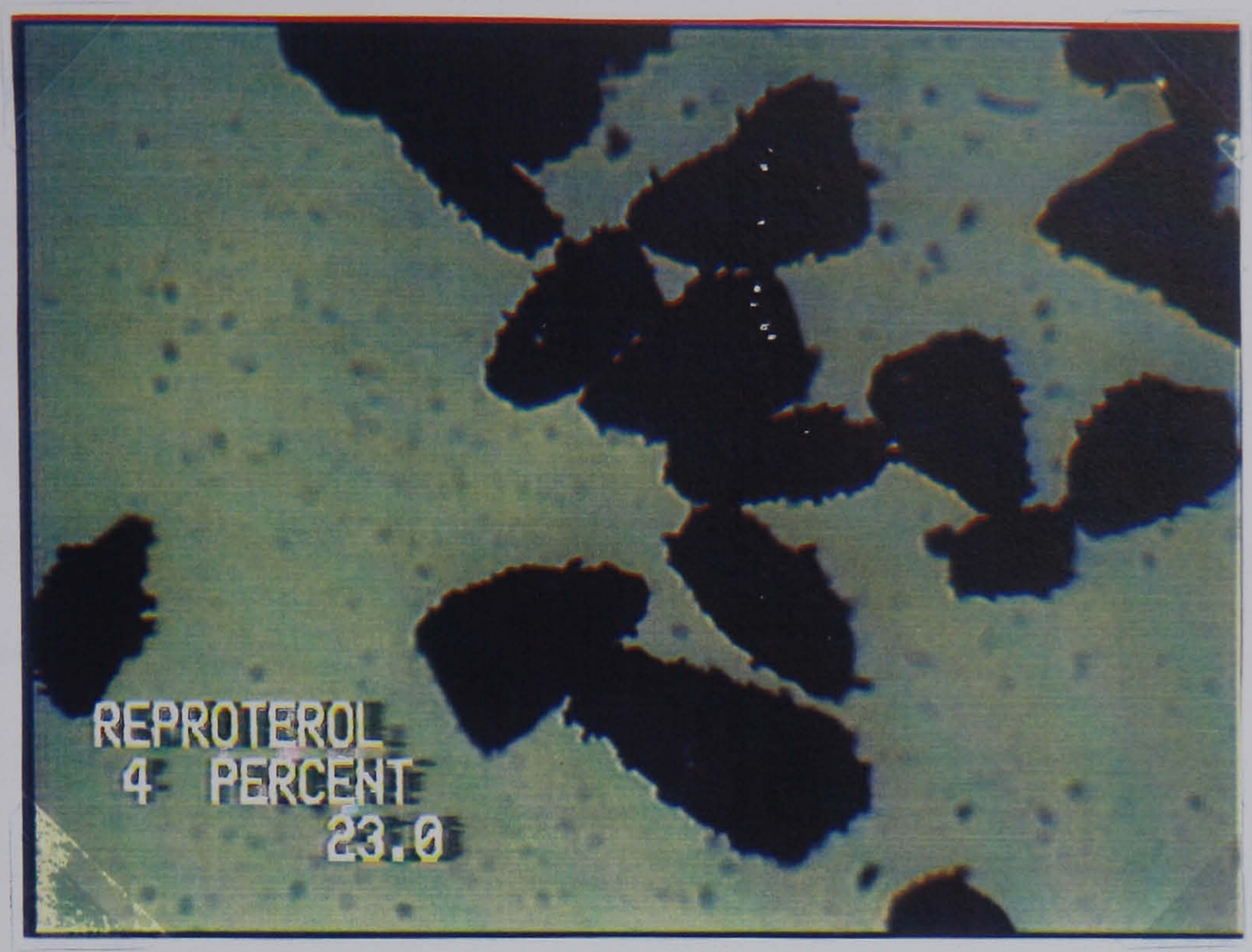

Figure 3.6.16. Reproterol/lactose powder mix 4.0 % w/w drug concentration. Magnification ×160 .

3.7 Discussion

The powder mixes, up to and including the 4 %w/w drug concentration, contain sufficient carrier surface to accommodate the drug particles in a monolayer arrangement as described by equation 3.5.1. However, from the micrographs it can be seen that a monolayer arrangement is not favoured. Small drug aggregates are adhered to the surface of the lactose particle. These surface-held aggregates are observed at all concentrations of each species of drug mix.

This confirms that the adhesion of fine particles occurs in a non-uniformed manner, as suggested by Ergermann [75]. The adhesion of small aggregates rather than isolated particles accounts for the large deviation of coefficient of variation (%) of samples taken from the powder mixes from that expected according to equation 3.5.1. Although the structure of the mixes indicates adhesive interactions take place, these do not occur at the expense of the cohesive interactions. This suggests that the formation of a carrier particle with a monolayer coating of drug is not the most energetically favourable situation.

Within each series of powder mixes the number of adhering aggregates increases with the drug load up to 4% w/w. These aggregates appear to be a similar size for each drug species throughout the series.

This suggests that an energy limiting factor may determine a critical size of adhering aggregate. The abrasion which occurs during the mixing process may remove large surface held drug aggregates.

These observations suggest that the formation and size of the adhered aggregates is not drug dependent

Further analysis using scanning electron microscopy provides more information about the structure of the drug/carrier interactive units. The surface held aggregates can be identified in all of the drug mixes at 4 %w/w concentration, as shown in Figures 3.7.1, 3.7.2 and 3.7.3.

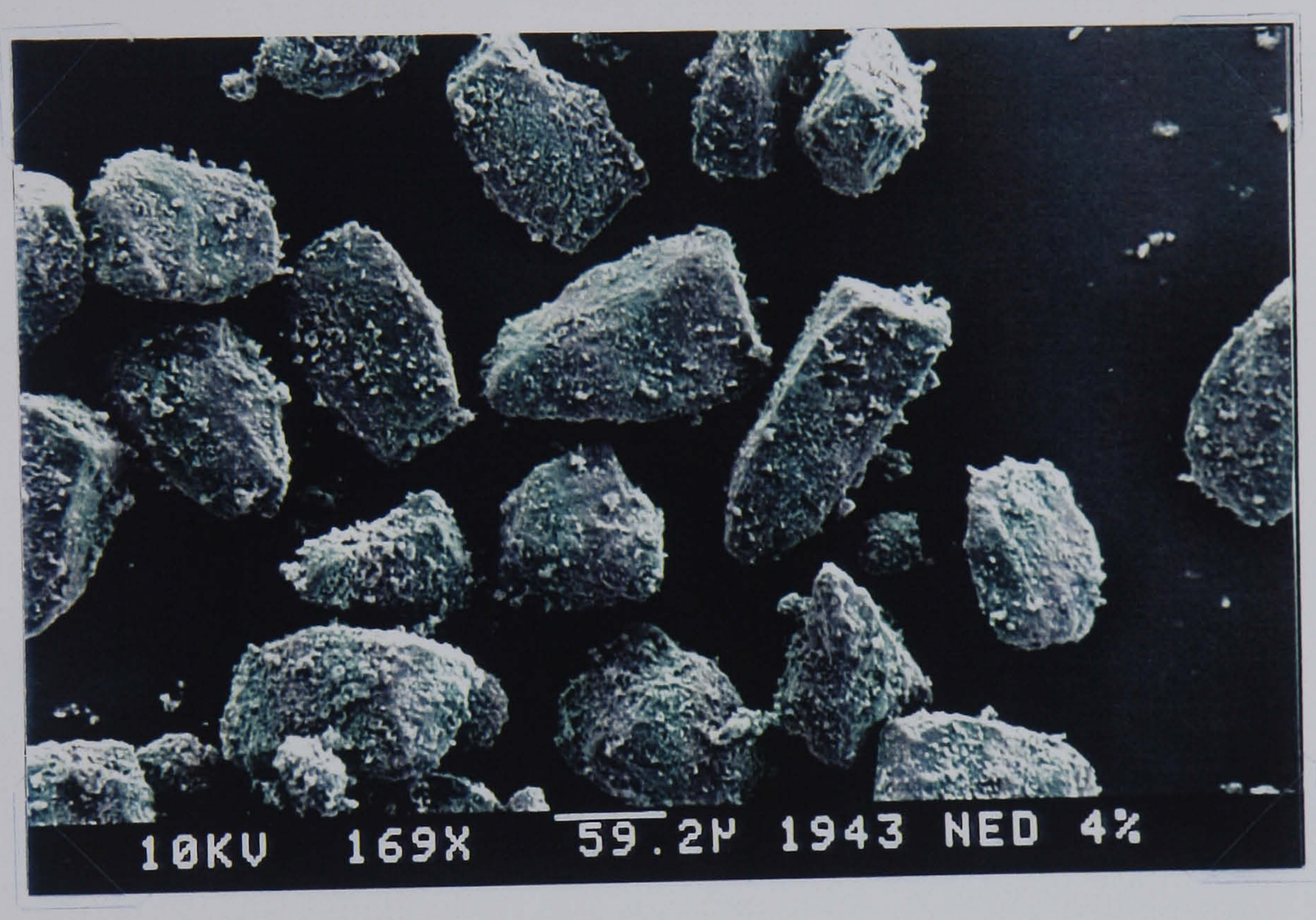

Figure 3.7.1 Scanning electron micrograph of nedocromil sodium/lactose powder mix 4.0 %w/w drug concentration. Picture number 1943.

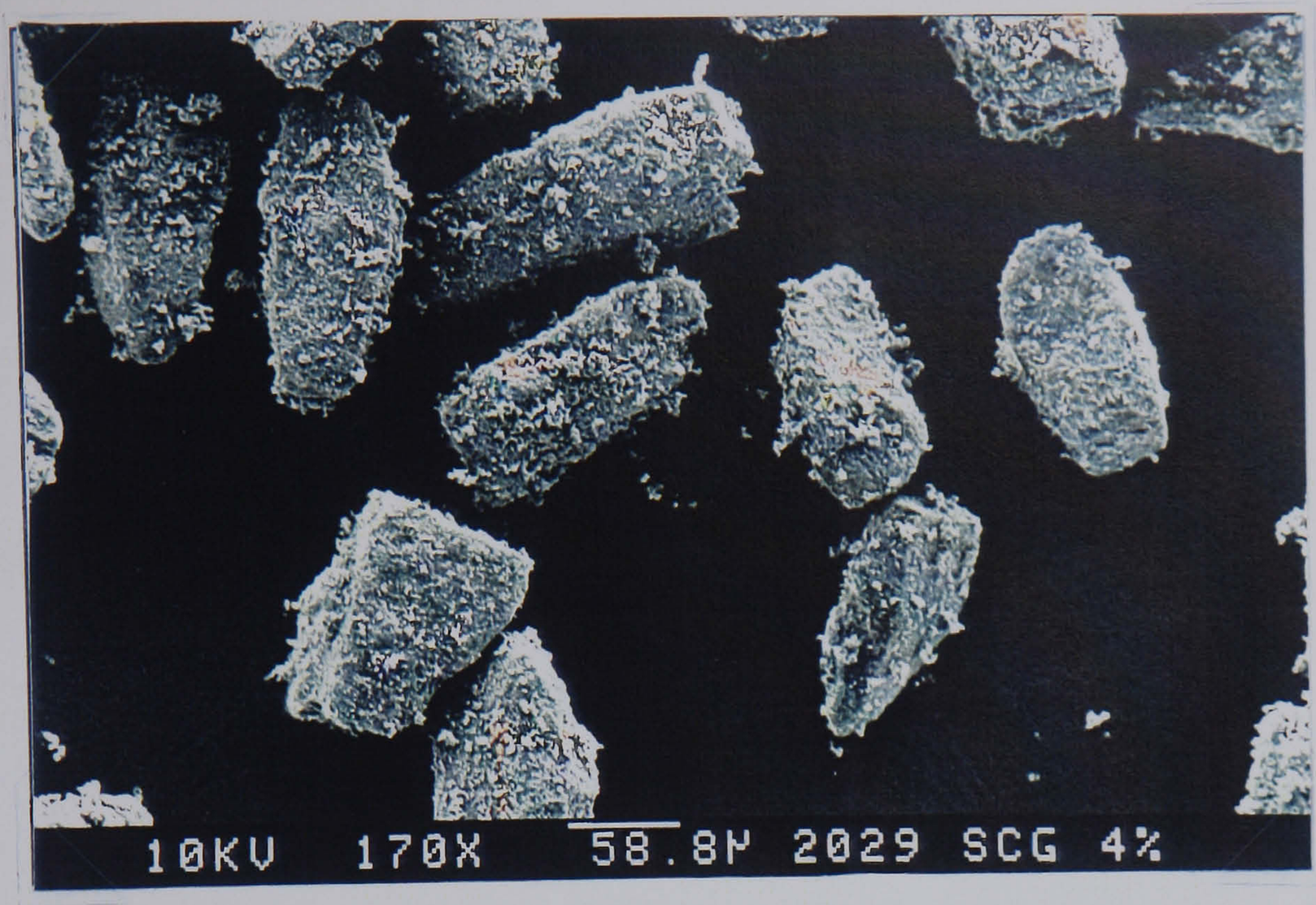

Figure 3.7.2 Scanning electron micrograph of sodium cromoglycate/lactose powder mix 4.0 %w/w drug concentration. Picture number 2029.

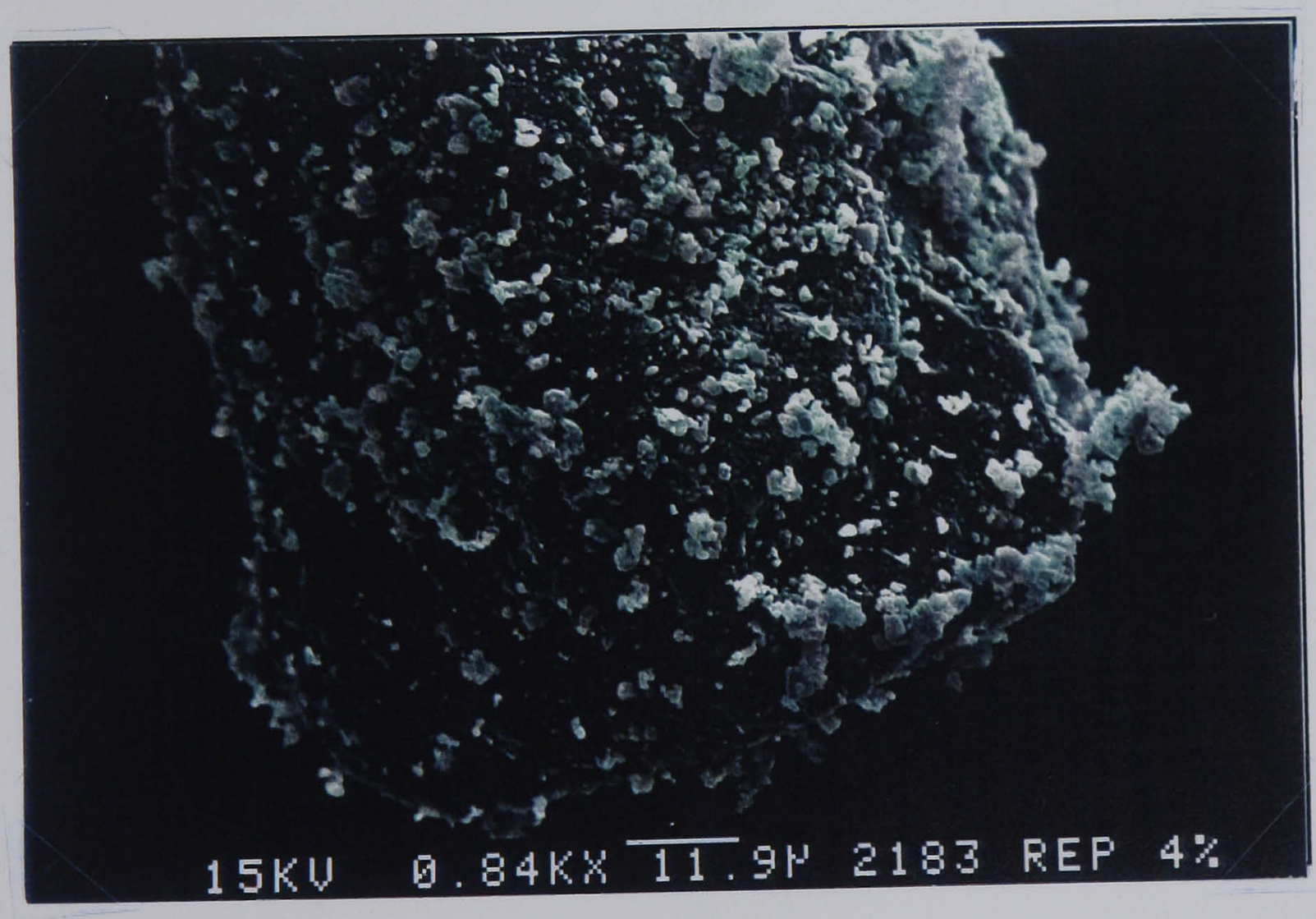

Figure 3.7.3 Scanning electron micrograph of reproterol/lactose 4.0 %w/w drug powder mix concentration. Picture number 2183.

Examining these surface-held aggregates at higher magnification shows that the cluster of drug particles appear to be attached via a small number of adhered particle. These can be seen in figures 3.7.4 and 3.7.5. These anchor particles may be single adhered drug particles, or fines of lactose which had previously been attached to the surface of the larger lactose crystals, as seen in Figure 2.2.9.

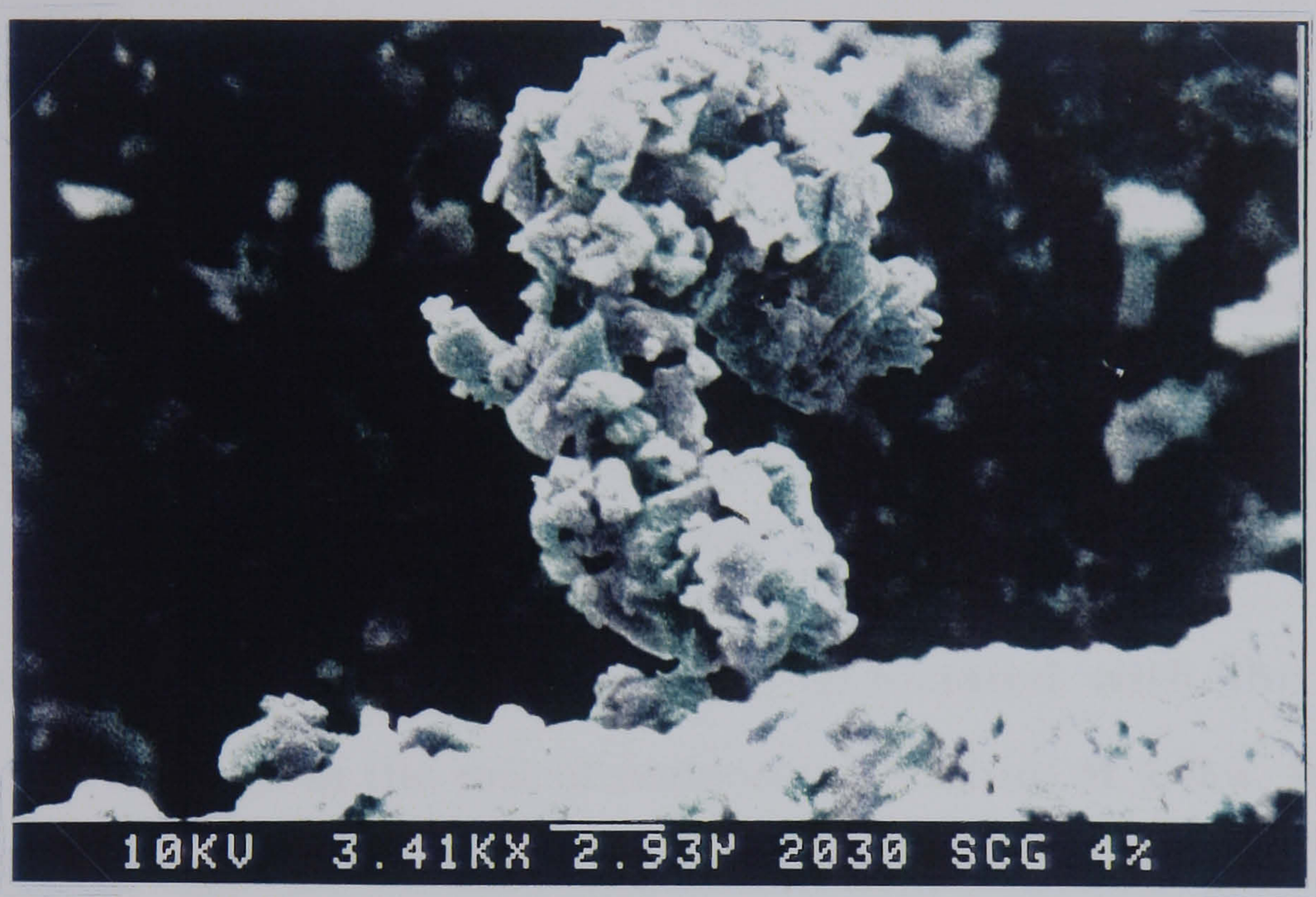

Figure 3.7.4 Scanning electron micrograph of sodium cromoglycate/lactose powder mix 4.0 %w/w drug concentration. Picture number 2039.

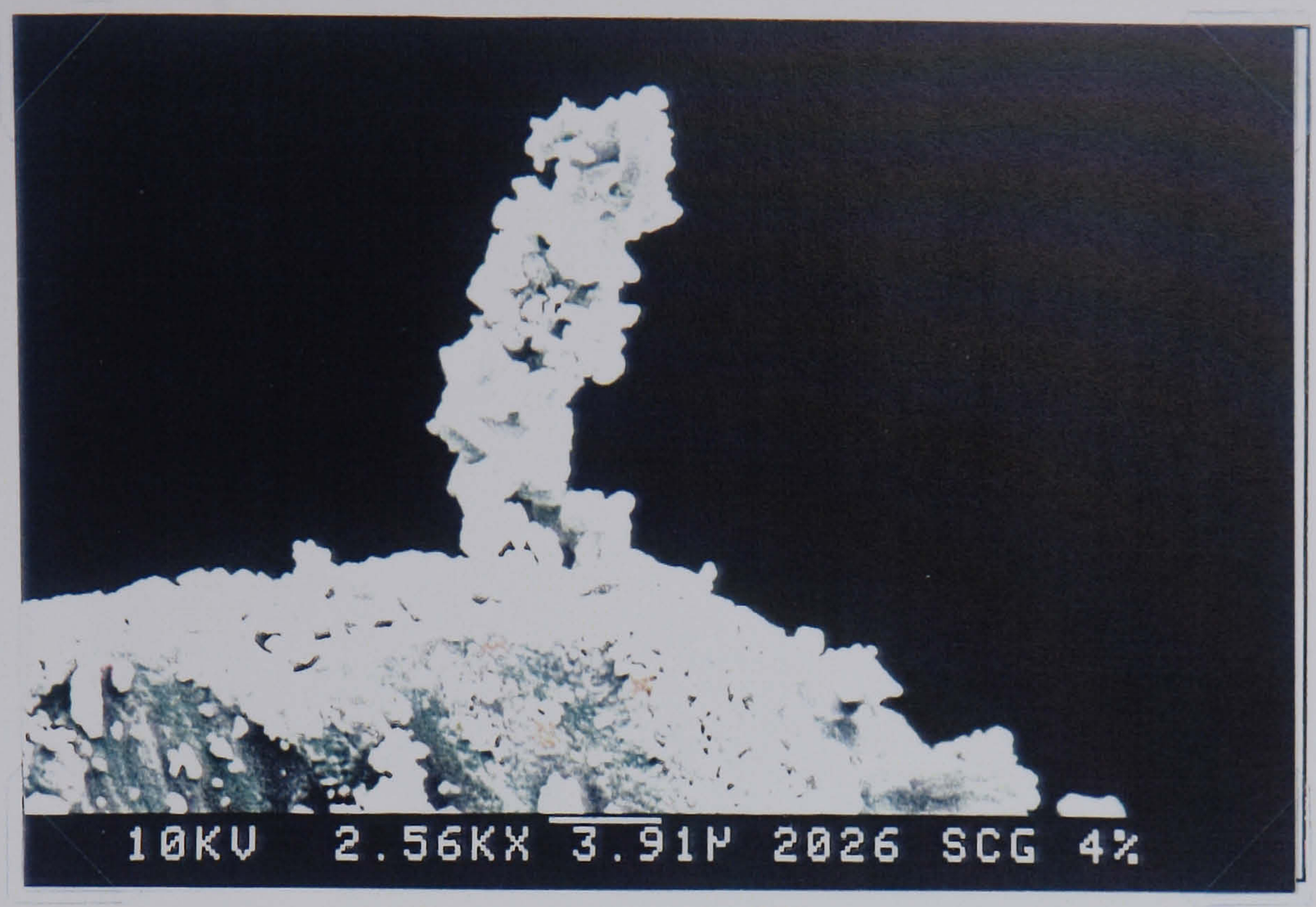

Figure 3.7.5 Scanning electron micrograph of sodium cromoglycate/lactose powder mix 4.0 %w/w drug concentration. Picture number 2026.

Drug aggregates which are not associated with the lactose surface can be seen in the mix of nedocromil sodium at 4 %w/w, Figure 3.7.6. These aggregates were not observed in the mixes of sodium cromoglycate and reproterol at the same concentration.

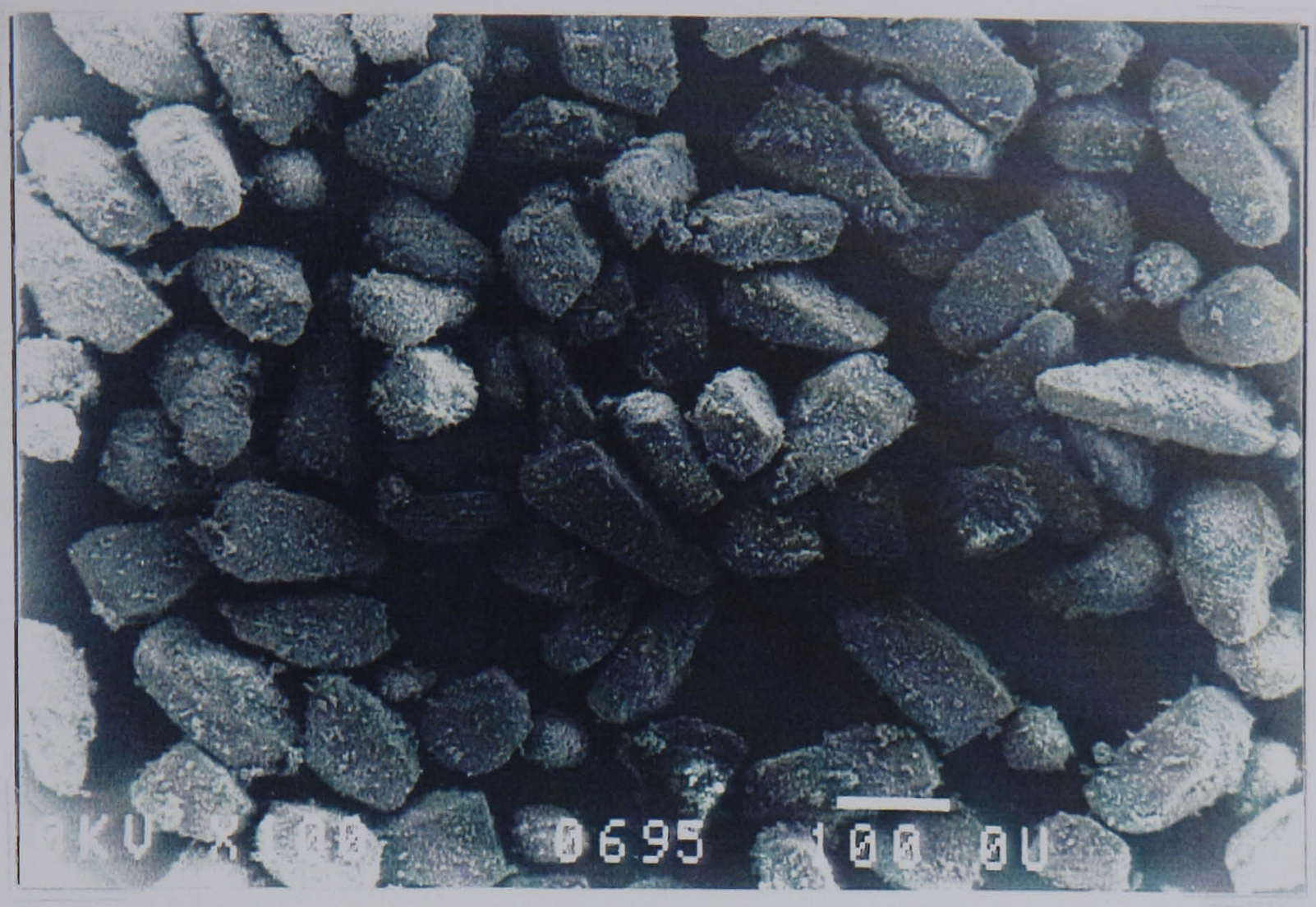

Figure 3.7.6 Scanning electron micrograph of nedocromil sodium/lactose powder mix 4.0 %w/w drug concentration. Picture number 0695.

At 40 %w/w drug load both the nedocromil sodium and sodium cromoglycate mixes contained large non-adhered aggregates. These co-exist with the surface held drug aggregates. These can be seen in figures 3.7.7 and 3.7.8. The small interacting drug clusters are associated with the surface of both the lactose particles and the non-interacting aggregates.

The image analysis micrographs of both mixes show that the non-adhered aggregates of nedocromil sodium are about 95 μm diameter compared with the non-adhered aggregates of sodium cromoglycate which are about 55 μm diameter.

The sample coefficient of variation (%) for these two mixes is 7.4 % and 2.1 % respectively. Non-adhered aggregates are present in both mixes, although only the mix prepared from sieved nedocromil sodium and lactose has a high coefficient of variation. The non-interacting aggregates formed in the mix of nedocromil sodium therefore, tend to segregate from the interactive units producing a mix with a poor homogeneity. The non-interacting aggregates formed in the sodium cromoglycate mix have a more random distribution producing a more homogeneous mix.

When compared with the non-interacting aggregates observed in the 4 % w/w drug concentration mix of nedocromil sodium, it appears that the drug load influences the aggregate size. Aggregates having a diameter < 50 μm are observed in the lower drug concentration mix (Figure 3.7.6) compared with the larger aggregates seen in the mix containing a higher concentration of drug.

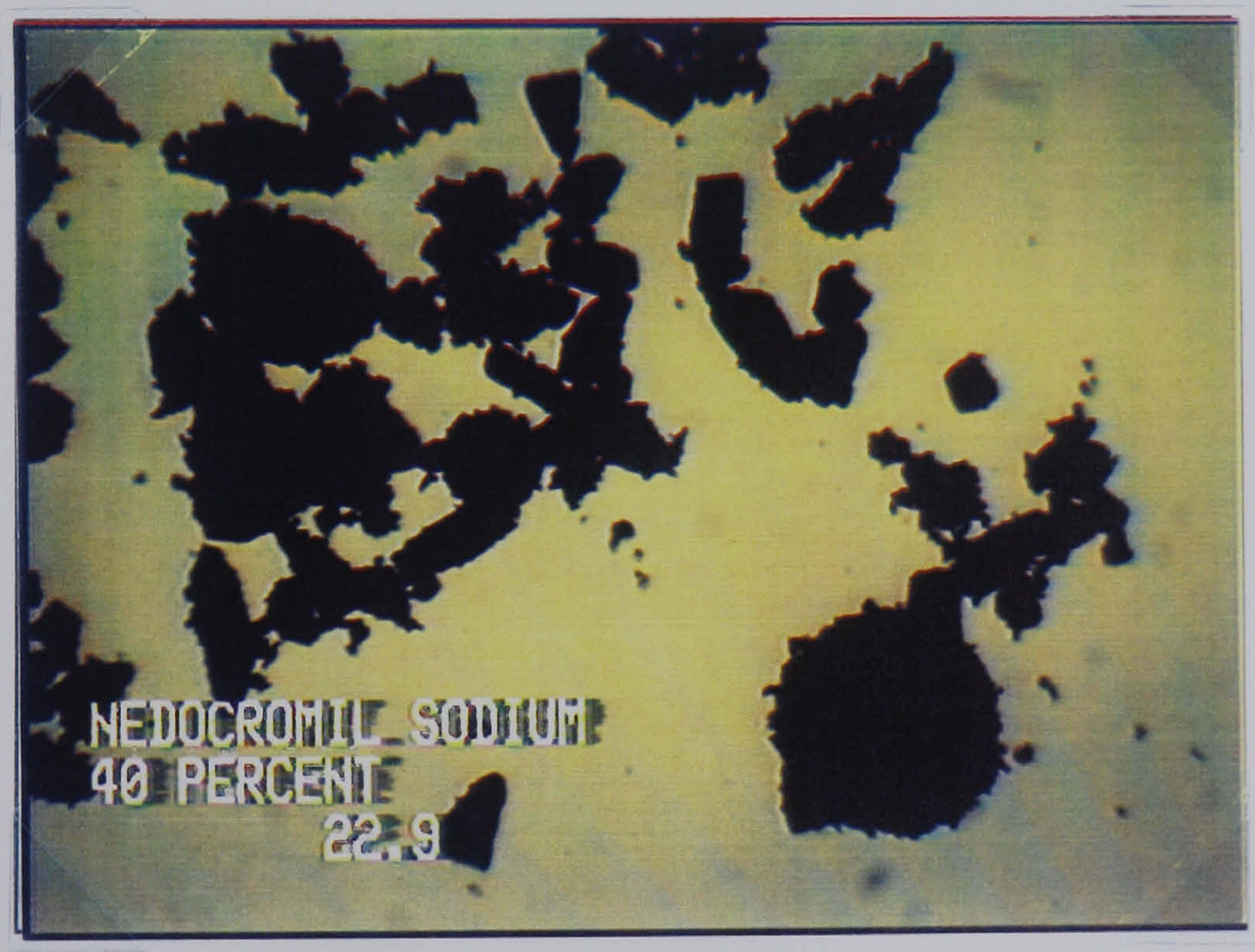

Figure 3.7.7. Nedocromil sodium/lactose powder mix 40 % w/w drug concentration. Magnification ×63 .

Figure 3.7.8. Sodium cromoglycate/lactose powder mix 40 % w/w drug concentration. Magnification ×63 .

3.8 Conclusions

An interactive powder mix resists segregation due to the adhesive interactions which occur between the small particles and the larger sized carrier species. A system which provides sufficient carrier surface to accommodate all of the small adhering particles has the potential to create the ideal monolayer coverage of the carrier by the adhered small particles. The tendency for the fine particles to form small aggregates in real binary powder mixes rejects the idea that monolayer coverage of the carrier particle with the fine particles will occur.

The structure of binary powder mixes of the drugs used for inhalation therapy and lactose deviated from that of an ideal interactive powder mix. Within powder systems which had the potential to create an ideal interactive mix, drug particles were adhered to the surface of the particles of lactose as single units and small drug clusters. The mechanism for the formation of these interactive units is unclear. It is possible that the small aggregates of drug are created in the mix due to the cohesive nature of the drug particles. These aggregates may then become adhered to the surface of the lactose particle. Alternatively, the surface held aggregates may be formed due to cohesive interactions taking place between drug particles which are adhered to the lactose and free drug particles. In either case the cohesive interactions of the drug particles are favoured rather than adhesive interactions between drug and lactose particles.

The cohesive interactions are responsible for the formation of non-interacting aggregates of drug. These are formed in the binary

mixes in which the drug load exceeds the surface available for adhesion provided by the lactose particles. The formation of these larger aggregates does not occur at the expense of the surface held small drug aggregates, as both types of drug cluster co-exist within the powder mixes. Drug load is a contributing factor to the formation of these non-adhering drug aggregates. However, their formation is not limited to systems which have a drug concentration greater than that required to cover lactose particles with a monolayer.

Competition exists, therefore, within the powder mixes between the cohesive interactions which are responsible for aggregate formation, and the adhesive interactions which are responsible for the formation of interactive units.

The structure of the mixes of the powder systems under investigation suggest that the equilibrium point between the adhesive and cohesive interactions is drug specific. Identical systems which differed only in type of drug varied in structure with respect to the drug load at which non-adhering aggregates were formed, the size of the non-adhering aggregates and the coverage of the lactose particles by surface held aggregates. The results suggests that the **cohesive** interactions are more dominant for mixes containing nedocromil sodium than they are for the corresponding mixes containing sodium cromoglycate and mixes of reproterol as the drug type.

As determined in Chapter Two, the size, shape and density of particles of nedocromil sodium, sodium cromoglycate and reproterol are similar. This suggests that these samples of drug would tend to behave

in a similar manner in a binary powder mix. As discussed in Section 2.12, very small differences in surface characteristics can be very influential upon surface energies of particles. Therefore, although similar in physical characteristics, it is possible that differences in surface characteristics between drug types have led to different interactive behaviour. It was not possible to identify these differences with the techniques used in this chapter.

The effect of the structure of these interactive mixes upon the performance of the dose as a dry powder inhalation were investigated in Chapter Four.

Chapter Four

Determination of the performance of binary powder mixes as inhalation dosage forms

4.1 Aim

The structure of the binary interactive mixes prepared for drug pulmonary delivery from a dry powder inhaler were evaluated in the previous chapter. The aim of this present chapter was to determine the performance of the powder mixes in their ability to deliver the dose of drug to the lungs, leading to the elucidation of a relationship between blend structure and performance.

4.2 Introduction

As described in Chapter One, the dimensions of drug particles must lie within a narrow size range for efficient pulmonary delivery and deposition. Deviation from these limits (2 μm to 5 μm) leads to deposition in the upper respiratory tract (if too large) or exhalation (if too small).

The inhalation system must therefore produce an aerosol cloud in which the drug particles exist as single entities. To do this, two distinct processes must take place. The first is the transfer of the powder from a static powder bed into an airstream. The second phase is the break-up and dispersion of the aggregates in the aerosol cloud into individual particles. The performance of the inhalation system is a measure of how efficiently the drug is fluidised and then dispersed into primary drug particles.

Several *in vitro* methods have been developed to mimic the deposition of an aerosol in the lungs. As discussed previously, (section 1.1), the depth of penetration into the lungs is dependent upon

the particle size. As the particle size decreases the particles can penetrate and are deposited further into the bronchial tree towards the alveoli. Experimental methods are based upon inertial impaction which dynamically separates the aerosol cloud into size fractions.

4.2.1 Inertial separation apparatus

Test equipment used to classify an aerosol cloud by inertial separation are based upon the 'cascade impactor' developed by May [95]. The principle of inertial impaction is described below.

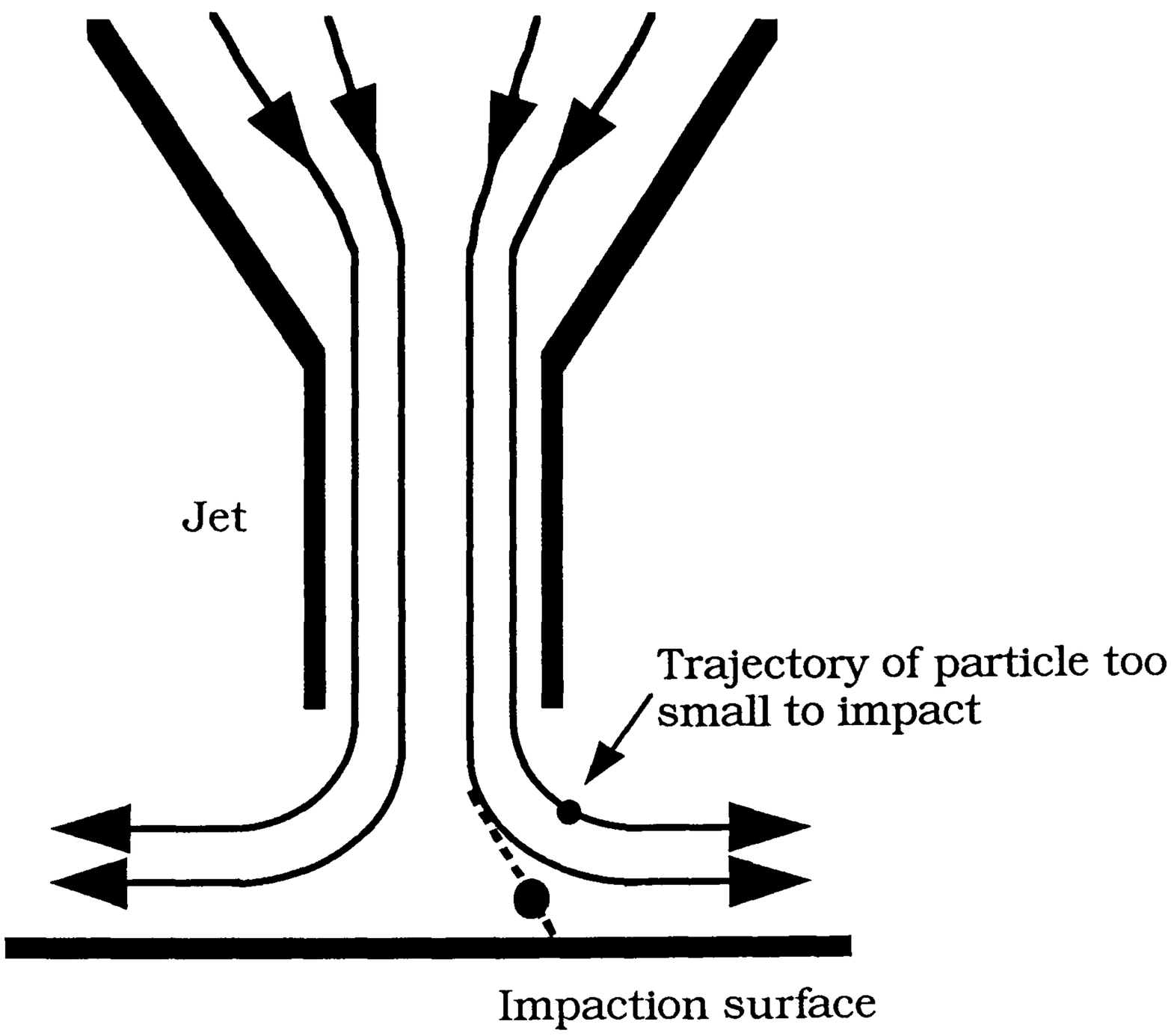

Figure 4.2.1 Process of inertial impaction

At each stage of the apparatus the airstream is presented with an obstacle such as a plate and has to deflect through 90°. The combination of the standard volumetric flow rate and the jet width determines the velocity of the air at the point of deflection. Particles with sufficient inertia (resistance to change in velocity) are unable to adapt to the change in direction at this point and become impacted onto the plate. Those particles which do not have sufficient inertia remain in the airstream and travel through the stage, further into the apparatus.

Each stage has progressively finer jets. Therefore the velocity of the air at the point of deflection is progressively greater. At each stage the largest remaining particles are removed due to their inertia and are deposited on the plate. Therefore the aerosol cloud is separated into progressively smaller sized particle fractions.

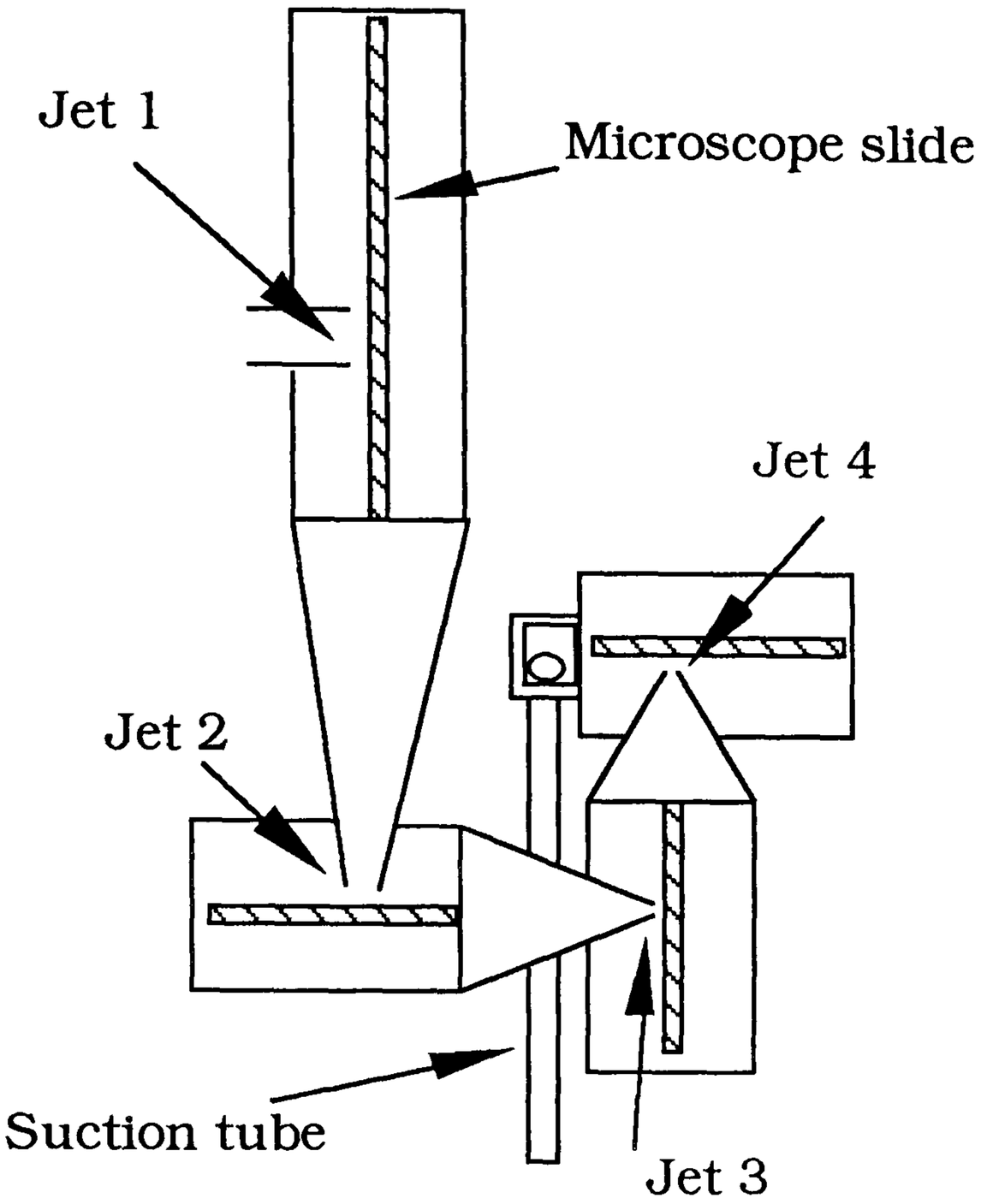

Figure 4.2.2 Sectional elevation of cascade impactor [95] (not to scale)

The cascade impactor designed by May has been the basis for the development of many instruments used to evaluate inhaler performance. All are based on the principle of inertial separation and can be classified into dry-stage impactors, wet-stage impactors and impingers.

4.2.2 Dry-stage impactors

These instruments vary significantly in design with respect to the number of stages, number of orifices at each stage, collection surfaces, recovery of the samples and recommended air flow rates. The collection surfaces of such apparati have to ensure the impacted particles remain associated with the impaction plate whilst the inhalation cycle takes place. Different materials can be used to construct the collection plate

[96, 97] or the surfaces can be coated with a range of materials [6, 98, 99]. However, the high jet velocity at the point of deflection still causes particles to be blown off the plate and become airborne once again [97, 98, 100]. Liquid aerosol particles are less prone to this overloading effect than solid aerosol particles [101, 102]. In order to evaluate the deposition at each stage the plates are removed from the apparatus and either weighed or washed and the solutions assayed for drug. The Anderson sampler has been widely used recently in the evaluation of metered dose and dry powder inhalation systems [97, 103-107]. Other dry impactors recently used in aerosol evaluation include the Pilat Mark 3 impactor [99], Delron stacked sampler [6, 96, 97, 108], and Castella Cascade Impactor [98].

4.2.3 Wet-stage impactors

A wet-stage impactor known as a multi-stage liquid impinger (MSLI) was developed by May [109]. In order to avoid particle 'bounce off', each stage of the apparatus contains a sintered glass disk moistened with a suitable liquid. The liquid is placed in each stage until the level just reaches the lower surface of this collection plate. The upper surface of the plate is kept moist by capillary action. Three upper stages each have a single jet and impaction plate. The final fourth stage of this apparatus consists of a liquid swirl impinger. This stage has no compaction plate, but the nozzle is directed tangential to the wall, such that the particles impinge into the liquid. It has been suggested that this type of instrument is more appropriate for analysis of concentrated powder aerosols than dry-stage impactors [110]. The multi-stage liquid impinger is currently used as a valuable research tool [98, 111-113].

4.2.4 Impingers

Instead of plates onto which particles impact, stages of impingers contain a quantity of liquid into which the particles impinge. The airstream is deflected and the cloud loses the large particles which do not adjust to the change in direction. Instead of becoming impacted onto collection plates, the particles are dissolved or suspended in the liquid. The two-stage impinger was developed as an instrument to quickly assess the performance of an inhalation device [114]. The second stage of the apparatus collects the fraction of the aerosol cloud which would penetrate into the lungs, known as the respirable fraction. This apparatus was accepted as a method for inhalation evaluation in the British Pharmacopoeia 1988 [115]. It has recently been used to evaluate both multi-dose pressurised inhalers and dry-powder inhalers [116-118].

4.2.5 Pre-separators

Most inertial separation instruments are used in conjunction with an induction port. This piece of apparatus is used to remove the very large aggregates from the cloud, and represents the deposition which would occur in the oro-pharyngeal area. The design of this 'throat' section has taken the form of either a cylindrical tube with a 90° bend [104, 110, 111], or a specially constructed piece of glassware [103, 119]. This pre-separator eliminates some error associated with particle bounce from the first impaction stage of the separator as the overloading effect of this first stage is decreased.

4.2.6 Aerodynamic diameter

Two particles which are aerodynamically indistinguishable because they have similar behaviour in a moving airstream may differ in their shape, size and/or density [120]. The aerodynamic property of a particle may be described by its aerodynamic diameter. This equivalent measurement corresponds to the diameter of a sphere of unit density which assumes the same terminal settling velocity as the particle in question, regardless of its shape and density.

Stokes' law determines the terminal settling velocity of a sphere in the laminar region, as described by equation 4.1.

$$v_{ts} = \left(\rho . D^2 . g\right) \Big/ (18 . \eta) \qquad \text{(equation 4.2.1)}$$

where

v_{ts} = terminal settling velocity
ρ = particle density
D = sphere diameter
g = gravitational acceleration
η = air viscosity

In terms of aerodynamic diameter, the sedimentation velocity can be described by equation 4.2 [121]

$$v_{ts} = \left(\rho_0 . D_{ae}^2 . g\right) \Big/ (18 . \eta) \qquad \text{(equation 4.2.2)}$$

where

ρ_0 = unit density (1 g/ cm^3)
D_{ae} = aerodynamic diameter

Stokes' law assumes an object moving in a continuous medium. If the particles are very small this picture is no longer applicable as the particle can 'slip' through the medium. In these cases, for particles smaller than 1 μm a slip correction factor, C_v, must be applied [5, 97, 114].

For spherical particles which are sufficiently large compared to the mean free path in the gas D_{ae} can simply be related to the diameter of the sphere and its density [97], as shown in equation 4.3.

$$D_{ae} = \left(\sqrt{\rho/\rho_0}\right).D \qquad \text{(equation 4.2.3)}$$

where D = particle diameter

The aerodynamic diameter of an airborne particle is the most important property in determining its respiratory deposition. The impaction surface in inertial separators act as a separator of the airborne particles into two sizes; those which are impacted are larger than the aerodynamic diameter parameter associated with the impaction surface, those which remain airborne are smaller.

The inertial impactor is therefore a useful tool to evaluate aerosol clouds as the parameter measured is that which determines pulmonary deposition.

Data provided by inertial impaction analysis is used to evaluate the inhaler device and formulation as a drug delivery system. This can

be presented either as particle size distribution within an aerosol (Mass Median Aerodynamic Diameter), or as the likely respiratory penetrability of an aerosols without determining the absolute particle size (Respirable Fraction).

4.2.7 Mass Median Aerodynamic Diameter

Each stage of an inertial separator can be described by its collection efficiency. This is defined as the percentage of particles of a particular aerodynamic diameter which are deposited on the stage. Ideally the collection efficiency should increase from 0 % to 100 % in a step function as shown below [122].

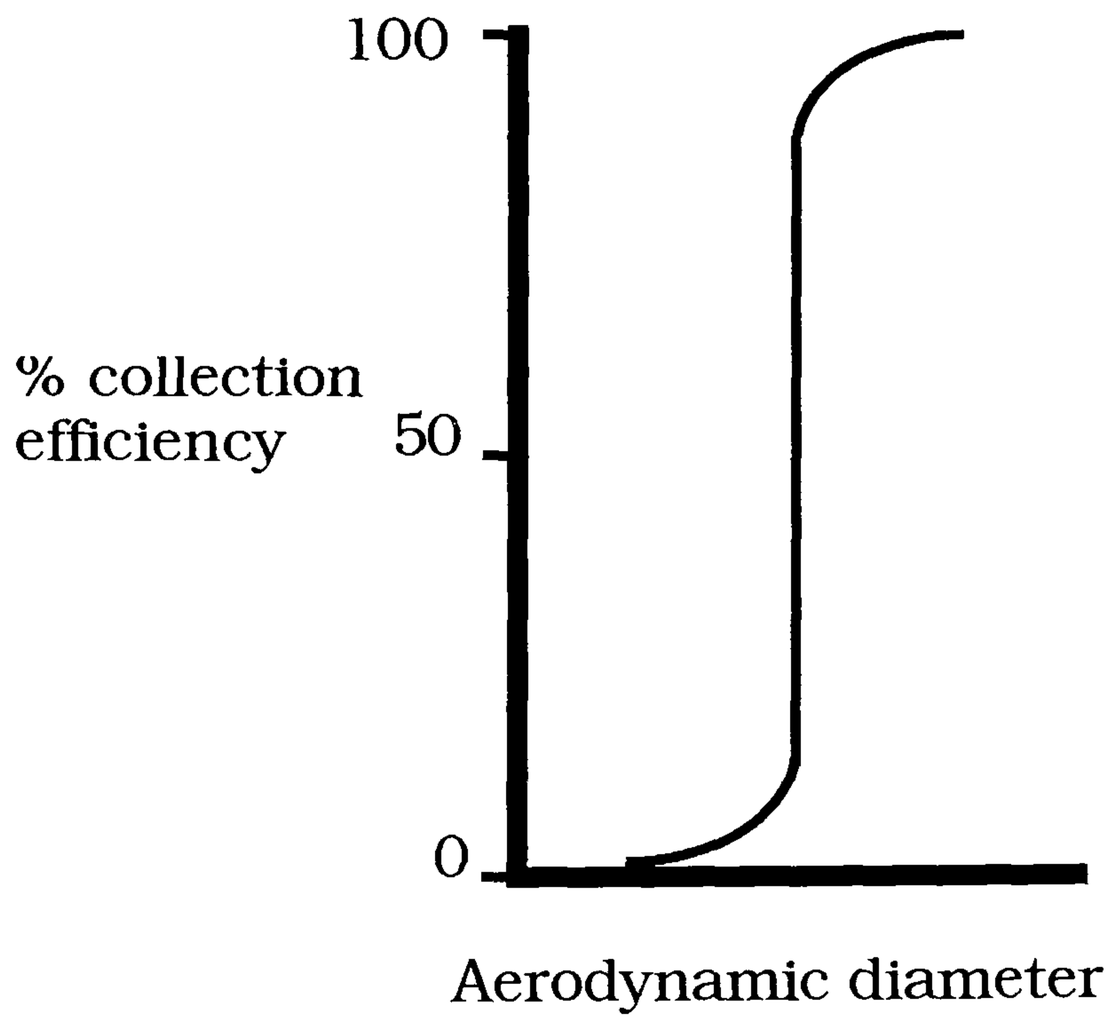

Figure 4.2.3 Ideal impaction curve

Inertial impactors can be calibrated in terms of the range of particle sizes collected at each stage at a given flow rate using monodisperse aerosols [123]. The aerodynamic diameter for which the stage has a 50% collection efficiency is known as its 'effective cut-off

diameter' and is used as the calibration value. When handling data it is assumed that all of the particles with a diameter larger than the effective cut off diameter are retained on the stage [96].

Cascade impactors have been used to estimate particle size and distribution within the aerosol cloud. In order to do this the amount of drug impacted onto each stage is quantified as a relative percentage of the total drug impacted on all of the stages. A cumulative percent value can then be determined for each stage. Log-probability plots of cumulative percent data versus the aerodynamic diameter of each stage can yield values for the Mass Median Aerodynamic Diameter and the Geometric Standard Deviation of particles in the cloud. The Mass Median Aerodynamic Diameter is obtained by determining the aerodynamic diameter which corresponds to 50 %. This is the single aerosol measurement which, according to the Task Group on Lung Dynamics of the International Commission on Radiological Protection [124], can estimate the regional deposition of particles within the respiratory tract. The Geometric Standard Deviation describes the degree of polydispersity of the aerosol. Using impactor data, this can be calculated by determining the aerodynamic diameter corresponding to 15.9 % and 84.1 % as shown below [120].

$$GSD = \sqrt{\frac{D_{84.1\%}}{D_{15.9\%}}} \qquad \text{(equation 4.2.4)}$$

Where GSD = Geometric Standard Deviation

$D_{84.1\%}$ = aerodynamic diameter corresponding to 84.1 %

$D_{15.9\%}$ = aerodynamic diameter corresponding to 15.9 %

4.2.7 Respirable Fraction

The Glaxo Twin Impinger apparatus does not provide sufficient data to permit analysis of a particle size distribution, but it does determine the respirable fraction of the aerosol cloud. This corresponds to the mass of drug deposited in the second stage of the apparatus. The first stage is designed to have an effective cut off diameter of 6.4 μm. The apparatus was designed such that the respirable fraction corresponds to particle deposition in stages 3, 4 and filter of the multi-stage liquid impinger [114].

4.2.8 Using impingers to evaluate aerosol clouds from dry powder inhalers

4.2.8.a Method

The British Pharmacopoeia [119], European Pharmacopoeia, and United States Pharmacopoeia all contain monographs covering the requirements to evaluate pressurised metered dose inhaler systems. Methods are described for analysing the respirable fraction and the emitted dose, but not to describe the particle size distribution within the aerosol cloud. For these tests the air flow rate through the apparatus is set at 1 litre per second with a continuous air flow through the apparatus. No standard monograph exists at present for the evaluation of dry powder inhaler systems.

All dry powder inhalers are, by design, breath actuated. Upon inspiration the patient creates a pressure drop across the device in order to create an air flow through it. An inherent resistance to the

passage of air through the device is necessary to create the turbulent airflow which fluidises and disperses the dose of drug. This resistance is unique to each device [125]. Therefore, testing devices at a constant air flow rate necessitates a range of pressure drops for a variety of devices. Conversely, a constant pressure drop across all dry powder inhalation systems results in a variety of air flow rates, depending on the device.

Valuable data for the clinical performance of an inhalation system can be provided by the determination of the pressure drop against the flow rate [125]. This is because the inspiratory effort required from the patient to deliver the dose is directly proportional to the pressure drop [14]. Without a standard monograph comparisons of dry powder inhalation devices are difficult due to the many different experimental methods employed, few of which consider the inspiratory effort.

4.2.8.b Data

The size distribution of particles present in an aerosol cloud can be described by the Mass Median Aerodynamic Diameter and the Geometric Standard Deviation. Recommendations have been made for values of these parameters which would achieve optimal lung delivery of the drug [124].

The mass distribution of drug throughout the apparatus is used to determine the particle size distribution in the aerosol. Several factors can produce errors in this determination. These are: lactose carrying drug particles deposited in calibrated 'throat' sections and 1st stages;

particle 'bounce off' associated with overloaded stages; wall deposition caused by interception of particles which remain airborne after passing the impaction plate, and increased later stage deposition due to non-spherical particles.

Particles attached to lactose

Carrier particles as well as drug are discharged from inhalation devices which use powder mixes. In theory all of the drug particles are removed from the surface of the carrier. The carrier particles, because of their size are impacted onto the pre-separator and 1st stage of the apparatus. It has been shown that some drug particles remain attached to the carrier particles [126]. This implies that the mass deposition of drug in the pre-separator and 1st stage is due to large drug aggregates and drug which is attached to the carrier. Particle size determination is then biased towards the larger particles and is not a true representation of the powder cloud.

Bounce off

As previously mentioned impaction plates may become overloaded. This is due to a very high number of particles being collected on the stage. It is possible that particles with an aerodynamic diameter greater than the effective cut off diameter for a stage may become impacted, but subsequently removed from the stage due to 'bounce off' or 'blow off' [108]. The particles then pass into the later stages of the apparatus where they are deposited. Therefore particles with a larger mass than the calibration values determine can be present in the later stages of impactor apparatus.

Wall deposition

The deflection of the air stream due to the position of the impaction plate is the point where particles are deposited due to their size. The air stream then flows through the next jet into the proceeding stage of the apparatus. The turbulent air flow within the stage causes drug particle to become deposited on the walls of the stage [98, 108]. According to the type of impactor used the errors incurred when particle sizing are different in nature. Impaction plates are removed from dry stage impactors and assayed for drug. The drug remaining on the walls of the stage is unaccounted for. This fraction of the particle cloud consists of increasingly smaller sized particles which are not impacted onto the plates. Therefore the overall cloud loses a proportion of the smaller sized particles. This effect is slightly different with wet stage impactors. Analysis of deposited drug in these instruments involves washing out the entire stage to collect drug not only impacted on the plates, but all of the internal surfaces. Therefore the wall deposits increase the mass of drug collected at each stage, although the particle sizes are smaller than the effective cut off diameter. Both effects lead to a size determination which is not a true representation of the powder cloud.

Non-spherical particles

Particles which are not spherical, particularly those with acicular structure, have aerodynamic diameters with a very weak dependence on the length [127]. Particles with very small aerodynamic diameters and a needle-like shape carry a much larger drug mass than

isodiametric particles [6]. When the lower stages of impinger apparatus are assayed the particle sizing towards the smaller sizes will be biased.

Therefore the determination of drug particle size distributions from dry powder inhalation systems incurs many errors. Added to this is the knowledge that different inertial separators yield different values for Mass Median Aerodynamic Diameter of an aerosol cloud from the same device [98]. Using different collection surfaces within the same instrument also gives rise to different determinations of Mass Median Aerodynamic Diameter [97].

Inertial impactors are useful instruments to determine the deposition of drug from an inhalation system. The particle size distribution can be determined for the particles of drug within the emitted dose. The size and distribution can then be described by the Mass Median Aerodynamic Diameter and Geometric Standard Deviation of particles within the cloud. It is assumed in the determination, however, that the drug particles behave in a similar manner to the calibration material used for the apparatus. This, of course is not always the case.

Without determining an absolute value, the regional deposition of drug particles can be expressed as the respirable fraction. The mass of drug from the powder cloud considered possible to penetrate and be deposited in the small branching airways of the lungs can be evaluated from deposition within particular stages of separation apparatus. Evaluation of the effect on deposition caused by changes to the

inhalation system can be carried out by direct comparison of the drug mass deposited on these stages.

4.3 Experimental

A multi-stage liquid impinger was used as an *in-vitro* model to assess the drug deposition characteristics from the binary powder mixtures. The inhaler device was developed at the Rijksuniversiteit Groningen, the Netherlands.

4.4 Materials

The following binary powder mixes were tested to evaluate their deposition profile.

Drug species	**Drug concentration (%w/w)**
Nedocromil sodium	0.4 1 2 4
Sodium cromoglycate	0.4 1 2 4 40
Reproterol	0.15 1.5

Table 4.4.1 Powder mixes investigated using multi-stage liquid impinger analysis

4.4 Apparatus

4.4.1. Multi-stage liquid impinger

The multi-stage liquid impinger is constructed of glass with sintered glass impaction plates. Based upon May's design [109], the apparatus incorporates the modifications made by Bell *et al.* [128].

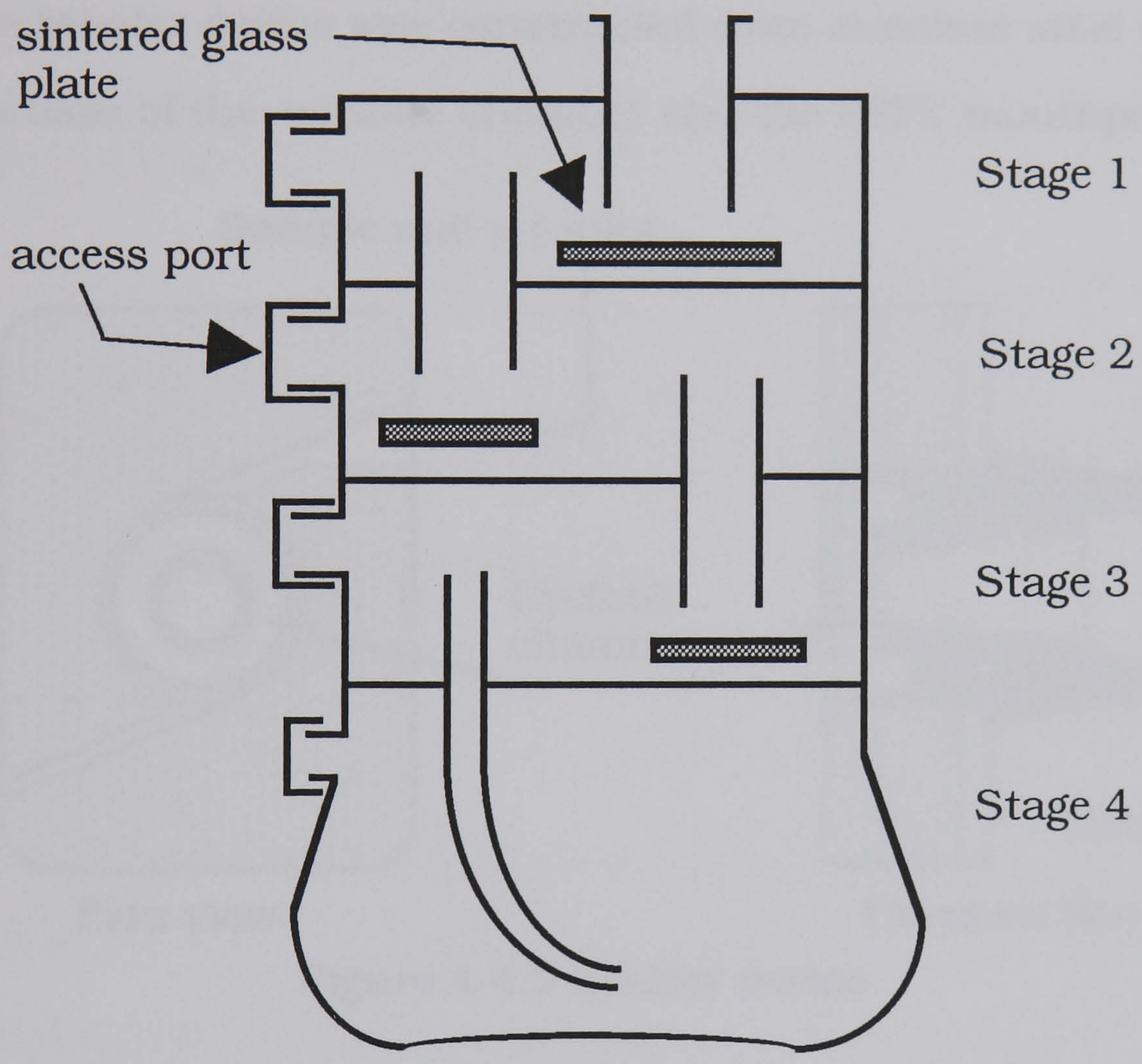

Figure 4.4.1 Diagram showing multi-stage liquid impinger

A tubular glass induction port with a 90° bend was used to simulate the oro-pharynx.

4.4.2. Inhaler device

The inhaler device used was a prototype of a cyclone type inhaler. Prior to inhalation the powder dose is introduced into the cyclone

chamber. During the inhalation cycle air is drawn into this chamber through two tangential inlets. The fluidised drug then leaves the chamber with the air stream which travels via the mouthpiece into the multi-stage liquid impinger. The particles of excipient, because of their larger size, do not undergo pneumatic transport, and remain in the cyclone chamber after the inhalation cycle.

The inhaler device was constructed from stainless steel except for the brass base of the cyclone chamber and the PTFE mouthpiece.

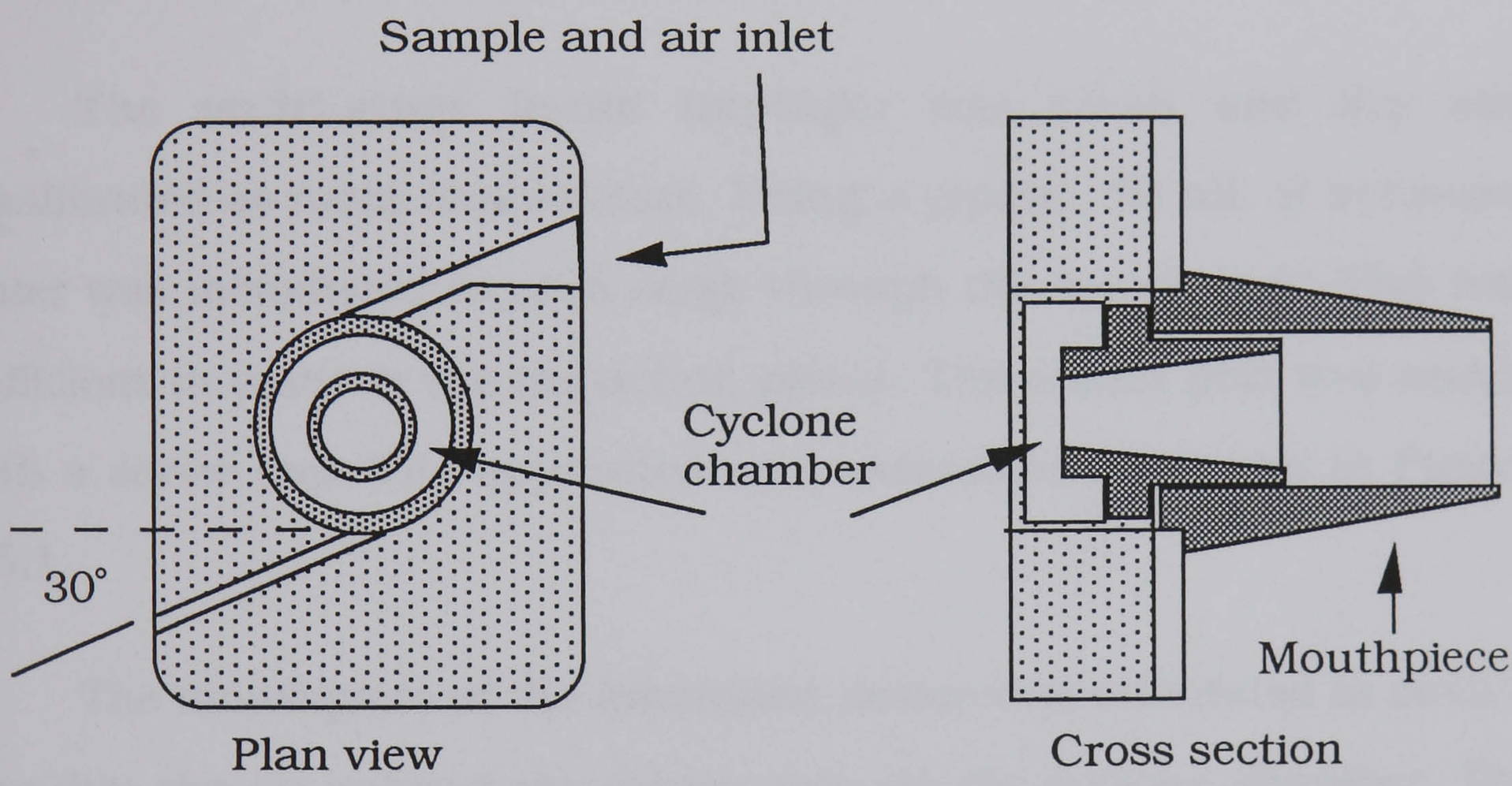

Figure 4.4.2 Inhaler device

4.5 Methods

4.5.1 Air flow calibration

Air flow through the inhaler device and impaction apparatus was determined with respect to the pressure drop across the device. Calibration of the apparatus to the pressure drop relating to 1 $L.sec^{-1}$ flow rate proceeded experimental analysis.

4.5.2 Multi-stage liquid impinger analysis

The multi-stage liquid impinger was clean and dry and equilibrated at room temperature. Using a pipette, 20 mL of deionised water was introduced to each stage through the access port. This was sufficient to moisten the impaction plates. The access port was sealed with a screw cap. The apparatus was assembled as shown in Figure 4.5.1 .

The mouthpiece of the inhalation device was orientated in such a way that the air entered the device only via the cyclone chamber. The brass bottom of the cyclone chamber was connected to earth.

The air flow through the apparatus was adjusted using the air flow regulator until the pressure drop across the inhaler device reached the calibrated value corresponding to 1 litre per second volumetric flow rate.

A single 25 mg dose of powder mix, previously weighed using a Mettler AT261 balance, was transferred into the cyclone chamber through the sample and air inlet (Figure 4.4.2).

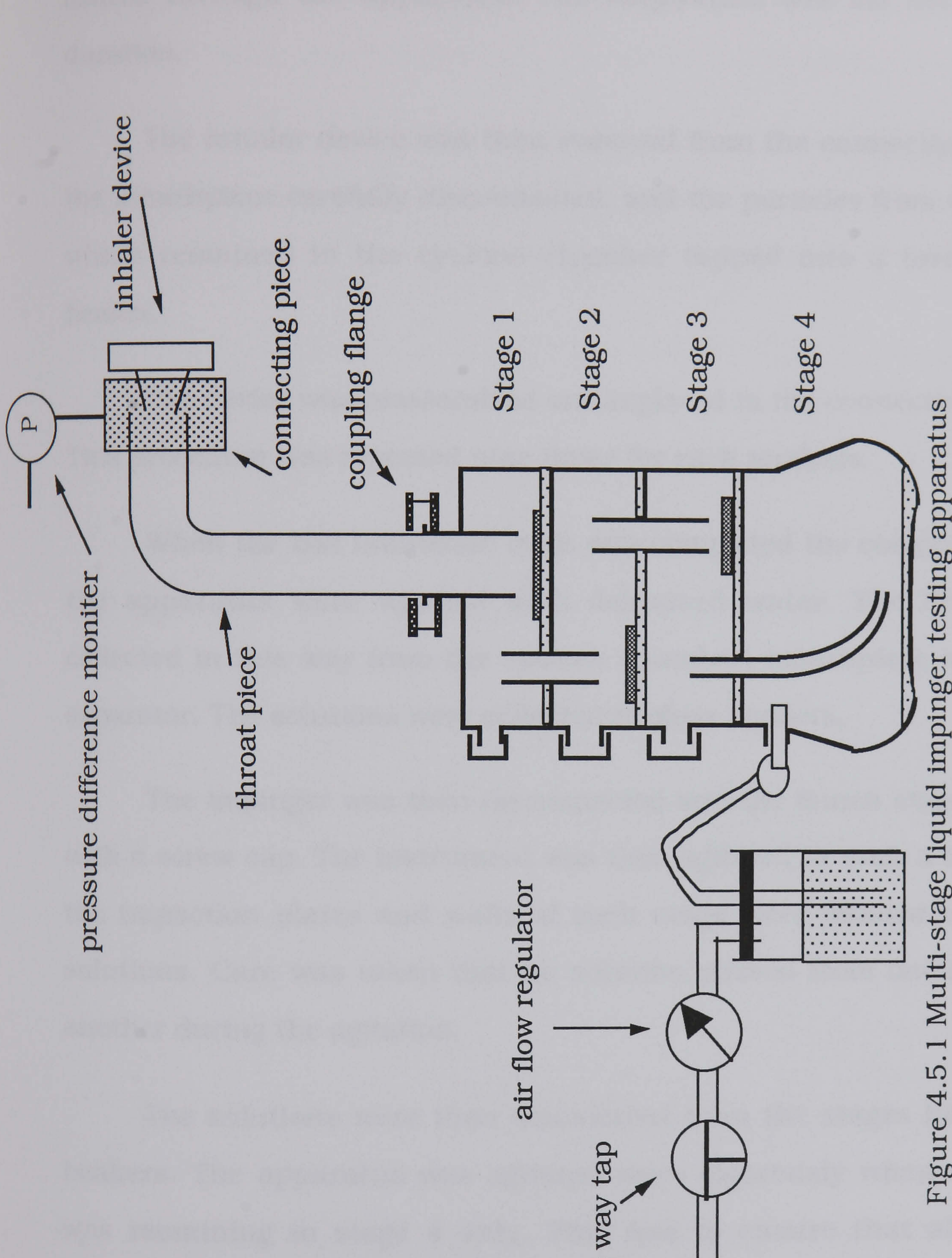

Figure 4.5.1 Multi-stage liquid impinger testing apparatus

The three-way tap was orientated such that the air flow was routed through the apparatus. The inspiration was six seconds in duration.

The inhaler device was then removed from the connecting piece, the mouthpiece carefully disconnected, and the particles from the dose which remained in the cyclone chamber tapped into a tared glass beaker.

The device was reassembled and replaced in the connecting piece. This procedure was repeated nine times for each analysis.

When the last inhalation cycle was completed the components of the apparatus were washed with deionised water. The drug was collected in this way from the cyclone chamber, mouthpiece and pre-separator. The solutions were collected in glass beakers.

The impinger was then disconnected and the fourth stage sealed with a screw cap. The instrument was then agitated in such a way that the impaction plates and walls of each stage were washed with the solutions. Care was taken that no solution passed from one stage to another during the agitation.

The solutions were then transferred from the stages into glass beakers. The apparatus was agitated more vigorously when solution was remaining in stage 4 only. This was to ensure that all of the surfaces of this awkwardly shaped stage had come into contact with the aqueous solution.

The total mass of powder which had been removed from the cyclone chamber after each inspiration was recorded. Sufficient deionised water was then added to this residue in order to dissolve both the drug and the lactose.

4.5.3 Drug assay

Solutions were assayed for drug content using the U.V assay described in section 2.11. There was no interference at the absorption maxima due to lactose.

4.6 Results

Deposition profiles were constructed for each of the powder blends. Drug was recovered from the following locations:

i. cyclone chamber
ii. mouthpiece
iii. pre-separator (throat)
iv. stage 1
v. stage 2
vi. stage 3
vi. stage 4
viii. attached to the lactose residue removed from the cyclone

Qualitative analysis of the powder residue which remained in the inhaler was carried out by image analysis and scanning electron microscopy.

4.6.1 Deposition profiles

The data obtained from each impinger analysis are expressed in the form of deposition profiles. The drug recovered at each location is expressed as a percentage of the total drug loaded into the inhalation device during the analysis.

Figure 4.6.1 Percentage of the loaded dose of nedocromil sodium recovered from ten doses of 25 mg of powder mix at each location of the *in vitro* inhalation testing apparatus

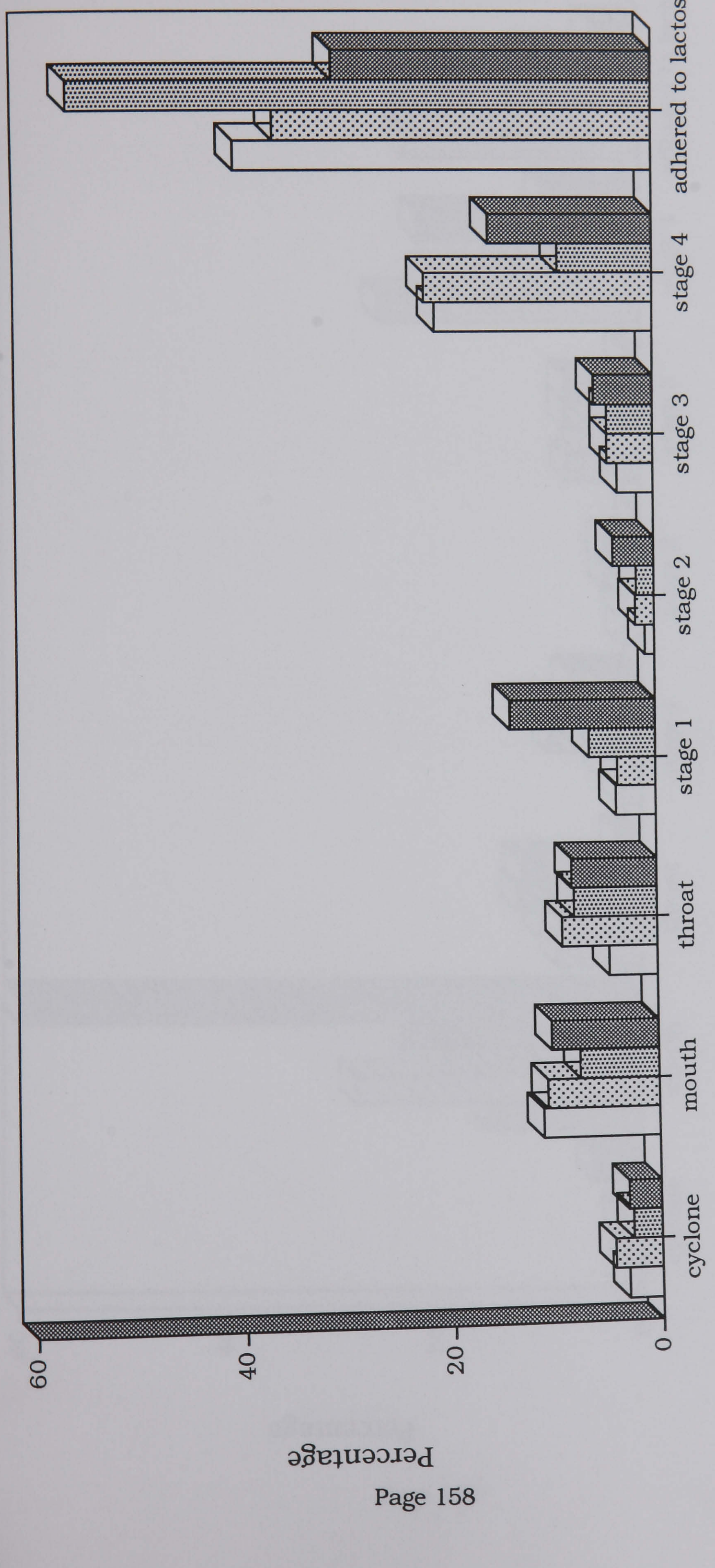

Figure 4.6.2 Percentage of the loaded dose of sodium cromoglycate recovered from ten doses of 25 mg of powder mix at each location of the *in vitro* inhalation testing apparatus

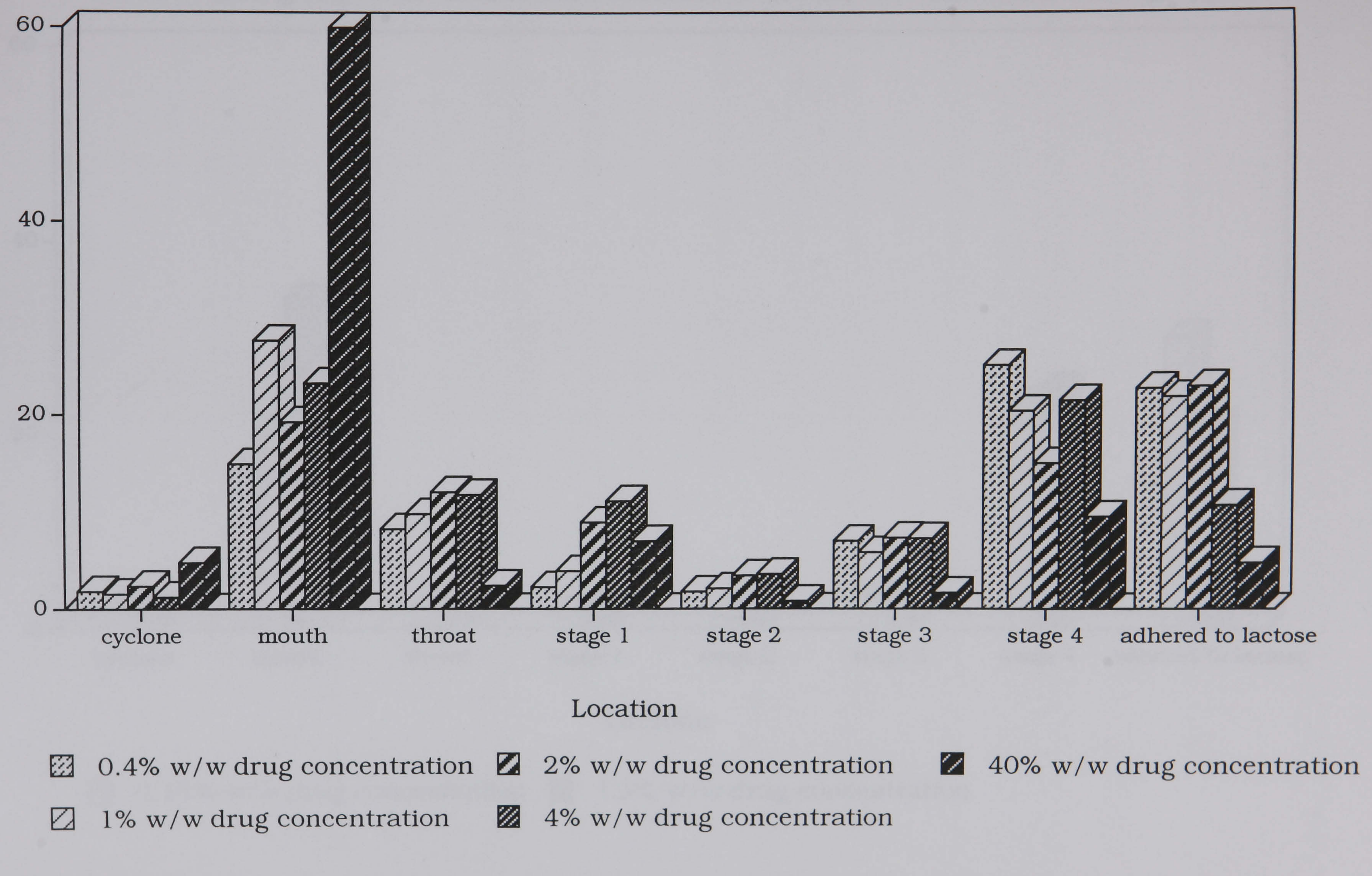

Figure 4.6.3 Percentage of the loaded dose of reproterol recovered from ten doses of 25 mg of powder mix at each location of the *in vitro* inhalation testing apparatus

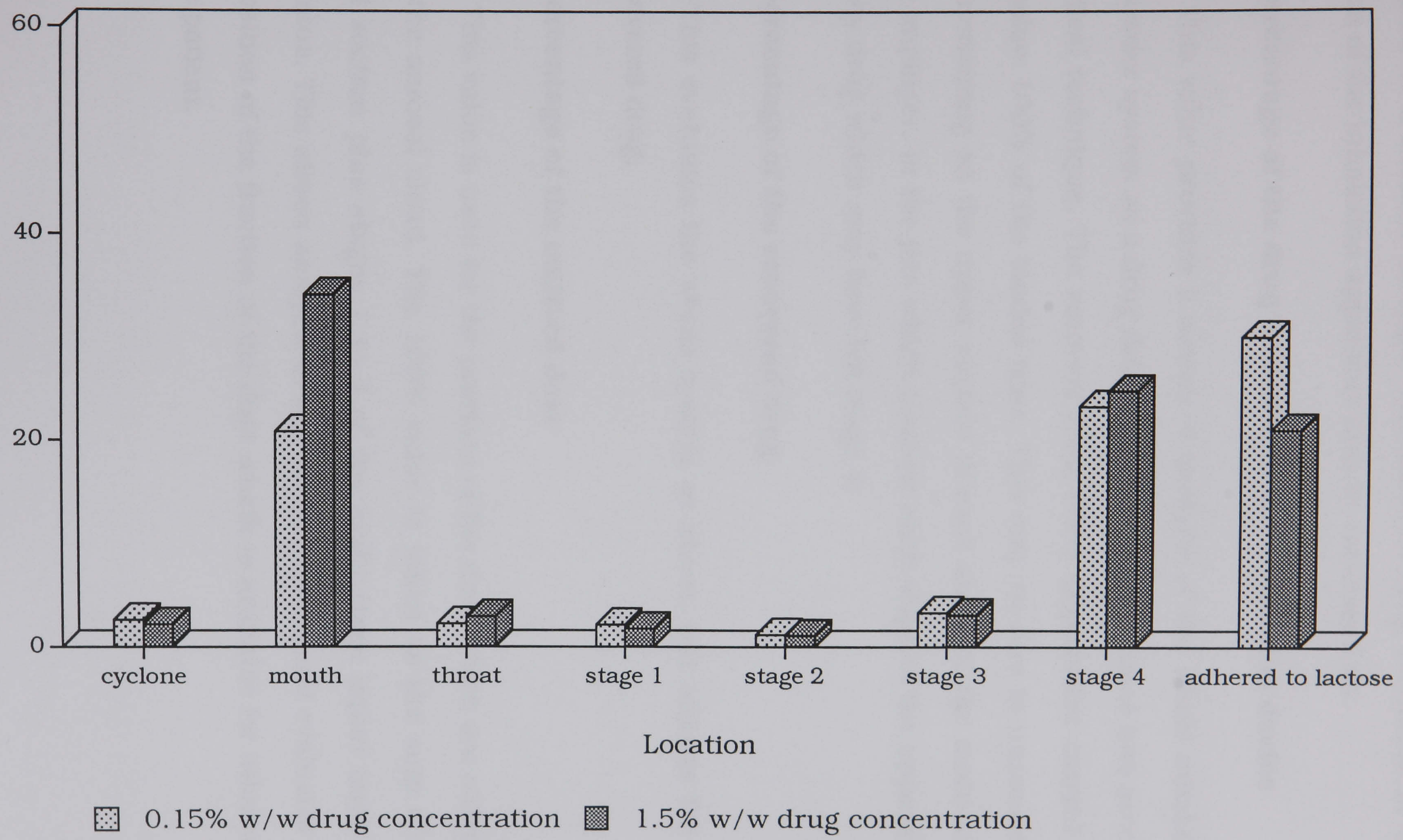

The data collected from the multi-stage liquid impinger can be presented in a number of ways. The mass of drug recovered at each location of the inhalation apparatus may be expressed as:

a) a percentage of the drug loaded into the inhalation device

This value provides a means of analysis of the whole inhalation and powder system as a drug delivery system. It also takes into account analytical technique. The recovery from every experiment carried out was below 100% of the loaded dose. This may be due to unrecovered drug remaining on the upper surface of each stage of the multi-stage liquid impinger, in the jets which connect each stage of the apparatus, and any drug which may have left stage 4;

b) a percentage of the recovered drug

This evaluates the whole system as above, but adjusts for the unrecovered drug;

c) a percentage of the emitted dose

This value is used for the portions of the dose which are collected from the aerosol cloud. The 100% value is taken as the sum of the throat section plus stages 1 to 4 of the multi-stage liquid impinger apparatus. This allows analysis of the aerosol cloud, and evaluates the composition of the fraction of the dose which is available for inhalation by the patient.

Analysis of the deposition results gives an indication of:

i-the role of adhesion within the powder mixes, and its influence on drug deposition;

ii- the role of cohesion within the powder mixes, and its influence on drug deposition;

iii- the consequent effect on the efficiency of the system to deliver drug to the target site;

iv- a comparison of the performance of powder mixes containing different drug entities.

4.7 Discussion

4.7.2 The role of adhesion within the powder mixes, and its influence on drug deposition

Adhesion is responsible for the direct association between the drug species and carrier particles in the powder mix. This adhesion maintains the integrity of the mix and prevents segregation of active and carrier particles. The inhaler device was designed such that the carrier particles of the dose are retained during the inhalation cycle. Analysis of this powder residue allowed the quantification of drug which was not detached during the air flow through the device. Drug which remained adhered was assayed using UV spectroscopy. Scanning electron microscopy was employed in order to analyse visually this portion of the dose.

4.7.2.i UV assay of drug remaining adhered

The residue powder was dissolved in double distilled water and assayed for drug content as described in Section 2.11. The percentage w/w of drug in the powder mix remaining in the device post inhalation was determined for each powder blend. The data from the quantification of this residue mix are presented in Table 4.7.1 and Figure 4.7.1. The error bars represent the standard deviation of the data.

Nedocromil sodium		Sodium cromoglycate		Reproterol	
Initial mix concentration (%w/w)	Residue mix concentration (%w/w)	Initial mix concentration (%w/w)	Residue mix concentration (%w/w)	Initial mix concentration (%w/w)	Residue mix concentration (%w/w)
0.392	0.171	0.394	0.097	0.150	0.050
0.985	0.381	0.960	0.225	1.475	0.330
1.956	1.205	1.951	0.430		
3.908	1.317	3.704	0.449		

Table 4. 7.1 %w/w drug content of mix residue after inhalation

Powder mix concentration after inhalation against powder mix concentration before inhalation

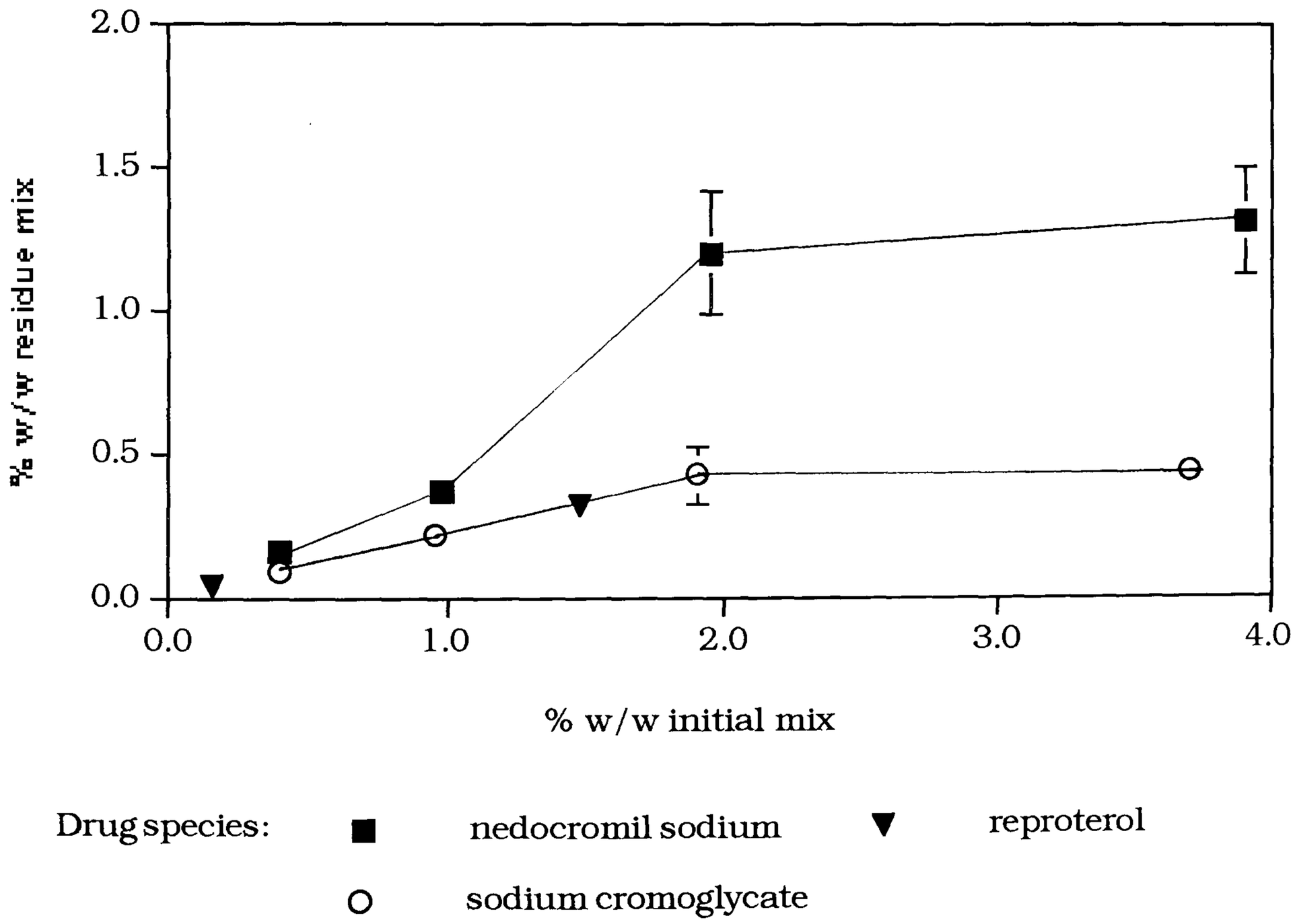

Figure 4.7.1 Relationship between %w/w initial powder mix and %w/w residue powder mix for three different drug species mixed with lactose

The error bars represent the standard deviation of the data.

The graph shows that an increasing mass of drug is retained on the lactose particles as the drug load in the initial mix increases. The number of adhered particles appears to reach a maximum as the %w/w concentration of the retained mix does not dramatically increase between the values of 2 %w/w and 4 %w/w initial drug mix.

Scanning electron micrographs of the powder mixes at 4 %w/w drug concentration pre and post inhalation show the distribution of the drug particles. The surface of the carrier particles in the pre inhalation mixes accommodate both single particles and small aggregates of drug. These can be identified in Figures 4.7.2 and 4.7.3 for mixes of nedocromil sodium and sodium cromoglycate at 4 %w/w nominal drug concentration. The distribution of these adhered aggregates throughout the initial mixes can be seen in the image analysis photographs, reproduced in Figures 3.6.4 to 3.6.16.

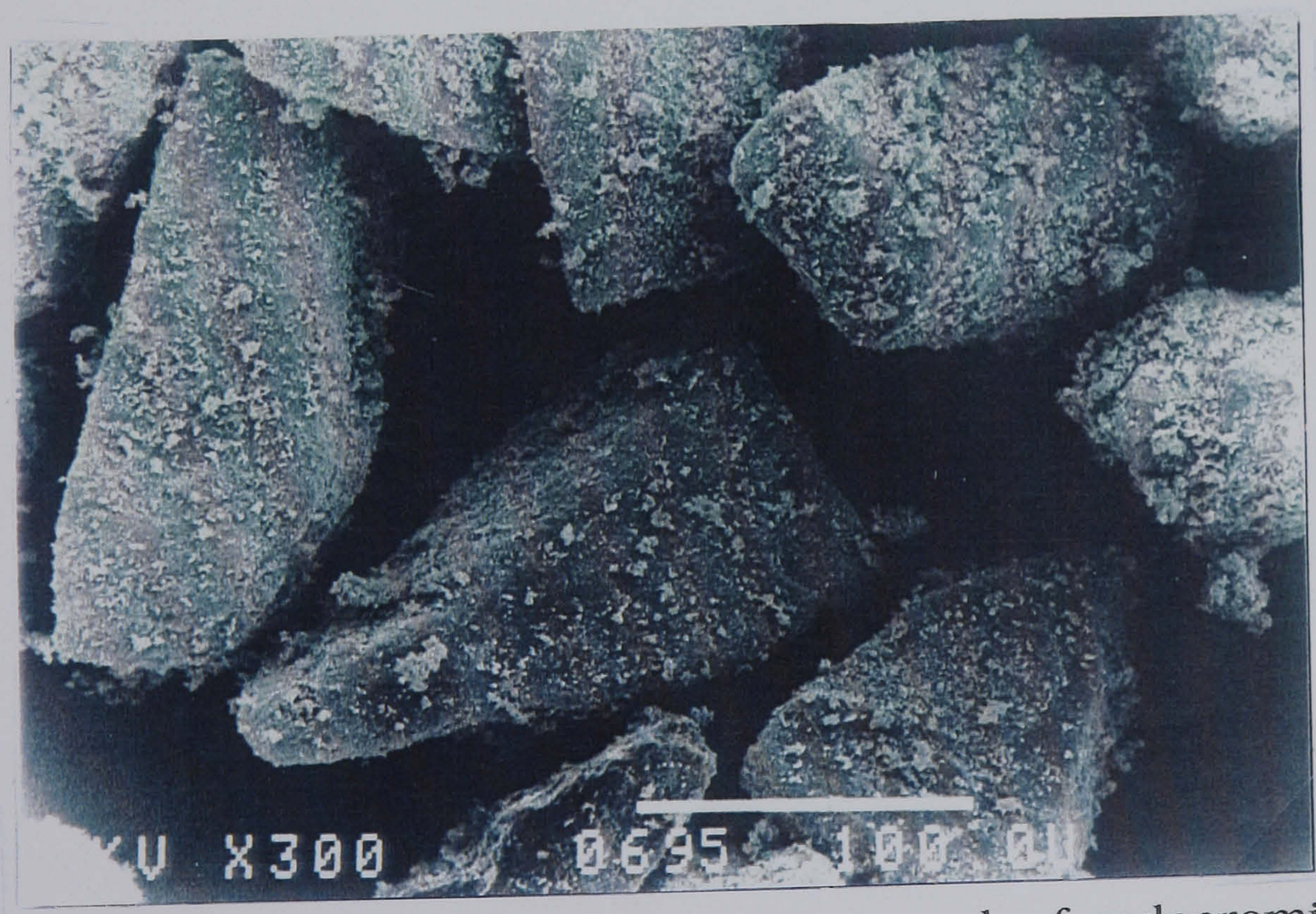

Figure 4.7.2. Scanning electron micrograph of nedocromil sodium/lactose powder mix 4.0 %w/w drug concentration. Picture number 0695.

Figure 4.7.3. Scanning electron micrograph of sodium cromoglycate/lactose powder mix 4.0 %w/w drug concentration. Picture number 0694.

Particles of drug can be identified on the surface of the carrier particles which were recovered from the device after the inhalation cycle. The adhered drug which has not been removed from the carrier exists as single isolated particles, or very small clusters of a few drug particles. These can be seen in the scanning electron micrographs reproduced in Figures 4.7.4 to 4.7.6. The larger aggregates which were associated with the carrier in the pre-inhalation mix are no longer present. Therefore, the drug which fluidises and leaves the cyclone chamber derives mainly from these surface held drug aggregates.

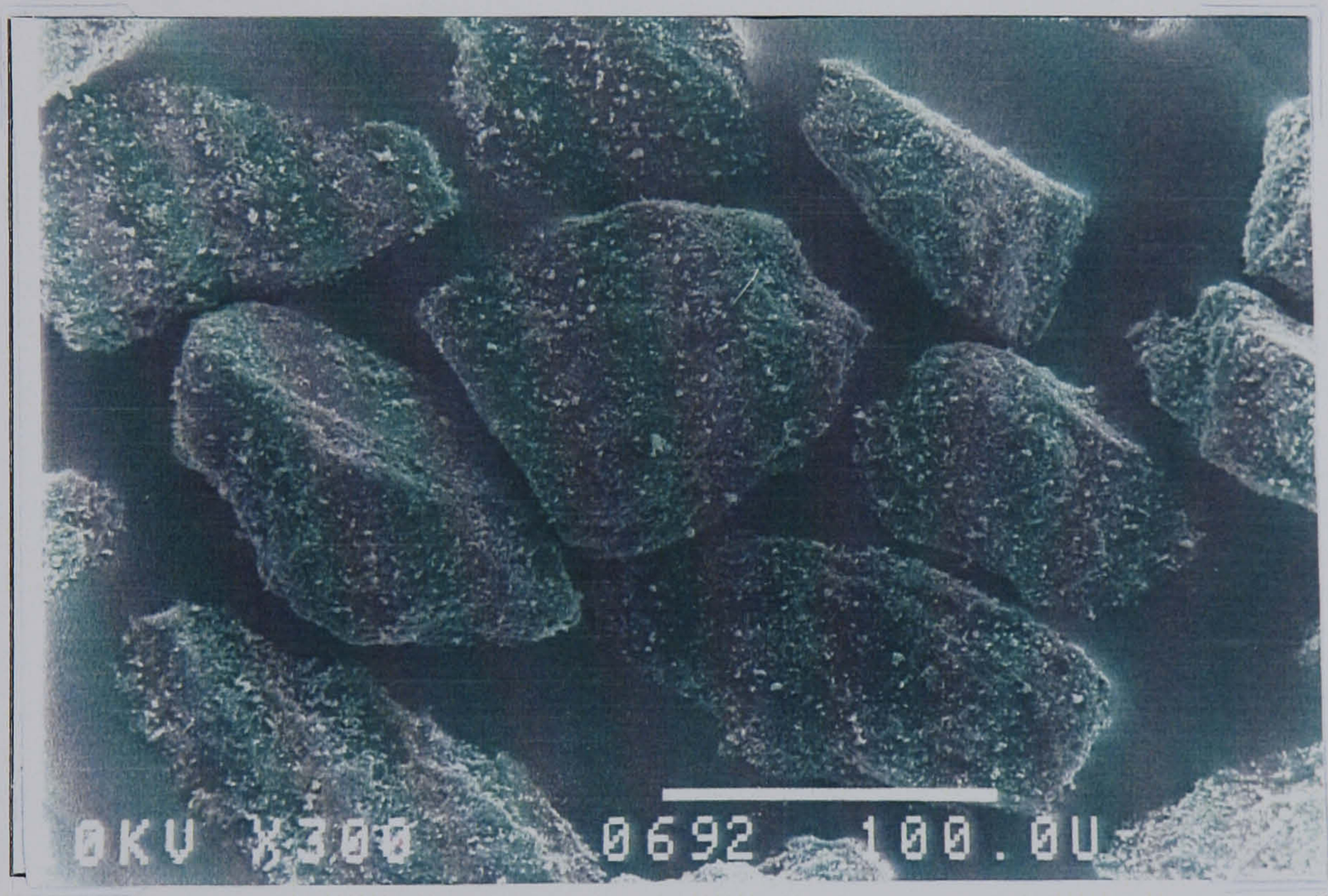

Figure 4.7.4. Scanning electron micrograph of nedocromil sodium/lactose powder residue after inhalation. Picture number 0692.

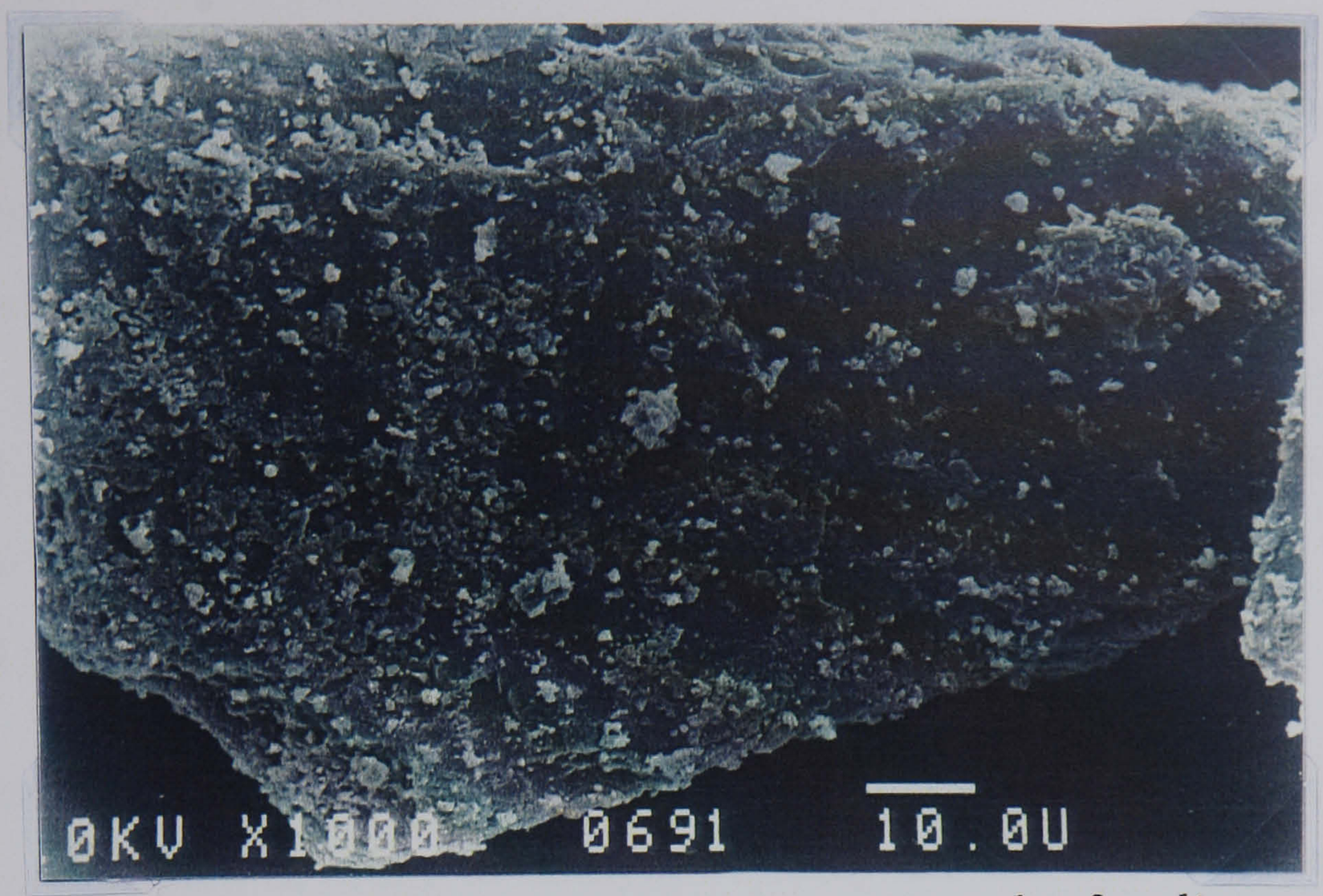

Figure 4.7.5. Scanning electron micrograph of sodium cromoglycate/lactose powder residue after inhalation. Picture number 0691.

Figure 4.7.6. Scanning electron micrograph of sodium cromoglycate/lactose powder residue after inhalation. Picture number 0691.

The percent remaining adhered to the lactose at an initial drug concentration of 40 %w/w was not determined. The composition of the binary mix pre-inhalation was such that it contained non-adhered drug agglomerates. Visual inspection of the powder remaining in the cyclone chamber post-inhalation determined that some of these agglomerates were still present. Therefore U.V. assay of this remaining powder mix would not provide information relating to the mass of drug which remained adhered to the carrier during the inspiration cycle.

Scanning electron microscopy was carried out on these post-inhalation particles in order to analyse visually the surface of the carrier particles. The resultant photomicrographs from the nedocromil sodium and sodium cromoglycate 40 %w/w mixes are reproduced in Figures 4.7.7 and 4.7.8 respectively.

Figure 4.7.7. Scanning electron micrograph of nedocromil sodium/lactose powder residue from 40 %w/w drug mix after inhalation. Picture number 1949.

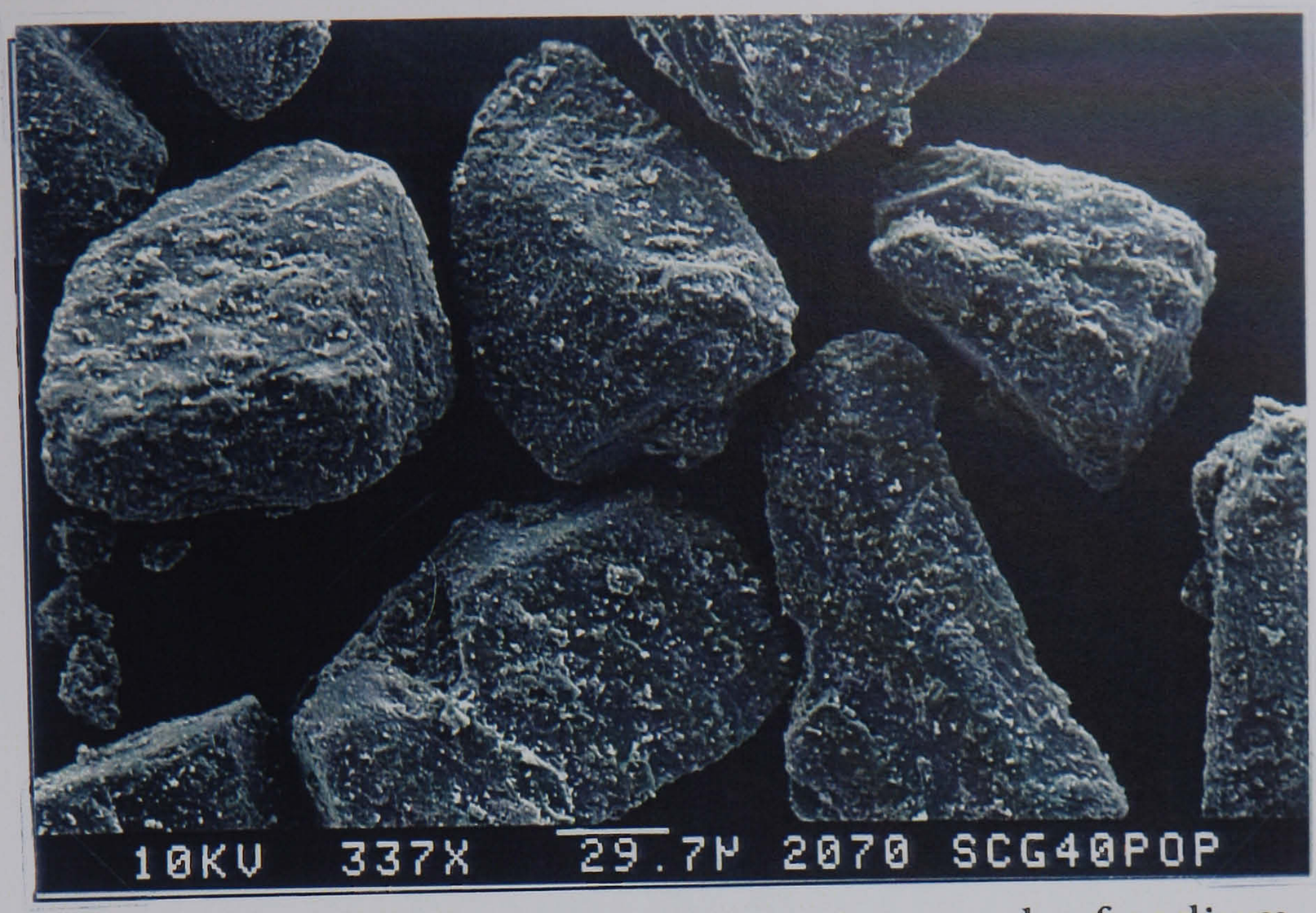

Figure 4.7.8. Scanning electron micrograph of sodium cromoglycate/lactose powder residue from 40 % w/w drug mix after inhalation. Picture number 2070.

The residue lactose particles from these 40 %w/w mixes have, associated with their surface, both single drug particles and small adhered aggregates. These aggregates appear much larger than the small clusters seen attached to the carrier particles of the lower concentration mixes. When compared with those which were adhered in the mix pre-inhalation, they are considerably smaller as shown in figures 4.7.9 and 4.7.10.

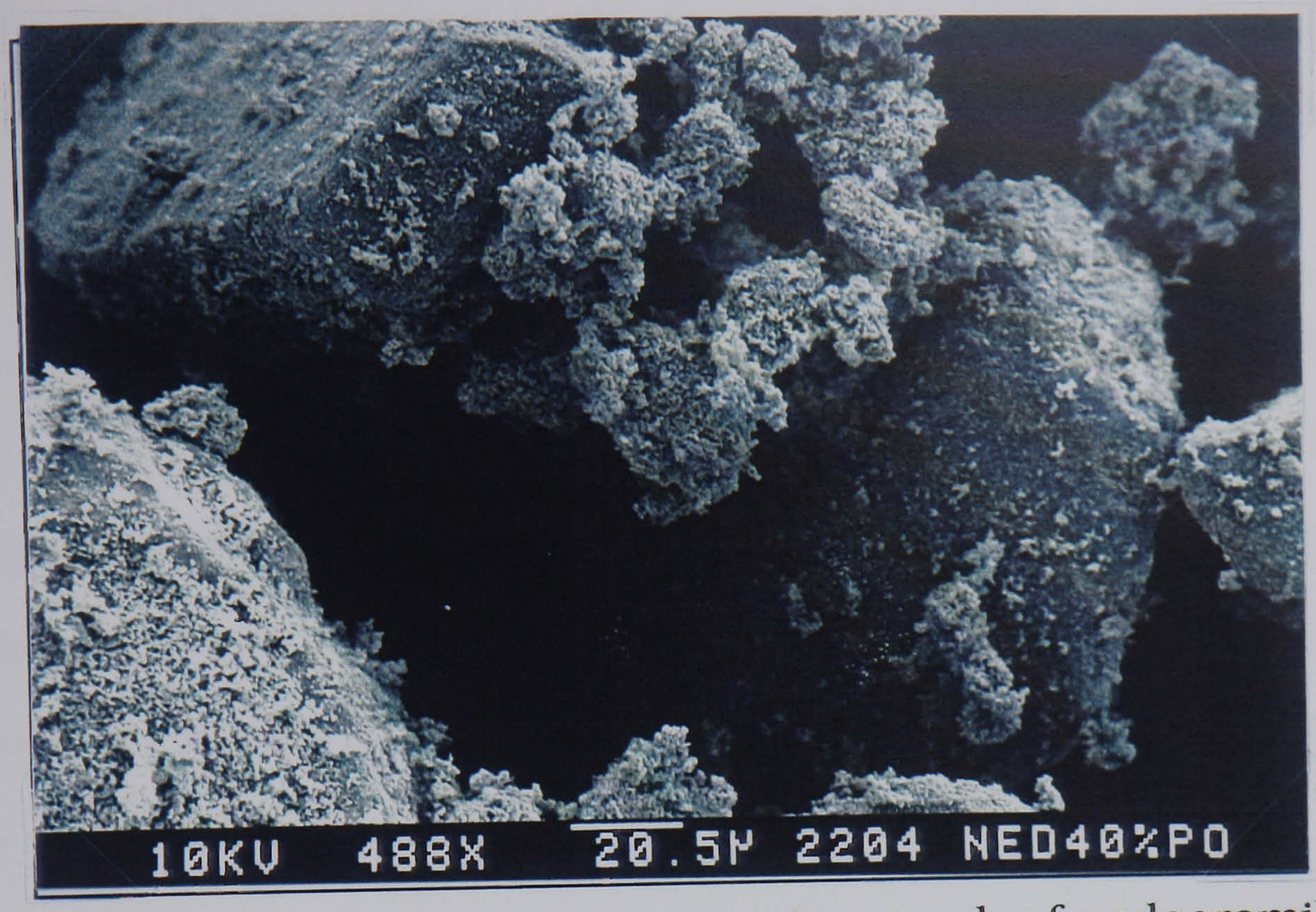

Figure 4.7.9. Scanning electron micrograph of nedocromil sodium/lactose 40 % w/w drug mix. Picture number 2204.

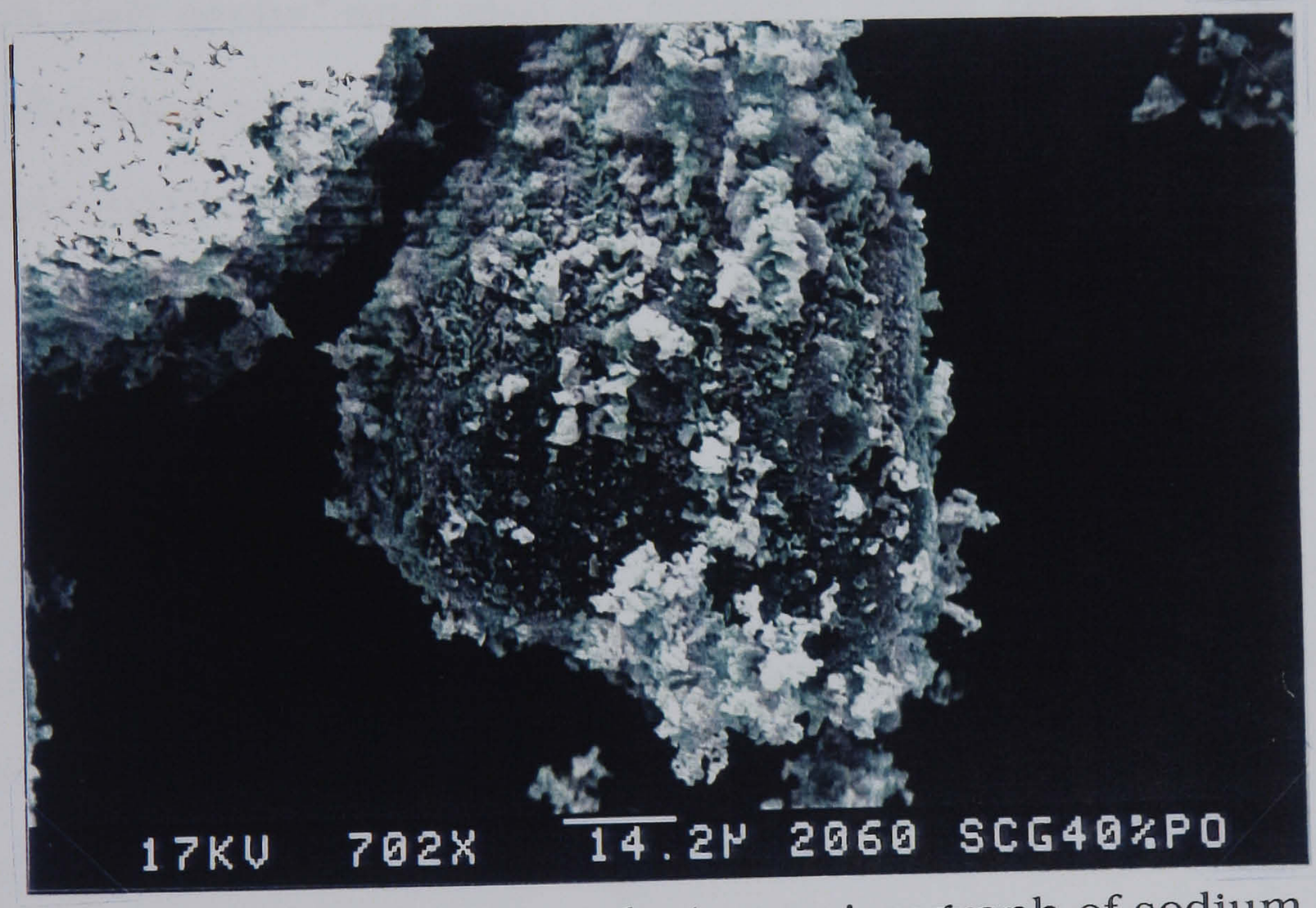

Figure 4.7.10. Scanning electron micrograph of sodium cromoglycate/lactose 40 % w/w drug mix. Picture number 2060.

Therefore it can be concluded that the energy supplied by the act of inspiration is not sufficient to remove all of the adhered drug. Drug which is removed from the carrier particles originated from cohesive

aggregates which are present in the powder mix. This suggests that the drug-lactose adhesive interactions are stronger than the drug-drug cohesive interactions.

As discussed previously in section 3.2 mechanisms of adhesion include van der Waals' forces, electrostatic forces and mechanical interlocking as well as forces due to liquid bridges, solid bridges and magnetic moments. The extent of the adhesive interactions within the binary powder mixes may be due to a combination of the electrostatic and van der Waals' forces.

During the mixing process contacts between surfaces of particles in the mix will occur, and also be broken. When this process occurs between two dissimilar materials static electrification, otherwise known as triboelectrification results. The triboelectrification of the two dissimilar surfaces in mutual contact occurs by transfer of electrons from one material to another [129] Therefore, the particles which experience contact events with carrier particles and the mixing vessel are able to form point charges on their surfaces. The strongly adhered drug particles may result from the electrostatic attractions between drug and lactose facilitating close particle contact which leads to increased van der Waals' interactions.

Triboelectrification may also cause the formation of the loosely packed cohesive aggregates. The large surface energy inherent to the small drug particles increases the cohesive tendency. Like-charging of these drug particles will cause a barrier for interparticle contact,

resulting in less opportunity for the van der Waal's forces to form between the particles of drug.

4.7.3 The influence of adhesion upon the deposition profile

The deposition of drug from the powder formulation is affected by the adhesion between the drug and carrier particles. Because a proportion of drug remains attached to the carrier it is not possible to deliver 100% of the loaded dose (as described in section 4.6) as a powder cloud. The reduction of the emitted dose (as described in section 4.6), therefore, decreases the performance of the inhalation system. The particles of drug which remain attached to the carrier are single entities, or very small clusters. If they were released from the carrier, these particles would be included in the respirable fraction of the dose. Therefore, it is suggested that the adhesion exhibited in the drug/carrier interactive unit, which is not disrupted during the inhalation cycle, adheres drug particles at the expense of the respirable fraction.

When expressed as a percentage of the recovered dose (as described in section 4.6), the reduction in the emitted dose can be expressed, as shown in Tables 4.7.1, 4.7.2, 4.7.3 and Figures 4.7.11, 4.7.12 and 4.7.13 for nedocromil sodium, sodium cromoglycate and reproterol respectively.

Nedocromil sodium

Drug conc. (%w/w)	Percentage of recovered drug from each location		
	mouth & cyclone (%)	powder cloud (%)	lactose (%)
0.4	14.50	39.70	45.80
1.0	15.54	45.87	38.59
2.0	12.47	39.17	48.37
4.0	17.58	49.42	33.01

Table 4.7.1 Distribution of recovered drug from nedocromil sodium powder mixes

Nedocromil sodium

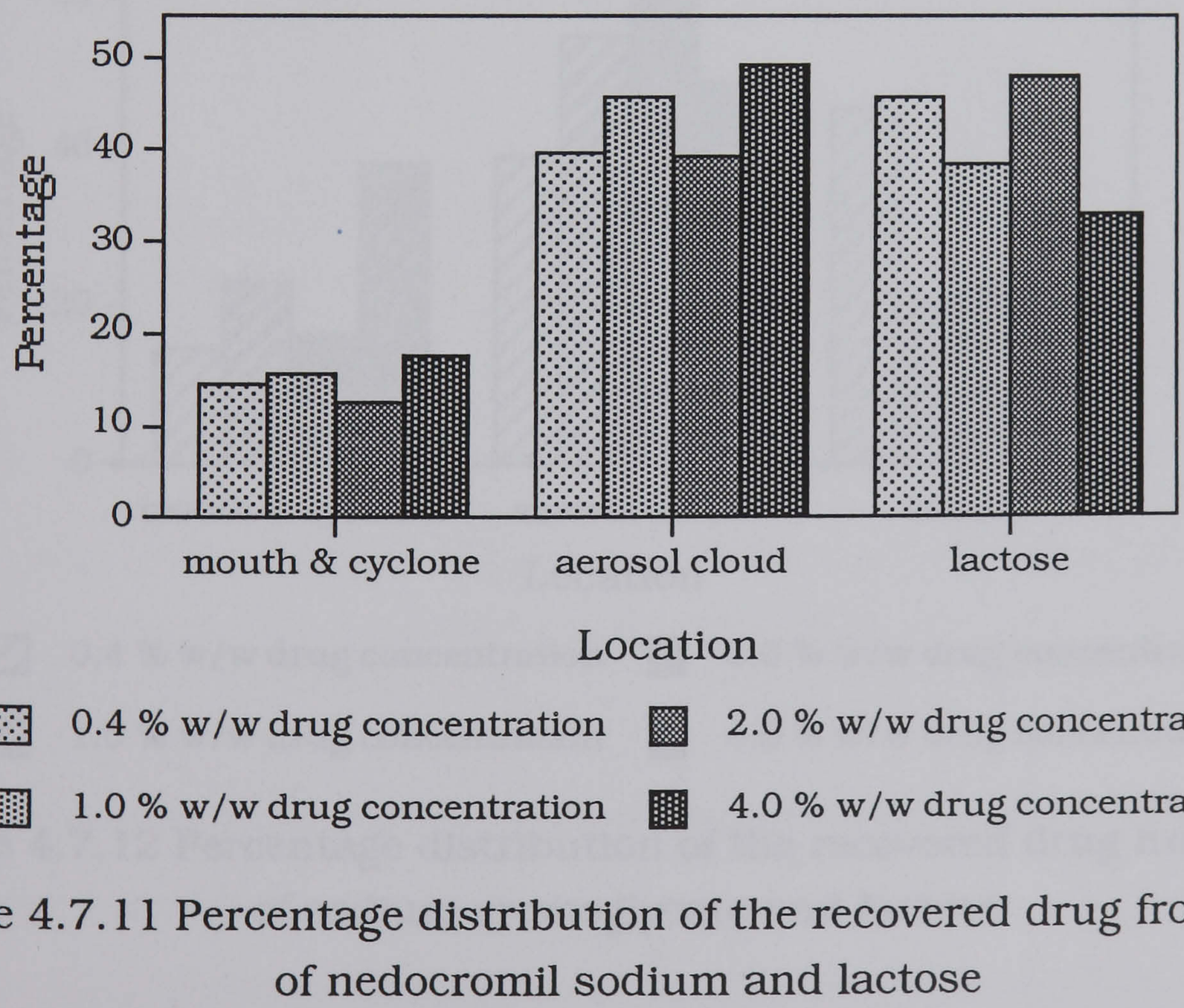

Figure 4.7.11 Percentage distribution of the recovered drug from mixes of nedocromil sodium and lactose

Sodium cromoglycate

Drug conc. (%w/w)	Percentage of recovered drug from each location		
	mouth & cyclone (%)	powder cloud (%)	lactose (%)
0.4	16.21	58.36	25.43
1.0	23.45	55.27	21.28
2.0	16.76	59.45	23.79
4.0	38.73	48.91	12.37

Table 4.7.2 Distribution of recovered drug from sodium cromoglycate powder mixes

Sodium cromoglycate

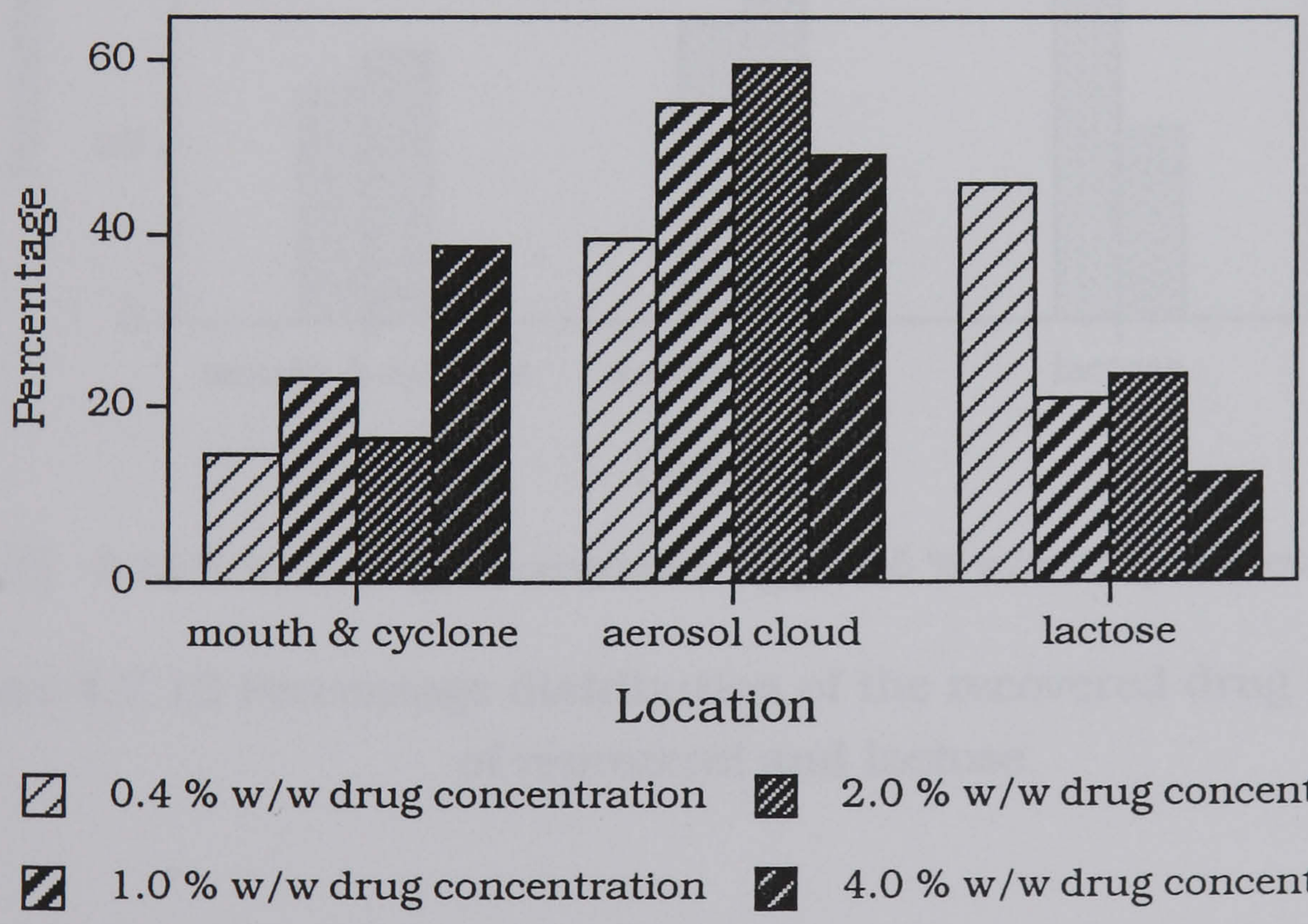

Figure 4.7.12 Percentage distribution of the recovered drug from mixes of sodium cromoglycate and lactose

Reproterol

Drug conc. (%w/w)	Percentage of recovered drug from each location		
	mouth & cyclone (%)	powder cloud (%)	lactose (%)
0.15	27.44	34.52	38.04
1.5	31.46	46.45	22.09

Table 4.7.3 Distribution of recovered drug from reproterol powder mixes

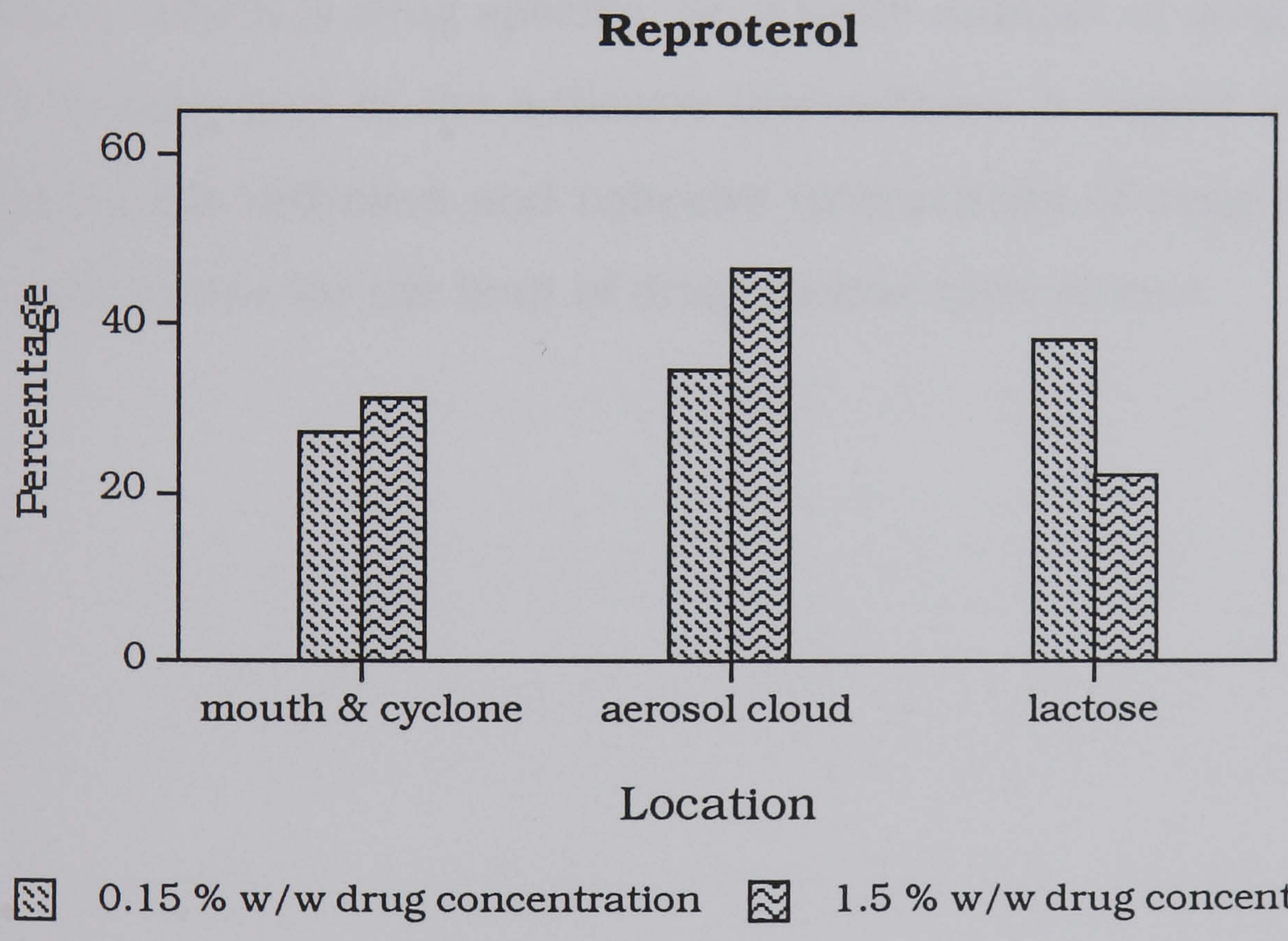

Figure 4.7.13 Percentage distribution of the recovered drug from mixes of reproterol and lactose

A constant mass of drug remains adhered to the carrier particles at 2 %w/w and 4 %w/w drug load for the mixes containing nedocromil sodium and sodium cromoglycate as the drug species(Figure 4.7.1). This is reflected by the percentage of the recovered dose due to drug

remaining adhered to the lactose particles decreasing at the higher concentration. An increase in mouthpiece deposition from sodium cromoglycate 4 %w/w drug concentration occurs at the expense of the emitted dose. This indicates an attractive interaction between the sodium cromoglycate particles and the surface of the mouthpiece that does not occur to such an extent for nedocromil sodium.

Therefore an effect of the adhesive interactions within the powder mixes is to decrease the respirable fraction of the drug. The results suggest that there is a finite number of sites for adhesion on the lactose surface, which is drug specific, or, a finite number of drug particles are able to take part in the adhesive interactions. A degree of competition between the adhesive and cohesive interactions of drug particles may be responsible for the limit of drug/lactose interactions.

4.7.5 The role of cohesion within the powder mixes, and its influence on drug deposition

The cohesive nature of the active species in the powder mix is responsible for the maintenance of the drug aggregates. The majority of these aggregates become airborne and leave the cyclone chamber. Deposition of the drug contained in these aggregates is dependent upon whether or not they disperse into primary particles. The aggregates which do not disperse will not travel to the stages of the multi-stage liquid impinger that correspond to reaching the target site. Because of their large size, these drug clusters will be deposited in the throat and stage 1 of the *in vitro* inhalation apparatus and therefore not reach the respiratory zone *in vivo*.

Drug deposition at these locations may also be due to the loss of carrier particles from the cyclone chamber of the device. As determined previously, some drug remains adhered to the carrier particles during the inhalation cycle. These particles of lactose have travelled with the air stream having been subjected to the cyclone effect within the chamber. Therefore, the drug associated with this fraction of the carrier particles will correspond to the concentration of drug which remains attached to the residue particles after the inhalation cycle. The values determined for the mass of lactose leaving the inhalation device and the associated drug are reproduced below.

Drug mix %w/w	Mass of lactose lost from 10 doses (mg). (±sd)	Mean %w/w remaining mix (±sd)	Mass of associated drug (mg) (±sd)
Mixes of nedocromil sodium			
0.4%	19.16 (±7.0)	0.17 (±0.02)	3.24×10^{-5} ($\pm1.1\times10^{-5}$)
1%	13.05 (±1.5)	0.38 (±0.3)	4.94×10^{-5} ($\pm2.5\times10^{-6}$)
2%	20.00 (±8.9)	1.21 (±0.2)	2.45×10^{-4} ($\pm1.4\times10^{-4}$)
4%	15.16 (±3.2)	1.31 (±0.2)	2.03×10^{-4} ($\pm6.5\times10^{-5}$)
Mixes of sodium cromoglycate			
0.4%	10.85 (±0.2)	0.09 (±0.01)	1.05×10^{-5} ($\pm6.1\times10^{-7}$)
1%	14.98 (±4.4)	0.22 (±0.04)	3.31×10^{-5} ($\pm7.6\times10^{-6}$)
2%	16.11 (±5.2)	0.48 (±0.1)	7.90×10^{-5} ($\pm4.2\times10^{-5}$)
4%	20.96 (±12.8)	0.45 (±0.01)	9.48×10^{-5} ($\pm5.9\times10^{-5}$)
40%	6.06 (±2.2)	3.08 (±1.0)	1.75×10^{-4} ($\pm3.6\times10^{-5}$)
Mixes of reproterol			
0.15%	22.08 (±12.6)	0.05 ($\pm4.5\times10^{-3}$)	1.16×10^{-5} ($\pm7.7\times10^{-6}$)
1.5%	12.48 (±1.2)	0.33 (±0.04)	4.09×10^{-5} ($\pm3.5\times10^{-6}$)

Table 4.7.4 Drug deposition in the throat and stage 1 of the multi-stage liquid impinger apparatus due to adhesion to lactose

When expressed as a percentage of the drug deposition by mass at the throat and stage 1, the largest value calculated was 0.08 %. The error therefore incurred due to lactose deposition in the impinger apparatus was considered to be negligible.

The sum of the throat and stage 1 deposition can be expressed both as a percentage of the drug loaded into the device, and a percentage of the emitted dose. Figures 4.7.14, 4.7.15 and 4.7.16 show the aggregate fractions recovered from the nedocromil sodium, sodium cromoglycate and reproterol powder mixes respectively.

Figure 4.7.14 Aggregate fractions from nedocromil sodium powder mixes

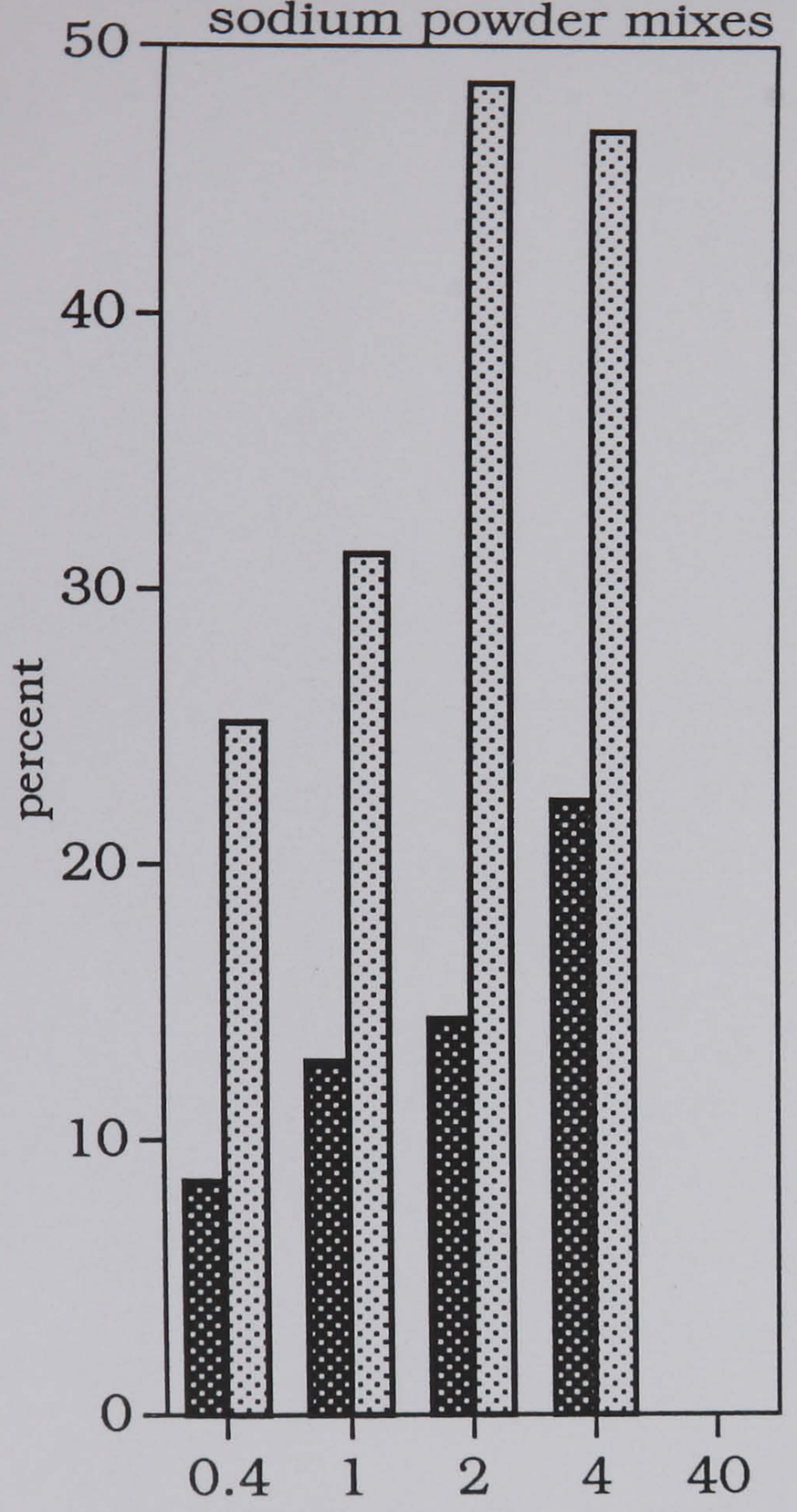

Figure 4.7.15 Aggregate fractions from sodium cromoglycate powder mixes

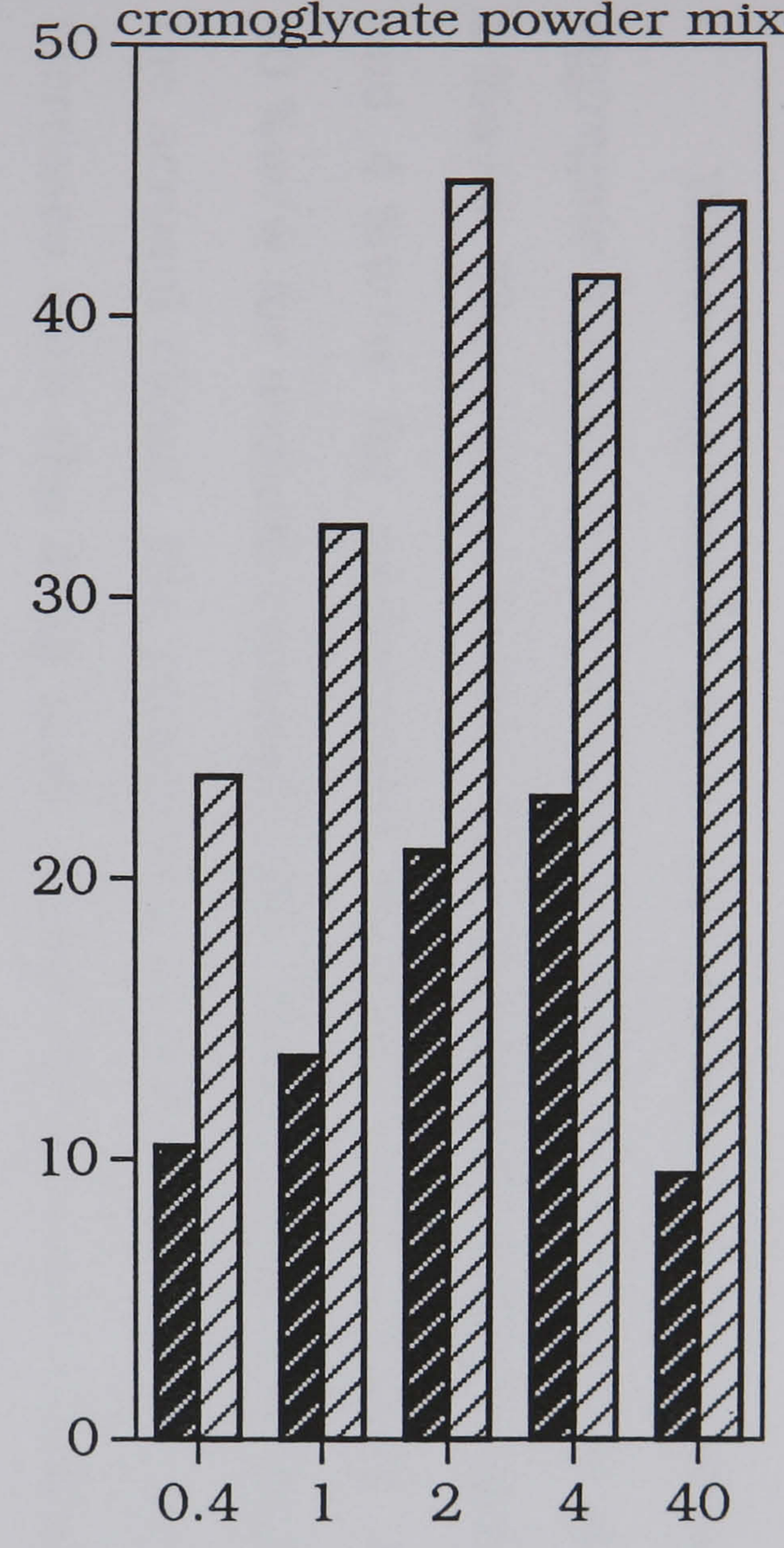

Figure 4.7.16 Aggregate fractions from reproterol powder mixes

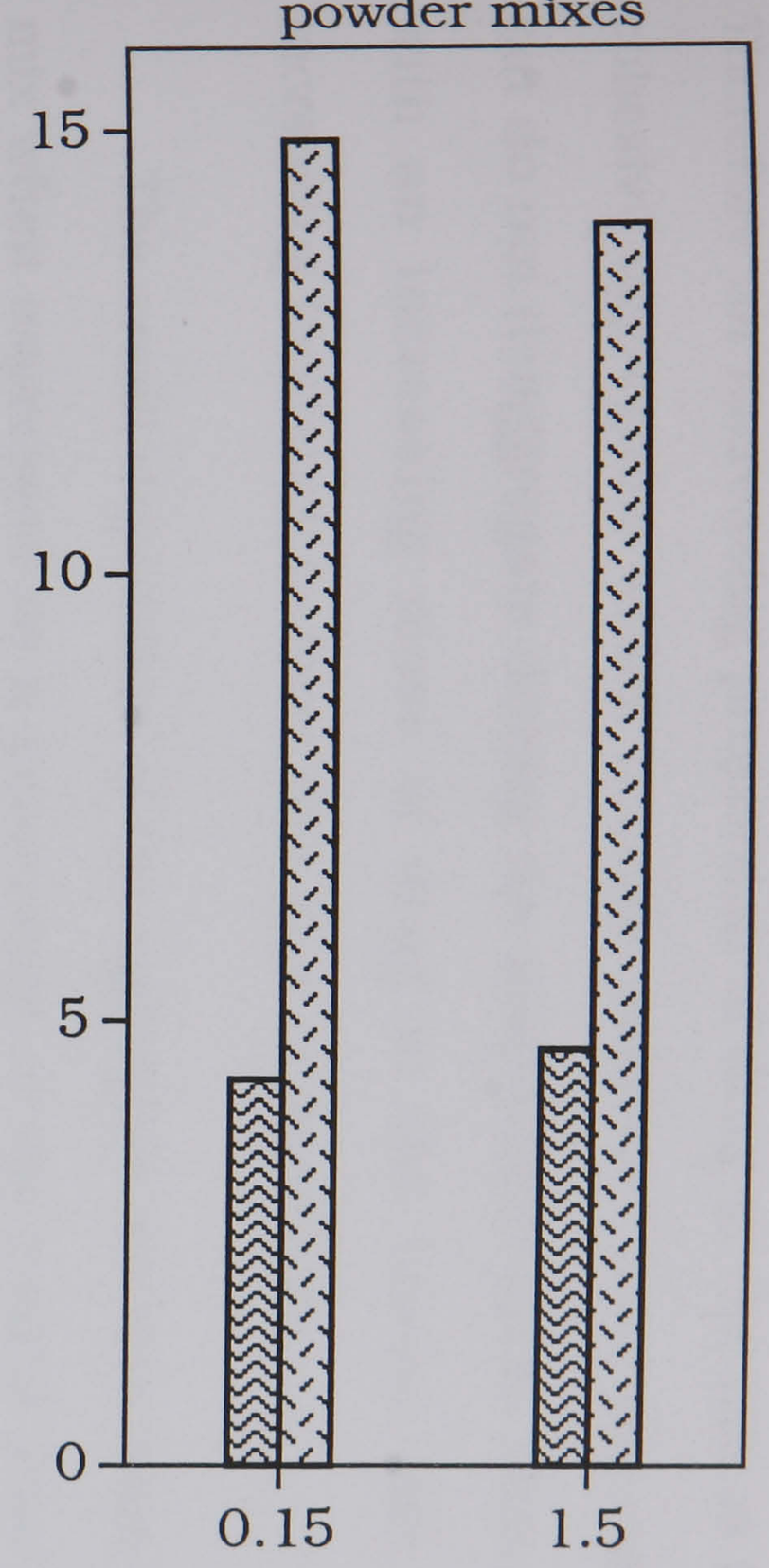

When expressed as a percentage of the loaded dose, the aggregate deposition tends to increase with an increasing drug load in the mix. Therefore an increasing proportion of drug in the mix is in the form of cohesive aggregates which become detached from the carrier particles but do not deaggregate during the inspiration cycle. This suggests that with an increasing mass of drug in the binary mix, there is an increasing tendency to form this type of aggregate.

The small deposition of the aggregate fraction from the 40 %w/w mix when expressed as a percentage of the loaded dose is due to the very high mouthpiece deposition of the drug.

When expressed as a percentage of the emitted dose the aggregate fraction tends to increase with an increase in drug load up to 2 %w/w. There is no further increase of this fraction between 2 %w/w and 4 %w/w for nedocromil sodium, and between 2 %w/w and 40 %w/w for sodium cromoglycate. Therefore, of the drug which forms the aerosol cloud, the proportion of non-dispersing drug aggregates increases with the drug load. Above drug concentrations of 2 %w/w this proportion tends to be constant and independent of the drug load.

4.7.6 The consequent effect of adhesion and cohesion on the efficiency of the system to deliver drug to the target site

Drug particles which account for the respirable fraction of the dose are deposited on stages 3 and 4 of the multi-stage liquid impinger. In order to travel through the apparatus to these stages the particles must be airborne as single entities.

The adhesive and cohesive interactions which occur within the powder mix combine to have an effect on the respirable fraction.

This respirable fraction can be expressed both as a percentage of the drug loaded into the device, and as a percentage of the emitted dose.

Figures 4.7.17, 4.7.18 and 4.7.19 show the respirable fractions recovered from the nedocromil sodium, sodium cromoglycate and reproterol powder mixes respectively.

Figure 4.7.17 Respirable fractions from nedocromil sodium powder mixes

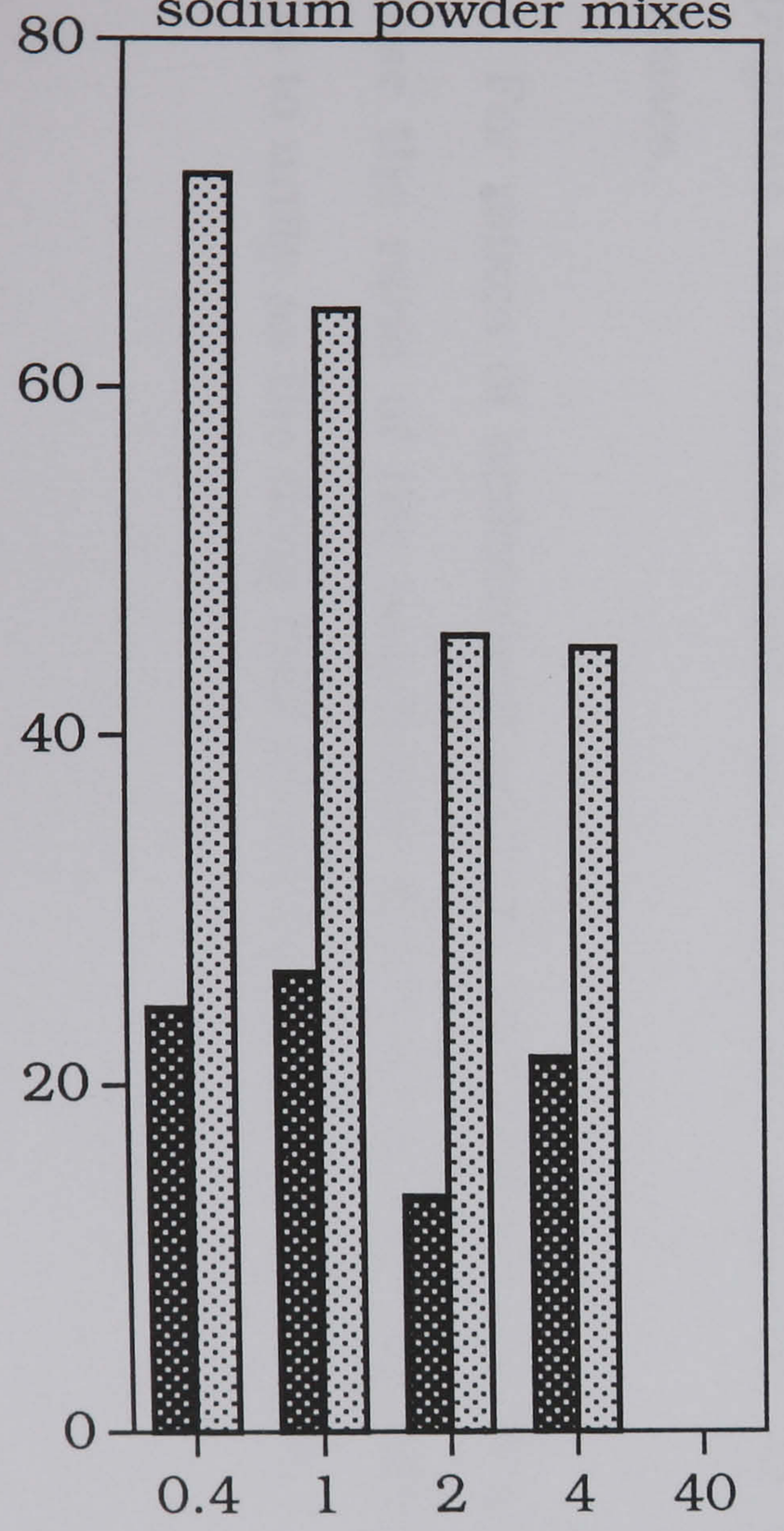

Figure 4.7.18 Respirable fractions from sodium cromoglycate powder mixes

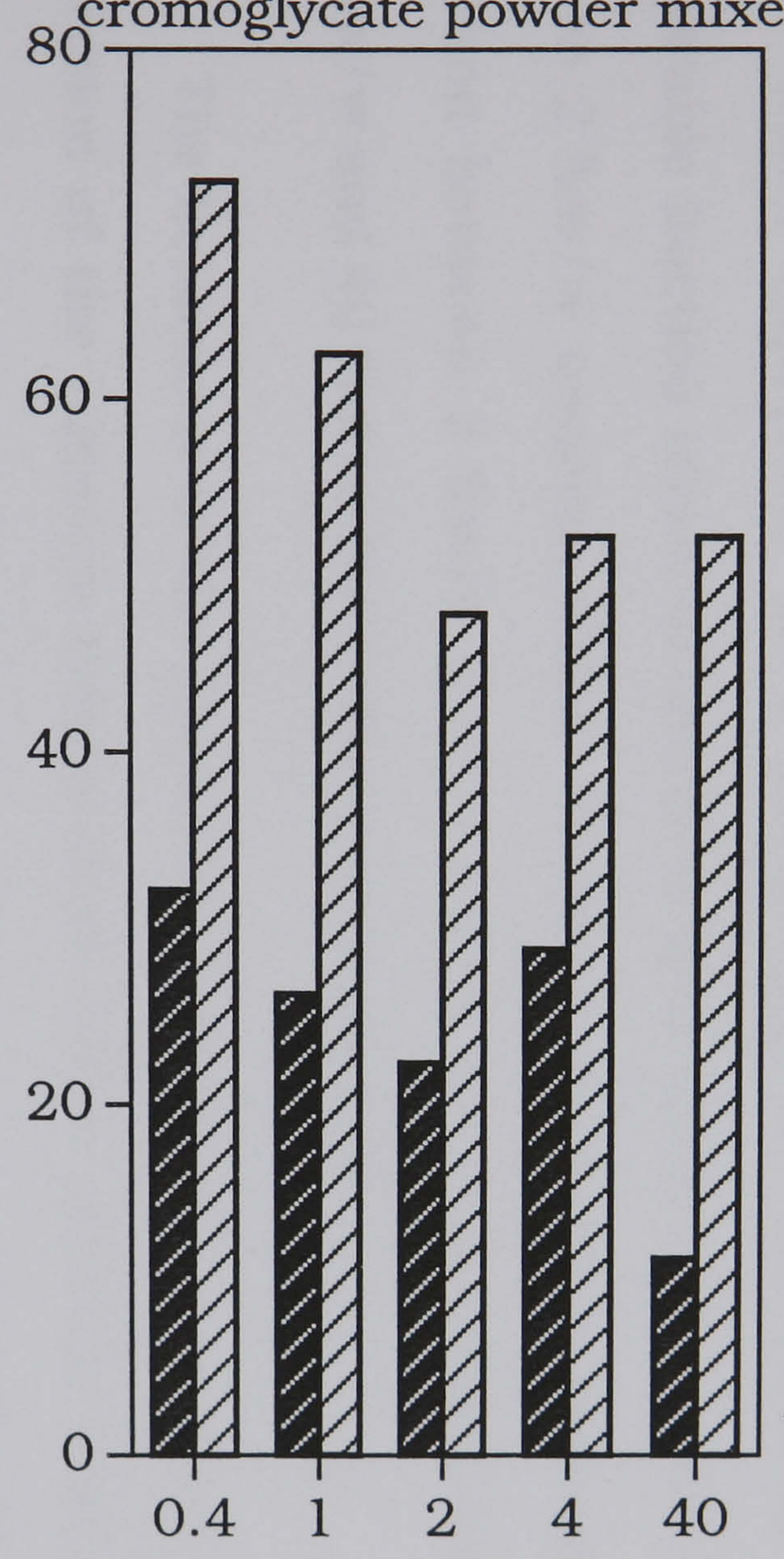

Figure 4.7.19 Respirable fractions from reproterol powder mixes

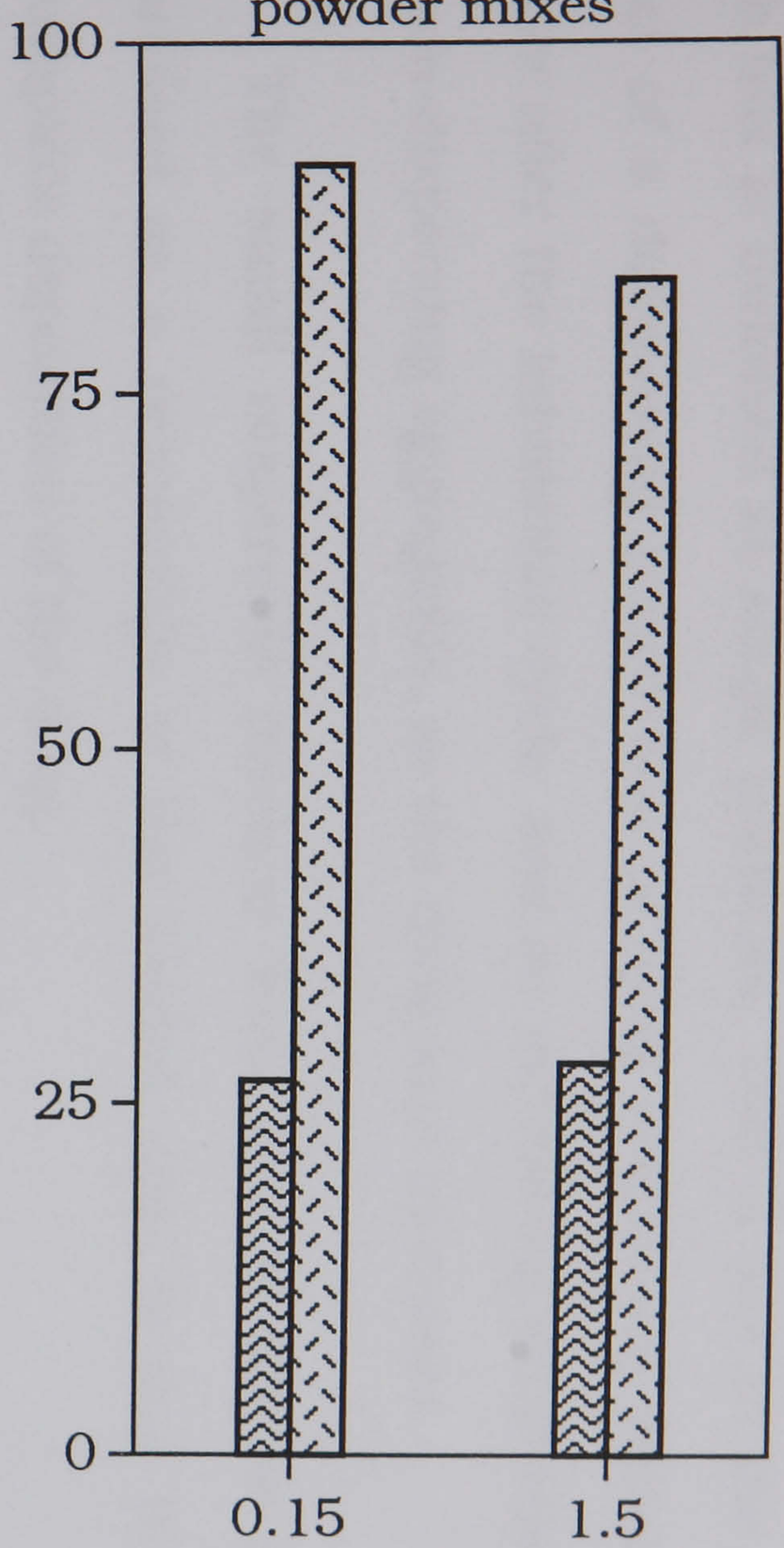

When expressed as a percentage of the loaded dose, the respirable fraction appears to be independent of the drug concentration. This suggests that a constant amount of the drug in each mix is fluidised as single particles. This is due to the combined effect of a decreasing proportion of drug remaining adhered to the carrier after the inhalation cycle, and an increasing proportion existing as non-dispersing aggregates, as the drug load increases.

The small respirable fraction from the 40 %w/w mix when expressed as a percentage of the loaded dose is due to the high mouthpiece deposition of the drug.

When expressed as a percentage of the emitted dose the respirable fraction tends to decrease with an increase in the drug load up to 2 %w/w concentration. There is no further decrease in this fraction between 2 %w/w and 4 %w/w for nedocromil sodium and 2 %w/w and 40 %w/w for sodium cromoglycate.

The behaviour of the respirable portion of the aerosol cloud is a reflection of the cohesive interactions which produce non-dispersing aggregates. As the proportion of the drug which exists in these aggregates increases, then the respirable fraction of the cloud decreases.

For mixes of nedocromil sodium and sodium cromoglycate with lactose the ratio of the respirable fraction to the aggregate fraction tends to unity as the drug load increases in the powder mix.

Figure 4.7.20 Ratio of respirable fraction to aggregate fraction for powder mixes

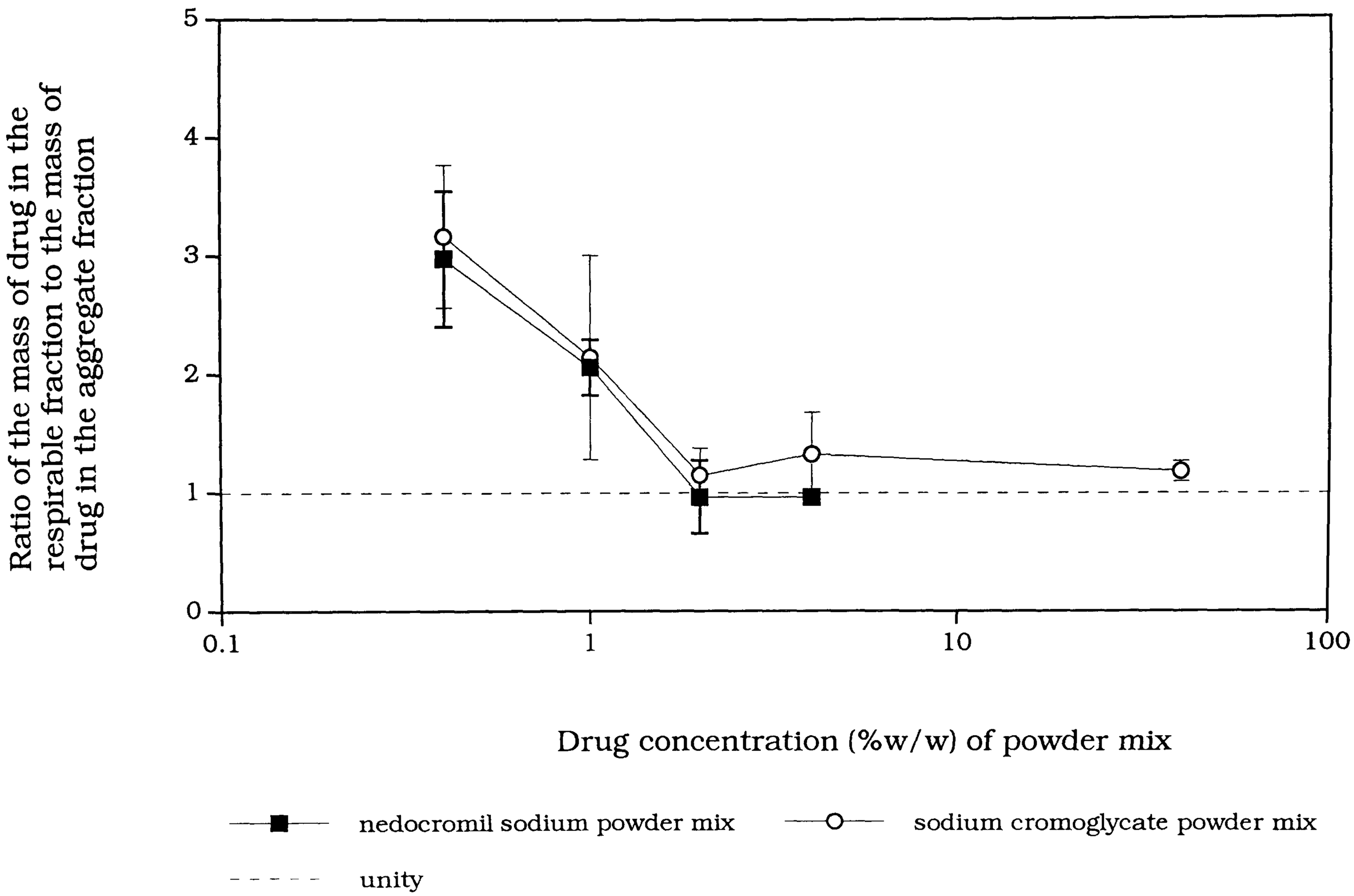

4.7.7 Effect of type of drug

Adhesive interactions

A significant difference exists when comparing the masses of drug adhered to the carrier particles at 2 %w/w and 4 %w/w for nedocromil sodium and sodium cromoglycate. Both drug species show a saturated effect at 2 %, but the mass of nedocromil sodium retained on the carrier surface is much greater than the corresponding mass of sodium cromoglycate. As the photomicrographs of the remaining fraction post inhalation show, the surface of the carrier particles from the nedocromil sodium powder mix contains more drug particles, covering a larger proportion of the lactose surface than in the sodium cromoglycate residue. Therefore the difference lies in a greater number of single particles remaining adhered, rather than stronger cohesive interactions which would cause aggregates to be retained on the lactose surface. The photomicrographs of the powder mixes containing nedocromil sodium and sodium cromoglycate show similar structures within the mix. Therefore the resultant difference in amount of drug remaining adhered is due to the difference in magnitude between the adhesive interactions of lactose and nedocromil sodium, and lactose and sodium cromoglycate.

Emitted dose composition

Considering the drug deposition as fractions of the emitted dose allows a comparison of the cloud composition of powder doses. The difference in adhesion behaviour between nedocromil sodium and sodium cromoglycate do not affect these values. The deposition

characteristics of the aerosol cloud from both types of mix are similar, as shown in Tables 4.7.5 and 4.7.6.

Drug concentration	Nedocromil sodium powder mixes (%)	Sodium cromoglycate powder mixes (%)
0.4 % w/w	72.19	72.36
1.0 % w/w	64.36	62.52
2.0 % w/w	45.73	47.79
4.0 % w/w	45.04	52.14

Table 4.7.5 Respirable fraction as a percentage of the emitted dose

Drug concentration	Nedocromil sodium powder mixes (%)	Sodium cromoglycate powder mixes (%)
0.4 % w/w	25.14	23.61
1.0 % w/w	31.27	32.49
2.0 % w/w	48.52	44.85
4.0 % w/w	46.68	41.37

Table 4.7.6 Aggregate fraction as a percentage of the emitted dose

These results are in contrast with mixes of reproterol, as shown below.

Drug concentration	Respirable fraction as a percentage of the emitted dose (%)	Aggregate fraction as a percentage of the emitted dose (%)
0.15 % w/w	91.53	14.88
1.5 % w/w	82.67	13.89

Table 4.7.7 Reproterol powder mixes

4.8 Conclusions

As shown in Chapter Two, nedocromil sodium and sodium cromoglycate are very similar with respect to size, shape and surface area. The performance of the powder blends of lactose with nedocromil sodium and sodium cromoglycate as inhalation dosage forms suggests that both species have a similar balance of adhesive/cohesive interactions, of a similar magnitude. The difference in the number of particles remaining adhered after inhalation may be due either to a difference in recognition of sites for adhesion, or different electrostatic behaviour. The difference in adhesion behaviour has no effect on the generation of the respirable fraction from the dose, which suggests that this portion of the powder cloud is cohesion dependent, rather than adhesion dependent.

The surface held cohesive aggregates are therefore the source of the respirable fraction of the dose. The limited respirable fraction is a reflection of the structure of the powder mix. The structures observed in the mix include adhered single particles, adhered aggregates and non-adhered aggregates. A dynamic equilibrium may exist between these structures as described in Figure 4.8.1.

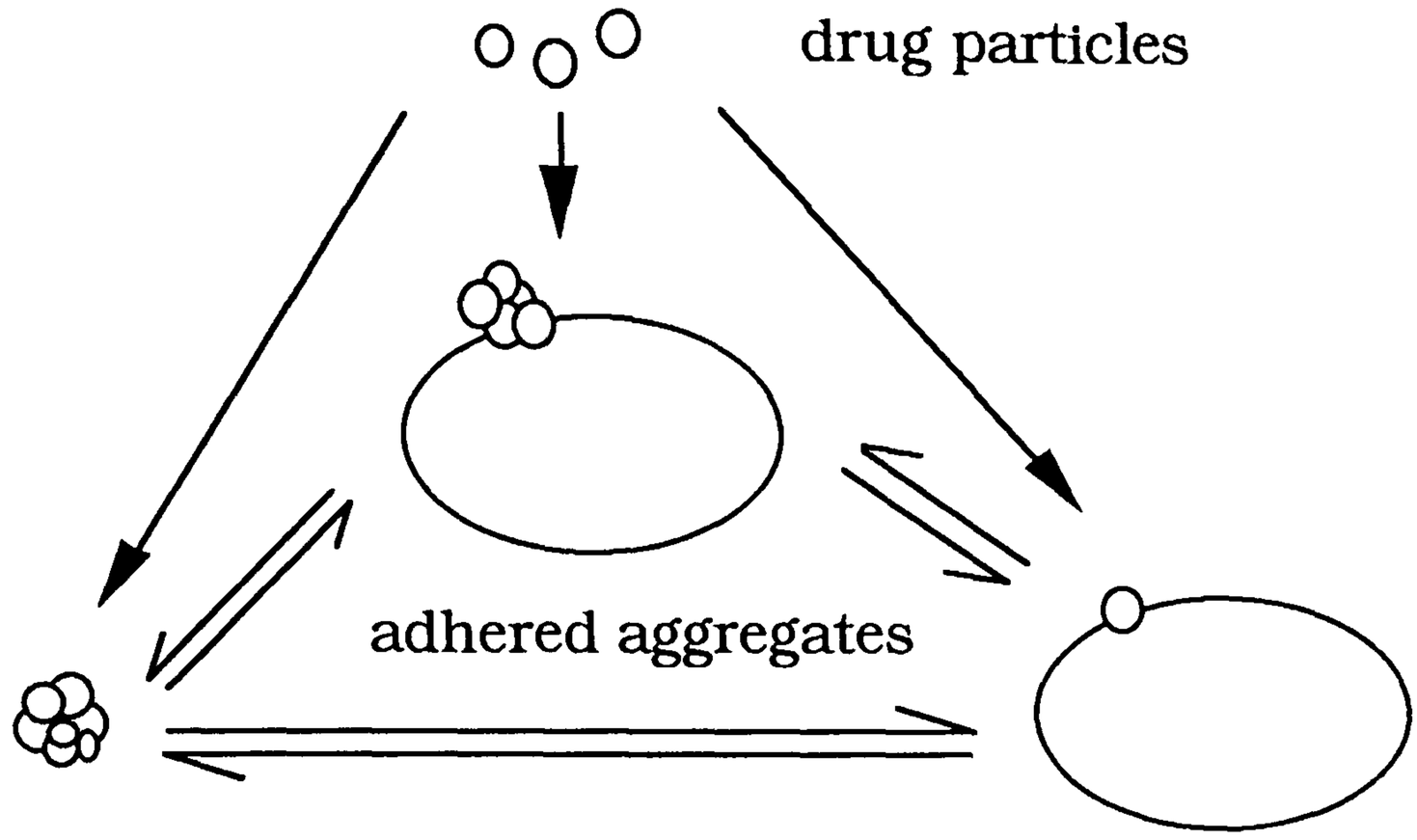

Figure 4.8.1 Structures within binary powder mixes

Therefore it is suggested that in order to optimise the respirable fraction of a powder dose manipulation of the structure of the mix towards the state of adhered aggregates would be favourable.

Chapter Five

Investigation of the adhesive interactions between powder particles by development of an ultracentrifuge technique

5.1 Aim

As a result of determining the structure of binary interactive mixes used in inhalation therapy it was apparent, as reported in Chapter 3, that some form of competition takes place between the drug-carrier adhesion and the drug-drug cohesion interactions. As reported in Chapter 4, these interactions influence the delivery of drug to the lower lung.

Therefore it was decided to investigate and attempt to quantify the magnitudes of these interactions.

The aim of this chapter was to elucidate the magnitude of the adhesive interactions between lactose carrier particles and nedocromil sodium. This was done by the development of a novel method based on an ultracentrifuge technique.

5.2 Introduction

A variety of methods employing the ultracentrifuge have recently been developed in order to quantify a force of adhesion associated with small particles. The ultracentrifuge method uses the principle that the magnitude of an induced centrifugal force which removes a powder particle from a substrate is equal to the attractive forces which existed between that particle and the substrate.

A centrifugal force is experienced by bodies which rotate around a central point. This force is directed outwards from the centre of

rotation, through the centre of gravity of the body. Newton's Second Law states that

$$\text{Force} = \text{mass} \times \text{acceleration} \qquad \text{(equation 5.2.1)}$$

In the case of centripetal force (which is directed towards the centre of the circle)

F = force acting upon the body (N)

m = mass of the particle (kg)

a = centripetal acceleration ($\text{rad}.\text{sec}^{-2}$)

The centripetal acceleration is the rate of change of velocity. This can be expressed as shown in equation 5.2.2.

$$a = r.\omega^2 \qquad \text{(equation 5.2.2)}$$

where r = distance between the centre of the particle and the axis of rotation (m)

ω = angular speed ($\text{rad}.\text{sec}^{-1}$)

Therefore, the force experienced by a particle which maintains its motion in a circle, can be describe by equation 5.2.3.

$$F = m.r.\omega^2 \qquad \text{(equation 5.2.3)}$$

If the force experienced by a particle is not sufficient to maintain the circular motion, the particle will assume a linear velocity in a direction tangential to the path of the circle.

This principle has been applied to a number of systems. The interaction between small particles and a metal substrate was the first

to be examined [130]. The particles under investigation were dusted onto the substrate which was then placed into a centrifuge rotor. The substrate was orientated such that it was parallel to the vertical axis of rotation. The force experienced by the particles to detach them from the substrate was determined by the speed of rotation of the rotor in the centrifuge. This led to the determination of the relationship between the proportion of small particles remaining adhered to the metal substrate after experiencing the centrifugal force, and the magnitude of the force.

A similar system has been used to evaluate the adhesion relationship between small metal spheres and a metal substrate [131].

This technique was first applied to pharmaceutical systems in order to evaluate the adhesion which takes place during the handling and processing of pharmaceutical powders [132]. The adhesion behaviour of various pharmaceutical excipients was investigated using metal and polymer substrates. Interactions between a stainless steel substrate and pharmaceutical excipients have also been extensively studied [133-135].

The centrifuge principle has been applied to pharmaceutical powder mixes in order to investigate their tendency for segregation. A chamber, divided by a sieve screen replaced the plane substrate. Mixes of glass beads and active drug [136-138], and mixes of pharmaceutical excipient and active drug [66, 139] were held behind the sieve screen in the chamber. Migration of the drug through the sieve into the collecting portion of the chamber took place when the centrifugal force was applied.

Distortion of the sieve screen at very high centrifuge speeds and accumulation of drug particles blocking the sieve apertures led to the development of a technique to evaluate species segregation from a single interactive unit [140, 141]. The single interactive units were adhered to a substrate and the proportion of drug removed after each time in the centrifuge was determined using scanning electron microscopy.

Analysis of data obtained from the centrifuge technique leads to the construction of an adhesion profile for the system under investigation. The ordinate of an adhesion profile relates to the percentage of drug which was not detached from the substrate during the time in the centrifuge. The abscissa is the magnitude of the force experienced by the particles. From this type of profile the median adhesion force (corresponding to 50 % retained drug) value can be determined ($adhesion_{50\%}$). This $adhesion_{50\%}$ value can then be used to describe the adhesion behaviour of a system. The standard deviation of adhesion can also be derived.

The standard deviation of adhesion was calculated by Kulvanich [136] from the relationship $\sigma = S_{16}^2 / S_{50}^2$ where S_{16} is the rotor speed at which 16% of the drug was retained on the carrier. This σ value measures the scatter of minimum and maximum rotor speeds required to detach the drug particles.

5.3 Experimental

A novel method was developed in this work which combined the plane substrate method as used by Krupp, Booth, St. John and Lam [130-135] with the investigation of adhesion between drug-carrier interactive systems as studied by Staniforth and Kulvanich [66, 136-139]. The method involved creating a powder covered plane substrate onto which carrier particles were dusted.

This centrifuge method was used to evaluate adhesive interactions between nedocromil sodium and α-lactose monohydrate. The influence upon the adhesion profile of impaction force, relative humidity and batch of nedocromil sodium were investigated.

5.4 Materials

The following materials were used.

Sample	Batch Number	Preparation
Nedocromil Sodium	Z403V & ZBB9A	Apex milled
α-lactose monohydrate	3217C	Electromagnetic vibratory sieved to collect size fraction 63 μm to 75 μm, followed by hand brushing through a 63 μm sieve to remove the < 63 μm fraction.

5.5 Apparatus

A specially designed cell was constructed from aluminium. A plane surface faced an internal collection chamber. The cell was supported in a perspex holder such that this surface was parallel to the axis of rotation of the centrifuge. The cell could be placed either with the surface innermost to impact carrier particles, or outermost in which case the lactose particles would be removed from the nedocromil sodium surface by the centrifugal force.

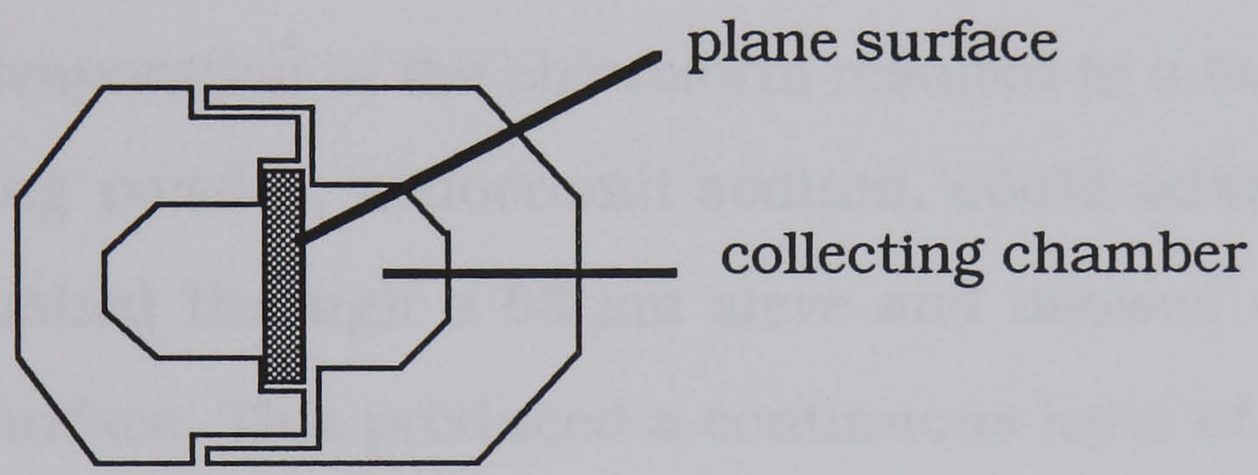

Fig. 5.5.1 Centrifuge cell

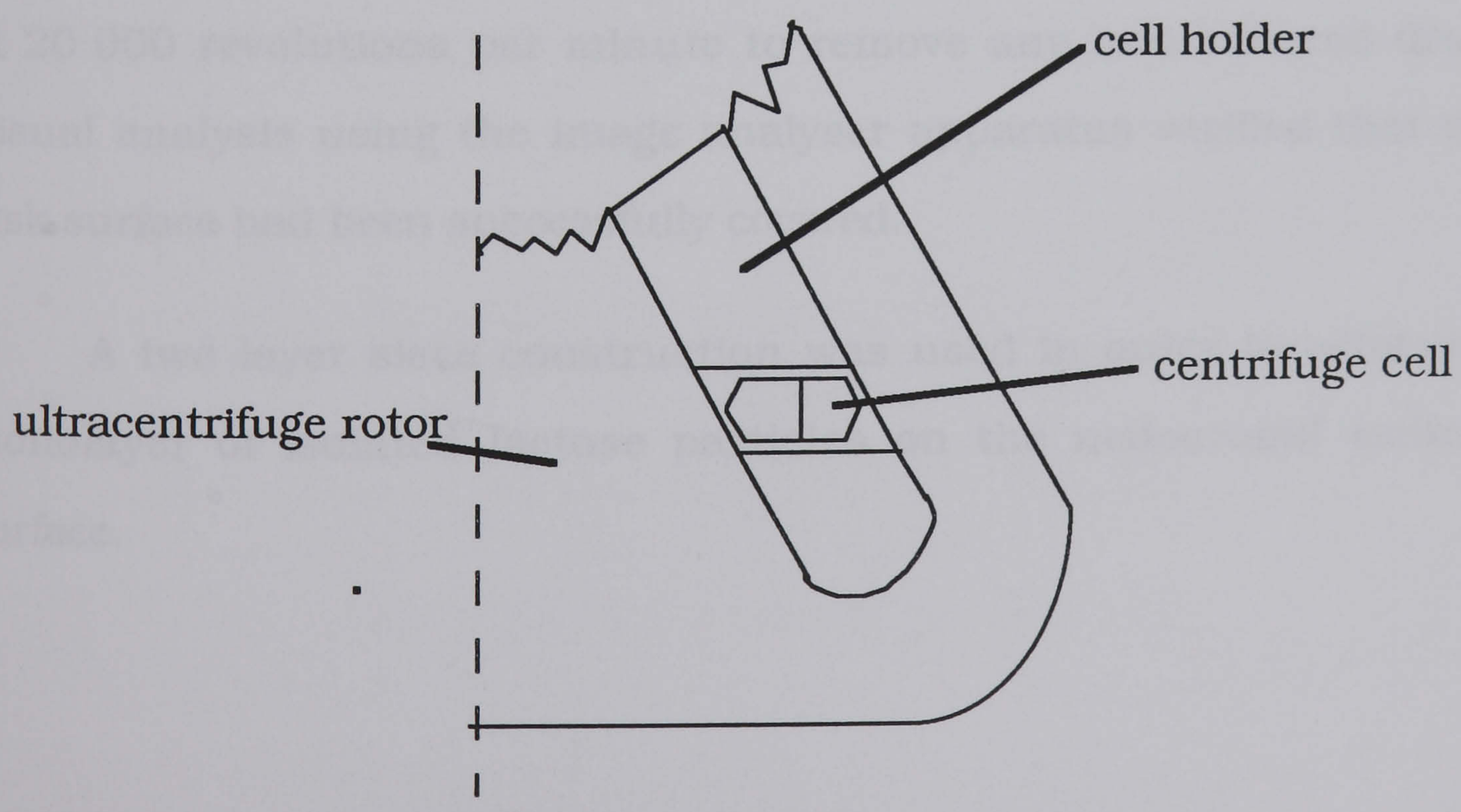

Fig. 5.5.2 Orientation of the cell within the ultracentrifuge rotor

The centrifuge rotor used was a 70Ti type used in a Beckman L8-80M centrifuge with a minimum speed of 1000 revolutions per minute (1.67×10^{-2}. Hz).

Image analysis was carried out using a Nikon SM-Z10 microscope, Hiatachi CCTV with an Eltime Image III image analyser.

5.6 Methods

5.6.1 Preparation of the cell

The plane surface of the centrifuge cell was coated with an adhesive solution prepared by dissolving clear adhesive tape in chloroform. Evaporation of the chloroform resulted in a tacky surface to which the drug powder, nedocromil sodium, could adhere. Sufficient drug was brushed through a 63 μm sieve and allowed to fall on this tacky plane surface. This produced a continuous layer of the drug. The cell was assembled and placed in the centrifuge with the nedocromil sodium surface facing outermost. The assembly was spun for 1 minute at 20 000 revolutions per minute to remove any non-adhered drug. Visual analysis using the image analyser apparatus verified that the disk surface had been successfully covered.

A two layer sieve construction was used in order to achieve a monolayer of isolated lactose particles on the nedocromil sodium surface.

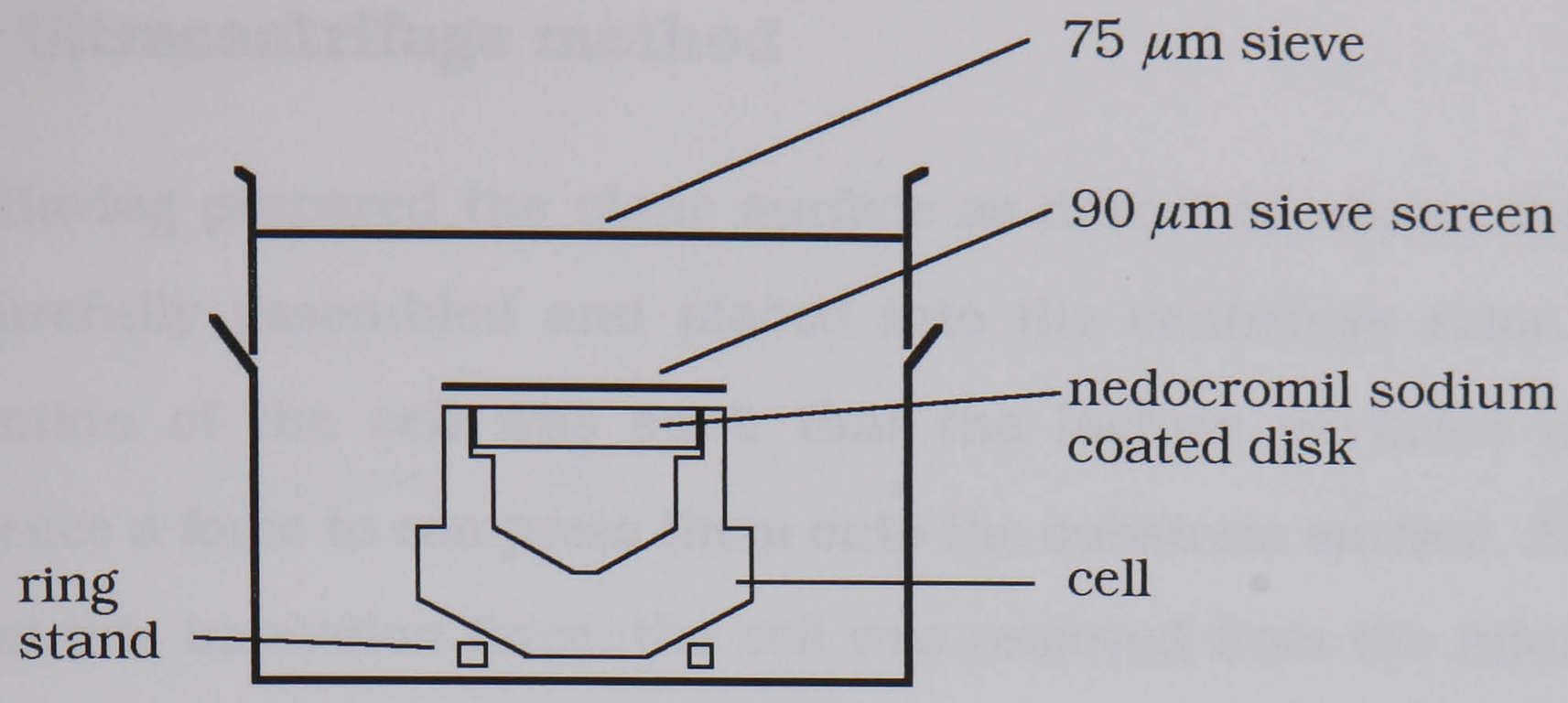

Fig. 5.6.1 Sieve assembly for lactose arrangement

About 10 mg of lactose was brushed through the upper sieve. It was necessary for each lactose particle to locate itself within a pore of the lower sieve in order to come into contact with the drug surface. Therefore interparticulate contact of the lactose particles could not occur. The arrangement of the layers on the aluminium disk is shown below.

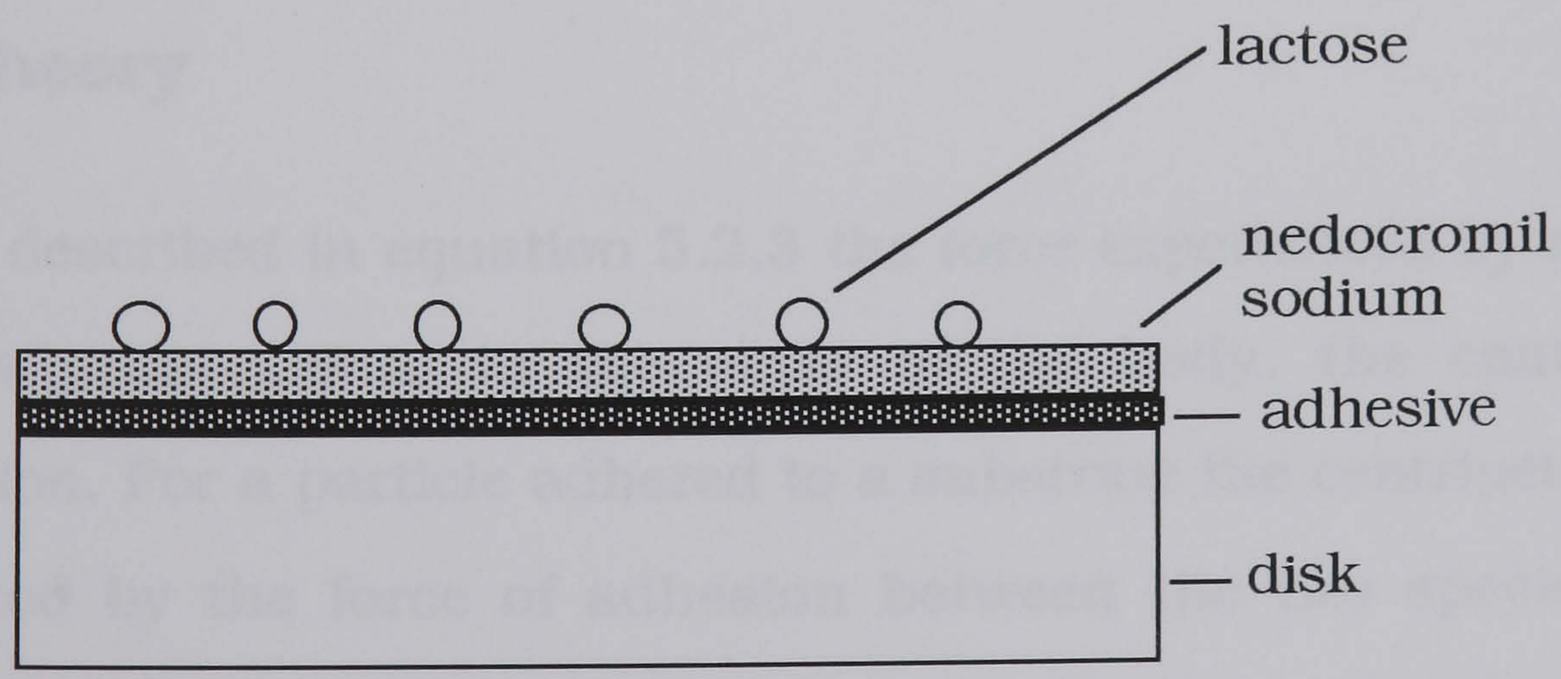

Fig. 5.6.2 Prepared disk arrangement

5.6.2 Ultracentrifuge method

Having prepared the plane surface as described above, the cell was carefully assembled and placed into the centrifuge rotor. The orientation of the cell was such that the lactose particles would experience a force to compress them onto the substrate surface. After a cycle at this impaction force, the cell was removed from the rotor and opened to expose the substrate. Image analysis was used to quantify the number of lactose particles present on the substrate. The cell was reassembled, and replaced in the rotor with the prepared surface facing outermost. The centrifugal force experienced by the particles of lactose this time was in the direction to remove them from the substrate. The rotor was held at the required speed for 60 seconds. After each time in the centrifuge the number of particles remaining on the disk was evaluated using image analysis. The cell was then replaced and spun at a faster rotation speed.

5.7 Results

5.7.1 Theory

As described in equation 5.2.3 the force experienced by rotating bodies is proportional to the mass of the body, the centripetal acceleration. For a particle adhered to a substrate the centripetal force is provided by the force of adhesion between the two species. The particle becomes removed from the substrate when the adhesive force is not sufficient to maintain the particle in circular motion. This is described in equation 5.7.1.

$$F_{det} = m.r.\omega^2 \qquad \text{(equation 5.7.1)}$$

The rotor speed of the centrifuge is related to the angular velocity as shown in equation 5.7.2.

$$\omega = (\pi/30) \times \text{rotor speed} \qquad \text{(equation 5.7.2)}$$

where the rotor speed is expressed in revolutions per minute.

The working formula used to calculate the centrifugal force for this work is shown in equation 5.7.3.

$$F_{det} = \left(\frac{d^3.\pi.\rho}{6}\right).r.\left(\frac{\pi.rpm}{30}\right)^2 \qquad \text{(equation 5.7.3)}$$

Where d is the particle diameter and ρ the density of the removed particle.

The relative centrifugal force ($F_{R.C.}$) acting on the particles at the rotor speeds used can be calculated from equation 5.7.4.

$$F_{R.C.} = \frac{\omega^2.r}{g} \qquad \text{(equation 5.7.4)}$$

A tabulation of the relative values for rotor speed, relative centrifugal force and adhesion force is shown in Table 5.7.1.

Removal speed (rev min^{-1})	Relative centrifugal force (g)	Adhesion force (N)
1000	82.34	1.93×10^{-7}
1500	185.26	4.34×10^{-7}
3000	741.03	1.74×10^{-6}
5000	2058.41	4.82×10^{-6}
10000	8233.62	1.93×10^{-5}
15000	18525.65	4.34×10^{-5}
20000	32934.49	7.72×10^{-5}
25000	51460.14	1.21×10^{-4}
30000	74102.60	1.74×10^{-4}
35000	100861.90	2.36×10^{-4}
40000	131738.00	3.09×10^{-4}

Table 5.7.1 Rotor speeds, Relative centrifugal force and Adhesion force for lactose particles in the centrifuge cell

5.7.2 Effect of force of impaction

Experimental analysis of the removal of lactose particles from the nedocromil sodium covered surface using the centrifuge technique was carried out. The samples were subjected to impaction forces ranging between 4.34×10^{-7}N (corresponding to 1 500 revolutions per minute of the centrifuge rotor) and 7.72×10^{-5}N (corresponding to 20 000 revolutions per minute of the centrifuge rotor).

Testing was also carried out with no impaction of the lactose particles onto the nedocromil sodium covered surface. The lactose samples were simply brushed through the sieve arrangement as shown in Figure 5.6.1. The number of lactose particles on the surface was determined by image analysis. The cell was then assembled and placed in the centrifuge rotor orientated such that the centrifugal force would

remove the particles of lactose from the nedocromil sodium covered surface.

In order to ascertain whether the nedocromil sodium had covered the adhesive layer sufficiently to act as a barrier between the lactose particles and the adhesive layer, the profile of lactose particles adhered directly to the adhesive layer was investigated. The particles of lactose were brushed through the sieve arrangement as shown in Figure 5.6.1. The number of lactose particles on the surface was determined by image analysis. The cell was then assembled and placed in the centrifuge rotor orientated such that the centrifugal force would remove the particles of lactose from the adhesive surface.

Adhesion profiles for lactose particles on a nedocromil sodium powder substrate

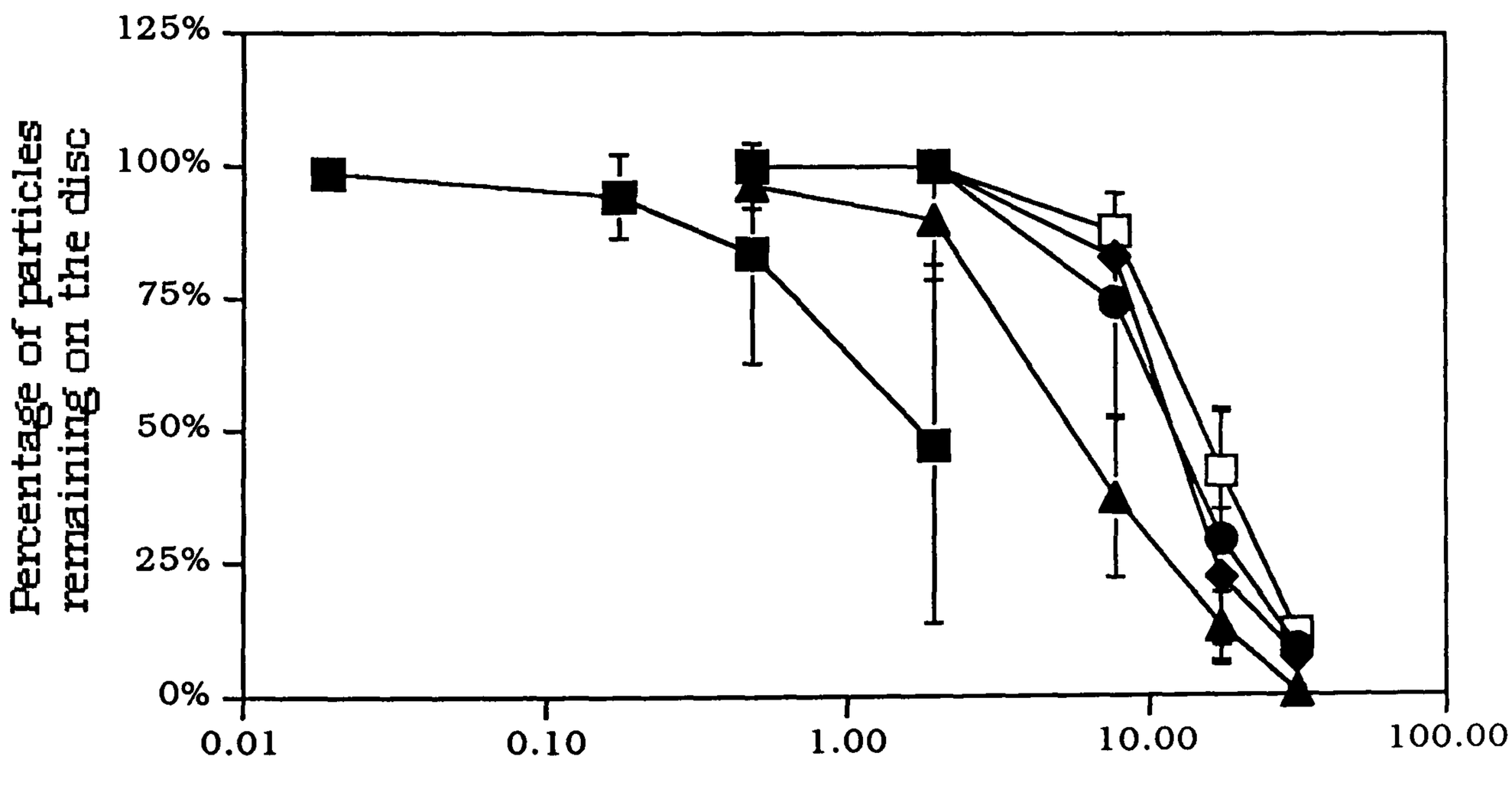

Figure 5.7.1 Effect of impaction force upon adhesion profiles

The error bars represent the standard deviation of the data.

The median adhesion force is the force at which 50% of the particles have been removed from the substrate surface. The respective median adhesion force ($adhesion_{50\%}$) for each impaction force profile are shown in Table 5.7.2.

Impaction force (N)	Measured $adhesion_{50\%}$ (N)
4.34×10^{-7}	1.8×10^{-5}
4.82×10^{-6}	5.4×10^{-5}
1.93×10^{-5}	1.2×10^{-4}
4.34×10^{-5}	1.2×10^{-4}
7.72×10^{-5}	1.6×10^{-4}

Table 5.7.2 Relationship between impaction force and measured adhesion force

Standard deviation values for the adhesion profiles are presented in Table 5.7.3. As described in section 5.2, the values S_{16}^2 and S_{50}^2 have been used to quantify the scatter of maximum and minimum rotor speeds required to detach the drug particles from a plane substrate. As seen in section 5.7, the force of adhesion (force of detachment) is directly proportional to the square of the rotor speed. The values of the standard deviation (σ) were calculated using equation 5.7.5.

$$\sigma = \frac{adhesion_{16\%}}{adhesion_{50\%}} \qquad \text{(equation 5.7.5)}$$

This expresses the scatter of force required to detach the drug particles from the substrate.

Impaction force (N)	Standard deviation of adhesion (N)
4.82×10^{-6}	2.96
1.93×10^{-5}	2.08
4.34×10^{-5}	1.85
7.72×10^{-5}	1.85

Table 5.7.3 Standard deviation of adhesion data

5.7.3 Discussion

Table 5.7.2 shows that the $adhesion_{50\%}$ values tend to increase as the impaction force increases. There is a large scatter in the data. When statistically tested using ANOVAR two way analysis $P<0.05$, there is no significant difference between each data point for all the adhesion profiles.

The interactions which are responsible for the lactose particles remaining associated with the surface of the disc after experiencing a force to remove them exist between the nedocromil sodium and lactose particles. The technique successfully covered the adhesive layer with nedocromil sodium. After experiencing a removal force of 7.72×10^{-5} N, 100 % of the lactose particles remained adhered directly to the adhesive layer when no impaction force had been applied. This is in contrast with the removal of lactose particles from the nedocromil sodium covered surface when no impaction force was applied. In this case the

removal force $1.93x10^{-7}$N (corresponding to the slowest possible removal speed 1 000 revolutions per minute) was sufficient to remove all but 5% of the lactose particles. The system developed, therefore, could not determine a value for the adhesion behaviour between particles of lactose and a nedocromil sodium substrate without applying a force to impact the two species.

Had the data been more reproducible, the construction of a plot of $adhesion_{50\%}$ against the impaction force would have allowed extrapolation to the intercept of the ordinate. This would have determine the value for $adhesion_{50\%}$ of a non-impacted system.

The increase in $adhesion_{50\%}$ values with an increasing impaction value may be due to deformation of the lactose particles, and distortion of the nedocromil sodium layer.

The force applied during the impaction process increases the pressure at the points of contact between the lactose particle and the nedocromil sodium covered surface. This can lead to plastic deformation as the contacting surfaces are flattened [133]. The increase in the interfacial bonding areas would then lead to an increase in van der Waal's attractions.

The bonding areas can increase in this case due to deformation of the adhesive and nedocromil sodium layers. As the lactose particle plastically deforms under the increased pressure, so do the layers on the disc. The result of such deformations is that the particle of lactose rests in a 'well' of nedocromil sodium as shown in Figure 5.7.2.

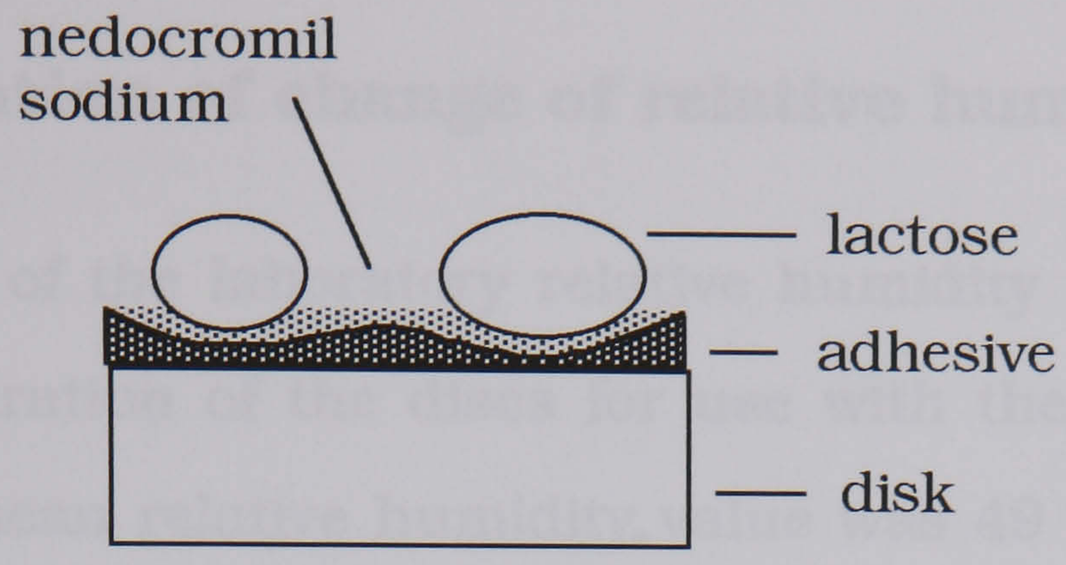

Figure 5.7.2 Representation of 'well' formation in the surface layers of the centrifuge disc

These 'wells' were observed at locations on the nedocromil sodium surface which had accommodated particles of lactose. They were more obvious at the larger magnitude impaction forces.

The combination of plastic deformation of the lactose particle and the layers covering the disc acts to increase the interparticulate bonding area. The higher the applied force, the greater the extent of the deformation, and therefore the greater resultant adhesive force. This is shown by the tendency of the adhesion profiles to shift to the right with an increasing impaction force.

Therefore the technique developed cannot provide an absolute value for the magnitude of the force of adhesion which exists between lactose and nedocromil sodium.

5.7.4 Investigation of change of relative humidity

Monitoring of the laboratory relative humidity was carried out during the preparation of the discs for use with the ultracentrifuge technique. The mean relative humidity value was 49 %, with a range from 46.5 % to 52.4 %. The adhesion data did not exhibit any consistent relationship with the changing values of relative humidity within this range. However, when experimental work was carried out at a much lower relative humidity the following data was obtained.

Adhesion profiles of lactose particles impacted at $7.7x10^{-5}$ N onto a nedocromil sodium covered surface

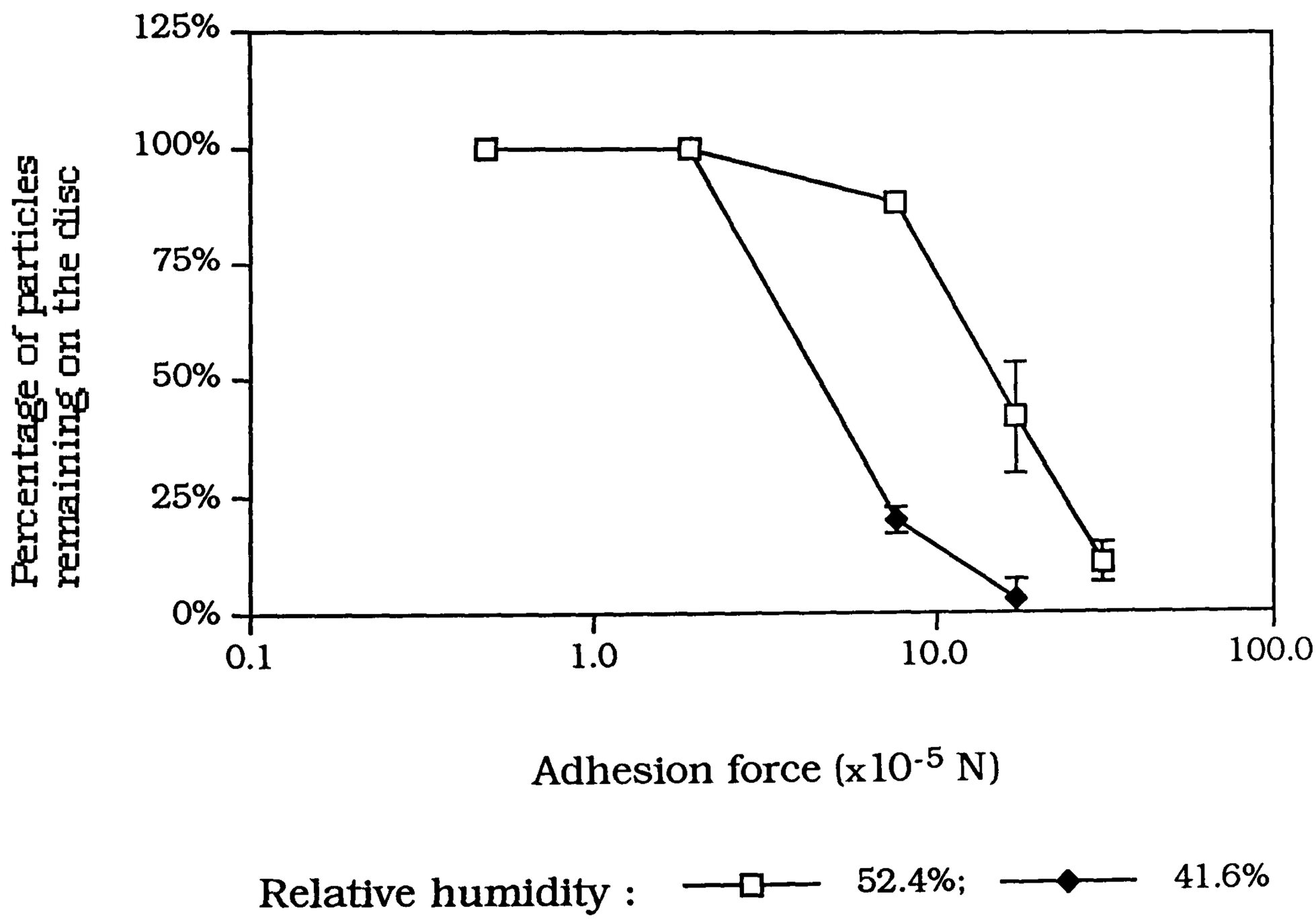

Figure 5.7.4 Effect of relative humidity upon impaction profiles

The calculated statistics for these two adhesion profiles are shown in Table 5.7.4.

Relative humidity (%)	**52.4**	**41.6**
$adhesion_{50\%}$ (N)	$1.06x10^{-4}$	$4.70x10^{-5}$
standard deviation of adhesion (N)	1.89	2.07

Table 5.7.4 Effect of relative humidity

5.7.5 Discussion

The tendency for adhesion to increase with an increase in relative humidity has previously been observed using particle-plane systems [142, 143], although the reverse has also been observed [138].

High relative humidity causes a rapid dissipation of electrical charge accumulated on a material's surface. This can be attributed to an adsorbed moisture film on the material which causes an increase on conductivity of the material's surface and surrounding atmosphere [144]. Charge decay has been shown to be responsible for the decrease in adhesion tendency of interactive mixes during storage [145]. The adsorbed moisture film, however, can also be responsible for an increase of adhesion due to capillary interaction [138]. The relative humidity at which this capillary interaction occurs can be lower than the critical relative humidity at which liquid bridges are formed.

Considering the system of lactose and nedocromil sodium it is suggested that the capillary force due to water condensation at the particle interface becomes more dominant than the associated loss of electrical activity. Therefore the adhesion tends to increase with an increase in relative humidity.

5.7.6 Effect of altering the batch of drug

Batch variation of nedocromil sodium deposition in the multistage liquid impinger has been noted [146]. Centrifuge analysis was carried out to try and establish any difference of adhesion profile caused by altering the drug batch. The adhesion profile following impaction at 4.34×10^{-7} N was determined as shown in Figure 5.7.5.

Adhesion profiles of lactose particles impacted at $7.7x10^{-5}$ N onto a nedocromil sodium covered surface

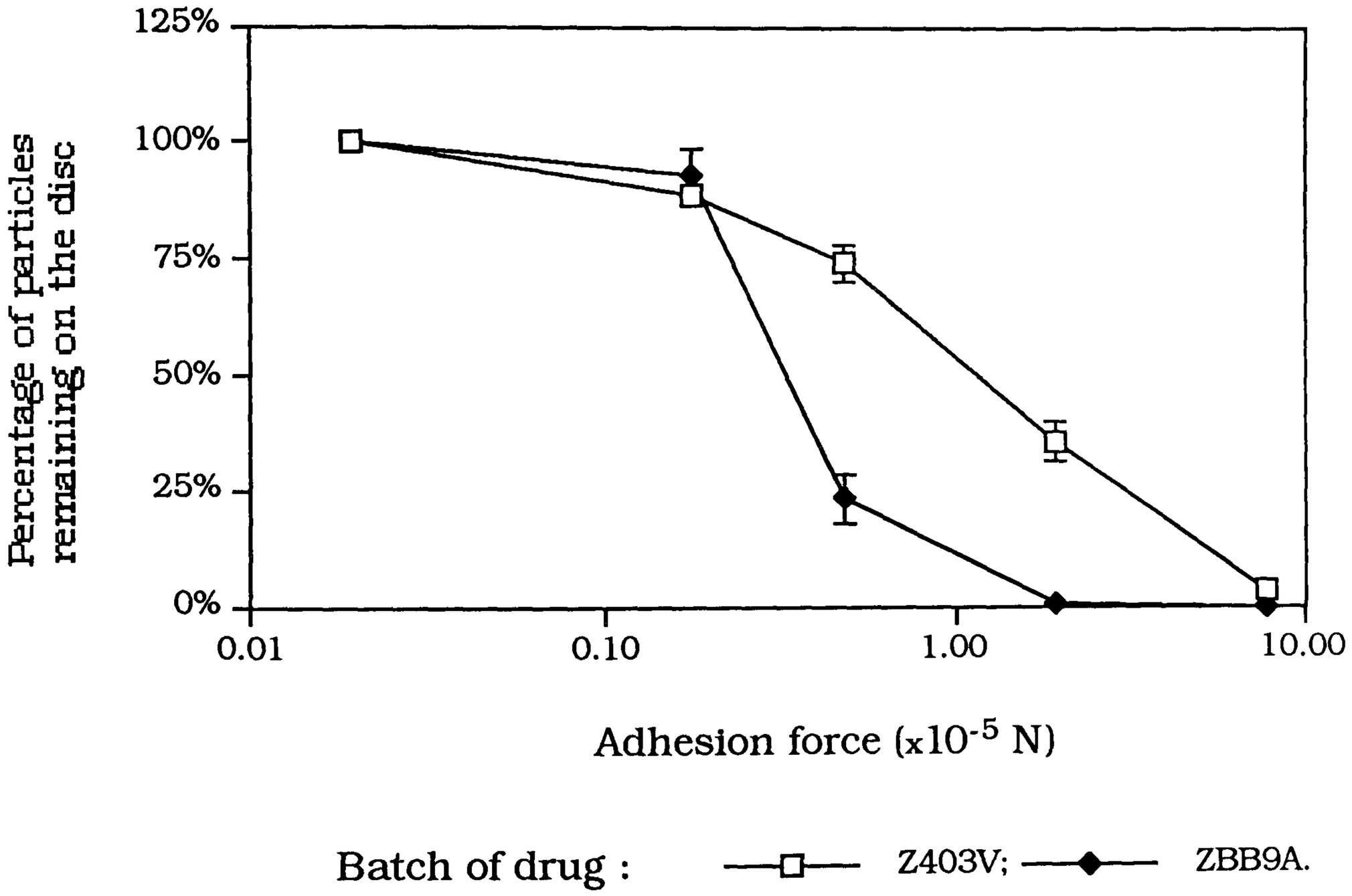

Figure 5.7.5 Effect of batch variation upon adhesion profile

The two batches were run concurrently, therefore environmental conditions were identical during analysis. Values for the adhesion$_{50\%}$ and standard deviation of adhesion are shown in Table 5.7.5.

Drug batch	Z403V	ZBB9A
$adhesion_{50\%}$ (N)	1.1×10^{-5}	3.1×10^{-6}
standard deviation of adhesion (N)	2.67	2.45

Table 5.7.5 Effect of batch variation

When tested statistically, the results at 5 000 and 10 000 revolutions per minute removal were significantly different.

These results correlate with the findings that less drug from batch ZBB9A is deposited in stage 4 of the multistage liquid impinger, suggesting that more may be retained adhered to the lactose portion of the binary mix.

5.8 Conclusion

A technique has been developed to attempt to quantify the force of adhesion between lactose particles and a substrate of drug particles. The results from this technique could be translated to the adhesive forces between drug particles and carrier particles within a binary powder mix used for inhalation therapy. However, the technique proved not to have the sensitivity capability to quantify these adhesive forces unless considerable force was applied to the system to encourage adhesion between the two powder species. This applied force distorted the system as it applied to binary powder mixes.

The use of the ultracentrifuge technique has previously been used to identify adhesive interactions between pharmaceutical excipients and processing apparatus where such forces of impaction are justified, such as during tabletting [132, 133]. When translated to the motion of the particles in a tumbling rotary mixer, a particle of lactose, to generate the same impaction force as generated in the ultracentrifuge system to achieve quantifiable adhesion would have to travel with an acceleration of 1.1×10^{3} $m.s^{-2}$. The action of the low energy mixer allows the particles to tumble under the force of gravity (9.81 $m.s^{-2}$), and due to turbulent rotation of the vessel. This would not produce such a large acceleration.

Therefore the system developed cannot provide absolute data relating to dry powder binary mixes prepared in a low energy mixer. However, when adhesion is enhanced, by impacting lactose particles onto the powder substrate, the method may be used as a tool to

distinguish differences in the adhesion behaviour of interacting systems, due to environmental or batch variation.

Chapter Six

Investigation of the cohesive interactions between powder particles by development of a cone penetration technique

6.1 Aim

As a result of determining the structure of binary interactive mixes used in inhalation therapy it was apparent, as reported in Chapter 3, that some form of competition takes place between the drug-carrier adhesion and the drug-drug cohesion interactions.

Therefore it was decided to investigate and attempt to quantify the magnitudes of these interactions.

The aim of this chapter was to elucidate the magnitude of the cohesive interactions between powder particles used in the formulation of these binary interactive mixes by the application of a cone penetrometry technique.

This technique, novel to this area, was assessed for its suitability to such an application.

6.2 Introduction

Cone penetration testing has been researched and developed primarily in the field of soil mechanics [147]. It has been used as a technique for measuring the mechanical properties of soils. This technology was transferred into the pharmaceutical sciences and used to investigate the measurement of the yield strength of pastes [148]. The application of a penetration test in powder mechanics followed [149], when it was assessed as a technique for measuring the cohesive strength of a powder. A reasonable correlation was observed between the penetrometer technique and a shear cell technique for the measurement of the cohesive caking strength of a powder.

The technique involves driving a cone into a powder bed. The force required to drive the cone is measured as a function of the depth of penetration into the bed. The theory (below) shows that the penetration force at a given depth is proportional to the unconfined compression strength of the powder.

6.2.1 Theory

As a cone penetrates into a powder bed, the powder fails in shear in successive surfaces emanating from the tip of the cone (Figure 6.1). As the stress from the weight of powder above the failure zone is low, the failure is effectively unconfined. This approximation is very good when the powder strength is large relative to the stress due to the powder above the failure surface.

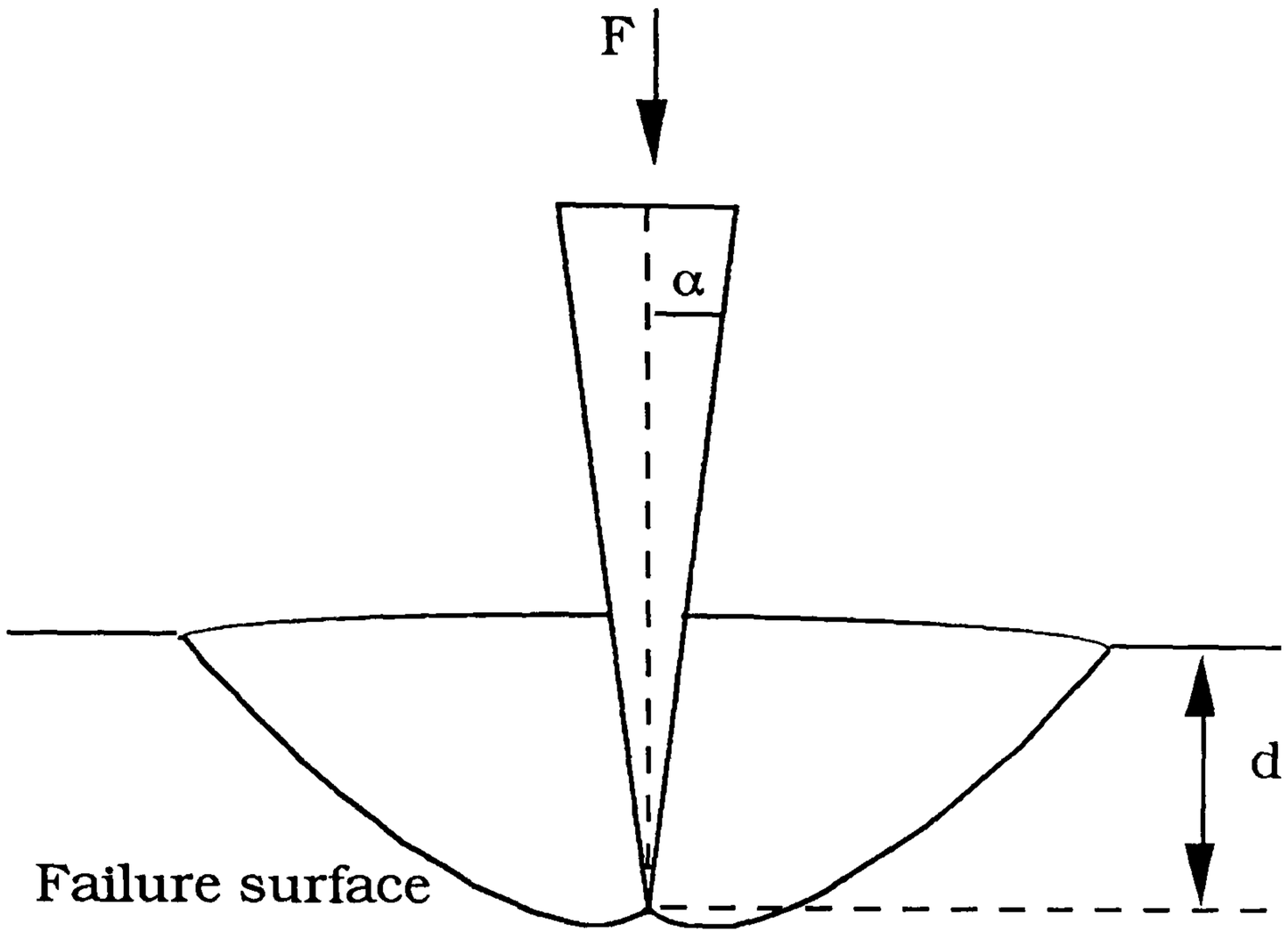

Figure 6.2.1 Failure surface for a cone penetrating an unconfined powder

Using a container sufficiently large for the powder to be effectively unconfined, and a low penetration speed so that inertial effects can be neglected the force applied to the cone, F, can be determined relative to the penetration depth, d.

The force applied to the cone is opposed by the frictional force F_f,between the cone and the powder, and the force required to cause failure of the powder under unconfined conditions, F_c.

$$F = F_f + F_c \qquad \text{(equation 6.2.1)}$$

The frictional force can be taken to be proportional to the applied force through a coefficient a_f which is a function of the dynamic friction coefficient μ for the cone-powder contact and the dynamic angle of internal friction of the powder ϕ_k.

$$F_f = a_f(\mu, \phi_k)F \qquad \text{(equation 6.2.2)}$$

Similarly, the force required to cause powder failure can be taken to be proportional to the unconfined compression strength of the powder specimen through a coefficient a_c, itself a function of μ and ϕ_k. The force is related to the penetration depth, d, through a power index, n, which, in order to satisfy dimensions must be equal to 2.

$$F_c = a_c(\mu, \phi_k) f_c / d^n \qquad \text{(equation 6.2.3)}$$

This unconfined compression strength is a measure of the cohesive interactions which exist within the powder bed.

Substituting equations 2 and 3 into equation 1, followed by rearrangement of the expression gives,

$$f_c = a_{fc}(\mu, \phi_k) \frac{F}{d^2} \qquad \text{(equation 6.2.4)}$$

For a given powder, a_{fc}, should be constant over a range of stresses for which μ and ϕ_k are constant. It has been shown that values of μ and ϕ_k are similar for dissimilar powders [149] suggesting that a_{fc} does not vary greatly from powder to powder.

6.3 Materials

The following materials were used. Kaolin and Starch 1500 were included in order to assess the sensitivity of the penetrometry technique

Sample	Batch Number
Nedocromil sodium	5B1
Nedocromil sodium	2002B1
α-Lactose monohydrate(325 M)	3217C
Light Kaolin B.P.	18CL
Starch 1500	DM 486

Table 6.3.1 Samples used for cone penetration testing

Scanning electron micrographs of these samples have been made and are presented in section 2.3.

6.4 Apparatus

A specially designed and constructed apparatus was used to prepare the powder bed. The powder sample was contained in a glass dish 76 mm diameter and 65 mm deep. The compaction apparatus is described in Figure 6.4.1.

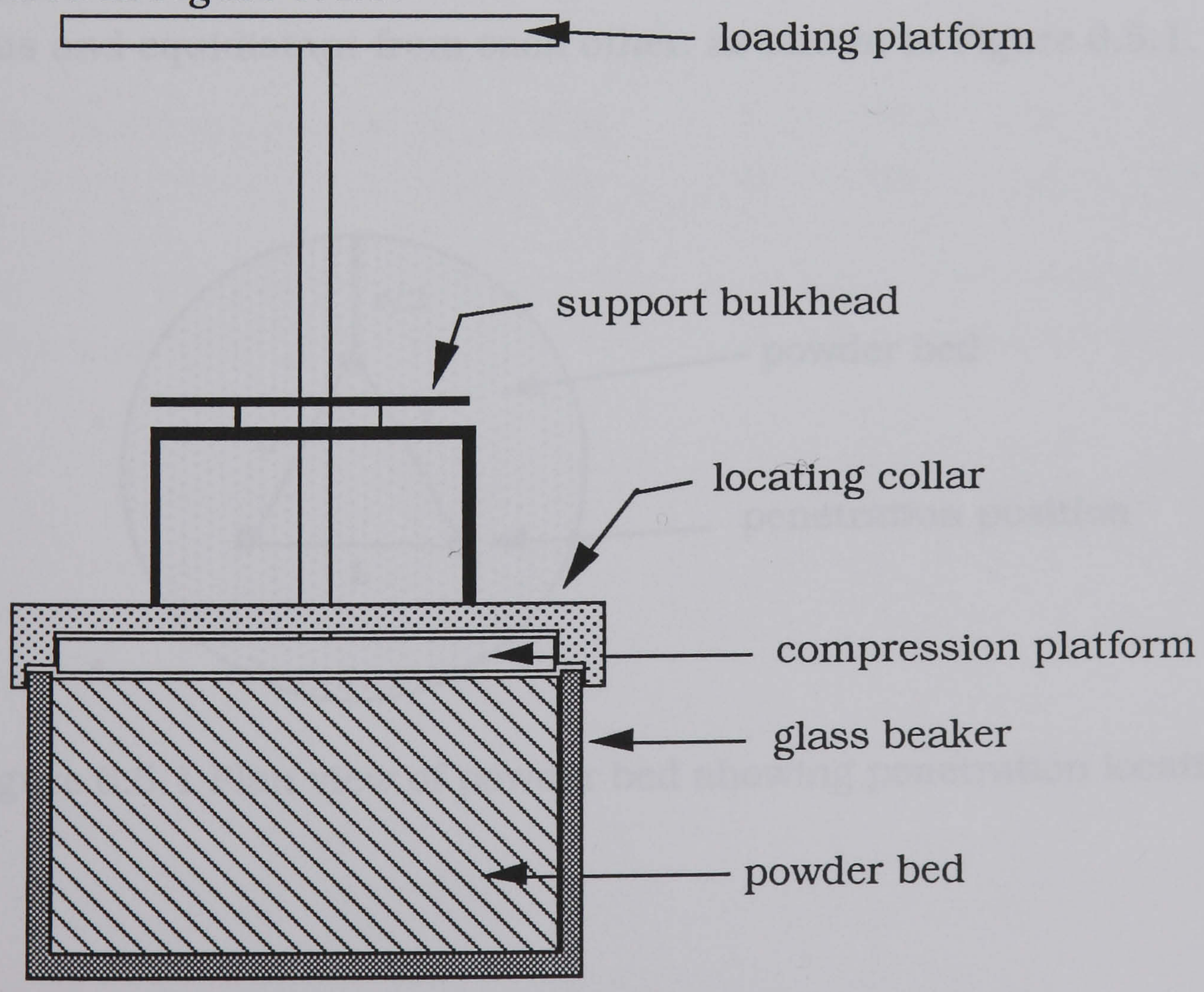

Figure 6.4.1 Powder bed compaction apparatus

The cone was constructed out of brass, had a half angle (α) of 5° and was 45 mm long.

A Tensometer 10 (Monsanto) was used to drive the cone into the powder bed. The force was recorded continuously by a chart recorder.

6.5 Methods

The powder sample was loaded into the dish such that the top surface was level and the same height as the dish. The powder bed compaction apparatus was located on the dish. The appropriate mass was placed gently on the loading platform. After compaction for 5 minutes the compaction apparatus was removed, and penetrometry tests carried out immediately. The cone was driven into the bed at a rate of 50 mm/min. Three penetration tests were carried out on each powder bed. The positions of the points of penetration were at half the radius and equidistant from each other, as shown in Figure 6.5.1.

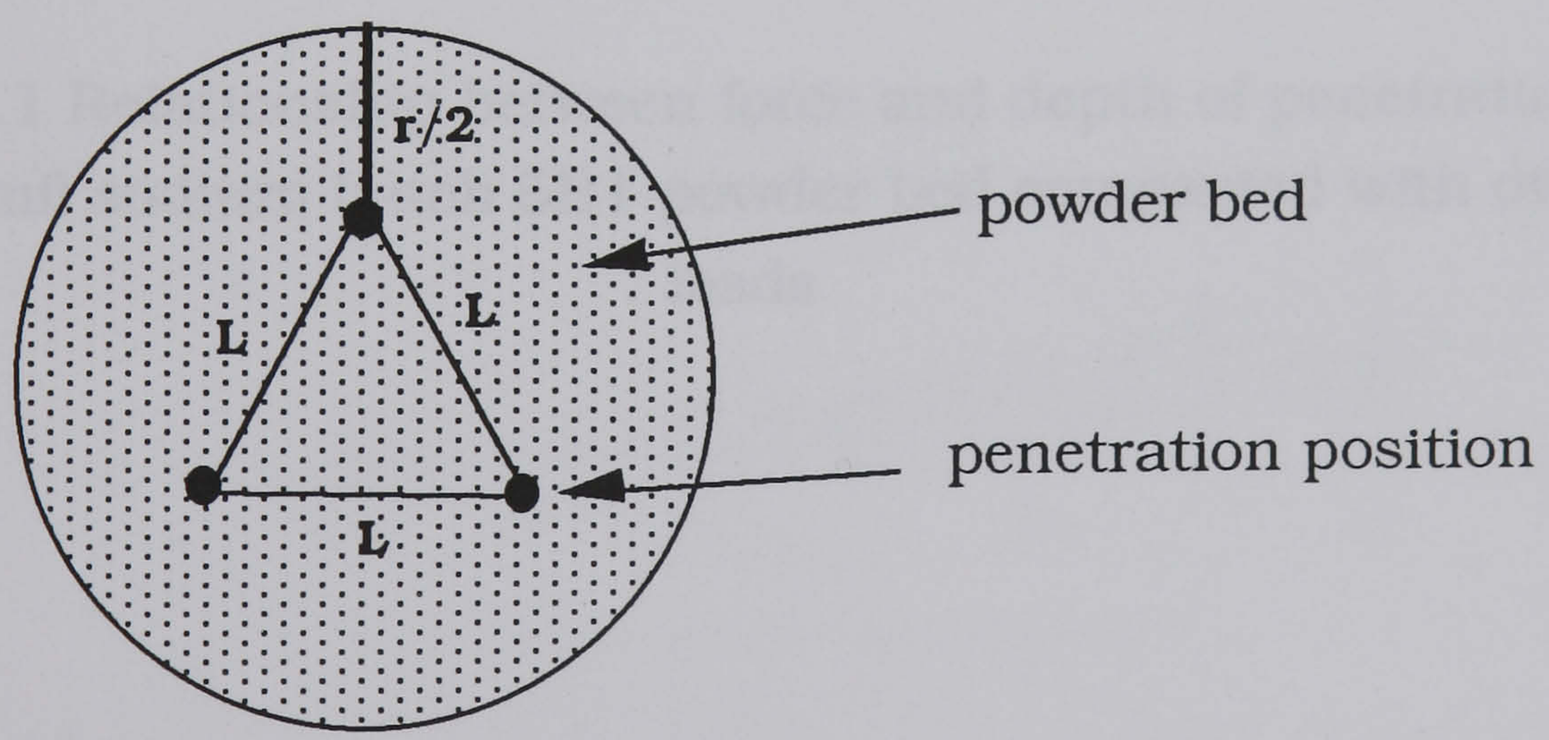

Figure 6.5.1 Plan view of powder bed showing penetration locations

6.6 Results

The relationships between the depth of penetration and the measured penetration force are shown in Figures 6.6.1 to 6.6.4.

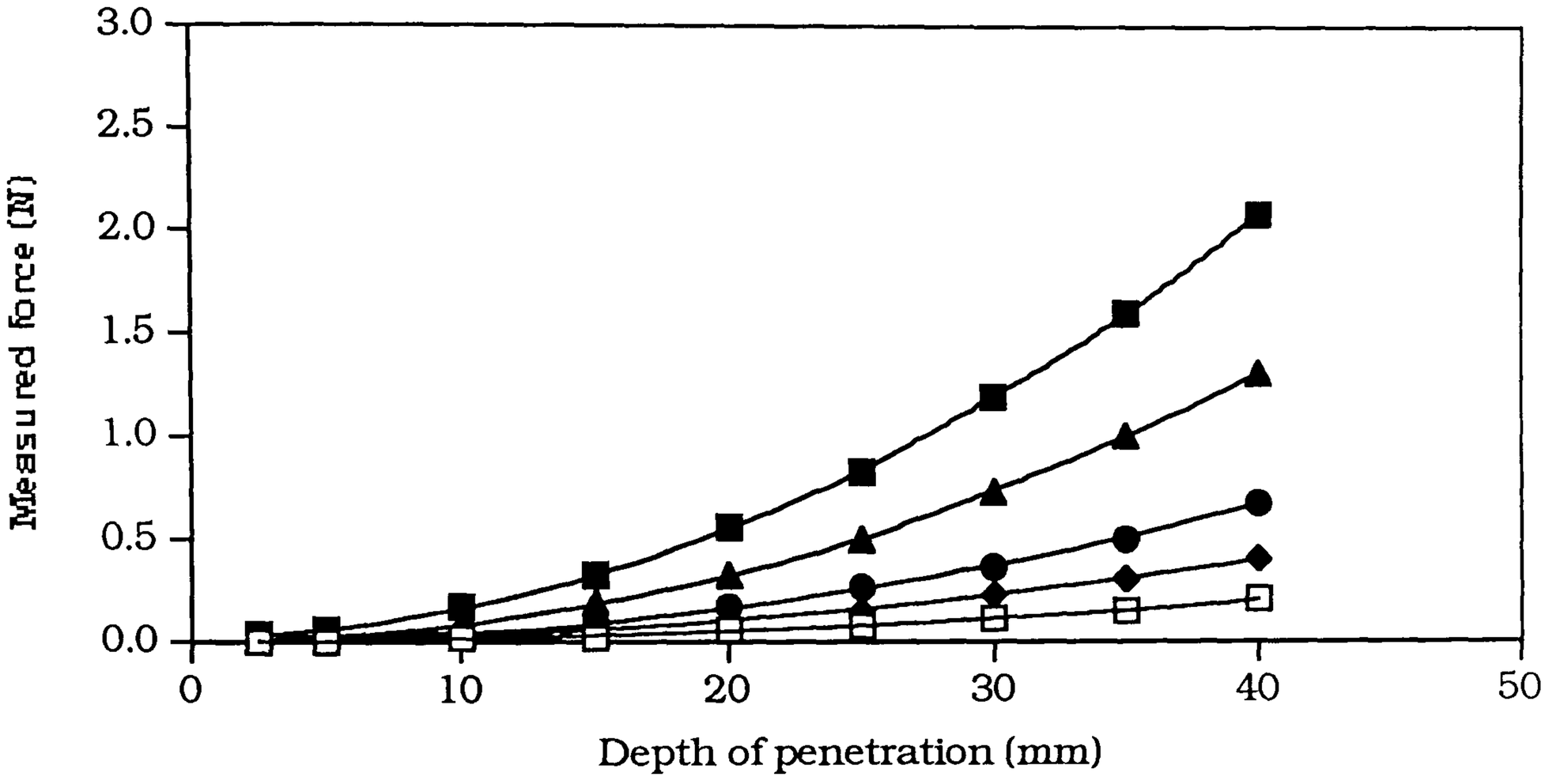

Figure 6.6.1 Relationship between force and depth of penetration into a nedocromil sodium batch 5B1 powder bed compacted with different loads

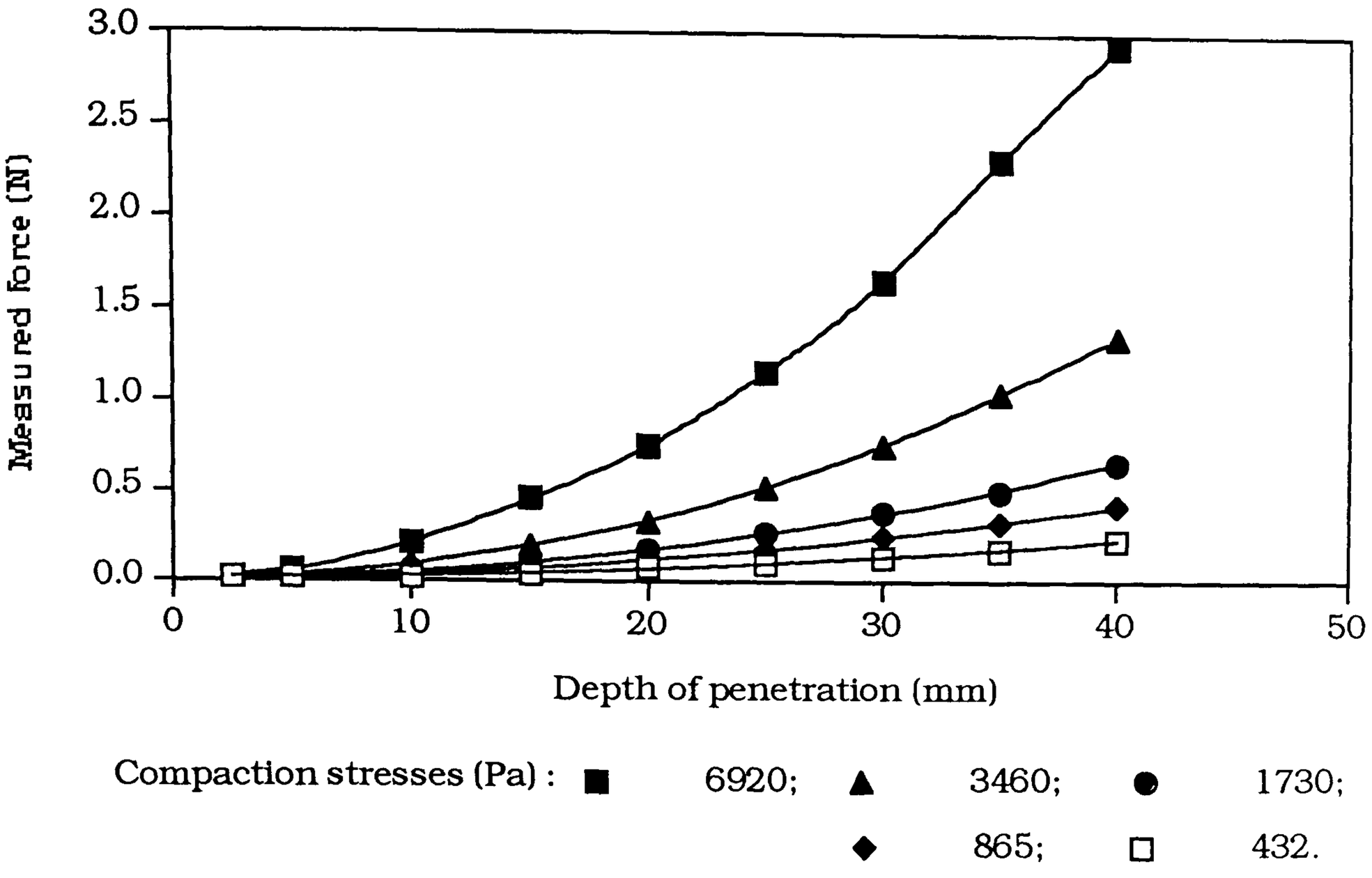

Figure 6.6.2 Relationship between force and depth of penetration into a nedocromil sodium batch 2002B1 powder bed compacted with different loads

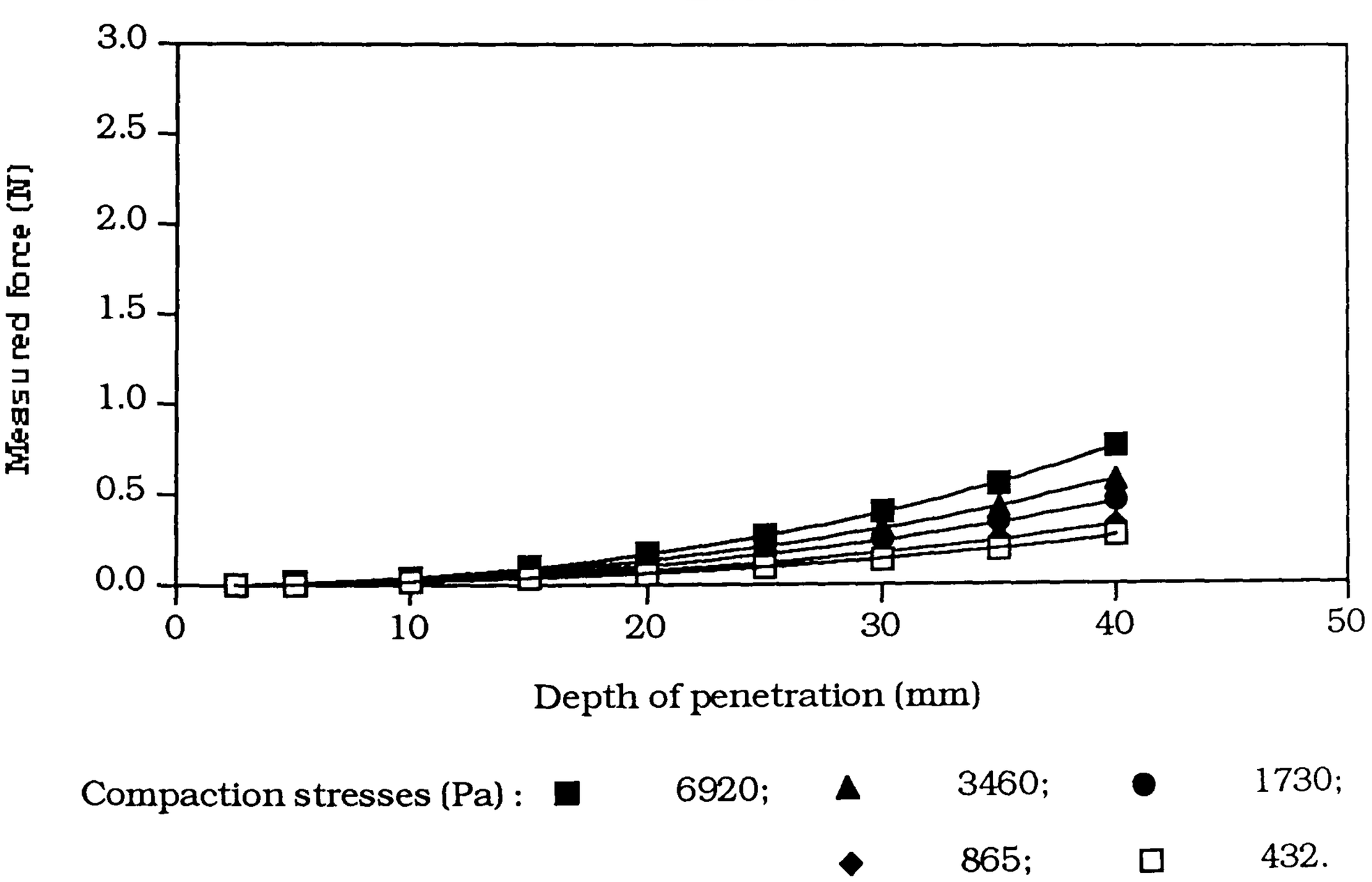

Figure 6.6.3 Relationship between force and depth of penetration into a lactose powder bed compacted with different loads

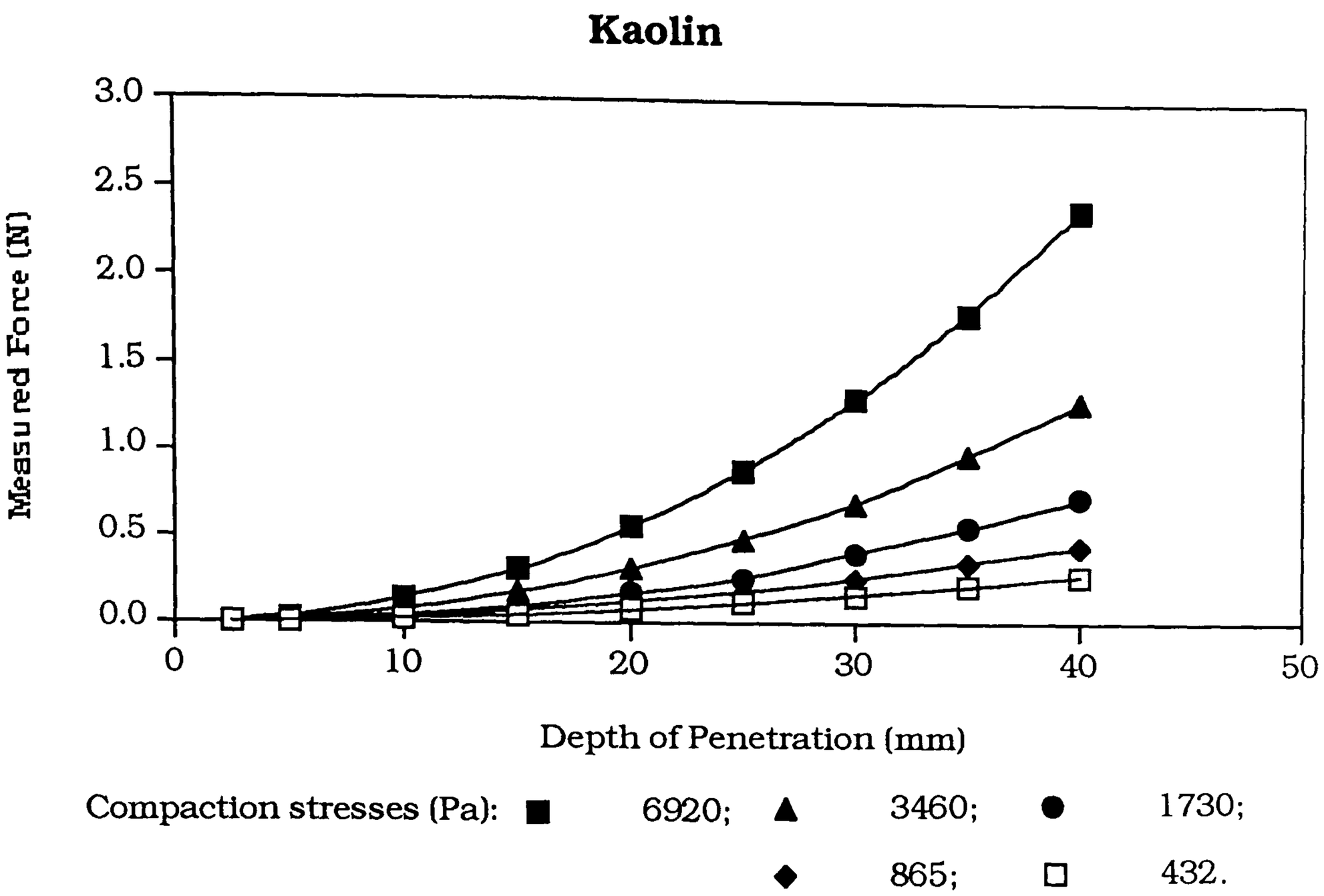

Figure 6.6.4 Relationship between force and depth of penetration into a kaolin powder bed compacted with different loads

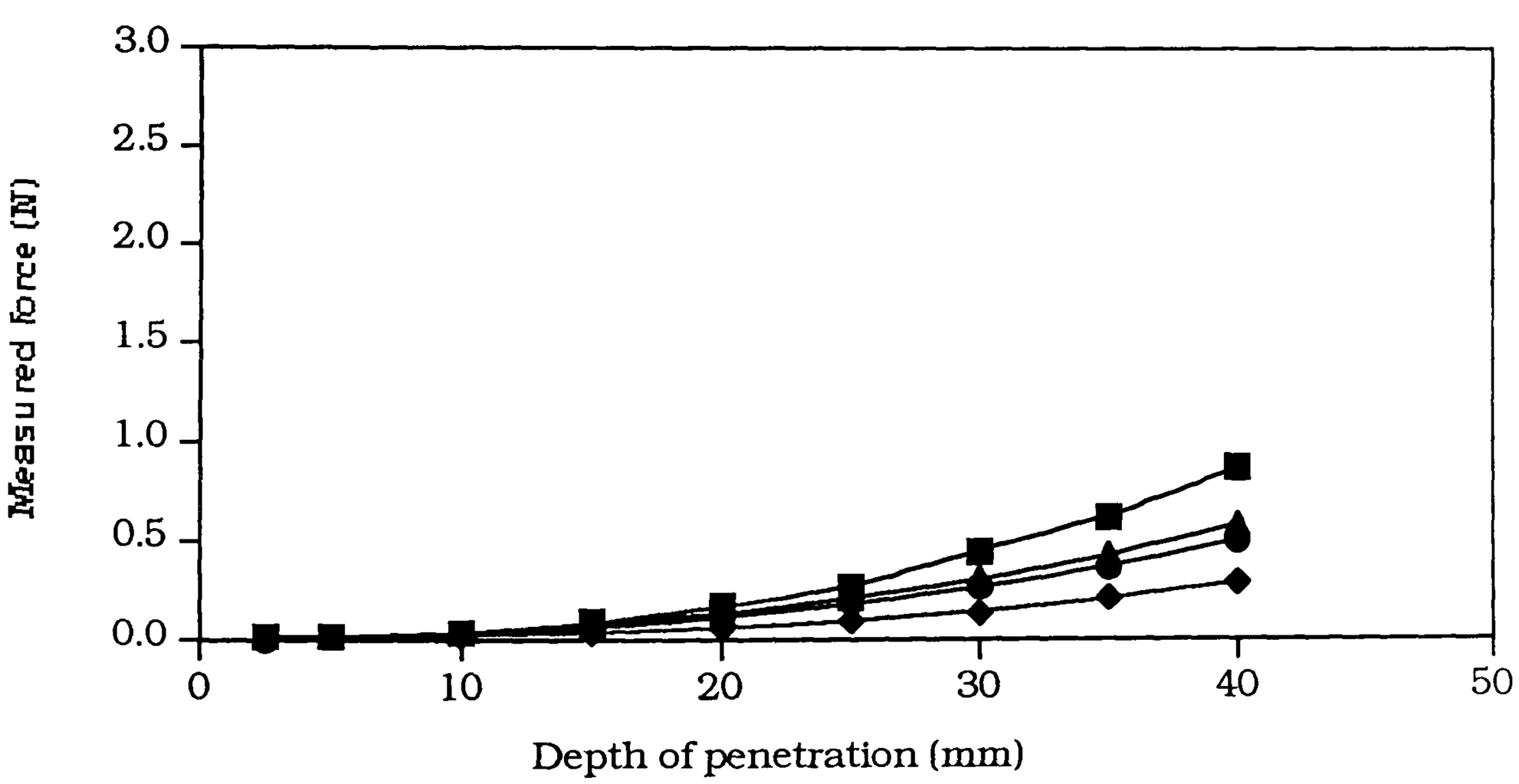

Figure 6.6.5 Relationship between force and depth of penetration into a Starch 1500 powder bed compacted with different loads

6.7 Discussion

All of the penetration force *versus* depth curves exhibit the typical parabolic shape. As expected, the force required to penetrate the powder bed increases as the force of compaction applied to the powder bed increases. This increase is more significant with the samples of nedocromil sodium and kaolin compared with the lactose and Starch 1500 samples.

The value of the unconfined compression stress was calculated using equation 6.2.4 with $a_{fc}=1.4$ [149]. The derived value for the unconfined compression stress showed very little variation over the replicate measurements at penetration depths greater than 10 mm. This can be seen in Figures 6.7.1 to 6.7.5. The error bars represent the standard deviation of the data.

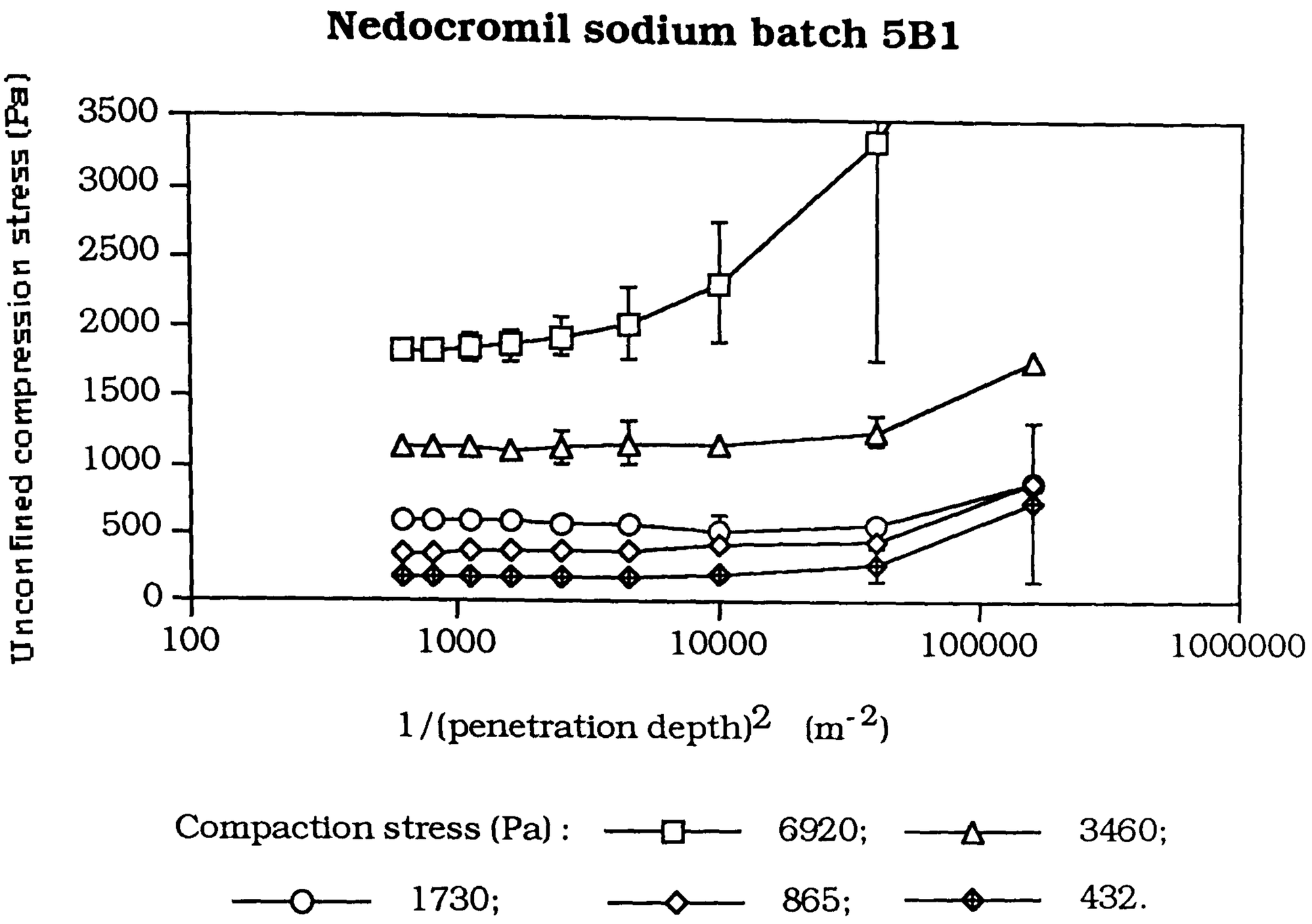

Figure 6.7.1 Relationship between the derived force of cohesion and the reciprocal of the square of the depth of penetration into a nedocromil sodium batch 5B1 powder bed compressed with different loads

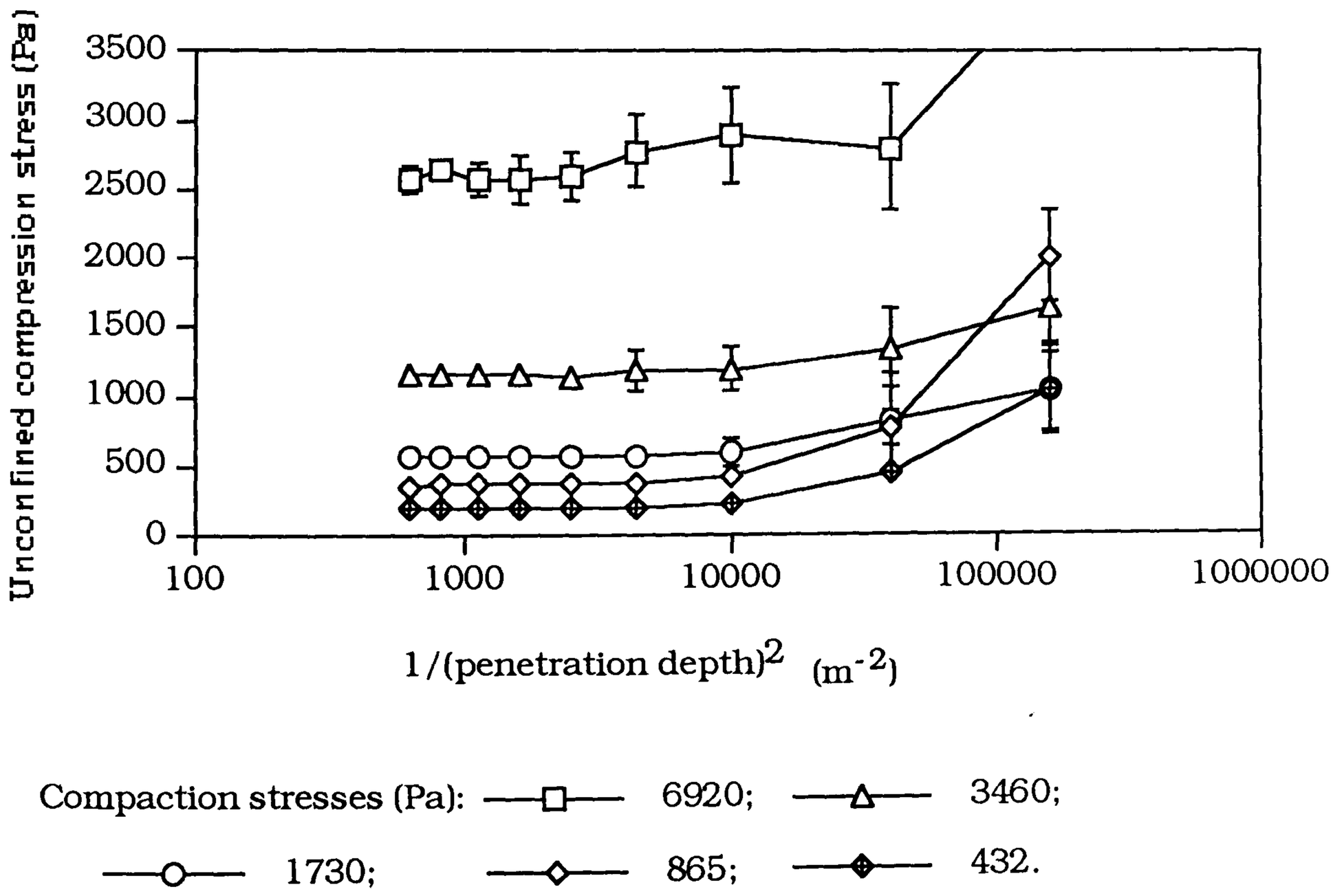

Figure 6.7.2 Relationship between the derived force of cohesion and the reciprocal of the square of the depth of penetration into a nedocromil sodium batch 2002B1 powder bed compressed with different loads

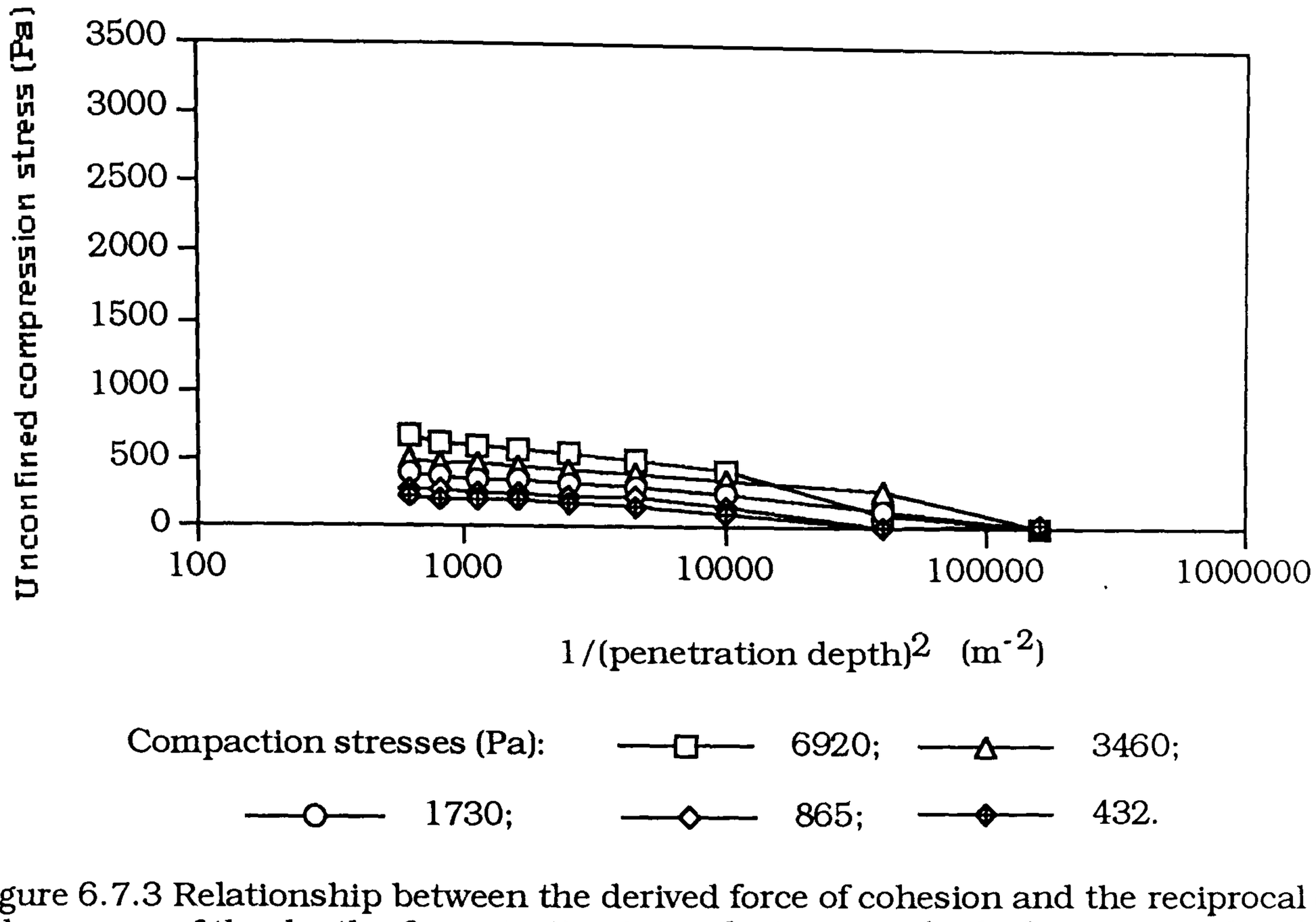

Figure 6.7.3 Relationship between the derived force of cohesion and the reciprocal of the square of the depth of penetration into a lactose powder bed compressed with different loads

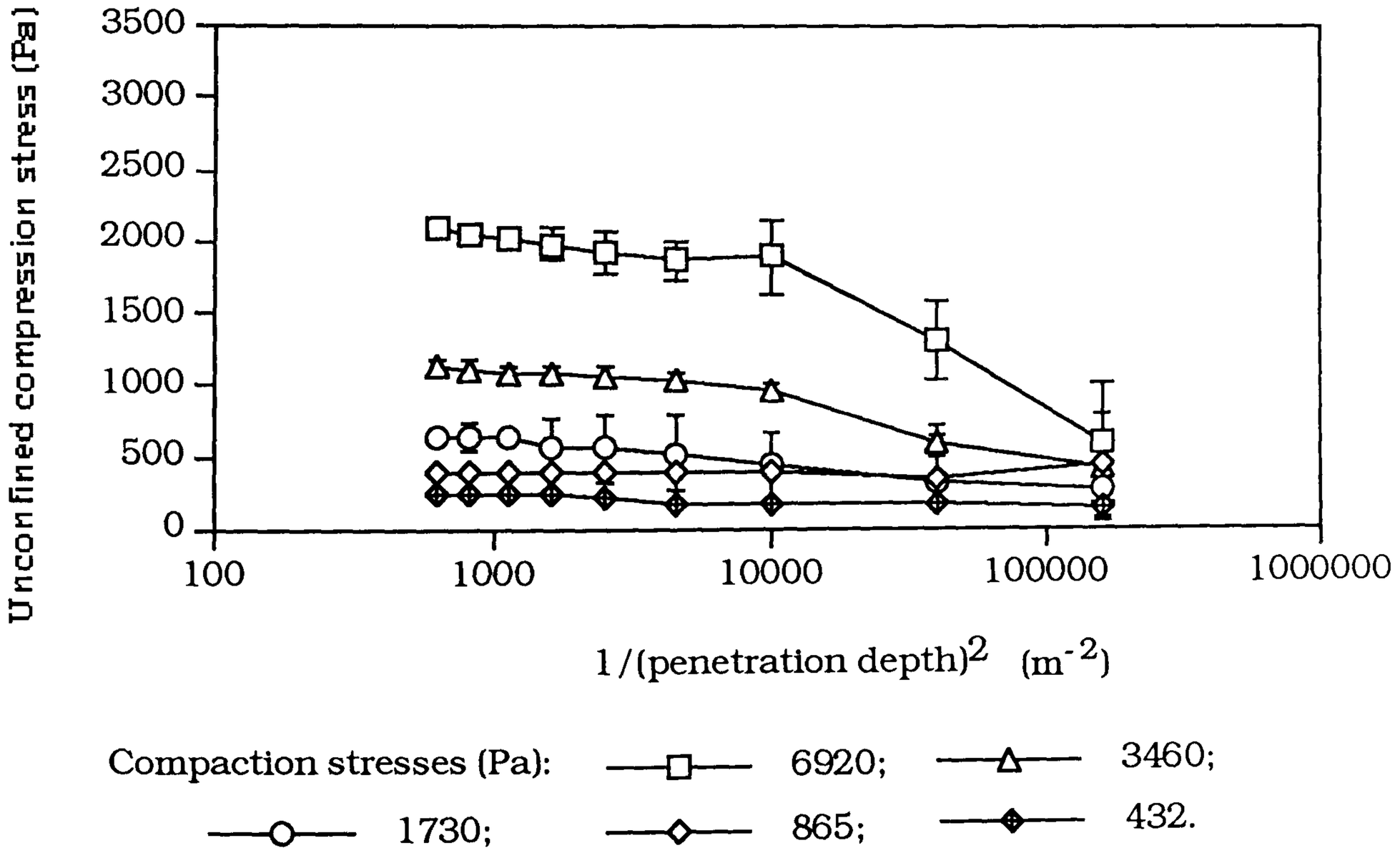

Figure 6.7.4 Relationship between the derived force of cohesion and the reciprocal of the square of the depth of penetration into a kaolin powder bed compressed with different loads

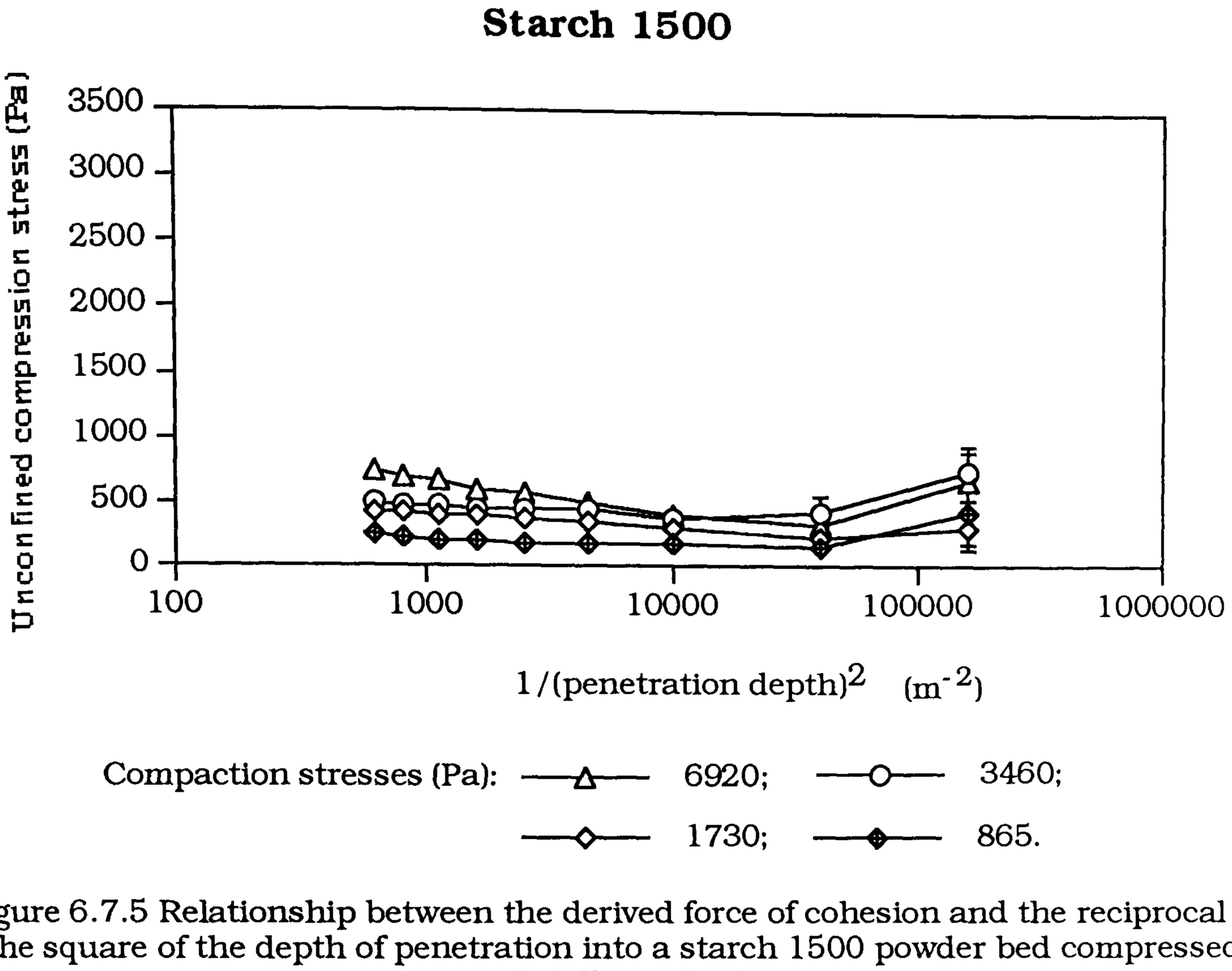

Figure 6.7.5 Relationship between the derived force of cohesion and the reciprocal of the square of the depth of penetration into a starch 1500 powder bed compressed with different loads

The derived values for the force of cohesion at penetration depths greater than 10 mm, and the respective coefficient of variation are shown in Table 6.7.1.

	Compaction stress				
	6920 Pa	3460 Pa	1730 Pa	865 Pa	432 Pa
Nedocromil sodium Batch 5B1					
F_c (Pa)	1951.8	1144.9	571.7	371.4	182.7
C.V. (%)	14.2	8.1	12.5	13.0	13.1
Nedocromil sodium Batch 2002 B1					
F_c (Pa)	2658.9	1171.6	580.8	380.5	206.4
C.V. (%)	8.8	9.6	8.3	8.6	15.3
Lactose					
F_c (Pa)	568.3	442.7	340.0	237.4	187.5
C.V. (%)	16.4	13.3	15.6	18.9	18.1
Kaolin					
F_c (Pa)	1975.4	1069.1	566.3	390.7	217.3
C.V. (%)	8.3	8.0	36.2	9.9	21.3
Starch 1500					
F_c (Pa)	588.3	455.1	380.4	202.5	not
C.V. (%)	20.9	17.1	12.7	16.0	available

Table 6.7.1 Derived values for the force of cohesion

As expected, the increase in the magnitude of the compaction procedure increases the unconfined compression stress within the powder bed. This is observed at all penetration depths, and is a reflection of the increased cohesive interactions within the powder bed due to the compaction procedure.

During the compaction procedure the volume of the powder bed is reduced. The rearrangement of the particles in the powder bed forms a less porous structure. This is achieved by the particles sliding past each other and coming into closer contact. The magnitude of the attractive forces which exist within the powder bed is dependent upon the interparticulate distance. Therefore as the compaction load increases the resulting decrease in the interparticulate distances within

the powder bed is reflected by the increase of the unconfined compression stress.

The relationships between the applied compaction stress and the derived measure of the cohesive interaction within the powder bed are shown in Figure 6.7.6.

Relationship between unconfined compression stress and compaction stress for five pharmaceutical powders

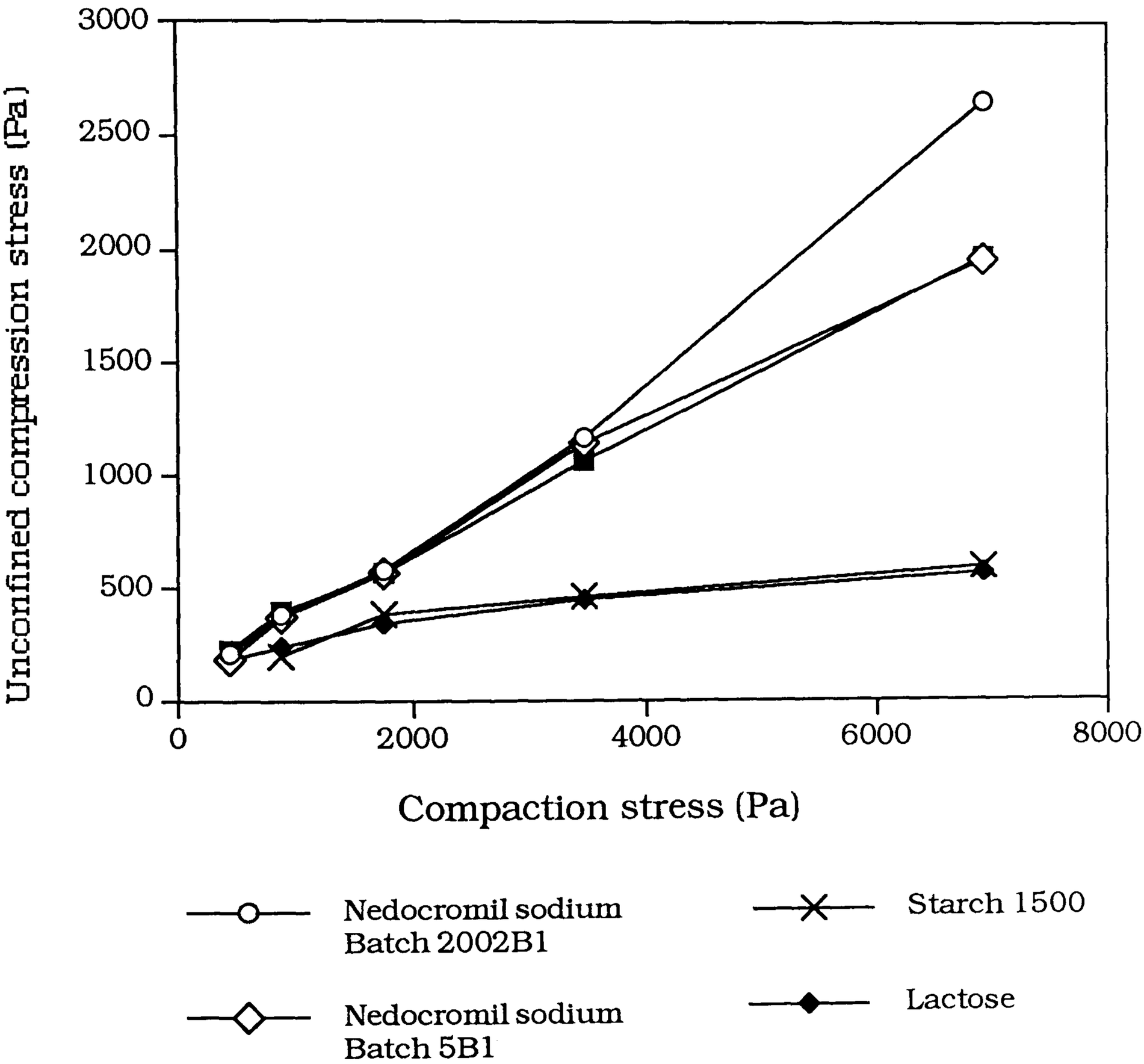

Figure 6.7.6

The magnitude of this measure of cohesive interaction at low compaction stresses is very similar for each of the five pharmaceutical powders investigated. Deviations in the behaviour due to the powder sample become apparent at compaction stresses in excess of 275 Pa. The cohesive interactions within the nedocromil sodium and kaolin powder beds increase in magnitude considerably more than those exhibited by the lactose and starch samples. This is a result of the particle size of the powder samples. As observed in section 2.2 particles of nedocromil sodium and kaolin have particle sizes ranging from 0.5 μm to 3 μm, whilst lactose and starch both have larger particles in the range of 50 μm to 90 μm.

At very small depths of penetration the derived magnitude of the unconfined compression stress tends to decrease for samples of lactose and kaolin, but increases for the nedocromil sodium samples. This suggests that the load is transmitted through the powder bed more effectively by the lactose and kaolin samples when compared with the samples of nedocromil sodium.

6.8 Conclusion

Using the cone penetrometry technique it is possible to differentiate between cohesive and free-flowing powders. This can be achieved by evaluating the unconfined compression stress within the powder bed having carried out a compaction process using a variety of loads.

The technique, however, does not have the sensitivity capability to evaluate the cohesive interactions between particles in a powder bed without preparing the bed by compaction.

At high bed compaction forces differentiation between the cohesive natures of the powders tested is possible. However, extrapolation to zero load, to yield the magnitude of the cohesive interaction within the uncompressed powder mass, resulted in values which could not differentiate between the fundamental cohesion properties of the powders under test. Thus a potentially useful test appears, unfortunately, to be insensitive to the subtle differences in powder cohesion which manifest themselves in significant differences in the performance of powder systems used in dry powder inhalation systems.

Chapter Seven

Preparation and evaluation of powder mixes for inhalation therapy using drug cohesive aggregates

7.1 Aim

As reported in Chapter 3 binary interactive mixes involve both adhesive and cohesive interactions, creating a powder mix which has characteristics of both an interactive mix and a random mix..

The aim of this chapter was to encourage the presence of cohesive aggregates within the binary powder mix, and assess the structure of such mixes in order to elucidate whether the structure of the mix would move towards the structure of an interactive mix.

This was done by preparing cohesive pellets of drug prior to mixing, by a tumbling method. The determination of the degree of adhesive and cohesive interactions within the powder mix was carried out as described in Chapters 3 and 4 respectively.

7.2 Introduction

Interactive powder mixes are formed when micronised powder particles adhere to the surface of larger crystals [53]. In powder mixes for inhalation therapy the micronised powder is the drug which is to be delivered to the lungs.

Adhesion of single particles of the drug to the surface of lactose particles has previously been encouraged by sieving the drug before mixing. During the mixing process adhesive interactions between the drug and particles of lactose have been established. Cohesive interactions were responsible for the formation of smaller drug aggregates within the powder mix. The structure of the binary powder

mix thus created was such that some aggregates were adhered to the surface of the lactose particles, whilst others were non-interacting. The presence of non-interacting aggregates and lactose particles in the mix is analogous to a random powder mix as described by Lacey [45].

In contrast to encouraging adhesion during the formation of binary interactive mixes by sieving the drug species prior to mixing, cohesion can be encouraged. This can be carried out by the preparation of cohesive drug aggregates. These can then be mixed with the lactose particles to form a binary mix. If such a system behaves as a random mixture no interparticulate interactions will occur. The homogeneity of a truly random mix of such a system can be determined by the Stange-Poole equation [81]. This determines the standard deviation of the sample composition for the best possible mix, as shown in equation 7.2.1.

$$\sigma_R = \left[ab\left(\overline{m}_a b + \overline{m}_b a\right) / M \right]^{\frac{1}{2}} \qquad \text{(equation 7.2.1)}$$

where

σ_R = standard deviation of the sample composition as a proportion of the sample mass M

a,b = mean proportion by mass of constituents A and B per sample

$\overline{m}_a$, $\overline{m}_b$ = representative mean particle mass of A and B

M = constant sample mass (dose size)

In contrast to this, adhesion/cohesion competition may take place. Adhesive interactions between the drug and carrier species may create a mix which tends towards the structure of an interactive mix. Such a powder mix would contain interactive units composed of drug

particles adhered to the surface of the carrier particle. As discussed in Chapter 3, the best possible interactive mix can be described by the coefficient of variation (%) derived from the Poisson equation, shown in equation 7.2.2 [86].

$$C_R = 100\sqrt{\frac{\overline{m}}{G}} \qquad \text{(equation 7.2.2)}$$

Where

$\overline{m}$ = representative mean particle mass

G = mean content of the adherent ingredient per sample

7.3 Experimental

Micronised material has been observed to form spherical aggregates when subjected to a tumbling action [150]. This procedure was investigated and optimised to prepare aggregates of nedocromil sodium. These aggregates were mixed with particles of α-lactose monohydrate. The quality of these mixes was determined by assessing the homogeneity. Image analysis and scanning electron microscopy were used to visualise the structure of the mixes.

7.4 Methods

7.4.1 Preparation of drug aggregates

About 25 g of nedocromil sodium directly from the stock bottle was placed into a clean dry Erweka copper coating pan type DK3. The internal diameter of the pan was 375 mm, with a 19 litre capacity. The tumbling cycle shown below was followed.

Step number	Speed number	Revolutions per second (Hz)	Time (seconds)
1	1	0.20	60
2	2	0.27	60
3	3	0.42	120
4	2	0.27	60

Table 7.4.1 Cohesive aggregate formation cycle

Subsequent to tumbling the prepared pellet batch was sieved using an Endecotts vibratory sieve shaker, model EVP1. The size fraction 180 μm to 250 μm was collected.

7.4.2 Mixing pellets

7.4.2.a Materials

Material	Batch	Aggregate sieve fraction
Nedocromil sodium	5B1	180 μm to 250 μm
α-lactose monohydrate	22301	63 μm to 90 μm

Table 7.4.2 Powder samples

7.4.2b Method

Drug and lactose samples were weighed using a Mettler AT261 balance. The quantity of each powder mix, 50 g and 25 g for 4 %w/w and 40 %w/w respectively, allowed a 50 % void space within the mixing vessel.

A specially constructed stainless steel mixing cylinder was used to prepare the mixes. Curved internal joints replacing the 90° angles reduced the dead space in the vessel. The capacity of the vessel was 160 cm^3.

The weighed samples were transferred to the mixing vessel and were mixed for 5 minutes using a Turbula mixer (T2C, W. A. Bachofen, Switzerland) set at 90 revolutions per minute (1.5 Hz). The vessel was then removed from the mixer and gently tapped in order to dislodge any

mix which had become adhered to the vertices of the vessel. This was followed by another 5 minute mixing time at the same settings.

7.4.3 Homogeneity testing

The quality of the mixes was assessed by determining the homogeneity. Samples of the dose size, 25 mg, were taken from the mix. These samples were dissolved in deionised water and immediately assayed for drug content by U.V spectroscopy as detailed in section 2.11.

7.4.4 Image analysis

Image analysis was employed in order to identify the structure of the drug aggregates. A Zeiss Axioskop microscope was used, the images being produced using a Mitsubishi colour video copy processor (CP 100B).

7.4.5 Scanning electron microscopy

Samples of powder mixes were analysed using an International Scientific Instruments DS130 scanning electron microscope, as described in section 2.3. The following samples were analysed:

1. 4 %w/w nedocromil sodium pellets/lactose mix;
2. 40 %w/w nedocromil sodium pellets/lactose mix;
3. Inhaler residue (as described in section 4.7.2) from 4 %w/w nedocromil sodium pellets/lactose mix;
4. Inhaler residue (as described in section 4.7.2) from 40 %w/w nedocromil sodium pellets/lactose mix.

7.4.6 Powder mix residue

The large value obtained for the sample coefficient of variation indicated that quantitative deposition testing using the multi-stage liquid impinger apparatus would incur large errors. The testing procedure was carried out, however, in order to collect the particles which remain in the cyclone chamber of the device after the inhalation cycle.

7.4.6a Materials

Analysis of the powder mixes containing 4 %w/w and 40 %w/w nedocromil sodium, prepared from drug aggregates was carried out.

7.4.6b Method

The *in vitro* inhalation testing procedure, detailed in Chapter Three was carried out. The powder which remained in the cyclone chamber was collected after each inhalation cycle. This residue powder was analysed using image analysis and scanning electron microscopy, as described in section 3.5.3.

7.5 Results

7.5.1 Analysis of drug aggregates

As shown in the photomicrograph, Figure 7.5.1, the aggregates have a spherical shape. Image analysis confirmed that the diameter of the aggregates were in the size range 180-250 μm.

Figure 7.5.1 Nedocromil sodium pellets. Magnification x 63.

The image shows small drug aggregates attached to the surface of these aggregates. These are very similar to the surface held aggregates seen in the interactive mixes of nedocromil sodium and lactose, observed in Figures 3.6.4 to 3.6.8.

The average aggregate mass was determined by assaying a known number of aggregates. The assay procedure was carried out as described in section 2.11. The mass of a single nedocromil sodium aggregate was determined as 2.76×10^{-6} g.

7.5.2 Homogeneity testing of the powder mix

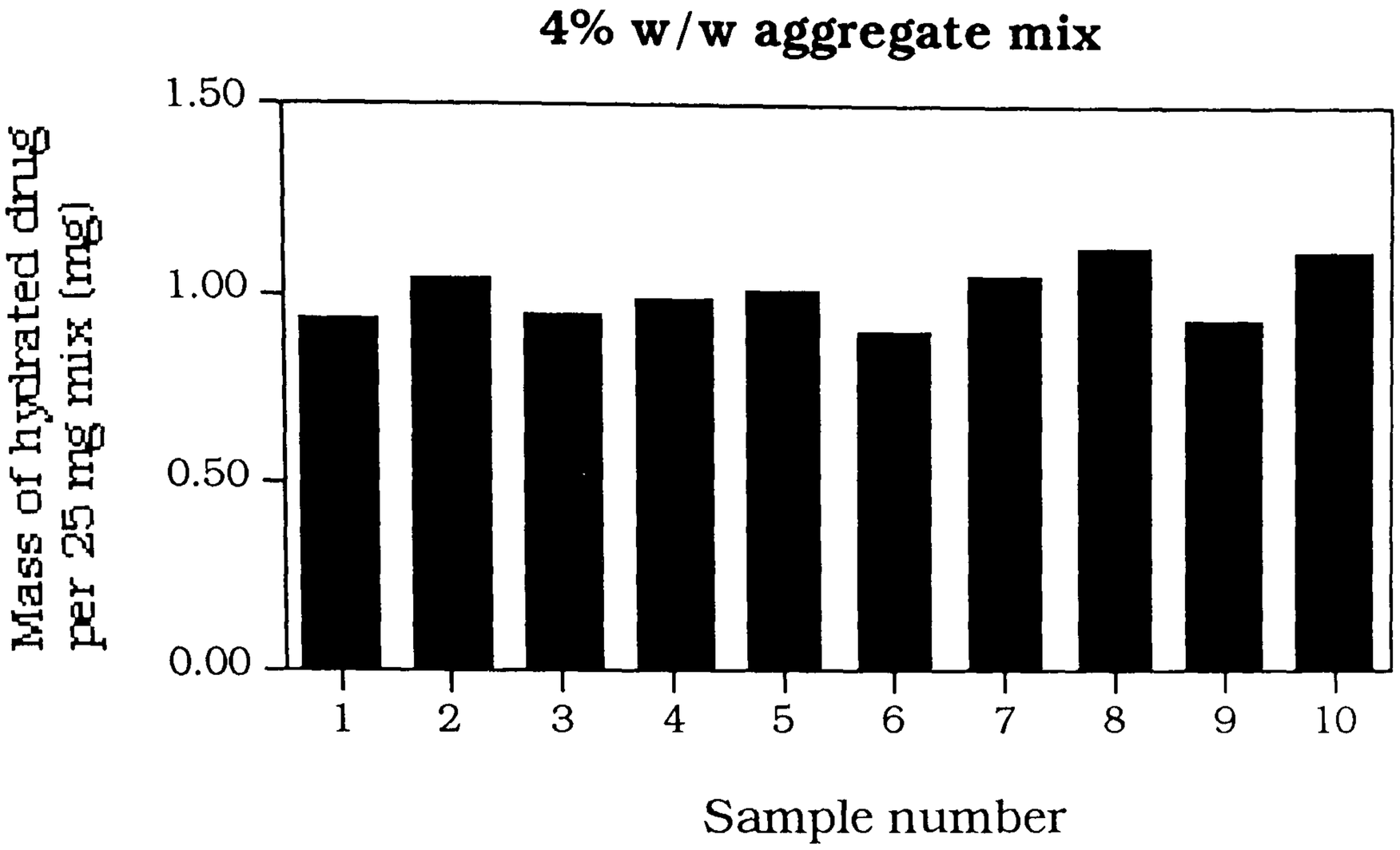

Figure 7.5.2 Assay results for 4 %w/w drug mix of nedocromil sodium aggregates with lactose

Theoretical hydrated drug content (% w/w)	Drug content coefficient of variation (%)	Standard deviation (mg)	Drug content by assay (% w/w)
4.0	7.71	0.077	4.003

Table 7.5.1. Assay results for 4 %w/w drug mix of nedocromil sodium aggregates with lactose

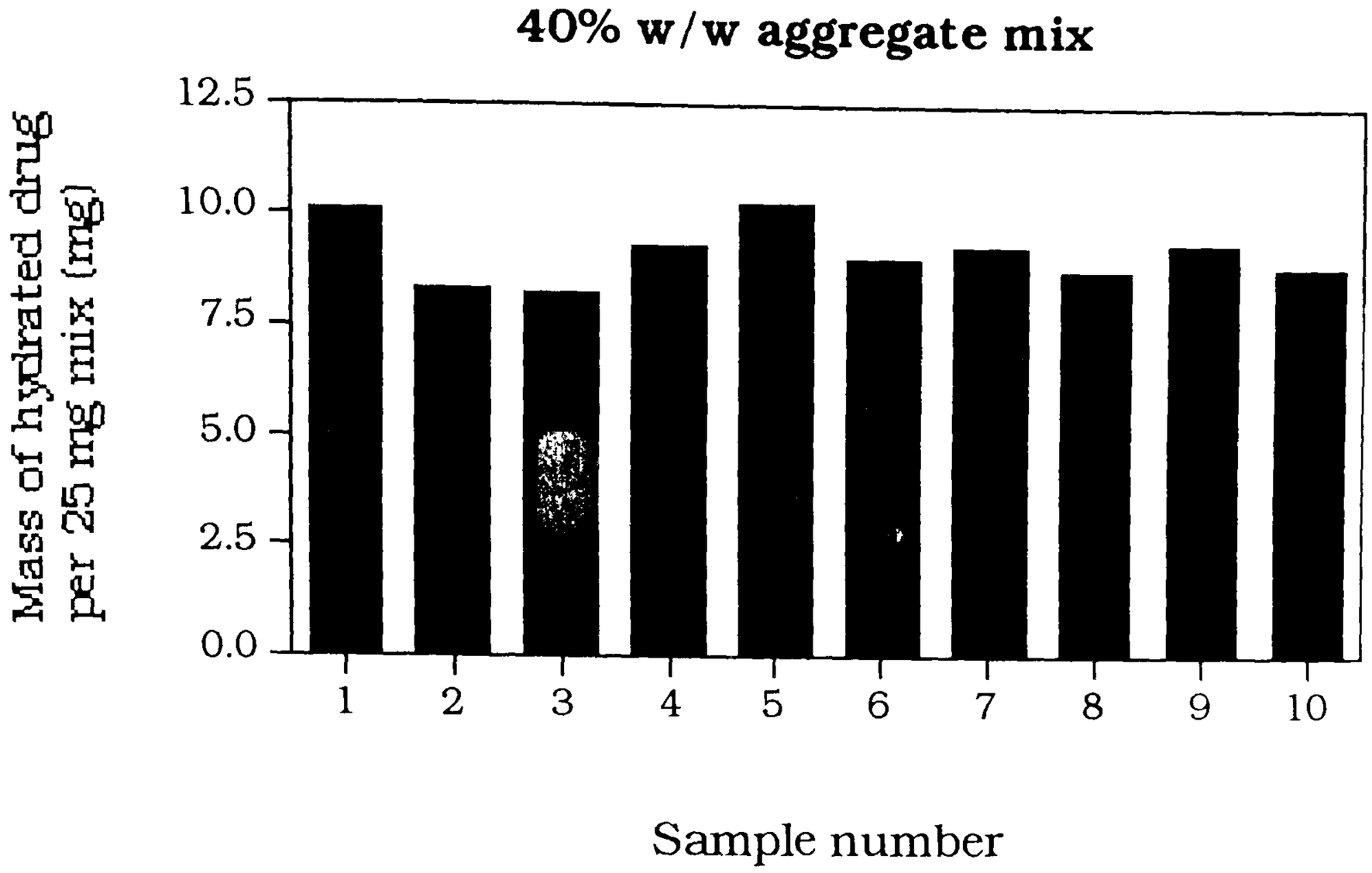

Figure 7.5.3. Assay results for 40 %w/w drug mix of nedocromil sodium aggregates with lactose

Theoretical hydrated drug content (% w/w)	Drug content coefficient of variation (%)	Standard deviation (mg)	Drug content by assay (% w/w)
40	7.33	0.668	36.41

Table 7.5.2 Assay results for 40 %w/w drug mix of nedocromil sodium aggregates with lactose

The theoretical values for the standard deviation of drug content per sample can be calculated for the best possible random mix, using the Stange-Poole equation (equation 7.2.1). These values for the theoretical best possible mix of nedocromil sodium aggregates (a) with lactose (b) are shown in Table 7.5.3..

	4 % w/w drug content	40 % w/w drug content
σ_R	0.002	0.004
CV %	0.202	0.042

Table 7.5.3 Homogeneity values calculated using the Stange-Poole equation for powder mixes of nedocromil sodium aggregates with lactose

Comparison of the experimental values for the sample coefficient of variation with the values determined theoretically show that the best attainable random mix has not been prepared. The theoretical values for the sample coefficient of variation for the best possible interactive mix, as described by Egermann [86] (equation 3.2.5.) are shown in Table 7.5.4.

	4.0 %w/w drug content	**40 %w/w drug content**
Coefficient of variation (%)	0.013	0.004

Table 7.5.4 Homogeneity values calculated using the Poisson-derived equation for powder mixes of nedocromil sodium with lactose

Comparison of the experimental values for the sample coefficient of variation with the values determined theoretically show that the best attainable interactive mix has not been prepared. Therefore, the sample variation of binary mixes prepared with particles of lactose and nedocromil sodium aggregates conformed neither to that of the best possible random mix, nor the best possible interactive mix.

7.5.3 Image analysis of powder mixes

Photomicrographs were obtained for the mixes of nedocromil sodium aggregates with lactose at drug concentrations 4 %w/w and 40 %w/w. These are reproduced in Figures 7.5.2 and 7.5.3.

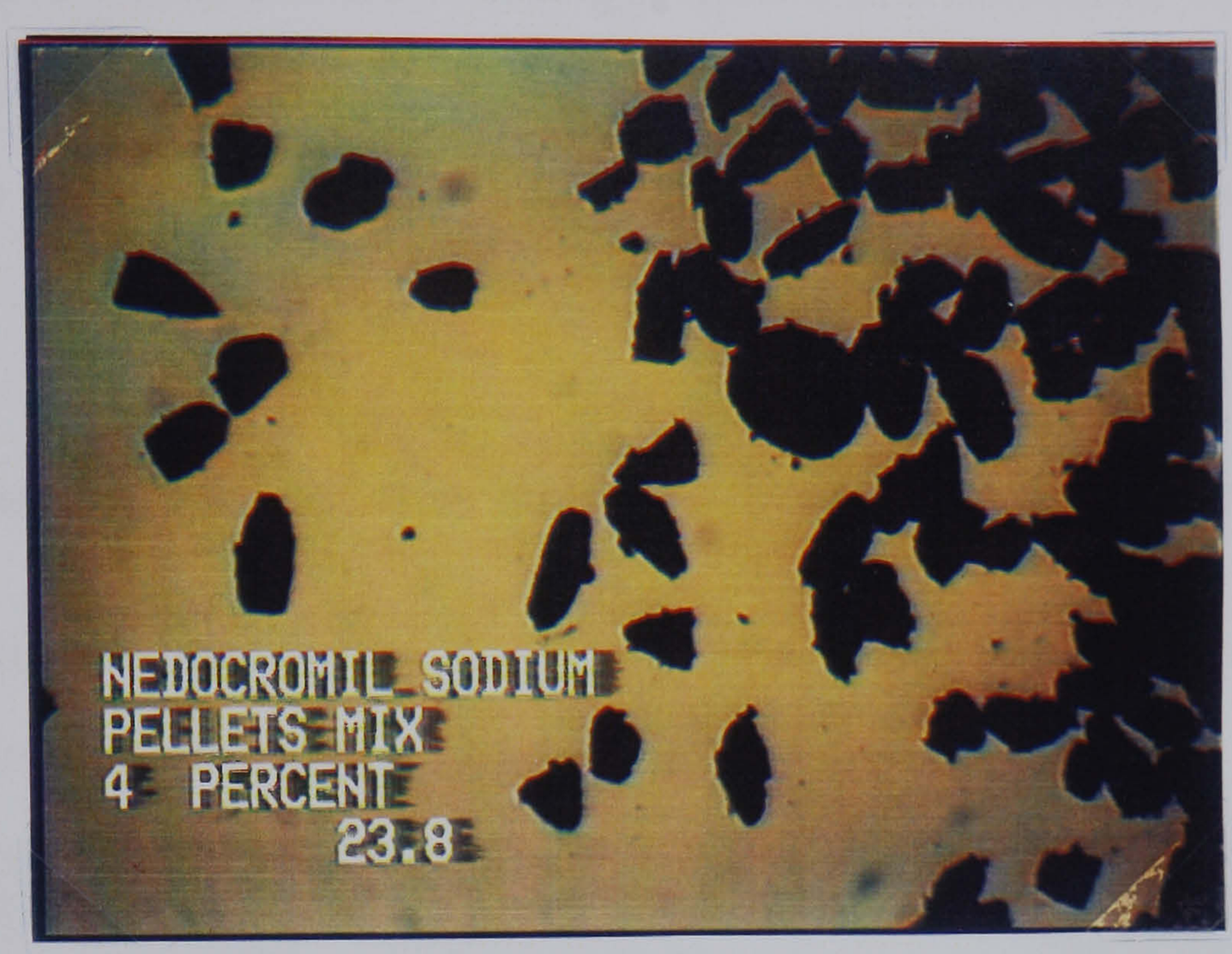

Figure 7.5.2 Nedocromil sodium aggregate 4 %w/w /lactose powder mix. Magnification x 63.

Figure 7.5.3 Nedocromil sodium aggregate 40 %w/w /lactose powder mix. Magnification x 63.

Particles of lactose in both of the powder mixes have small aggregates of the drug associated with their surface. These surface held aggregates are more abundant in the higher concentration mix.

As seen with the interactive mixes using pre-screened drug (Figures 3.6.20 and 3.6.21), the aggregates are attached to the lactose particle via a small number of anchor particles. These small aggregates can also be seen on the surface of the drug pellets in the mix.

7.5.4 Scanning electron microscopy of powder mix

Photomicrographs of the 4 %w/w and 40 %w/w powder blends are reproduced in Figures 7.5.4 to 7.5.7.

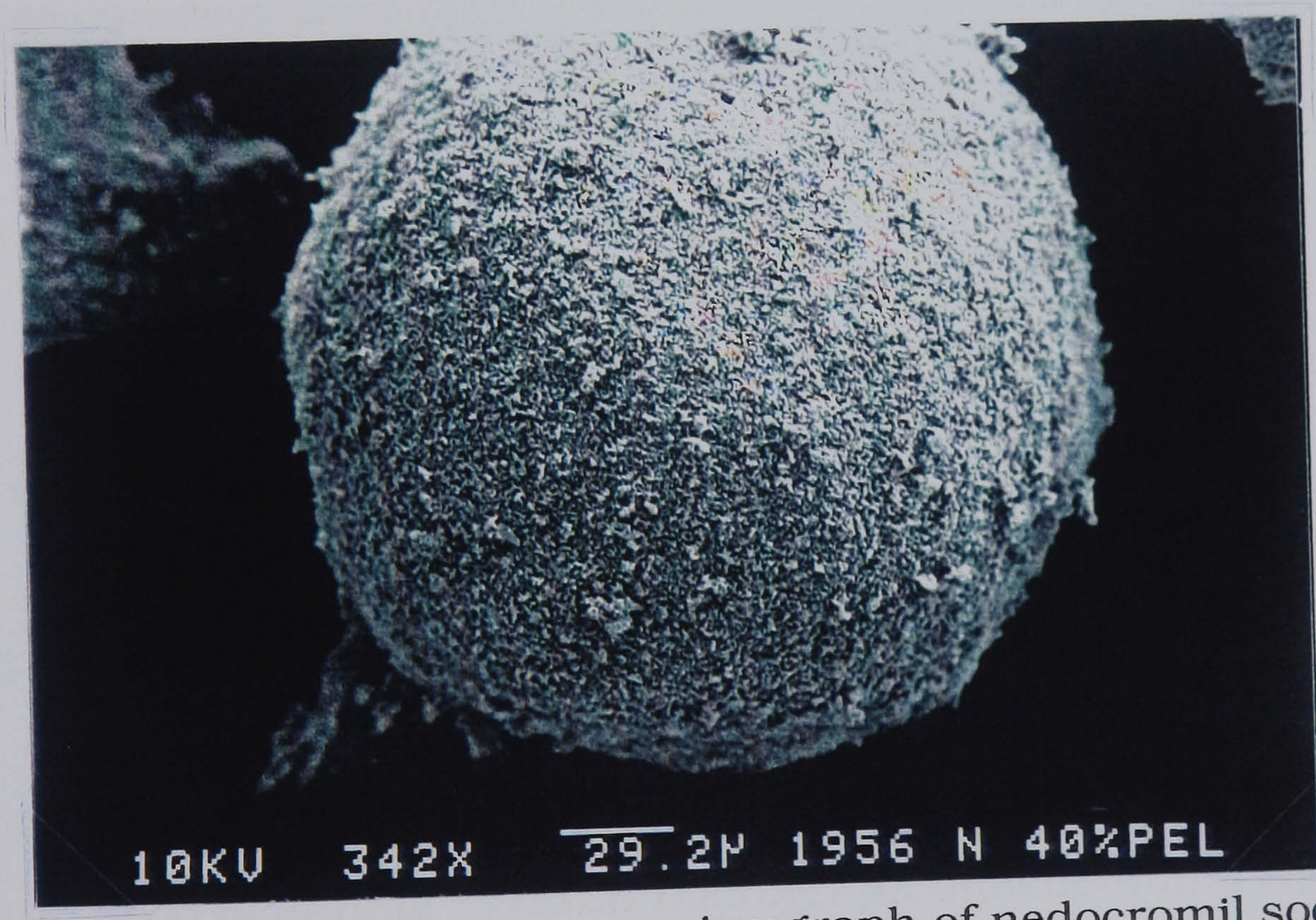

Figure 7.5.4 Scanning electron micrograph of nedocromil sodium aggregate/lactose 4 %w/w powder mix with lactose. Non-adhered pellet. Picture number 1956.

Figure 7.5.5 Scanning electron micrograph of nedocromil sodium aggregate/lactose 4 %w/w powder mix with lactose. Lactose particles. Picture number 1957.

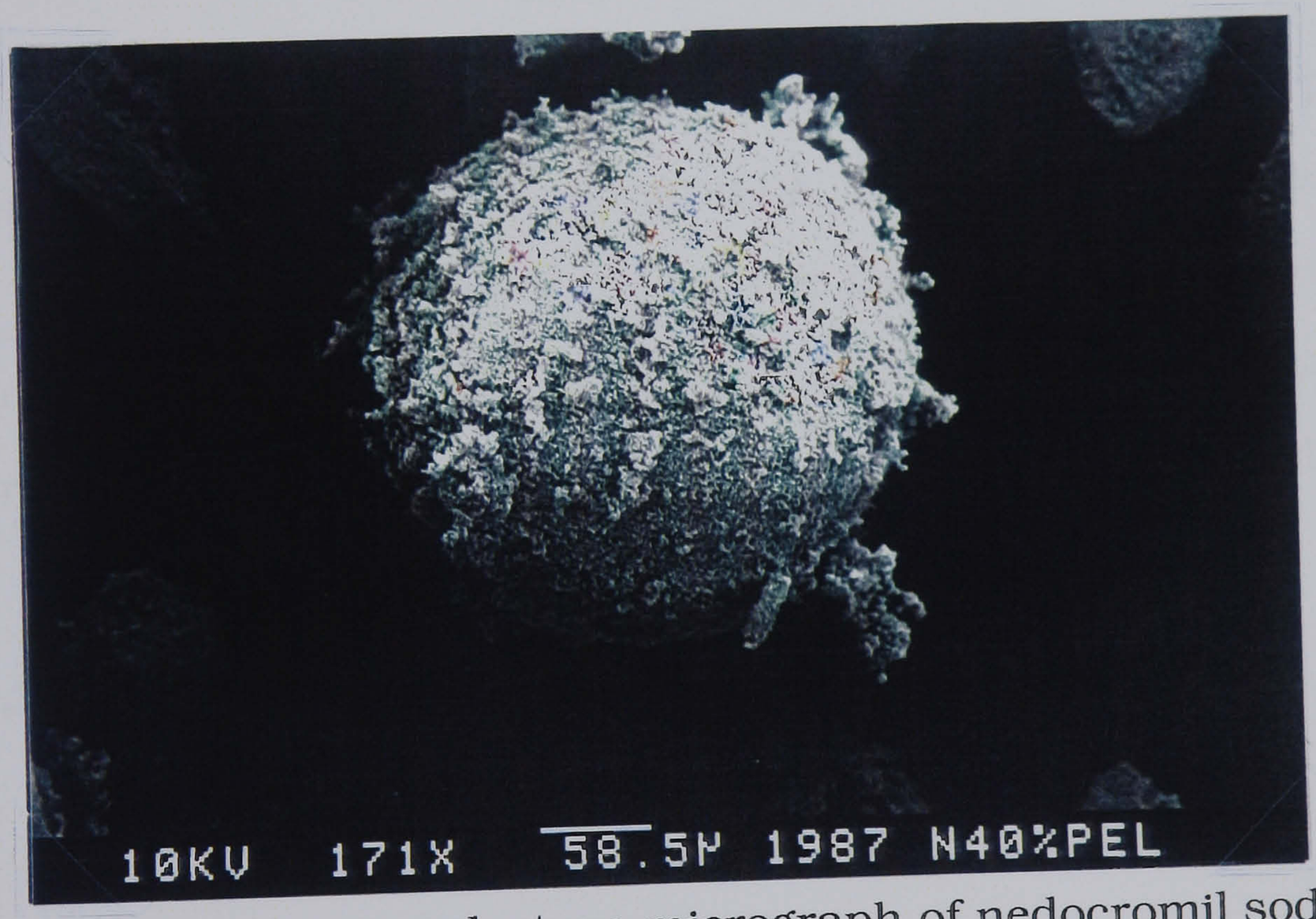

Figure 7.5.6 Scanning electron micrograph of nedocromil sodium aggregate/lactose 40 %w/w powder mix with lactose. Non-adhered pellet. Picture number 1987.

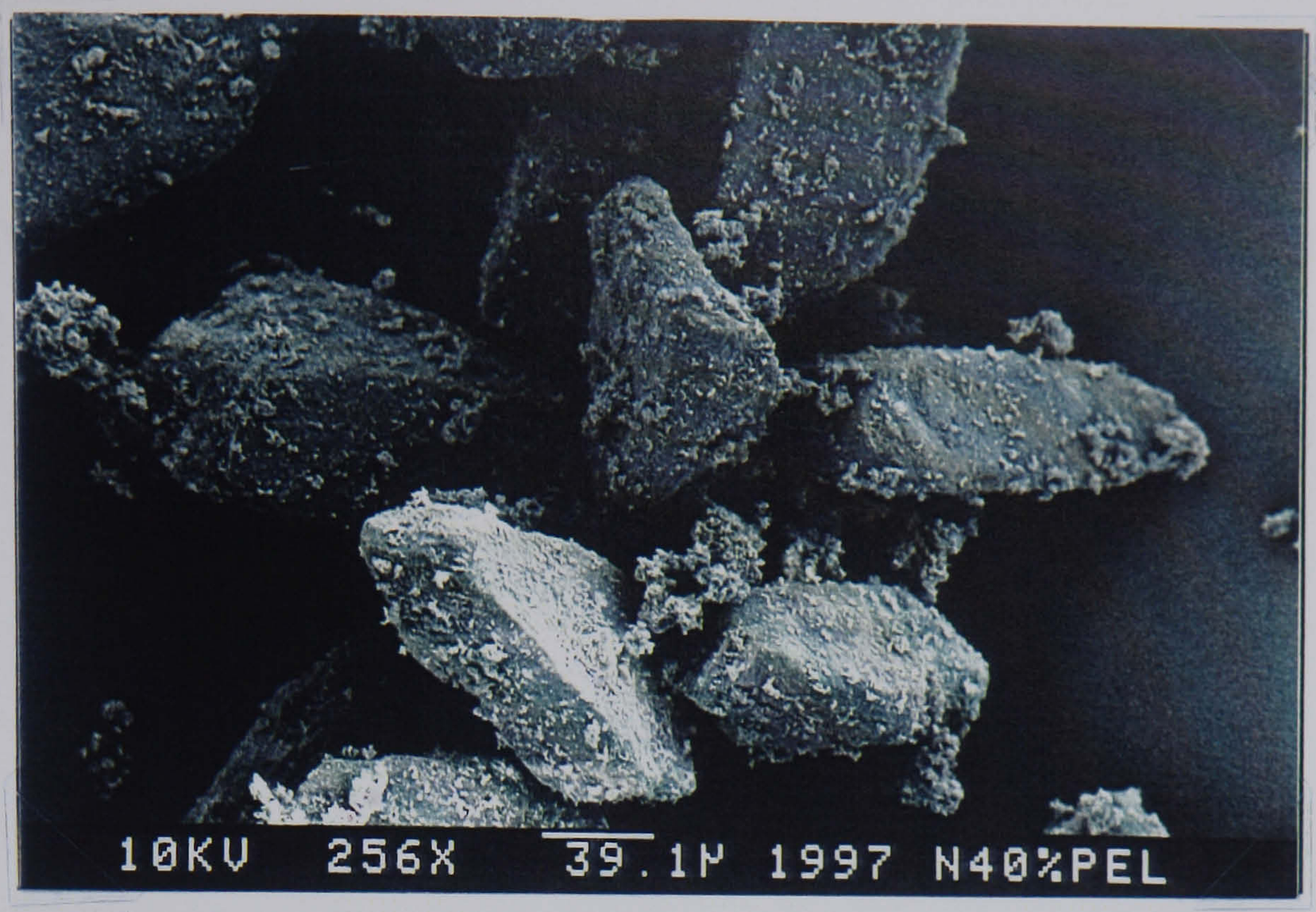

Figure 7.5.7 Scanning electron micrograph of nedocromil sodium aggregate/lactose 40 %w/w powder mix. Lactose particles. Picture number 1997.

Small adhered aggregates are present in both of the powder mixes, as shown in the photomicrographs. These small aggregates are present both on the surfaces of the lactose particles and the surface of the larger aggregates. The size of these small aggregates is independent of the drug load, but the number is proportional to the drug load.

7.5.5 Scanning electron analysis of the mix residue

Photomicrographs of the powder residue, collected after the inspiration cycle, are reproduced in Figures 7.5.8 and 7.5.9.

Figure 7.5.8 Scanning electron micrograph of nedocromil sodium aggregate/lactose powder residue from 4 %w/w drug mix after inhalation. Picture number 1976.

Figure 7.5.9 Scanning electron micrograph of nedocromil sodium aggregate/lactose powder residue from 40 %w/w drug mix after inhalation. Picture number 2010.

Surface held aggregates are no longer present in the powder residue from the lower drug load mix. This is in contrast to the residue from the 40 %w/w mix which retained some surface held aggregates throughout the inhalation cycle.

Further magnification, Figure 7.5.10, of the surface of a lactose particle retained from the 4 %w/w powder mix shows the very fine drug particles which remain adhered.

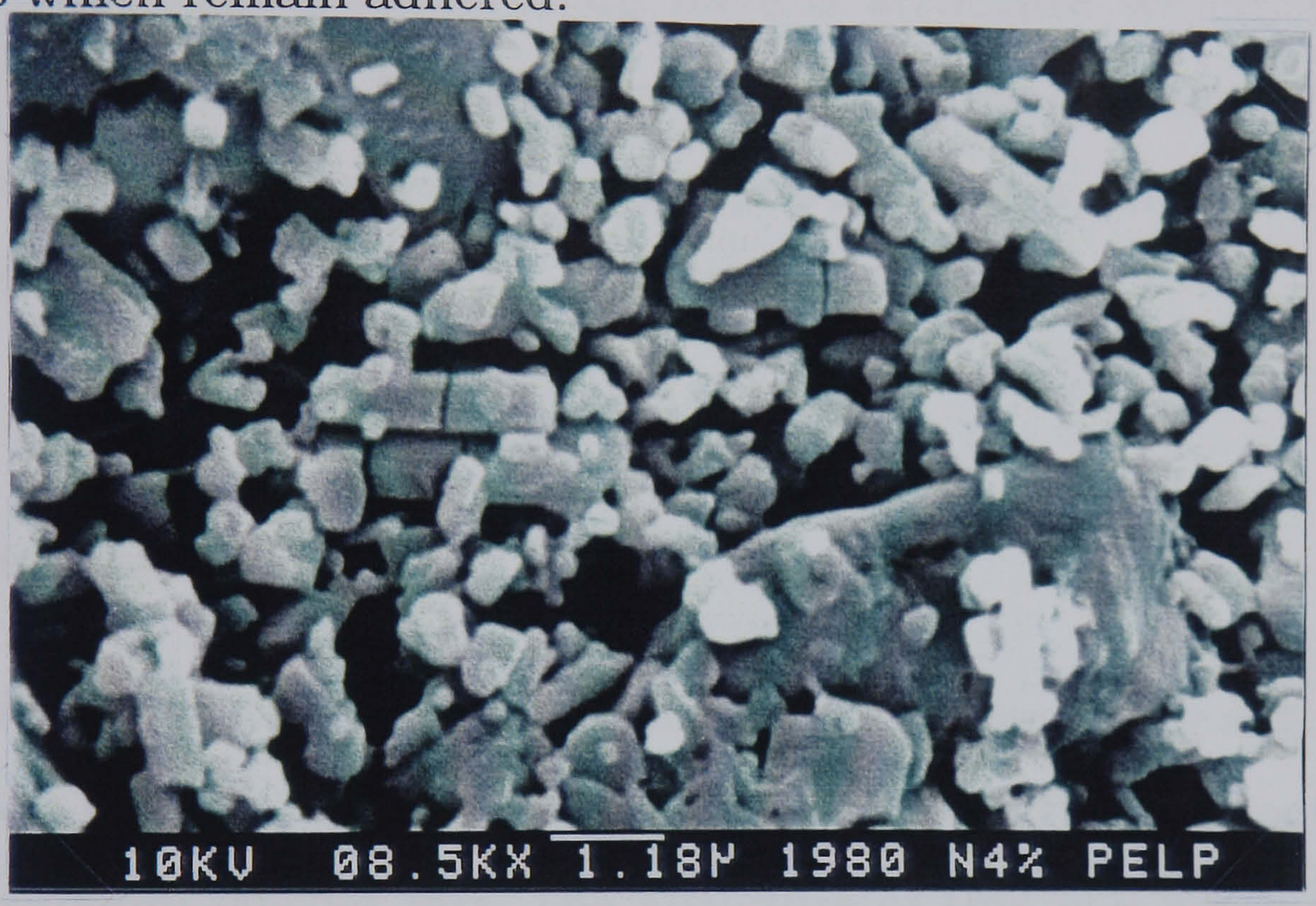

Figure 7.5.10 Scanning electron micrograph of nedocromil sodium aggregate/lactose powder residue from 4 %w/w drug mix after inhalation. Picture number 1980.

7.6 Discussion

The structure of the aggregate mixes deviates from the random behaviour of a binary mix due to adhesive interactions between particles of drug and lactose. This is reflected in the poor homogeneity exhibited by the mixes when compared with the best possible mix. The

structure of the mix tends towards an interactive mix due to the surface held particles of drug. However, the incomplete distribution of the drug from the aggregates onto the surface of the lactose prevents the best possible interactive powder mix being formed. A proportion of the non-interacting drug aggregates remain after the mixing process has been carried out. Therefore the powder mixes prepared by mixing lactose particles with aggregates of drug have a structure which, due to adhesive and cohesive interactions competing for particles of drug, combines the structures of random powder mixes and interactive powder mixes.

7.7 Conclusion

A method has been developed in order to prepare drug aggregates of a narrow size fraction. These were mixed with particles of lactose to create a random powder mix. The structure of this mix when viewed using scanning electron microscopy, deviated from that of a random mix due to adhesive interactions existing between the drug species and the carrier species. These adhesive interactions caused drug to be removed from the aggregates and become associated with the surface of the lactose particles. This process did not continue to completion, and so the structure of the powder mix was a combination of drug adhered to the surface of the lactose particles, and aggregates of drug which were not interacting with the particles of lactose.

The structure of the mix prepared from samples which encourage the formation of a random mixture of particles did not correspond to a

true random distribution. Cohesive and adhesive interactions between the two powder species created a combined structure of an interactive binary powder mix and random mix of two powder species.

Chapter Eight

Conclusions

8.1 Conclusion

Mixing very small sized drug particles with larger carrier particles theoretically produces an interactive powder mix in which the drug particles adhere to the surface of the carrier. Mixing two particle species which are similar in terms of size and density theoretically produces a random type of powder mix.

The structure of binary powder mixes prepared for inhalation therapy reflect neither an interactive nor a random type of mix.

Theoretical interactive powder mixes assume complete adhesion of the smaller particle species to the surface of the carrier to complete a monolayer coverage of the larger particle. This assumes adhesive interactions take place over the whole surface of the carrier particle, and neglects any cohesive, drug-drug, particle interactions.

Theoretical binary random powder mixes describes a random distribution of two species of powder particle within the powder bed. This assumes that adhesive interactions between the species do not take place.

The real binary powder mixes combined the adhesive element of interactive mixes with the non-interacting element of random mixes.

The interactive units of the real mixes are composed of a particle of lactose with associated particles of drug. This drug is adhered either as individual particles or as small cohesive aggregates. Non-interacting

aggregates of drug are also present in the mix, depending upon the drug load.

This is the structure for binary powder mixes regardless of the method of the drug preparation. Sieving the drug in order to encourage adhesion and preparing drug aggregates in order to encourage a random mix results in a similar structure.

The structure of the mix is due to both adhesive and cohesive interactions between the drug and carrier particles, and the drug-drug particles respectively.

Adhesive interactions do not take place over the whole surface of the particle of lactose. Specific areas appear to be preferential points for adhesion. These specific areas are identified by the examination of particles which remain in the inhaler device after the inspiration cycle. The number of single particles associated with the surface of a carrier particle appears to be finite.

Regardless of the drug preparation prior to mixing, drug particles are adhered as either single entities or small clusters. These small clusters are associated to the particle of lactose via small anchor particles, making the adhesive interaction. The clusters are held together by the cohesive forces which act within the aggregate.

The mechanism of formation of these surface held aggregates may either be at the adhesive site, or before adhesion takes place. An initial adhered particle may be the focus of cohesive interactions of more drug particles to form a small drug cluster. This is similar to the

mechanism suggested by Stephenson [67] for the formation of an interactive mix. An alternative mechanism may be that the small drug clusters are created within the powder mix and adhere onto the surface of the carrier particle. Because of their small size, the drug particles have a correspondingly high surface energy. Reduction of the surface free energy is the favourable result of aggregate formation. If created within the mix, these aggregates come into contact either with an adhesive site on the surface of the carrier particle, or other small aggregates. The energy supplied by the mixer may be responsible for removing surface held aggregates from the particles of lactose, leaving single surface held particles of drug.

When the drug load is high, non-interacting aggregates of drug are formed, but not at the expense of the surface held drug clusters.

The formation of these larger drug aggregates coincides with the plateau of the % w/w drug remaining adhered to carrier particles after the inhalation cycle. This may be due to the number of sites for adhesion of drug to the carrier being saturated. This would encourage the non-adhered small clusters to cohere, forming larger drug aggregates. Alternatively, the large drug load, and correspondingly large number of drug particles may readily cohere to form drug aggregates which are too large to adhere to the carrier particles. These may then be in competition with the lactose particles to be associated with the smaller clusters of drug. These small drug clusters may transfer from the surface of the lactose particles to the surface of the drug aggregates depending upon the magnitude of the adhesive and cohesive forces respectively.

Drug particles are removed from prepared drug aggregates to form surface held aggregates of drug on the surface of the carrier. The mechanism for this, as above, may be removal of single drug particles from the aggregate to adhere to the lactose, or cohere to drug particles already adhered. Alternatively, these small clusters of drug may form on the surface of the aggregate. Small clusters of drug were observed on the surface of the aggregates prior to mixing. These may then transfer to the lactose particles, or remain associated with the drug aggregate depending upon the magnitudes of the adhesive and cohesive interactions.

These surface held aggregates appear to be the source of the drug from the powder mix which travels to the lower stages of the multi-stage liquid impinger apparatus. These clusters of drug appear either adhered to the particles of lactose, or to the surface of non-interacting drug aggregates.

The creation of these larger drug aggregates provides more surface area in the powder mix with which the smaller drug clusters can be associated. Therefore, although the aggregate fraction of the powder mix increases due to the formation of non-dispersing drug aggregates, the number of dispersing, surface held aggregates also increases. The proportions of drug presented as respirable fraction and aggregate fraction, once this structure of the powder mix has been established, tends to be constant.

At a high drug load the formation of drug aggregates from sieved powder during the process of mixing led to a poor homogeneity of the

powder mix. The system in this case tended towards cohesive interactions between the particles of drug in order to form these aggregates. When the aggregates were prepared in a controlled way to obtain a specific size fraction, the mix presented a better value for homogeneity. However, when the system tended towards adhesive interactions, at low drug loads, mixing with prepared drug aggregates hinders the formation of interactive units. The preparation of the drug to encourage adhesion of small particles results in the mix with a better homogeneity.

Drug concentration (%w/w)	Sieved drug. Sample coefficient of variation (%)	Drug as aggregates. Sample coefficient of variation (%)
4.0	0.750	7.710
40.0	10.266	7.336

The structure of the binary mixes was slightly different according to the drug species used. Particles of nedocromil sodium and sodium cromoglycate differed only slightly with respect to physical characteristics such as size, shape and density. The particles of nedocromil sodium in the mix tended to display a more cohesive nature than the particles of sodium cromoglycate. However, when comparing the performance of the formulations in the multi-stage liquid impinger, their behaviour was very similar.

The mixes using a smaller sized drug particle were prepared at drug concentrations which contained the same number of drug particles as the mixes of the larger drug species. Poor homogeneity due

to non-interacting aggregate formation and segregation occurred at a much lower drug concentration than observed with the mixes containing larger drug particles. However, when comparing the performances of the same number concentration mixes, the mixes containing the smaller sized particles perform better as an inhalation formulation. At low drug concentrations, the very small proportion of the dose recovered as the aggregate fraction, and the good homogeneity of the mix suggests that the drug interactive units formed release the drug as small particles rather than aggregates. The photomicrographs of these units have shown that the drug is adhered as single particles and small drug clusters. Therefore, the drug clusters from these mixes easily deaggregate to deliver a large proportion of drug to the lower stages of the impinger.

In conclusion, drug delivered from binary powder mixes of a drug with carrier particles aims to travel to the pulmonary sites of action in order to exert a local pharmacological effect. The behaviour of these particles within the powder mix determines whether or not this result is achieved.

It has been determined that due to both cohesive and adhesive interactions taking place between the drug and drug/carrier particles respectively, the drug particles may be located within a number of structures. It has been elucidated that drug particles with the potential to reach pulmonary target sites originate from surface held drug aggregate structures.

Having determined the relationship between binary powder mix structure and drug delivery performance, investigation of the magnitude of particle interactions with a view to optimising the structure of the mix for drug delivery led to the development of two techniques. The insensitivity of the techniques suggests that binary powder blend optimisation will result from the application of more sensitive surface energy analysis of powder particles.

In conclusion, this work has elucidated that binary powder mixes of micronised drug or micronised drug pellets, with lactose particles, prepared in a tumbling-rotary type blender exhibit a structure which has characteristics of both interactive and random mixes.

Methodologies developed in order to quantify the magnitude of the adhesion and cohesion within the powder blends did not have the sensitivity capability to determine these forces.

The respirable fraction delivered from the powder blends originates from small cohesive aggregates which are associated with the surface of the lactose particles.

There is a difference in the mix structure and the deposition characteristics of the drug from the blend for different drug species.

There is a difference in deposition characteristics from a powder blend due to the drug load.

When the drug load is low, the respirable fraction is high. As the drug load increases, so does the number of non-adhered aggregates, which increases the aggregate fraction of the dose and therefore decreases the respirable fraction. However, this stabilises as the non-adhered aggregates provide a surface onto which the small surface-held aggregates can attach.

References

1. Health, D.o., *Asthma An Epidemiological Overview*. Central health monitoring unit epidemiological overview series, 1995, HMSO.

2. Montefort, S. and S.T. Holdgate, *Asthma as an immunological disease.* Medicine International, 1991. **89**: p. 3699-3702.

3. Walters, E.H., *Inhaled versus oral treatment with salbutamol.* Research and Clinical Forums, 1984. **6**(1): p. 73.

4. Newman, S.P., *et al.*, *Deposition of pressurised aerosols in the respiaratory tract.* Eur. J. Respir. Dis, 1981. **62**: p. 3-21.

5. Hinds, W.C., *Aerosol Technology*. 1982, New York: Jonh Wiley & Sons.

6. Chan, H. and I. Gonda, *Respirable Form of Crystals of Cromoglycic Acid.* Journal of Pharmaceutical Sciences, 1989. **78**(2): p. 176-180.

7. Gonda, I., *A semi-emperical model of aerosol deposition in the human respiratory tract for mouth inhalation.* J. Pharm. Pharmacol., 1981. **33**: p. 692-696.

8. Crompton, G.K., *The adult patient's difficulties with inhalers.* Lungs, 1990. **168**(Suppl.): p. 658-662.

9. Hilton, S., *An audit of inhaler technique among asthma patients of 34 general practitioners.* Br. J. Gen. Pract., 1990. **45**: p. 505-506.

10. Crompton, G.K., *New inhaler devices.* Eur. Respir. J., 1988. **1**: p. 674-680.

11. Molina, M.J. and F.S. Rowland, *Stratospheric sink for chlorofluoromethanes: chlorine atomc-atalysed destruction of ozone.* Nature, 1974. **249**: p. 810-812.

12. Daly, J.J., *Replacements for CFC propellants: a tachnical and environmental overview.* J. Biopharm. Sci., 1992. **3**: p. 265.

13. Clarke, A.R. and A.M. Hollingworth, *The Relationship Between Powder Inhaler Resistance and Peak Inspiratory Conditions in Healthy Volunteers - Implications for In Vitro Testing.* J. Aerosol. Med., 1993. **6**(2): p. 99-110.

14. Sumby, B.S., S.M. Cooper, and I.J. Smith, *A comparison of the inspiratory effort required to operate the Diskhaler and Turbohaler inhaler in the administration of powder drug formulations.* British Journal of Clinical Research, 1992. **3**: p. 117-123.

15. Olsson, B. and L. Asking, *Critical Aspects of the Function of Inspiratory Flow Driven Inhalers.* Journal of Aersosol Medicine, 1994. **7**(1): p. S43-S47.

16. Kassem, N.M., K.K.L. Ho, and D. Ganderton, *The effect of air flow and carrier size on the characteristics of an inspirable cloud.* Journal of Pharmacy and Pharmacology, 1989. **41**((suppl)): p. 14.

17. Vidgren, M., *et al.*, *Effect of powder inhaler design on drug deposition in the respiratory tract.* Int. J. Pharm., 1988. **42**: p. 211-216.

18. Timsina, M.P., *et al.*, *Drug delivery to the respiratory tract using dry powder inhalers.* International Journal of Pharmaceutics, 1994. **101**: p. 1-13.

19. Dickens, C.J. and J.J. McAughey, *Factors Affecting In Vitro Testing of Inhalers.* Journal of Aerosol Medicine, 1994. **7**(2): p. 193-196.

20. Jashnani, R.N., P.R. Byron, and R.N. Dalby, *Testing of dry powder aerosol formulations in different environmental conditions.* International Journal of Pharmaceutics, 1995. **113**: p. 123-130.

21. Pitcarn, G., *et al.*, *A comparison of the lung deposition of salbutamol inhaled from a new dry powder inhaler, at two inhaled flow rates.* International Journal of Pharmaceutics, 1994. **102**: p. 11-18.

22. Newman, S.P., *et al.*, *Terbutaline sulphate Turbuhaler: effect of inhaled flow rate on drug deposition and efficacy.* International Journal of Pharmaceutics, 1991. **74**: p. 209-213.

23. Vidgren, M.T., P.A. Vidgren, and T.P. Paronen, *Comparison of physical and inhalation properties of spray-dried and mechanically micronised disodium cromoglycate.* International Journal of Pharmaceutics, 1987. **35**: p. 139-144.

24. *A.B.P.I Data Sheet Compendium.* 1993-1994, Datapharm Publications Ltd.

25. Khankari, R.K. and D.J.W. Grant. *Solution-mediated transformation of nedocromil sodium hemihydrate to nedocromil sodium trihydrate.* in *American Association of Pharmaceutical Scientists 9th Annual Meeting*. 1994. San Diego, USA:

26. *British Pharmacopoeia.* ed. B.P. Commission. Vol. 1. 1993, London: H.M.S.O.

27. Allen, T., *Particle size measurement.* Fourth ed. Powder Technology Series, ed. B. Scarlett. 1990, Chapman and Hall.

28. Staniforth, J.N., *Particle size reduction,* in *Pharmaceutics The science of dosage form design,* M.E. Aulton, Editor. 1988, Churchill Livingstone: p. 581-590.

29. Gjaltema, D. and P. Hagendoorn, Rijksuniversiteit Groningen. Dept Pharmaceutical Technology, .

30. Steel, G., *Nedocromil sodium verbal communication* 1996.

31. Cox, J.S.G., G.D. Woodward, and W.C. McCrone, *Solid-State Chemistry of Cromolyn Sodium (Disodium Cromoglycate).* Journal of Pharmaceutical Sciences, 1971. **60**(10): p. 1458-1465.

32. Lerk, C.F., *et al.*, *Alterations of a- lactose during differential scanning calorimetry.* J. Pharm. Sci., 1984. **73**(6): p. 856-857.

33. Lowell, S. and J.E. Shields, *5. The single point BET method,* in *Powder Surface Area and Porosity.* 1984, Chapman and Hall: p. 30-35.

34. Allen, T., *16. Gas adsorption,* in *Particle size measurement,* T. Allen, Editor. 1990, Chapman and Hall: London. p. 540-566.

35. Buckton, G., *et al.*, *The effect of comminution technique on the surface energy of a powder.* Int. J. Pharm., 1988. **47**: p. 121-128.

36. Florence, A. and E. Salole, *Changes in crystallinity and sloubility on comminution of digoxin and observations on spironolactone and oestradiol.* J. Pharm. Pharmac., 1976. **28**: p. 637-642.

37. Otsuka, M. and N. Kaneniwa, *Effect of grinding on the crystallinity and chemical stability in the solid state of cephalothin sodium.* Int. J. Pharm., 1990. **62**: p. 65-73.

38. Lerk, C.F., *et al.*, *Transitions of lactoses by mechanical and thermal treatment.* Journal of Pharmaceutical Sciences, 1984. **73**(6): p. 857-859.

39. Buckton, G., *Surface characterisation: Understanding sources of vaiability in the production and use of pharmaceuticals.* J. Pharm. Pharmac., 1995. **47**: p. 265-275.

40. Ward, G.H. and R.K. Schultz, *Process-Induced crystallinity changes in albuterol sulfate and its effect on powder physical stability.* Pharmaceutical Research, 1995. **12**(5): p. 773-779.

41. Briggner, L., *et al.*, *The use of microcalorimetry in the study of changes in crystallinity induced in the processing of powders.* Int. J. Pharm., 1994. **105**: p. 125-135.

42. Buckton, G., P. Darcy, and A.J. Mackellar, *The use of isothermal microcalorimetry in the study of small degrees of amorphous content of powders.* Intenational Journal of Pharmaceutics, 1995. **117**: p. 253-256.

43. Saleki-Gerhardt, A., C. Ahlneck, and G. Zografi, *Assessment of disorder in crystalline solids.* Int. J. Pharm., 1994. **101**: p. 237-247.

44. Travers, D.N., *Mixing*, in *Pharmaceutics. The science of dosage form design*, M.E. Aulton, Editor. 1988, Churchill Livingstone: p. 550-564.

45. Lacey, P.M.C., *The mixing of solid particles.* Trans. Inst. Chem. Engineers, 1943. **21**: p. 53-59.

46. Staniforth, J.N., *Advances in powder mixing and segregation in relation to pharmaceutical processing.* Int. J. Pharm. Tech. & Prod. Mfr., 1982. **3 (suppl)**: p. 1-12.

47. Egermann, H. and P.Frank, *Novel Approach to Estimate Quality of Binary Random Powder Mixtures: Samples of Constant Volume.1:Derivation of Equation.* Journal of Pharmaceutical Sciences, 1992. **81**(6): p. 551-555.

48. Fairman, M.D. and E.G. Rippie, *Segregation Kinetics of Particulate Solid Systems III.* J. Pharm. Sci, 1965. **54**(5): p. 719-722.

49. Williams, J.C., *The Mixing of Dry Powders.* Powder Technology, 1968/69. **2**: p. 13-20.

50. Lai, F.K., J.A. Hersey, and J.N. Staniforth, *Segregation and Mixing of Fine Particles in an Ordered Mixture.* Powder Technology, 1981. **28**: p. 17-23.

51. Travers, D.N. and R.C. White, *The mixing of micronised sodium bicarbonate with sucrose crystals.* J. Pharm. Pharmacol., 1971. **23 (suppl.)**: p. 260S-261S.

52. Jones, T.M. and N. Pilpel, *Some physical properties of lactose and magnesia.* J. Pharm. Pharmacol, 1965. **17**: p. 440-448.

53. Hersey, J.A., *Ordered Mixing: A New Concept in Powder Mixing Practice.* Powder Technology, 1975. **11**: p. 41-44.

54. Thiel, W.J., F. Lai, and J.A. Hersey, *Comments on "Suggestions on the Nomenclature of Powder Mixtures".* Powder Technology, 1981. **28**: p. 117-118.

55. Egermann, H. and N.A. Orr, *Comments on the paper 'Recent developments in solids mixing' by L. T. Fan et al.* Powder Technology, 1991. **68**: p. 195-196.

56. Egermann, H. and N.A. Orr, *Ordered mixtures-Interactive mixtures.* Powder Technology, 1983. **36**: p. 117-118.

57. Egermann, H. and N.A. Orr, *Comments to 'Order out of Chaos'.* J. Pharm. Pharmacol., 1989. **41**: p. 142-143.

58. Hartley, P.A., G.D. Parfitt, and L.B. Pollack, *The role of van der Waals force in the agglomeration of powders containing submicron particles.* Powder Technology, 1985. **42**: p. 35-46.

59. Visser, J., *Van der Waals and other cohesive forces affecting powder fluidisation.* Powder Technology, 1989. **58**: p. 1-10.

60. Israelachvili, J., *Intermolecular & Surface Forces*. 2nd ed. 1992. Academic Press Limited.

61. Mosser, S. and K. Sommer, *Calculation of van der Waals forces in adhering systems.* Powder Technology, 1977. **17**: p. 191-195.

62. Staniforth, J.N., *Order out of Chaos.* J. Pharm. Pharmacol., 1987. **39**: p. 329-334.

63. Yip, C.W. and J.A. Hersey, *Ordered powder mixtures.* Nature, 1976. **262**: p. 202-203.

64. Schmidt, P.C. and K. Benke, *"Supersaturated" Ordered Mixtures on the Basis of Sorbitol.* Drugs made in Germany, 1985. **28**: p. 49-55.

65. Crooks, M.J. and R. Ho, *Ordered Mixing in Direct Compression of Tablets.* Powder Technology, 1976. **14**: p. 161-167.

66. Staniforth, J.N., *et al.*, *Determination of interparticulate forces in ordered powder mixes.* J. Pharm. Pharmacol., 1981. **33**: p. 485-490.

67. Stephenson, P.L. and W.J. Thiel, *The Effect of Humidity on the Production of Ordered Mixtures.* Powder Technology, 1980. **25**: p. 115-119.

68. Yeung, C.C. and J.A. Hersey, *Ordered Powder Mixing of Coarse and Fine Particulate Systems.* Powder Technology, 1979. **22**: p. 127-131.

69. Chang, R.-K., *et al.*, *A comparison of free-flowing, segregating and non-free-flowing, cohesive mixing systems in assessing the performance of a modified V-shaped solids mixer.* Drug Development and Industrial Pharmacy, 1995. **21**(3): p. 361-368.

70. Chowhan, Z.T. and E.E. Linn, *Mixing of Pharmaceutical Solids. 1. Effect of Particle Size on Mixing in Cylindrical Shear and V-Shaped Tumbling Mixers.* Powder Technology, 1979. **24**: p. 237-244.

71. Yeung, C.C. and J.A. Hersey, *Criteria for Ordered Mixtures.* Powder Technology, 1979. **24**: p. 106-107.

72. Hersey, J.A., W.J. Thiel, and C.C. Yeung, *Partially Ordered Randomised Powder Mixtures.* Powder Technology, 1979. **24**: p. 251-256.

73. Yip, C.W. and J.A. Hersey, *Perfect Powder Mixtures.* Powder Technology, 1977. **16**: p. 189-192.

74. Egermann, H., I. Kemptner, and E. Pichler, *Effects of interparticulate interactions on mixing homogeneity.* Drug Development and Industrial Pharmacy, 1985. **11**(2&3): p. 663-676.

75. Egermann, H., *Effects of Adhesion on Mixing Homogeneity Part 1: Ordered Adhesion-Random Adhesion.* Powder Technology, 1980. **27**: p. 203-206.

76. Staniforth, J.N. and J.E. Rees, *Segregation of vibrated powder mixes containing different concentrations of fine potassium chloride and tablet excipients.* J. Pharm. Pharmacol., 1983. **35**: p. 549-554.

77. List, P.H. and B.W. Müller, *Untersuchungen über den FST-Komplex.* Pharm. Ind., 1972. **34**(12): p. 963-972.

78. Thiel, W.J. and P.L. Stephenson, *Assessing the Homogeneity of an Ordered Mixture.* Powder Technology, 1982. **31**: p. 45-50.

79. Sallam, E.A., A. Badwan, and M. Takieddin, *Surface characterisation of sucrose and antibiotics powder mixes with relevance to mixing theories.* Drug development and Industrial Pharmacy, 1986. **12**(11-13): p. 1731-1748.

80. Verraes, J. and R. Kinget, *Ordered powder mixing: theory and practice*. Int. J. Pharm. Tech. & Prod. Mfr., 1980. **1**(3): p. 36-41.

81. Poole, K.R., R.F. Taylor, and G.P. Wall, *Mixing powders to ine-scale homogeneity: studies of batch mixing*. Trans. Inst. Chem. Eng., 1964. **42**: p. T305-T315.

82. Egermann, H., *Effects of Adhesion on Mixing Homogeneity II: Highest Attainable Degree of Mixing of a Polydisperse Ingredient and a Monodisperse Diluent*. J. Pharm. Sci., 1985. **74**: p. 999-1000.

83. Egermann, H., *Ordered powder mixtures: reality or fiction ?* J. Pharm. Pharmacol., 1989. **41**: p. 141-142.

84. Davies, O.L. and P.L. Goldsmith, *Statistical methods in research & production*. 4th ed. 1988, Longman scientific & technical.

85. Johnson, M.C.R., Pharm. Acta. Helv., 1972. **47**: p. 546-559.

86. Egermann, H., *Extension of Johnson's equation of homogeneity of random mixtures*. J. Pharm. Pharmacol., 1985. **37**: p. 491-492.

87. Williams, J.C., *The Properties of Non-Random Mixtures of Solid Particles*. Powder Technology, 1969/70. **3**: p. 189-194.

88. Orr, N., *Assessment of an ordered mix.* Powder Technol., 1979. **24**: p. 105-107.

89. Lai, F.K.Y. and J.A. Hersey, *Simulated ordered powder mixture.* International Journal of Pharmaceutics, 1987. **36**: p. 157-164.

90. Yip, C.W. and J.A. Hersey, *Segregation in Ordered Powder Mixtures.* Powder Technology, 1977. **16**: p. 149-150.

91. Johnson, M.R.C., *The effect of particle size upon mixture homogeneity.* Pharm. Acta Helv., 1975. **50**(3): p. 60-63.

92. Staniforth, J.N. and J.E. Rees, *Effect of vibration time, frequency and acceleration on drug content uniformity.* J. Pharm. Pharmacol., 1982. **34**: p. 700-706.

93. Stephenson, P.L. and W.J. Thiel, *The Mechanical Stability of ordered Mixtures when Fluidised and their Pharmaceutical Application.* Powder Technology, 1980. **26**: p. 225-227.

94. deBoer, A.H., 1993, Universitaire Centruum voor Technologie en Receptur, Rijksuniversiteit Groningen, Netherlands:

95. May, J.R., *The Cascade Impactor: An Instrument for Sampling Coarse Aerosols.* J. Sci. Intrum., 1945. **22**: p. 187-195.

96. Groom, C.V. and I. Gonda, *Cascade Impaction: The performance of different collection surfaces.* J. Pharm. Pharmacol., 1980. **32(suppl)**: p. 98P-.

97. Hickey, A.J., *Factors Influencing Aerosol Deposition in Inertial Impactors and Their Effect on Particle-Size Characterisation.* Pharmaceutical Technology, 1990. **14**: p. 118-130.

98. Hallworth, G.W. and U.G. Andrews, *Size analysis of suspension inhalation aerosols by inertial separation methods.* J. Pharm. Pharmac., 1976. **28**: p. 898-907.

99. Zanen, P., *et al.*, *The effect of the inhalation flow on the performance of a dry powder inhalation system.* International Journal of Pharmaceutics, 1992. **81**: p. 199-203.

100. Gonda, I., *et al.*, *Characteristics of Hygroscopic Inhalation Aerosols,* in *Particle Size Analysis 1981,* N.G. Stanley-Wood and T. Allen, Editors. 1981, Wiley Heyden Ltd: Chichester. p. 31-42.

101. May, K.R., *An "ultimate" cascade impactor for aerosol assessment.* J. Aerosol Science, 1975. **6**: p. 413-419.

102. May, K.R., *Aerosol impaction jets.* J. Aerosol Science, 1975. **6**: p. 403-411.

103. Kim, C.S. and L. Garcia, *Delivery Characteristics of Albuterol Powder Inhaler by Rotahaler.* Journal of Aerosol Medicine, 1993. **6**(3): p. 199-211.

104. Vidgren, M., *et al.*, *In vitro and in vivo deposition of drug particles inhaled from pressurised aerosol and dry powder inhaler.* Drug development and industrial pharmacy, 1988. **14**((15-17)): p. 2649-2665.

105. Waldrep, J.C., *et al.*, *Operating Characteristics of 18 Different Continuous-Flow Jet Nebulisers With Beclomethasone Diproprionate Liposome Aerosol.* Chest, 1994. **105**(1): p. 106-110.

106. Martin, G.P., A.E. Bell, and C. Marriott, *An in vitro method for assessing particle deposition from metered pressurised aerosols and dry powder inhalers.* International Journal of Pharmaceutics, 1988. **44**: p. 57-63.

107. Kassem, N.M. and D. Ganderton, *The influence of carrier surface on the characteristics of inspirable powder aerosols.* J. Pharm. Pharmacol., 1990. **42(suppl.)**: p. 11P.

108. Hickey, A.J., *An Investigation of Size Deposition Upon Individual Stages of a Cascade Impactor.* Drug Development and Industrial Pharmacy, 1990. **16**(12): p. 1911-1929.

109. May, K.R., *Multistage Liquid Impinger.* Bacteriol. Rev., 1966. **30**(3): p. 559-570.

110. Bell, J.H., P.S. Hartley, and J.S.G. Cox, *Dry Powder Aerosols 1: A New Powder Inhalation Device.* Journal of Pharmaceutical Sciences, 1971. **60**(10): p. 1559-1564.

111. Newman, S.P., *et al., Pressurised aerosol deposition in the human lung with and without an "open" spacer device.* Thorax, 1989. **44**: p. 706-710.

112. Wong, D.Y.T., *Reports for Fisons Pharmaceuticals* 1995, Leicester Polytechnic:

113. O'Callaghan, C., *et al., Improvement in sodium cromoglycate delivery from a spacer device by use of an antistatic lining, immediate inhalation, and avoiding multiple actuations of drug.* Thorax, 1993. **48**: p. 603-606.

114. Hallworth, G.W. and D.G. Westmoreland, *The twin impinger: a simple device for assessing the delivery of drugs from metered dose pressurised aerosol inhalers.* J. Pharm. Pharmacol., 1987. **39**: p. 966-972.

115. *British Pharmacopoeia.* ed. B.P. Commission. Vol. 2. 1988, London: H.M.S.O.

116. Kassem, N.M., M.A. Shamat, and C. Duval, *Inspirable properties of a carrier free dry powder aerosol formulation.* J. Pharm. Pharmacol., 1991. **43(suppl.)**: p. 75P.

117. Wetterlin, K., *Turbuhaler: A New Powder Inhaler for Administration of Drugs to the Airways.* Pharmaceutical Research, 1988. **5**(8): p. 506-508.

118. Vidgren, M. and H. Sormunen. *In vitro comparison of the novel multiple dose powder inhaler, metered dose inhaler and Rotadisk® powder device.* in *The 12th Pharmaceutical Technology Conference.* 1993. Elsinore, Denmark:

119. *Appendix XVII C,* in *British Pharmacopoeia.* 1988, p. A204-A207.

120. Wiggins, N.A., *The development of a mathematical approximation technique to determine the mass median aerodynamic diameter (MMAD) and geometric standard deviation (GSD) of drug particles in an inhalation aerosol spray.* Drug Development and Industrial Pharmacy, 1991. **17**(14): p. 1971-1986.

121. Gonda, I., *Targeting by Deposition,* in *Pharmaceutical Inhalation Aerosol Technology,* A.J. Hickey, Editor. 1992, Dekker: New York.

122. Hallworth, G.W., *The formulation and evaluation of pressurised metered-dose inhalers,* in *Drug delivery to the respiratory tract,* D.

Ganderton and T. Jones, Editors. 1987, Ellis Horwood: Chichester. p. 18-118.

123. Byron, P.R. and A.J. Hickey, *Spinning-Disk Generation and Drying of Monodisperse Solid Aerosols with Output Concentrations Sufficient for Single -Breath Inhalation Studies.* J. Pharm. Sci., 1987. **76**(1): p. 60-64.

124. *Task Group on Lung Dynamics of the International Commission on Radiological Protection.* Health Phys., 1966. **12**: p. 173-207.

125. Richards, R. and M. Saunders, *The need for a comparative performance standard for dry powder inhalers.* Thorax, 1993. **48**: p. 1186-1187.

126. Clarke, A.S., *et al. Composition of binary interactive mixes before and after in vitro inhalation testing*. in *A.A.P.S.* 1994. San Diego:

127. Gonda, I. and A.F.A.E. Khalik, *On the calculation of aerodynamic diameters of fibres.* Aerosol Sci. Technol., 1985. **4**: p. 233-238.

128. Bell, J.H., K. Brown, and J. Glasby, *Variation in delivery of isoprenaline from various pressurised inhalers.* J. Pharm. Pharmacol., 1973. **25(suppl)**: p. 32P-36P.

129. Staniforth, J.N. and J.E. Rees, *Investigation of triboelectric and ionistaion methods for electrostatic charging of powder particles.* Int. J. Pharm. Tech. & Prod. Mfr., 1982. **3**(3): p. 69-72.

130. Krupp, H., *Particle adhesion, theory and experiment.* Adv. Colloid Interface Sci., 1967. **1**: p. 111-239.

131. St.John, D.F. and D.J. Montgomery, *Adhesion of small metal spheres to plane metal substrates.* Journal of Applied Sciences, 1971. **42**(2): p. 663-668.

132. Booth, S.W. and J.M. Newton, *Experimental investigation of adhesion between powders and surfaces.* J. Pharm. Pharmacol., 1987. **39**: p. 679-684.

133. Lam, K.K. and J.M. Newton, *Investigation of applied compression on the adhesion of powders to a substrate surface.* Powder Technology, 1991. **65**: p. 167-175.

134. Lam, K.K. and J.M. Newton, *Influence of particle size on the adhesion behaviour of powders, after application of an initial press on force.* Powder Technology, 1992. **73**: p. 117-125.

135. Lam, K.K. and J.M. Newton, *Effect of temperature on particulate solid adhesion to a substrate surface.* Powder Technology, 1992. **73**: p. 267-274.

136. Kulvanich, P. and P.J. Stewart, *Fundamental considerations in the measurement of adhesional forces between particles using the centrifuge method.* International Journal of Pharmaceutics, 1987. **35**: p. 111-120.

137. Kulvanich, P. and P. Stewart, *The effect of particle size and concentration on the adhesive characteristics of a model drug-carrier interactive system.* J. Pharm. Pharmacol., 1987. **39**: p. 673-678.

138. Kulvanich, P. and P.J. Stewart, *Influence of relative humidity on the adhesive properties of a model interactive system.* J. Pharm. Pharmacol., 1988. **40**: p. 453-458.

139. Staniforth, J.N., *et al.*, *Interparticle forces in binary and ternery ordered powder mixes.* J. Pharm. Pharmacol., 1982. **34**: p. 141-145.

140. Laycock, S. and J.N. Staniforth, *A method for determining interparticulate forces in ordered mixes.* Labo-Pharma-Probl. Tech, 1984. **32**(340): p. 185-189.

141. Laycock, S. and J.N. Staniforth, *Problems encountered in accurate determination of interparticle forces in ordered mixes.* Particulate Science and Technology, 1983. **1**: p. 259-268.

142. Corn, M., *The adhesion of solid particles to solid surfaces.* Air Pollution Control Assoc., 1961. **11**: p. 566-575.

143. Corn, M. and F. Stein, *Re-entrainment of particles from a plane surface.* Am. Ind. Hyg. Assoc. J., 1965. **26**: p. 325-336.

144. Boschung, P. and M. Gloor, *methods for investigating the electrostatic behaviour of powders.* J Electroststt., 1980. **8**: p. 205-219.

145. Kulvanich, P. and P.J. Stewart, *Correlation between total adhesion and charge decay of a model interactive system during storage.* Int. J. Pharm., 1987. **39**: p. 51-57.

146. Communication, Research and Development Group, Fisons Pharmaceuticals, .

147. Robertson, P.K. and R.G. Campanella, *Interpretation of cone penetration tests. Part 1: Sand.* Can. Geotech. J., 1983. **20**: p. 718-733.

148. Benbow, J.J. and J. Bridgwater, *Measurement of Paste Yield by Cone Penetration.* Chemical Engineering Science, 1987. **42**(4): p. 915-919.

149. Knight, P.C., *Measurement of Powder Cohesive Strength with a Penetration Test.* Powder Technology, 1988. **54**: p. 279-283.

150. Bruff, W. and J. Novosad, *Balling of Silica Dust by Mechanical Handling (Meeting Report).* Powder Technology, 1979. **23**: p. 273-276.